NASA-CR-197185

Orion

NASw-4435

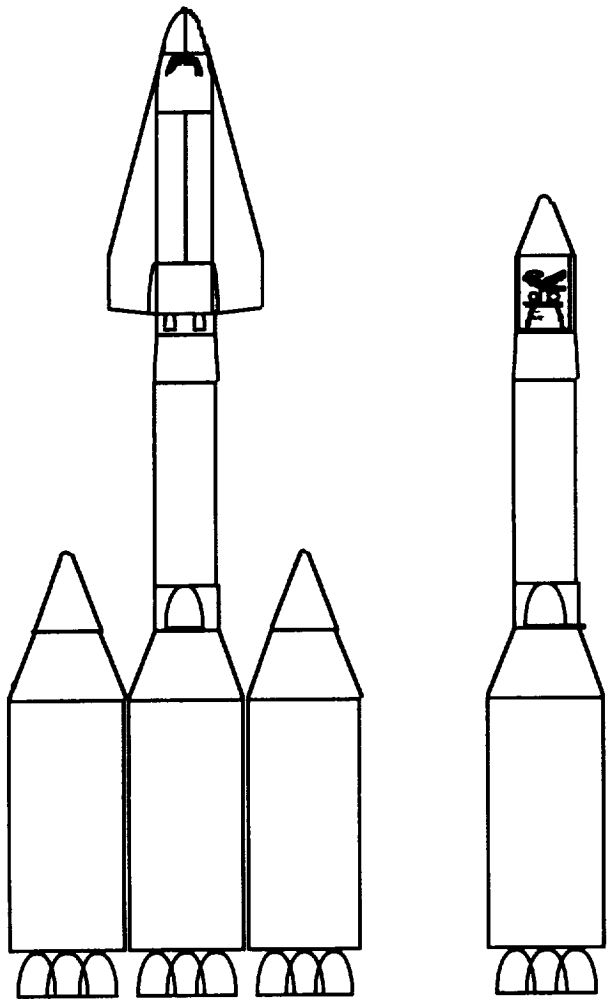

(NASA-CR-197185) ORION: DESIGN OF A SYSTEM FOR ASSURED LOW-COST HUMAN ACCESS TO SPACE (Maryland Univ.) 314 p

N95-12564

Unclas

G3/18 0026167

Design of a System for Assured Low-Cost Human Access to Space

University of Maryland at College Park
Department of Aerospace Engineering
ENAE 484 Design Project
Spring 1994

Abstract

In recent years, Congress and the American people have begun to seriously question the role and importance of future manned spaceflight. This is mainly due to two factors: a decline in technical competition caused by the collapse of communism, and the high costs associated with the Space Shuttle transportation system. With these factors in mind, the ORION system was designed to enable manned spaceflight at a low cost, while maintaining the ability to carry out diverse missions, each with a high degree of flexibility. It is capable of performing satellite servicing missions, supporting a space station via crew rotation and resupply, and delivering satellites into geosynchronous orbit. The components of the system are a primary launch module, an upper stage, and a manned spacecraft capable of dynamic reentry. For satellite servicing and space station resupply missions, the ORION system utilizes three primary modules, an upper stage and the spacecraft, which is delivered to low earth orbit and used to rendezvous, transfer materials and make repairs. For launching a geosynchronous satellite, one primary module and an upper stage are used to deliver the satellite, along with an apogee kick motor, into orbit. The system is designed with reusability and modularity in mind in an attempt to lower cost.

Orion

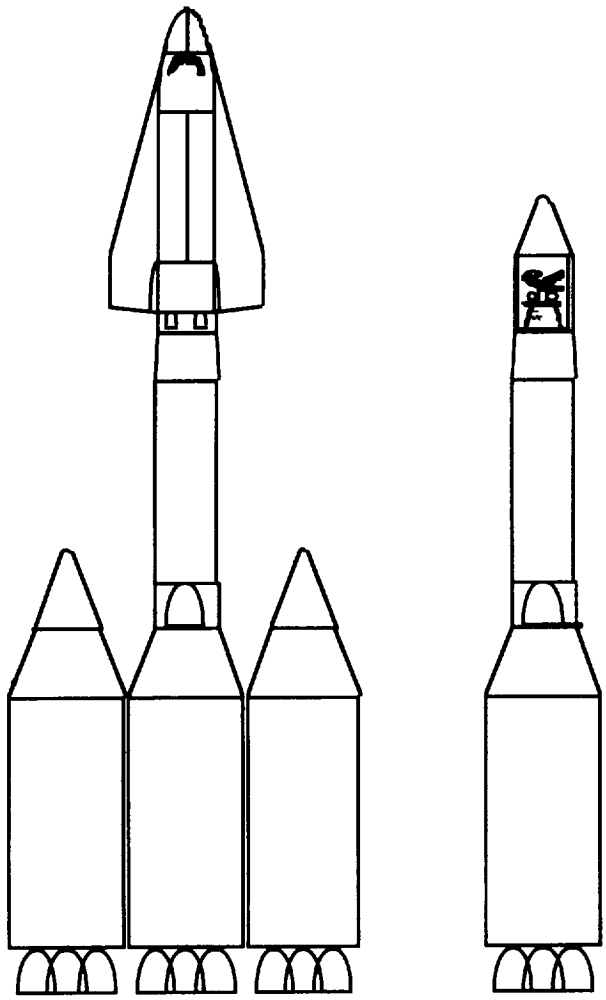

Design of a System for Assured Low-Cost Human Access to Space

University of Maryland at College Park
Department of Aerospace Engineering
ENAE 484 Design Project
Spring 1994

The ORION system was designed by undergraduate students in the University of Maryland's ENAE 484 Spacecraft Design class, a one-semester course taught by Dr. Dave Akin. The purpose of the class was to expose students to engineering design on a systems level, using a format and organization similar to industry. The following is a list of the students who participated in the class, with a description of their respective contributions.

Kourosh Amin	Systems Integration: Spacecraft
Teresa Hunt	Systems Integration: Programmatics and Reliability; Final Presentation
Brian Whalen	Systems Integration: Spacecraft
Martin Zhu	Systems Integration: Launch Vehicle; Final Presentation
Andy Heifetz	Avionics: Data Management; Final Presentation
Andrew Langsdale	Avionics: Communications
Andrew Muhs	Avionics: Navigation, Guidance and Control
Johnny Gee	Propulsion: Engine Design; Power
Taral Patel	Propulsion: Propellants and Engine Design, Thrust Vectoring
Rizwan Ramakdawala	Propulsion: OMS and RMS
David Brent	Mission Analysis: Rendezvous
Mike Drever	Mission Analysis: Launch Trajectory
Alan Ricks	Mission Analysis: Abort Analysis and Systems, Pre-Launch Scheduling and Ground Operations
Josh Elvander	Human Factors; Final Presentation
Kevin Johnson	Human Factors; Spacecraft Integration
Gabriele Barigelli	Structures: Launch Vehicle
Robert Evans	Structures: Thermal Protection; Re-entry Trajectory
Angel Rittle	Structures: Wing and Crew Cabin

The final report was edited by Josh Elvander, Andy Heifetz, Teresa Hunt and Martin Zhu. The class would like to thank Dr. Akin for his invaluable assistance, direction, and above all, patience. It would also like to thank J. Corde Lane, his able, qualified and punctual teaching assistant.

ORION
DESIGN OF A SYSTEM FOR ASSURED LOW-COST HUMAN ACCESS TO SPACE

University of Maryland at College Park
Aerospace Engineering Department
College Park, Maryland

Professor David Akin
J. Corde Lane, Teaching Assistant
Josh Elvander, Andy Heifetz, Teresa Hunt, Martin Zhu,
and Students of the ENAE 484 Design Class

Abstract

In recent years, Congress and the American people have begun to seriously question the role and importance of future manned spaceflight. This is mainly due to two factors: a decline in technical competition caused by the collapse of communism, and the high costs associated with the Space Shuttle transportation system. With these factors in mind, the ORION system was designed to enable manned spaceflight at a low cost, while maintaining the ability to carry out diverse missions, each with a high degree of flexibility. It is capable of performing satellite servicing missions, supporting a space station via crew rotation and resupply, and delivering satellites into geosynchronous orbit. The components of the system are a primary launch module, an upper stage, and a manned spacecraft capable of dynamic reentry. For satellite servicing and space station resupply missions, the ORION system utilizes three primary modules, an upper stage and the spacecraft, which is delivered to low earth orbit and used to rendezvous, transfer materials and make repairs. For launching a geosynchronous satellite, one primary module and an upper stage are used to deliver the satellite, along with an apogee kick motor, into orbit. The system is designed with reusability and modularity in mind in an attempt to lower cost.

Introduction

The main goal of the class was to design a vehicle capable of transporting payload and crew into space at a low cost. The system's cost per manned mission was to be less than $100M (all dollar values FY94), and the cost of transporting payload to orbit was to be reduced to $1000/kg bulk cargo. It was to be based on current technology with a technology cut-off date of January 1, 1994. The system was expected to be fully operational by the year 2000 with safe crew abort modes in all flight regimes, and a mission reliability of 99%. The preliminary design and analysis of the system was performed by a team of eighteen students during the Spring 1994 semester.

Mission Objectives

Reference Missions

The system was required to perform the following three reference missions:

Mission 1: Transport four astronauts and a 5000 kg logistics module to the Space Station and return to Earth with the same size crew and payload. The crew of four was not permitted to participate in flight operations.
Mission 2: Perform the Hubble Space Telescope (HST) servicing mission from STS-61.
Mission 3: Transport a 2000 kg communications satellite, along with necessary apogee kick stage, for insertion into geosynchronous transfer orbit.

Mission Model

The system was required to perform the three preceding reference missions according to the mission model in Table 1. Three developmental flights were planned in the year 1999 to test the system.

Table 1 Baseline Mission Model

Interval	Space Station Resupply	HST Servicing	Satellite to GEO	Total per year
2000-2004	4/year	2/year	5/year	11
2005-2009	6/year	3/year	6/year	15
2010-2014	8/year	4/year	8/year	20
2015-2019	10/year	3/year	10/year	23
2020-2024	4/year	1/year	4/year	9

ORION System Overview

The components of the system were a primary launch module, an upper stage, and a manned spacecraft capable of dynamic reentry. The ORION spacecraft was designed to support a crew of six astronauts for up to 15 days in low earth orbit (LEO). The spacecraft was a delta winged vehicle capable of gliding to a horizontal landing on a runway. Its primary landing site was

Kennedy Space Center. It was 21 m in length with a height of 4.1 m and a wingspan of 10.75 m. Primary control surfaces for landing were located on the winglets of the wings. It was equipped with three sets of landing gear arranged in a tricycle configuration for landing.

Figure 1 Top View of Spacecraft

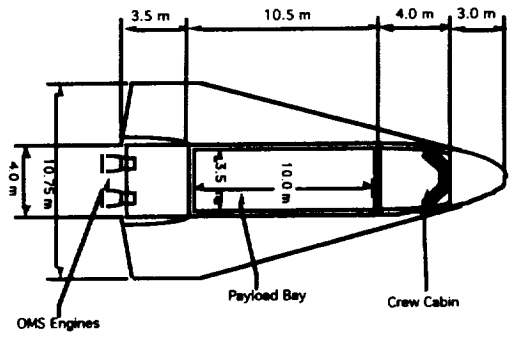

The launch vehicle primary modules used a liquid oxygen (LOX) liquid hydrogen (LH_2) propellant system with three engines. The modules were 22.4 m in length with a diameter of 8.0 m, and had a mass of approximately 28,000 kg. The upper stages also used a LOX/LH_2 system with only one engine. The upper stages were 19.5 m in length with a diameter of 4.4 m. and a mass of approximately 8700 kg.

Vehicle Configurations

ORION was designed with two configurations. The first configuration was a manned system designed to perform reference missions 1 and 2. The three stage launch vehicle used two primary modules as its first stage (stage 1m), one primary module as its second stage (stage 2m), and one upper stage as its third stage (stage 3m). The launch vehicle was capable of boosting approximately 50,000 kg of payload into low earth orbit in this configuration. The spacecraft sat on top of the stack and was attached to stage 3m.

The second configuration was an unmanned two stage vehicle designed to perform reference mission 3. The first stage (stage 1u) used one primary module and the second stage (stage 2u) used one upper stage. This configuration delivered approximately 7,800 kg to GTO. The spacecraft was not used since the mission was unmanned. In its place on stage 2u was a payload shroud designed to protect the satellite during launch.

Programmatics

Launch Vehicle Programmatics. Analysis showed that manufacturing expendable rockets and using a reusable spacecraft was more cost-effective than manufacturing reusable rockets. The launch vehicle was scheduled for 393 missions: 227 manned and 166

Figure 2 ORION Manned & Unmanned Configurations

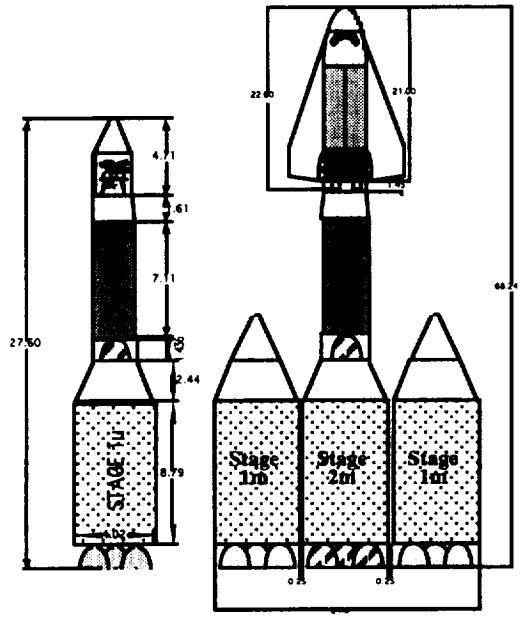

Unmanned **Manned**

unmanned. The primary launch site was Kennedy Space Center. The module and upper-stage production rates are shown in Table 2 below.

Table 2 Module and Upper Stage Production

Interval	Modules per year	Upper Stages /year	Total Modules	Total Upper Stages
1999	7	3	7	3
2000-2004	23	11	115	55
2005-2009	33	15	165	75
2010-2014	44	20	220	100
2015-2019	49	23	245	115
2020-2024	19	9	95	45
Total			**847**	**393**

Spacecraft Programmatics. Three reusable spacecraft were needed to complete the baseline mission profile (Table 1). The first spacecraft was built in 1999, the second in 2000, and the third in 2005. The first and second spacecraft were retired in 2020, the first having completed 74 missions and the second 72 missions. The third spacecraft had flown a total of 81 missions at the end of the program.

Launch Trajectory

The launch vehicle was capable of delivering the necessary payload to the three orbits listed in the table below. The ΔV's necessary to achieve these orbits are also listed. The launch vehicle was capable of achieving the low earth orbits with approximately 4500 kg of spare fuel.

Table 3 Launch Vehicle Performance Requirements

Mission	ΔV (km/s)	Altitude(km)	Inclination
Space Station	9.2	500	52°
Hubble Servicing	8.9	520	28.5°
GEO Satellite	10.6	36,000	0°

Orbital Rendezvous

Orbital rendezvous maneuvers were required by the spacecraft to perform reference missions 1 and 2. Following the release of the last booster stage, the spacecraft was left in a coplanar orbit 18.5 km below the target. The spacecraft maneuvered to a distance of 300 m from the target, ahead and slightly below the target, with the payload bay oriented towards the target. The spacecraft then performed a V-bar maneuver to position itself within 10 m of the target. The RMS was used to either capture or berth with the target. Upon completion of orbital operations with the target, the spacecraft maneuvered via a reverse V-bar to a range of 300m. Once it reached this distance it could safely deorbit.

Spacecraft Overview

The ORION spacecraft was capable of supporting six astronauts for 15 days, orbital maneuvers, and on-orbit operations to support the two manned missions. Upon completion of a mission, the ORION spacecraft performed a lifting body reentry and glided to a landing at the Kennedy Space Center. It was possible to land under emergency conditions at Edwards Air Force Base, California; White Sands, New Mexico; Zaragosa, Spain; Casablanca, Morocco; Rota, Spain; and Guam.

The main components of the spacecraft were the crew cabin, payload bay, wings, reaction control system (RCS), and the orbital maneuvering system (OMS). Spacecraft components forward of the payload bay were referred to as the forward fuselage. It included the crew cabin, forward RCS, forward landing gear, avionics and attitude sensors.

The crew cabin was the largest component of the forward fuselage, measuring 3.5 m in diameter by 4.0 m in length. It provided life support and other support facilities for a crew of up to six people for up to 15 days, and was designed so that part of the crew cabin could be ejected in an emergency, carrying the crew to safety. An airlock exited into the payload bay. All life support except the cryogenic oxygen supply was located within the pressurized volume of the crew cabin, along with most of the avionics. Nose landing gear and attitude sensors were located forward of the crew cabin.

The payload bay was sized to carry a docking module and pressurized logistics module for the station resupply/crew transfer, or the HST repair equipment. Three fuel cells and supporting reactant tanks were located underneath the bottom of the payload bay

Figure 3 ORION Spacecraft

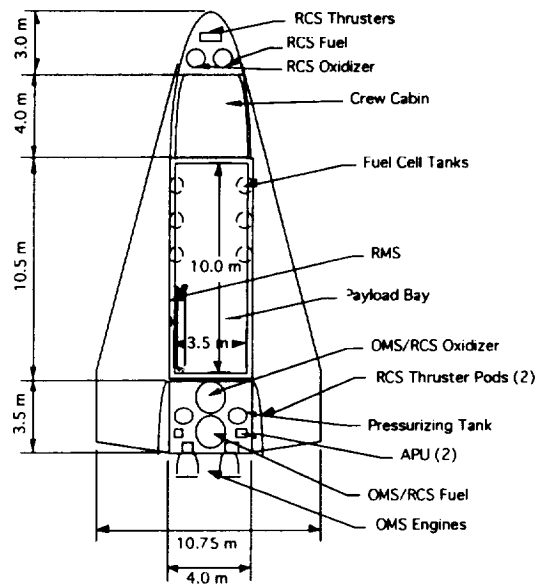

between the support frames. Radiators covered the inner surfaces of the payload bay doors, used to reject heat from the crew cabin. The RMS was mounted on the port side of the payload bay, halfway down its length. The mid fuselage also provided the support for the wing loads.

The aft fuselage housed the Orbital Maneuvering System, the aft RCS, and supporting auxiliary power units (APUs), which provided power to operate the control surfaces. The OMS and RCS were bipropellant systems, using the same propellant and oxidizer, which simplified the tanks, fuel lines and valves. The OMS had two engines, which were gimbaled by the APUs, and were used for orbital insertion, maneuvering, rendezvous and deorbit.

Spacecraft Components

Crew Cabin

The crew cabin was divided into the upper deck and the lower deck. The upper deck is shown in Figure 4. This area served as the control cockpit for launch and reentry, equipped with seats that could be removed and stowed away during on-orbit operations where they become unnecessary. The flight controls in the fore of the cabin also contained atmosphere control panels and other controls necessary to maintaining the cabin. The

rear of the cabin contained the galley, waste control area, and storage space for Extra-vehicular Maneuvering Units, personal belongings and sleeping hammocks. The RMS control station was located on the aft wall with RCS controls for rendezvous operations, and two windows looking up and aft for on-orbit operations.

Figure 4 Crew Cabin Upper Deck

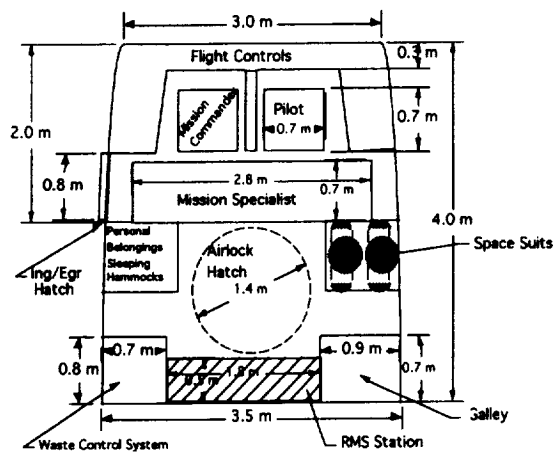

The lower deck contained the airlock and support systems for the crew. The airlock was entered via the upper deck. The egress of the airlock passed through the lower deck into the payload bay. The forward section of the lower deck contained nitrogen, emergency oxygen, water supplies and the avionics package. Escape rockets for propelling the upper deck escape capsule were located at the middeck point, along with blast charges to separate the bulkhead.

Figure 5 Crew Cabin Side View

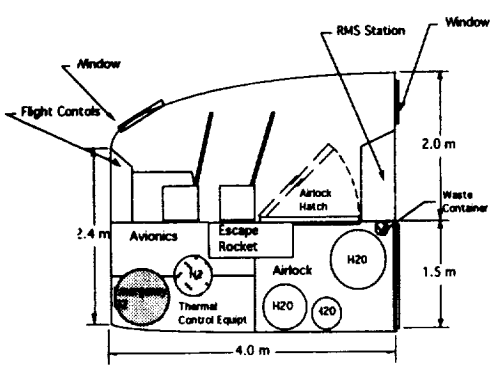

Atmosphere. The crew cabin contained oxygen and nitrogen mixed in a 35/65 ratio at a combined pressure of 0.68 atm. This reduced pressure allowed less structural load, less fire hazard and only requires about an hour of prebreathing before EVA. The diatomic oxygen was supplied to the atmospheric control system by the liquid oxygen fuel cell used in the power system. The liquid oxygen passed from the fuel cells through a series of regulators to provide cabin oxygen partial pressure. The diatomic nitrogen was stored in two tanks pressurized to 204 atm that each contain 23.5 kg of nitrogen.

Removal of CO_2 took place via a LiOH scrubber. Approximately 1.1. kg of LiOH per person per day was expected to be consumed. Contaminants were removed with an activated charcoal adsorption filter. Air in the cabin was ventilated through an air contaminant removal loop which combined the LiOH scrubber and charcoal filter.

The spacecraft was cooled using a dual-loop heat-rejection system. A heat transfer loop ran through the crew cabin using water as a working fluid. Atmosphere was ventilated over heat exchangers located in the rear of the cabin, from where the cooling water continued on through the avionics bay via modular "cold boxes" utilizing thermal interfaces. A radiator fluid loop received heat at exchangers located in the rear of the crew cabin and transferred it to space via radiators located in the payload bay doors. The working fluid in the radiator loop was Freon-12, chemically known as dichlorodiflouromethane. Figure 6 shows a loop diagram of the thermal system.

Figure 6 Thermal Loop Diagram

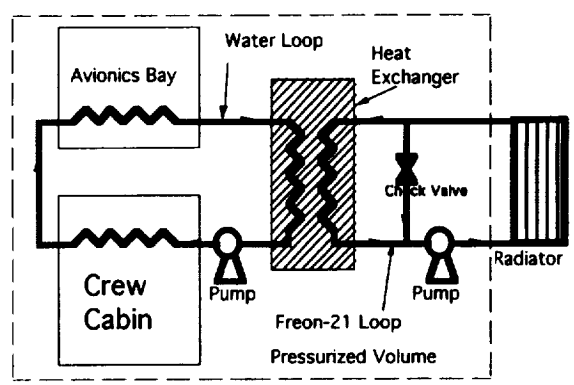

Emergency oxygen was carried with the nitrogen in the pressurized cabin, in two vessels each containing 4.5 kg of diatomic oxygen at 204 atm, enough for six crew members for one day. Emergency breathing masks were provided which interfaced directly with the cabin control panel. Other emergency equipment included two halon fire extinguishers (one per deck), a photoelectric smoke detector located near the intake of the contaminant control system, and emergency lighting.

EVA Ops. The ORION spacecraft carried five EMUs, one per EVA astronaut and one spare. The airlock was designed to hold two EVA-suited astronauts. The spacecraft was equipped with a Remote Manipulator System (RMS), which measured slightly over 10 m at

full extension. The RMS was constructed of graphite-epoxy with seven joints: three in the shoulder, two in the elbow and three in the wrist (similar to a human arm). It was capable of exerting a maximum torque of 620 N-m to brake its payload, and can provide a holding force of 2000 N.

Escape System. The purpose of the escape system was to get the crew out of the path of any explosions caused by a failure of the launch vehicle. A trade study determined that ejecting a portion of the crew cabin was more mass effective than individual ejection seats. The escape capsule (the upper deck of the crew cabin) was equipped with a drogue parachute which was to be deployed 20 seconds into the abort, and a 33.5 m diameter ring sail parachute which would decelerate the astronauts to the point where impact with the ground or water would occur at or less than 25 g deceleration, deemed safe for human survival.

Avionics

The three reference missions were decomposed into sixteen top level functions. The avionics systems were responsible for performing the guidance, navigation, control, systems health monitoring and management, and communications functions. Systems health monitoring and management includes:

- Avionics system configuration monitoring and management
- propulsion monitoring and management
- fluids (propellant) monitoring and management
- power monitoring and management
- fire monitoring and management
- life support monitoring and management
- thermal monitoring and management

The avionics system also has the ability to initiate abort procedures if the situation requires faster than human reaction times.

The avionics systems were required to meet three requirements which were to achieve .9975 system level reliability, to reduce ground operation costs, and to standardize components so that they might be used on both the crewed and un-crewed vehicle configurations. Reducing ground operation costs (maintenance, pre-launch testing, etc.) was identified as a major cost savings strategy. Using the same components on all configurations was required to reduce Research and Development costs and to increase the economy of scale for production of these components.

Data Management and Processing. The data management and processing sub-system was divided into two areas; the computer resources area and the vehicle network area.

The vehicle network gathers information from sensors and other devices (man-machine interfaces, communication receiver, etc.) and delivers this information to the computer resources. The computer resources process the information and return command signals or telemetry back to the network for distribution to the proper actuators/effectors and other control devices.

The computer resources area was sub-divided into hardware and software. The hardware elements of composed of five modular computer units. Each computer unit was composed of nine standard modules, used RISC instruction set architecture, and could perform 15 million instructions per second (15 MIPS).

The five computer units were linked together in a functionally distributed architecture. In this architecture, any computer can perform processing tasks of any function that was delegated to the avionics systems (guidance, navigation, control, systems health monitoring and management, and communications). Responsibility for given function is allocated to a specific computer in real time by the avionics systems software. This architecture has the following advantages of only needed one type of computer unit, having graceful degradation, and sharing sensor information.

Requiring only one computer type lowers research and development cost and increases the economy of scale for production. Graceful degradation is the ability of a system to operate in the presence of a know fault. If one of the five computer units fails, the functions it was responsible for are redistributed to another computer. If more computers fail, the remaining operation computers are distributed the flight critical functions. Sharing of sensor information allows for fewer data buses.

The software on-board the spacecraft allows for a high degree of autonomy requiring less ground support. The size of the software required to performs the avionics system functions were estimated as 1.5 million lines of code costing $262 million dollars.

The vehicle network is a quad redundant high speed fiber optic bus arranged in a linear topology using a token passing protocol. Sensors and control devices gain access to the network through remote data units. The remote data units provide D/A and A/D conversion, "Byte-to-Light" and "Light-to-Byte" conversion implementation of network protocol, and limited signal conditioning.

There are 24 remote data units (RDUs) distributed throughout the spacecraft.

Figure 7 Conceptual diagram of the data management and processing sub-system

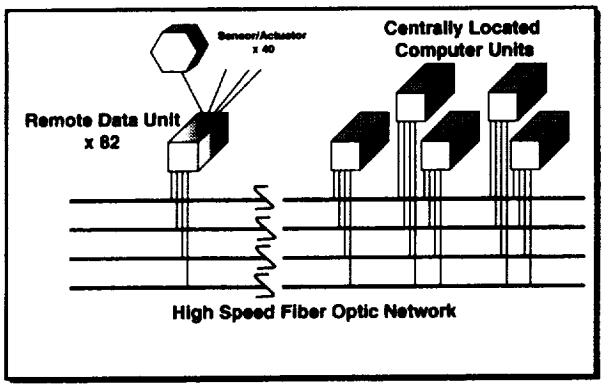

Navigation, Guidance, and Control. The navigation, guidance, and control functions were configured by mission phase. The mission phases were as follows:

Ascent phase- Launch to orbit insertion (0-500+ km)
On-orbit phase
Entry Phase - Initiation of re-entry (120 - 3 km). Radio Blackout occurs from 100 - 50 km. Terminal Area Energy Management occurs from 21 - 3 km.
Precision landing phase - (3 - 0 km)

The primary navigation system is a tightly integrated Internal Navigation System (INS) and Global Positioning System (GPS). This integrated system is more accurate than a pure INS or GPS. Navigation software handles the configuration of the Kalman filter. The Kalman filter is configured by mission phase.

Table 4 Kalman filter configurations

Mission Phase	Configuration	Situation
Ascent	INS/GPS	Normal
On-Orbit	INS/GPS	Normal
On-Orbit	Relative INS/GPS	Docking
Entry	INS/GPS	Normal
Entry	Standalone INS	Black-out
Precision Landing	Standalone INS	Normal
Any	Standalone GPS	INS Failure

During the on-orbit phases, a star tracker regularly updates the INS system. A radar altimeter (RA) and a Microwave Landing System (MLS) were used with the INS in the precision landing phase since the INS/GPS system did not meet the accuracy requirements. A differential GPS was considered for the precision landing phase; however it did not meet the 1994 technology cut-off date. Throughout the mission phases, attitude determination will come from the INS measurements.

Guidance will provided for the ascent and entry phases. A closed loop guidance scheme based on Spherical Atmospheric Linear Tangent guidance[1] was used for ascent. This scheme allows for feed-forward compensation of wind gusts which are calculated in real time using winds ahead sensors (small Doppler radar). Linear Tangent steering, where the optimal thrust angle in terms of time with respect to a fixed coordinate axis, is solved for in both the pitch and yaw planes (Hanson 1992). The ascent profile is as follows:

1) Vertical Liftoff, initiate closed loop guidance
2) At 15 sec into ascent wind parameter is phased into guidance profile. Angle of attack is held to zero.
3) At 45 sec wind is fully modeled. Angle of attack continues being held to zero.
4) At vacuum, guidance commands precise control of velocity and position.
5) At orbit insertion, guidance commands strict velocity control.
6) After orbit insertion, terminate guidance.

The reentry guidance function is prediction of azimuth to terminal area energy management (TAEM). Closed loop control is initiated at initial reentry maneuver. Steering is broken up into horizontal guidance and vertical guidance. Horizontal guidance controls spacecraft heading by steering according to roll angle[2]. Horizontal guidance, using a predictive method, keeps the vehicle in a desired heading error by maneuvering the spacecraft through a series of S-turns. Vertical guidance is an energy controller, adjusting range by varying the angle of attack and the commanded traveling altitude(Buhl 1992). At the start TAEM, guidance is terminated.

The vehicle has three types of control devices which are thrust vector gimbaling, reaction control system (RCS), and aerodynamic control surfaces. Each device is used as follows:

Ascent Phase Guidance commands will perform attitude pitch and yaw control by thrust vector gimbaling. INS gyros will measure attitude.

On-orbit Phase INS will perform Attitude measurement by use of gyros and by input from star tracker. Control will be accomplished by the RCS system.

Return Phase Return guidance commands initiate prior to re-entry and terminate at terminal area energy management (TAEM). Control will be accomplished by RCS cold gas thrusters and phasing in of aerodynamic surfaces at 150 km. INS gyros will make attitude measurement. Air data system will be phased in as an additional sensor to make atmospheric measurements.

Precision Landing phase Atmospheric data will come from the air data sensors. INS will measure attitude with respect to a glide slope provided by microwave scanning beam and ground mapping by radar altimeter. Control will be accomplished by aerodynamic control surfaces.

During the on-orbit mission phase, control commands can be from either manual inputs or from an automatic stabilization program. After TAEM, guidance is terminated and the pilot issues the control commands.

Figure 8 On-orbit control structure

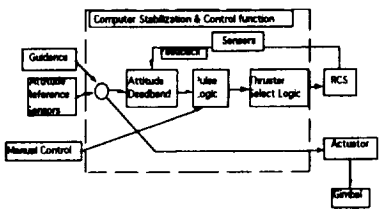

Electrical mechanical actuators (EMAs) were used to control engine gimbals, engine and RCS valves, and aerodynamic control surfaces. EMAs offer substantial mass savings, reduced ground operation costs, and quicker turn around time than due hydraulic actuators.

Communications. Two systems currently exist which ORION would permitted to use, namely the Satellite Tracking and Data Network (STDN) and the Telemetry and Data Relay Satellite System (TDRSS). Therefore, the primary communications link for the manned ORION missions will be through the TDRSS. A secondary back up link will provide direct spacecraft to ground communications through the STDN in the event that the TDRSS link should fail. Other supplemental links include spacecraft to astronauts in Extra-Vehicular Activity (EVA), Merritt Island tracking facility to launching vehicle, spacecraft to space station All links will be digital, (except EVA where the lower frequencies limit the amount of data transmitted at any given time). Digital communications have decreased error rates and several sources of information can be multiplexed into a single link. The following is a summary of communication links.

- S-band through TDRSS
- K-Band through TDRSS
- S-band through to STDN
- S-band through to STDN
- S-band though launch facility
- EVA astronaut to spacecraft
- S- band to space station

Crew Cabin Structure

Aluminum 2024 was selected as the material for the crew cabin because of its high strength and low density. The thickness of the aluminum was determined by analyzing the loads and stresses on the cabin. The main loads on the crew cabin were the ultimate load (P_{ult}) and the critical buckling load ($P_{cr.}$) Since the crew cabin was cylindrical, the main stresses that acted on the structure were hoop and longitudinal stresses. The safest minimum crew cabin thickness was 0.01 m.

Spacecraft Wing Structure

The spacecraft used a delta wing, with the properties shown in Table 5, for reentry and landing. The wings were sized for optimum performance in the hypersonic and subsonic flight regimes. In the hypersonic regime the wings were designed with a low ballistic coefficient, a high lift to drag ratio, and low mass. In the subsonic region the wings were designed with a low landing speed and a low wing loading.

Table 5 Wing Properties

Wing Span	10.75 m	Wing Area	88.06 m^2
L/D	1.43	Bal. Param.	265 kg/m^2
CLmax	1.4	Vstall	75.6 m/s^2
Loading	4900N/m^2	root thick.	1.5 m
Ult. Ld Fac	12	Mass	140 kg

Wing tips with vertical control surfaces were located on the wings for added performance and increased stability. Each wing tip was 5 m^2, with a length of 4m and a height of 2.5 m.

Orbital Maneuvering System (OMS)

The Orbital Maneuvering System (OMS) was designed to enable the spacecraft to perform Hohmann transfers to rendezvous with either the space station or the Hubble Space Telescope (HST), and to perform deorbits. A maximum ΔV of 375 m/s was required. A hypergolic bipropellant combination of hydrazine fuel with a nitrogen tetroxide oxidizer was chosen for ideal performance. Combustion chamber analysis indicated that performance was optimal at a chamber pressure of 689500 Pa, yielding 7500 N of thrust and an Isp of 351 s. The thrusters utilized a bell shape nozzle and a self-impingement injector plate, with like doublet impinging injectors. Table 6 provides general performance characteristic of the OMS thruster.

The 2 OMS engines each used regenerative cooling wherein fuel was bled from the tanks and injected into the walls of the nozzle, using a non-impinging injector at 298 °K. Thrust vectoring was accomplished with a large electric gimbal on each engine, each powered by Auxiliary Power Units (APUs), rotating it over ±15°.

The APUs used the same fuel as the OMS, yet only required 2% of the margined OMS fuel supply.

Table 6 OMS Thruster Performance Data

Propellant	$N_2O_4+N_2H_4$	R (reac)	101
Isp (vac) (s)	343.8	R (prod)	101
Oxidizer/Fuel	1.42	Isp (thr.ch)(s)	351
dens.(kg/m^3)	1220	Thr/Eng (N)	7500
Temp(thr.ch.)	3266	Ue (m/s)	3373
c* (m/s)	1573	mass flow (kg/s)	2.22
Cf	.512	Gamma	1.26
Expnsn Ratio	8	Throat Area	.0212
Exit Diameter	.465	Nozzle Length	.567
Throat Dia.	.164	Chamber Dia.	.201
Exit Area	.170	Chamber Length	.304

Reaction Control System (RCS)

The Reaction Control System was a set of thrusters used to perform small translational and rotational changes during rendezvous operations. To ensure redundancy in groups of three over each axis, multiple thrusters were used, so that a total of 36 RCS thrusters existed on the spacecraft, 14 in the nose and 22 in the two aft pods. The thrusters utilized a standard cylindrical thrust chamber with a 15° half-angle cone-shaped nozzle. The same propellant was used as in the OMS system, hydrazine fuel with nitrogen tetroxide for an oxidizer. Regenerative cooling, the heat-transfer method used in the OMS, was not practical with a thruster of such a small size, and ablative cooling was used instead. Although radiative cooling systems are simpler and more cost-effective, the RCS was to serve as a backup for the OMS, which would require such a continuous burn of the RMS to build up thrust that the nozzles would melt with a radiative cooling system. The characteristics of the engine were almost the same as the OMS engines. Refer to Table 6 for details. The only differences are the mass flow (.296 for RCS). Table 7 gives the dimensions of the RCS engines.

Table 7 RCS Engine Data

Expnsn Ratio	8	Throat Area	.00283
Exit Diameter	.17	Nozzle Length	.211
Throat Dia.	.06	Chamber Dia.	.0735
Exit Area	.0227	Chamber Length	.156

Propellant feed was accomplished with a gas pressure feed system, for both the OMS and RCS. Helium was used at a pressure of about 20 MPa to blow down the propellant into the engine. Redundancy existed in the system to a high degree to prevent catastrophic accidents. Quad check valves and pressure regulators were located after each tank to prevent back flow and pressure loss, and a parallel isolation solenoid valve with pressure regulators was placed after the helium tank to ensure constant pressurized flow. Figure 9 shows the pressure line schematic of the aft system.

Figure 9 Aft RCS/OMS Propellant Schematic

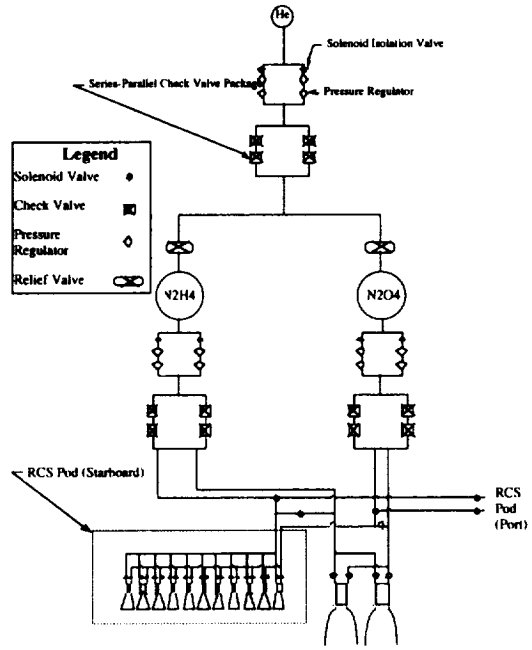

Power

Electrical power was provided by liquid hydrogen/liquid oxygen fuel cells with nickel hydrogen batteries as a secondary (backup) source. The OMS required electrical power to gimbal the thrusters, and flight controls required power to move the control surfaces. These systems received power from the APUs mentioned above, with maximum power of 61.6 kW at any given time.

Three fuel cells provided 5.5 kW of power for the entire mission, with a triple degree of redundancy: if one of the fuel cells failed, the 11 kW of power from the two remaining cells provided enough power to complete the mission. If two cells failed, the remaining cell provided enough power for emergency reentry. One of the liquid oxygen fuel cells contained an additional supply of oxygen for the life support system.

The secondary batteries could supply 5.5 kW of power for a period of 24 hours, enough time for emergency reentry. Table 8 shows the power requirements of the various spacecraft subsystems. Figure 10 provides a schematic of the electrical system.

The electrical distribution system was designed to provide redundancy in all aspects for reliability. All three fuel cells were connected to a distribution bus by three separate relays. The distribution bus supplied power to three separate sub-buses which supply life support and avionics.

Table 8 Subsystems Power Requirements

Subsystem	Power (kW)	Usage	Duration (hrs)	Power Load (kWhr)
Lighting	.25	Cont	300	75
Ventilation & Fans	1	Cont	360	360
Pumps	1	Cont	360	360
Airlock	.5	Temp	30	15
RMS	1	Temp	30	30
Galley	.0125	Temp	60	.75
Electronics	1.5	Cont	300	450
Comm.	1.5	Cont	300	450
Nav.	.2	Cont	360	72
OMS Gimbal	18.5	Temp	5	92.5
OMS Valve	7.7	Temp	30	231
RCS Valve	7.7	Temp	15	115.5
Flt. Servos	61.6	Temp	7	431.2
Max Power	102.5		**Max Load**	2683
Essential Power	5.45		**Essntl Load**	1767

Figure 10 Electrical System Schematic

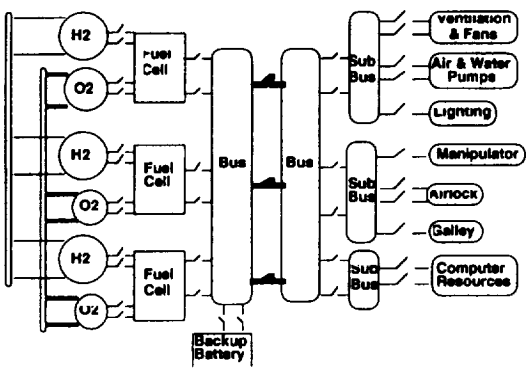

Launch Vehicle

Introduction and Overview

The goal of the ORION project was "affordable human access to space." Therefore, reducing cost was the driving factor in the design of the launch vehicle. The resulting design had four major cost-reducing features.

1) The vehicle was customized for the manned and unmanned missions. For the manned missions, the vehicle would use all three stages. For the unmanned missions, the vehicle would use only the top two stages.

2) The design used a custom top stage, one module for the 2nd stage, and two modules for the 1st stage. Extensive trade studies examined the launch vehicle cost per mission of three cases: pure modular design, conventional staging design with ideal ΔV distributions, and semi-modular design, which was the cheapest.

3) Both the custom top stage and the modules used the same LOX/LH2 engine with different expansion ratios. The top stage used one engine and the modules used three engines. Two nozzles were designed for the launch vehicle with different expansion ratios. For the manned missions, the top stage and 2nd stage module used the nozzles with higher expansion ratio than the ones used by the 1st stage modules, and for the unmanned missions the top stage used the higher expansion ratio nozzle while the 2nd stage module used the lower one. This design would require research, development, and testing of just one engine. No other launch system in the present or history had this characteristic.

4) The launch vehicle was expendable. For the specific mission model and the configuration, an expendable vehicle had a cost advantage over the reusable one.

Figure 11 Launch Vehicle Overview (unmanned)

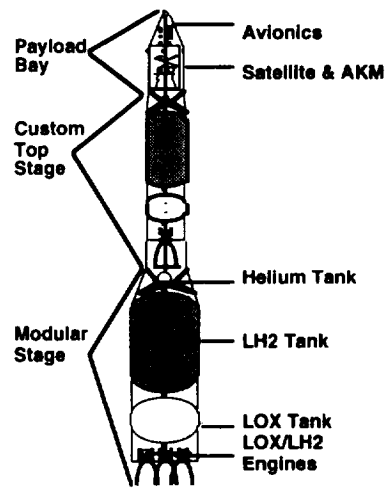

For the manned missions, the payload bay would be replaced by the spacecraft. Also, there would be an additional stage consisting of two modules.

Launch Vehicle Components

Structures. The structures of the launch vehicle would be subjected to axial and hoop stresses due to static and dynamic loads, as well as vibrations before and during ascent. The dynamic loads could be characterized by load factors.

Table 9 Load Factors

Type	Steady State	Transient	Total
lateral	±4.0 g's	±2.0 g's	±6.0 g's
axial	±4.0 g's	±3.0 g's	±7.0 g's

By analogy to other launch systems, the vibration that the launch vehicle would experience was estimated at 20 Hz. Therefore, the natural frequency of the structural members was designed to be above 20 Hz to avoid dangerous resonance.

The material for the major structural components was chosen to be aluminum 2024 after trade studies comparing several cases for the lowest cost. The material for the helium tank was chosen to be Kevlar-49 due to the fact that the helium tank was subject to high internal pressures.

The shape of the LOX and LH2 tanks was chosen for the lowest mass for the entire vehicle. The resulting design was able to withstand all the loads with a safety factor of 1.6 for yield and 2.0 for ultimate, and was optimized for lowest cost. The geometry and orientation of the components of the upper stage and the module were identical.

Figure 12 Module Dimensions

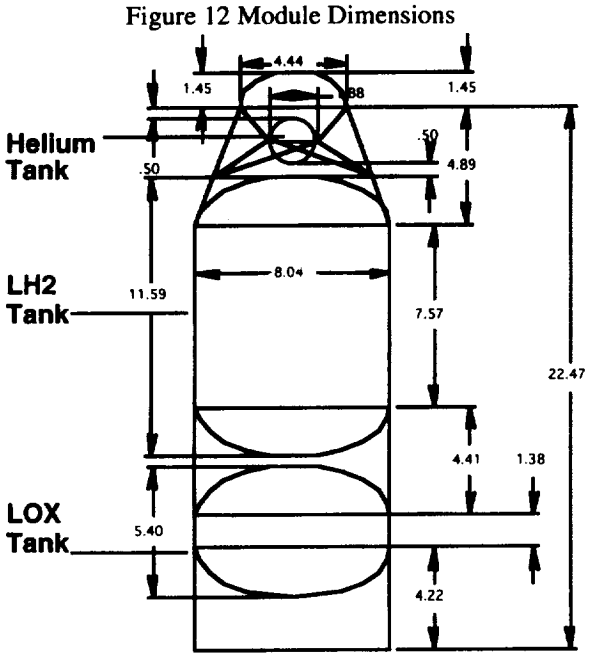

The LH2 tank was placed above the LOX tank to minimize CG travel during accent.

Table 10 Upper Stage Masses & Dimensions

Part	Thickness	Pressure	Radius
Helium tank	8.3 mm	20 MPa	.57 m
Interstage fairing	2.16 mm		2.22 m
Hydrogen tank	7.47 mm	0.52 MPa	2.22 m
Intertank fairing	2.60 mm		2.22 m
LOX tank	3.84 mm	0.45 MPa	2.22 m
Nozzle shroud	4.73 mm		2.22 m

Table 11 Module Masses & Dimensions

Part	Thickness	Pressure	Radius
Helium tank	14 mm	20 MPa	0.94 m
Interstage fairing	4.22 mm		4.02 m
Hydrogen tank	12.3 mm	0.52 MPa	4.02 m
Intertank fairing	8.72 mm		4.02 m
LOX tank	6.05 mm	0.45 MPa	4.02 m
Nozzle shroud	9.26 mm		4.02 m

Propulsion and Power. The launch vehicle main propulsion system would be based on cryogenic LOX/LH2 rockets engines with an Isp of approximately 430 s. The main propulsion system would consist of combustion chambers, propellant feed systems, tanks, injection systems, ignition systems, thrust vectoring control systems, and nozzles. Power required for the ignition systems, valves, and gimbal actuators would be provided by APUs located on the launch vehicle.

The chamber pressure was chosen to be 16.5 MPa after trade studies considering the relationship between the chamber pressure, thrust coefficient, mass, and complexity. Using one engine for the top stage and three of the same engines for the modular stage would yield the lowest cost while maintaining good reliability.

A single combustion chamber was designed for both the top and modular stages. Two nozzles of similar design but with different expansion ratios were designed. The expansion ratios of the nozzles were chosen to achieve a good balance between performance and mass.

The high expansion nozzle would expand the flow to an exit pressure of 26.5 kPa, equivalent to the ambient pressure corresponding to a standard altitude of 10 km. The low expansion nozzle would expand the flow to an exit pressure of 70.1 kPa, equivalent to the ambient pressure corresponding to a standard attitude of 3 km.

Propellant feed system trade studies showed that staged combustion cycle was optimum after comparing it to a pressure feed system, a gas generator cycle, a combustion tap-off cycle, and an expander cycle.

Optimization studies were done on turbo pump inlet pressures and compressor/turbine characteristics. From these analysis the turbo pumps were designed.

Propellant tank storage pressures were determined from the turbo pump inlet pressures and were used in the design of the propellant and helium tanks.

The non-impinging concentric "ring groove" type manifold was designed for the injection system. This design offered high performance and combustion stability for gaseous fuel and liquid oxidizer. For the main combustion chamber the area required for injection of LH2 was determined to be $0.0115 m^2$ while the area

required for injection of LOX was determined to be $0.0058m^2$.

Figure 13 Turbo Pump Cycle Schematic

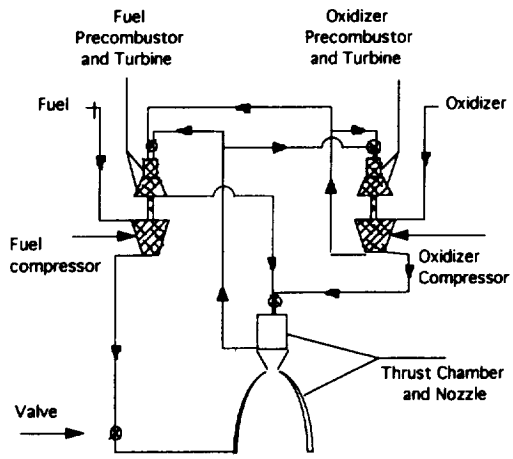

Table 12 Compressor Characteristics

Engine Feed System	Pump Characteristics	
Designation	LOX Pump	LH_2 Pump
Type	Radial	Radial
No. of impeller stages	3	4
Impeller diameter (cm)	32.6	23.2
No. of inducer stages	1	1
Inducer diameter (cm)	16.2	12.5
Flow rate (kg/s)	382	78
Inlet pressure (MPa)	0.32	0.29
Discharge pressure (MPa)	22.3	32.66
Pump pressure rise (MPa)	21.9	32.36
Shaft speed (rpm)	5840	35840
Fluid power output (kW)	8203	35564

Table 13 Turbine Characteristics

Engine Feed System	Turbine Characteristics	
Designation	LOX Pump	LH_2 Pump
	TURBINES	TURBINE
Type	Low-reaction	Low-reaction
No. of stages	2	2
Flow rate (kg/s)	137	137
Inlet temperature (K)	811	811
Inlet pressure (MPa)	23.3	23.3
Pressure ratio	1.13	1.49
Shaft speed (rpm)	5840	35840
Turbine power (kW)	12594	54714
Mixture ratio (Precombustor)	0.79	0.79

Four types of ignition systems were investigated: pyrotechnic igniters, hypergolics, spark plug igniters, and spark torch igniters. Spark torch igniters were chosen for their simplicity and reliability.

Four systems were investigated for thrust vector control of the launch vehicle: gimbals, liquid side injection, jet vanes, and auxiliary thrust chambers. Gimbals were chosen for their reliability and their ability to provide relatively large angular displacements (on the order of 15 degrees or more).

Figure 14 Injector Element & Manifold Schematics

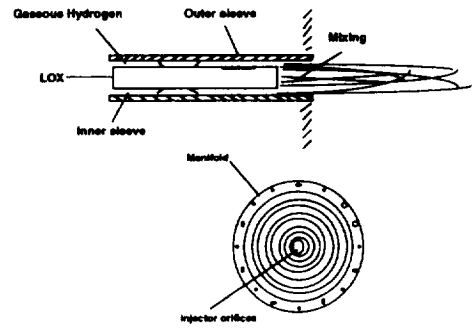

The power system for the modules consisted of four APUs similar to the ones on the spacecraft, except they would supply up to 135 kw each. Only three were necessary to satisfy the power required by the stage, and the fourth one was used for redundancy. The top stage would use one APU of similar design.

Heavy-Lift Capability

The modularity of the ORION launch vehicle was successful not only in reducing cost but also in customizing the vehicle for a specific mission. It could accomplish missions far more demanding than the reference missions by using additional modules. With two more modules as an additional stage, the four stage launch vehicle would be able to place the spacecraft into geosynchronous orbit. This ability would be valuable for possible geosynchronous satellite service missions. The same configured vehicle would be able to deliver 51000 kg bulk cargo into GEO, and 84000 kg to the space station. With a more ambitious configuration (four more modules as an additional stage), the launch vehicle could place the spacecraft with over 30000 kg payload into a hyperbolic orbit. The same configuration would deliver 80000 kg into GEO, and 117000 kg into LEO. This configuration surpassed the capability of all pre-existing launch systems on this planet.

Cost Estimation

A cost analysis was performed to estimate the cost per mission. The cost per mission was determined by setting the net present value of the total expenditures equal to the net present value of the total revenue. The total revenue is the cost per mission multiplied by the number of missions. Knowing the number of missions and the net present value of the total expenditures one can solve for the cost per mission. The total expenditures, which include research and development cost, ground operation costs, expendable parts cost, spacecraft costs, and spacecraft refurbishment costs are discussed below.

Research & development costs were approximated for each component using empirical formulas that relates costs to mass (Appendix 5.3.1). The total R&D costs are $1.5 billion FY94 dollars. The R&D also includes the $393 M FY94 dollars for software development. The R&D costs are distributed linear over six years.

Ground operation costs included launch operations, recovery operations, facilities, ground support equipment, management, and engineering support costs. The total ground operation costs were $122.5 M FY94 per year.

Expendable parts are components that form the expendable launch vehicle. The parts and their respective costs are as follows.

Table 14 Theoretical first unit costs

Expendable Part	Theoretical First Unit Cost [$M FY94]
Module	$34.14
Upper Stage	$19.68
Engine	$45.28
Avionics Package	$16.20

A learning curve factor is multiplied to the theoretical first unit cost of each additional unit produced. A learning curve is mathematical technique to account for productivity improvements as a larger number of units are produced[3].

The total spacecraft costs is $429 M FY94. Spacecraft refurbishment costs were estimated as 15% of the total spacecraft costs per flight.

Table 15 Cost per mission

Mission	Cost $M FY94
Crewed	$ 283
Un-crewed	$ 85

Figure 15 Cost and Revenue per year

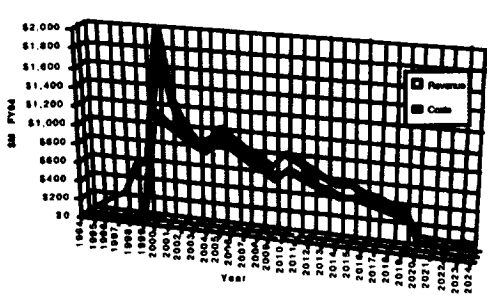

Figure 16 Total expenditure breakdown

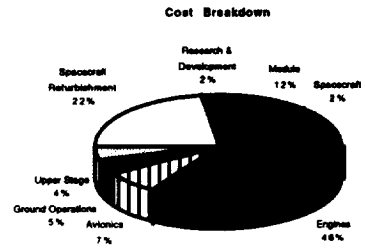

The net present value of the total expenditures equal $16.276 billion FY94. The cost per mission of an un-crewed mission is was estimated to be .3 of the cost of a crewed mission. The total discounted launch charges for the program to break-even are shown in Table 15. Overall spending and revenue histories are shown in Figure 15. The breakdown of expenditures is shown in Figure 16.

Acknowledgments

The ORION system was designed by undergraduate students in the University of Maryland's ENAE 484 Spacecraft Design class, taught by Dr. David Akin. The following students participated in the class: Kourosh Amin, Teresa Hunt, Brian Whalen, Martin Zhu, Andy Heifetz, Andrew Langsdale, Andrew Muhs, Johnny Gee, Taral Patel, David Brent, Mike Drever, Alan Ricks, Josh Elvander, Kevin Johnson, Gabriele Barigelli, Robert Evans, and Angel Rittle.

The final report was edited by Josh Elvander, Andy Heifetz, Teresa Hunt and Martin Zhu. The class would like to thank Dr. Akin for his invaluable assistance, direction, and above all, patience. It would also like to thank J. Corde Lane, his able and resourceful teaching assistant, and Dr. Mark Lewis and Dr. Rob Sanner for attending our Critical Design Review. Finally, thanks go to the USRA for providing us with this opportunity, and to Dr. Vicki Johnson of the USRA for attending our Critical Design Review.

References

[1] Hanon J.S., Wade M., Chang H., and Freeman, S.E., "Guidance and Dispersion Studies of National Launch Ascent Trajectories," *IEEE Journal*, 1992, pp.22-32

[2] Buhl, W. and Paris,D.,"Guidance and Control for Re-entry Vehicles," *IEEE Journal*, 1991, pp.131-135

[3] Larson, W.J. and Wertz, J.R.,*Space Mission Analysis and Design*, 2nd edition, Microcosm, Inc. and Kluwer Academic Publishers, 1992, pp.734

Table of Contents

1.0	**Introduction**	
1.1	Motivation	1
1.2	Mission Objectives	1
1.2.1	Reference Missions	1
1.2.2	Mission Model	2
1.3	Design History	2
1.3.1	Launch Vehicle Fuel System Studies	3
1.3.2	Conventional Staging vs. Modular Staging	3
1.3.3	Learning Curve Analysis	4
1.3.4	Optimum Modular Configuration	5
1.3.5	Re-usable vs. Expendable	6
1.3.6	Conclusions	7
1.4	ORION System Overview	7
1.4.1	Introduction	7
1.4.2	Vehicle Components	8
1.4.3	Vehicle Configurations	10
1.4.4	Heavy Lift Capability	13
2.0	**Mission Analysis**	
2.1	Introduction	14
2.2	Launch Trajectory Analysis	14
2.2.1	Purpose	15
2.2.2	Vehicle Model	16
2.2.3	Results	18
2.2.4	Drag and Gravity Loss Determination	19
2.2.5	Conclusions	21
2.3	Orbital Analysis	25
2.3.1	Rendezvous Maneuver Sequence	25
2.3.2	Proximity Operations	26
2.4	Reentry	27
2.4.1	Introduction	27
2.4.2	Reentry Trajectory	27
2.5	Programmatics	32
2.5.1	Spacecraft Programmatics	32
2.5.2	Launch Vehicle Programmatics	33
2.5.3	System Reliability	34
3.0	**Spacecraft**	
3.1	Spacecraft Configuration	37
3.1.1	Introduction	37
3.1.2	Spacecraft Layout	38
3.1.3	Mass Breakdown	39

3.2	Center of Gravity	40
3.3	Crew Cabin	41
3.3.1	Introduction	41
3.3.2	Requirements	41
3.3.3	Crew Cabin Configuration	48
3.3.4	Life Support Systems	52
3.3.5	Escape Capsule	59
3.3.6	Safety Equipment	62
3.3.7	EVA & RMS Requirements	63
3.4	Avionics	66
3.4.0	Introduction	66
3.4.1	Data Management and Processing	70
3.4.2	Navigation, Guidance, and Control - Manned Mission	87
3.4.3	Communications	106
3.5	Structures	115
3.5.1	Introduction	115
3.5.2	Crew Cabin	115
3.5.3	Wings	118
3.5.4	Heating and Heat Transfer	121
3.6	Propulsion and Power	128
3.6.1	Orbital Maneuvering System	128
3.6.2	Reaction Control System	131
3.6.3	Power	138
4.0	**Launch Vehicle**	
4.1	Introduction and Overview	145
4.2.	Module Configurations	146
4.3.	Mass and Center of Gravity Analysis	147
4.4.	Avionics	151
4.4.1	Introduction	151
4.4.2	Navigation, Guidance, and Control-Unmanned Mission	153
4.4.3	Communications	155
4.5.	Structures	156
4.5.1	Introduction	156
4.5.2	Design Margins and Load factors	156
4.5.3	Material Selection and tank end-cap geometries	157
4.5.4	Third Stage Masses and Dimensions	158
4.5.5	Dimensions and Masses of the Modules	161
4.6	Propulsion and Power	163
4.6.1	Introduction	163
4.6.2	Engine Design	164
4.6.3	Propellant Feed System	167
4.6.4	Propellant Tank Requirements	171

4.6.5	Injection System	172
4.6.6	Ignition System	173
4.6.7	Thrust Vector Control	174
4.6.8	Power	175
5.0	**Conclusion**	
5.1	Introduction	176
5.2	Overall Mass and Center of Gravity	176
5.3	Cost Estimation	180
5.3.1	Research & Development	180
5.3.2	Ground Operation Costs	180
5.3.3	Expendable Parts	180
5.3.4	Spacecraft Costs	182
5.3.5	Total Program Costs	182
5.4	Final Conclusions	183

Appendices

A.2.2.1	Details of the program used to calculate the trajectories
A.2.4.2.1	Reentry Trajectory Selection and Analysis
A.3.2.1	Component Level Mass Breakdown
A.3.3.2.3	Contaminant Standards
A.3.3.2.4	Acceleration Guidelines
A.3.3.2.11	Radiation
A.3.3.4.2.3	Carbon Dioxide Removal and Scrubbers
A.3.3.4.3	Thermal Control System Refrigerant
A.3.3.5	Mass vs Escape Option
A.3.3.7.4	Airlock Trade Study
A.3.3.7.5	RMS Trade Study
A.3.4.0.1	Mission sub-functions
A.3.4.0.2	Function Performance Levels
3.4.1.4.1.1	Sensor Data Rates
A.3.4.2.2	GPS/INS Comparison
A.3.4.3.2	General Information on TDRSS and STDN
A.3.4.3.3	Power vs. Data Rate
A.3.4.3.4.1	Power vs. Data Rate
A.3.4.3.5.2	Earth Coverage Beamwidth
A.3.4.3.7	Link Budgets
A.3.5.1	Mass Estimating Relations from NASA CR 2420
A.3.5.3.1	Wing Size Selection Spreadsheet
A.3.6.3.2	Mass and Cost Analysis on Various Power Sources
A.4.5.4	Third Stage Mass Spreadsheet
A.4.5.5	Module Mass Spreadsheet
A.4.6.2.1	Mass Analysis of the Combustion Chamber and Nozzle

A.4.6.2.3.a Equations Used for Combustion Chamber and Nozzle Design
A.4.6.2.3.b Specifications of Modular Engine and Top-Stage Engine
A.4.6.3.1 Turbopump Cycles
A.4.6.3.3 Turbopump Analysis
A.5.2 Center of Gravity Analysis Spreadsheet
A.5.3.1 Cost Estimating Relations
A.5.3.4 Raw Component Level Costs

1.0 Introduction

1.1 Motivation

In recent years, Congress and the American people have begun to seriously question the role and importance of future space exploration. This is mainly due to two factors: a decline in technical competition caused by the collapse of communism, and the high costs associated with the Space Shuttle transportation system. With these factors in mind, the main goal of the class was to design a vehicle capable of transporting payload and crew into space at a low cost. The system's cost per manned mission was to be less than $100M (all dollar values FY94), and the cost of transporting payload to orbit was to be reduced to $1000/kg bulk cargo. It was to be based on current technology with a technology cut-off date of January 1, 1994. The system was expected to be fully operational by the year 2000 with safe crew abort modes in all flight regimes, and a mission reliability of 99%. The preliminary design and analysis of the system was performed by a team of eighteen students during the Spring 1994 semester.

1.2 Mission Objectives

1.2.1 Reference Missions

The class was given three reference missions that the vehicle was expected to perform. They were as follows:

Mission #1: Transport four astronauts and a 5000 kg logistics module to the Space Station in order to resupply it. Return to Earth with the same crew size and payload. The crew on the return mission was not permitted to participate in flight operations.

Mission #2: Perform the Hubble Space Telescope servicing mission from STS-61.

Mission #3: Transport a 2000 kg communications satellite, along with necessary kick stage, for insertion into geosynchronous transfer orbit.

1.2.2 Mission Model

The ORION system was expected to perform the reference missions outlined in section 1.2.1 according to the following mission model:

Time Interval	Space Station Resupply	HST Servicing Mission	Satellite Transport to GEO	Total Missions per year
2000-2004	4/year	2/year	5/year	11
2005-2009	6/year	3/year	6/year	15
2010-2014	8/year	4/year	8/year	20
2015-2019	10/year	3/year	10/year	23
2020-2024	4/year	1/year	4/year	9

Table 1.2.2.a Baseline Mission Model

Three developmental flights, occuring in the year 1999, were added to the mission model to test the ORION system before the actual program began in the year 2000. The mission model was split into manned and unmanned phases. The first two reference missions were grouped into the manned phase and the third reference into the unmanned phase. This was done because the third mission was not required to be manned.

Time Interval	Total manned missions per year	Total unmanned missions per year
2000-2004	6	5
2005-2009	9	6
2010-2014	12	8
2015-2019	13	10
2020-2024	5	4

Table 1.2.2.b Manned and Unmanned Missions per Year

1.3 Design History

The configuration of the launch vehicle was chosen after extensive trade studies of different cases. These included different fuel systems, conventional staging vs. modular staging, and re-usable vs. expendable. The factor which complicated this study was that the mission model placed significantly different ΔV requirements on the launch vehicle. And since the goal was affordable human access to space, customizing the launch vehicle for different missions to reduce cost was the principle driving the design.

The first study done was to determine the optimal number of stages for the launch vehicle. Using the Lagrange multiplier method it was determined that

a three stage vehicle would best suit the mission model. All subsequent studies were based on a three stage vehicle.

1.3.1 Launch Vehicle Fuel System Studies

Four fuel systems were considered in this study.
1) LOX/LH2
2) LOX/RP1
3) HYBRIDS
4) N204-A50

The result was summarized in the following graph:

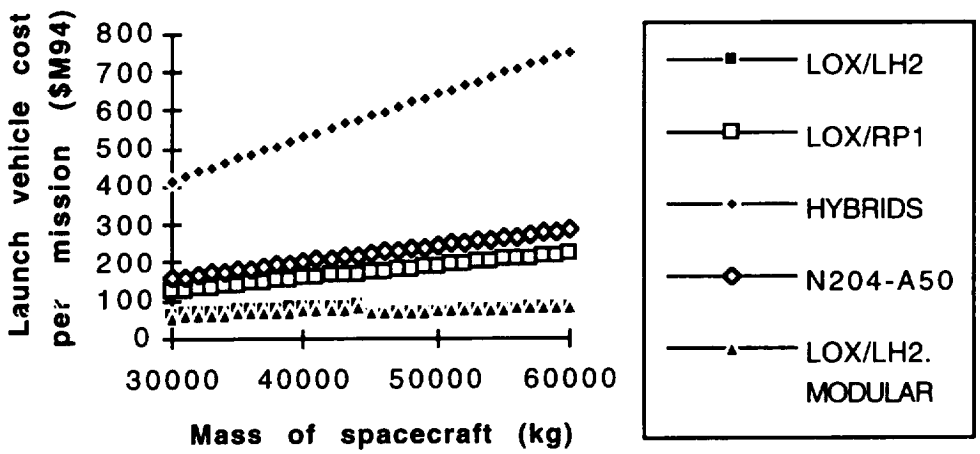

Figure 1.3.1.a Fuel System Comparison

In this graph, the inert masses of the launch vehicle using different fuel systems were calculated and then the non-recurring and recurring costs for the first unit were calculated via empirical formulae relating cost to mass. Total production cost was obtained by applying learning effect to the first unit recurring cost. Finally, summing the production cost and non-recurring cost and dividing that by the number of missions obtained the launch vehicle cost per mission. From this analysis, one could conclude that the launch vehicle had the lowest cost per mission for the entire range of payload under study by using LOX/LH2 as fuel system.

1.3.2 Conventional Staging Vs. Modular Staging

After LOX/LH2 was chosen for the fuel system, a study was done to evaluate the cost differences between a conventionally staged vehicle with ideal ΔV

distribution and a modular design using a number of 2nd stage modules as 1st stage. The result of this study was presented in the following graph:

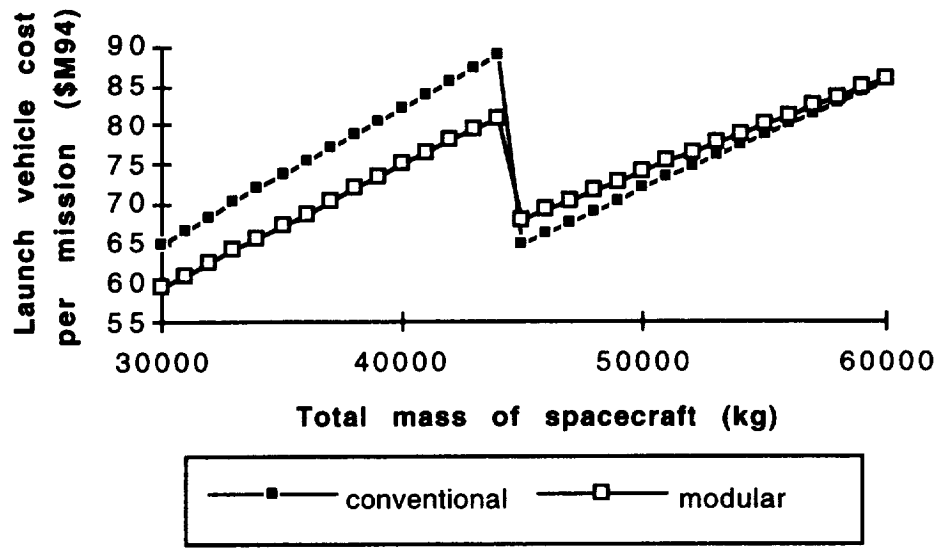

Figure 1.3.2.a Study of Conventional Versus Modular Staging

The discontinuity in the graph was due to the fact that if the mass of the spacecraft was below about 45000kg, the top stage could be taken off for the unmanned mission and if the mass of the spacecraft was above 45000kg, the 1st stage could be taken off for the unmanned mission.

One key note about this analysis was that the modular design was obtained by simply using three 2nd stage modules for the 1st stage. This design was yet optimized for the mission model and outperformed the requirements for all missions. It was determined that the optimized modular design would cost less for the entire range of payload under study, and therefore the modular design was chosen for further development.

1.3.3 Learning Curve Analysis

After the modular design with LOX/LH2 as fuel system was chosen, what needed to be determined next was how many modules would be employed for the launch vehicle. For example, a fully modular design would probably have one module for the 3rd stage, 4 for the second stage, and 7 for the 1st stage. Or a semi-modular design might have a different 3rd stage, two modules for the 2nd stage and 5 modules for the 1st stage. This question was answered by performing a learning curve analysis to relate cost per module to

the total number of modules needed for the entire mission model. The result was as follows.

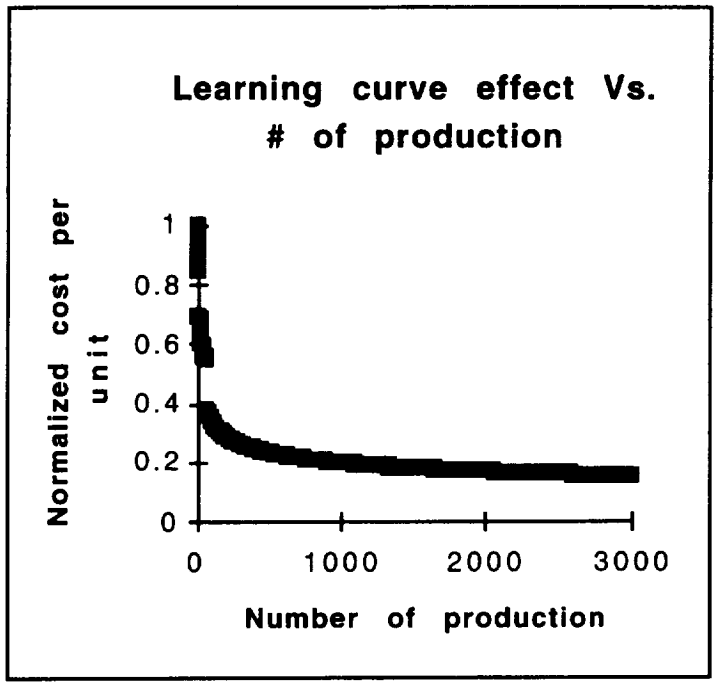

Figure 1.3.3.a Learning Curve Effect on Production Costs

From this analysis, one could conclude that the savings due to the learning curve effect leveled off for productions of more than about 1000 units. Based on the mission model, if one module was used for the 2nd stage and between 2 to 4 modules were used for the 1st stage, the total number of modules that would be produced ranged from 840 to 1290. Note that these values fell into the region where learning curve had the greatest effect. Increasing the number of modules for the 2nd stage added undesired complexity without much improvement in savings due to learning curve effect. Therefore, the decision was made to use one module for the 2nd stage and 2 to 4 modules for the 1st stage.

1.3.4 Optimum Modular Configuration

The mass of the spacecraft was frozen at 51000kg with a 20% margin. With this information, the modular launch vehicle could be optimized for the specific mission model. The result was as follows:

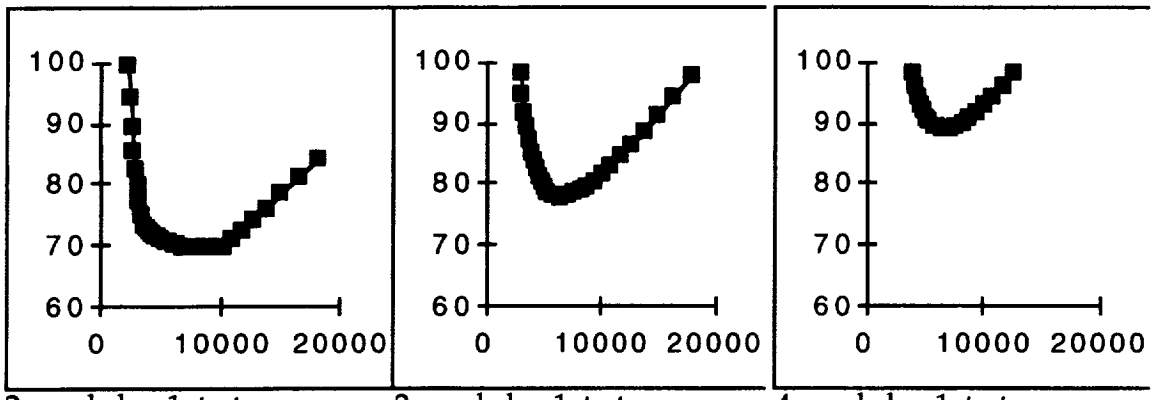

2 modules 1st stage 3 modules 1st stage 4 modules 1st stage
X-axes: Top stage inert mass (kg)
Y-axes: Launch vehicle cost per mission ($M94)

Figure 1.3.4.a Optimum Modular Configuration for the Launch Vehicle

From this analysis, it was concluded that the optimum modular launch vehicle would have 2 modules for the 1st stage with the following properties:

	Inert Mass (kg)	Propellant Mass (kg)
Top Stage	8,860	50,200
Modules	38,560	218,480

Table 1.3.4.a Modular Launch Vehicle Properties

1.3.5 Re-usable Vs. Expendable

The analysis used in this section was valid for the specific mission model (table 1.2.2.a) and the specific configuration. In this analysis, the difference in cost, instead of the actual cost, between the re-usable vehicle and the expendable vehicle was studied and the result showed that the expendable launch vehicle would cost less for the mission model. Note: all cost were in $M94.

Cost Category	Re-usable ($M94)	Expendable ($M94)
Total N/R & R/C	19,100	27,150
Additional Avionics N/R	45	0
Refurbishment	6460	0
Recovery	260	0
Additional Maintenance	2,600	0
Total	**28,465**	**27,150**

Table 1.3.5.a Cost Comparison of Re-usable and Expendable Launch Systems

Total re-usable - expendable = -1315 ($M94)
Note: ground equipment and cost discounting were not included in the above analysis; however, both factors would make the expendable vehicle more favorable.

Assumptions made during the analysis:
1) Structural mass ratio increased 40% for re-usable vehicle.
2) Average cost per kg increased 20% for re-usable vehicle.
3) First unit avionics recurring cost increased $M7 for the re-usable vehicle.
4) Approximately 10% of the modules which optimally be recovered would be lost or damaged.
5) Refurbishment cost was about 10% of the average production cost of modules.
6) A crew of 100 would be needed for recovery.
7) A crew of 1000 would be needed for additional maintenance and ground operations associated with the re-usable vehicle.
Sensitivity tests on the assumed parameters were performed to validate the final result.

1.3.6 Conclusions

Based on the trade studies, the configuration for the launch vehicle was chosen. The launch vehicle would exhibit the following properties:
1) Expendable
2) Three stages
3) Semi-modular design where only the 2nd and 1st stages used the same modules.
4) 1 module for the 2nd stage and 2 modules for the 1st stage
5) Mass properties:

	Inert Mass (kg)	Propellant Mass (kg)
3rd Stage	8,860	50,200
Modules	38,560	218,480

Table 1.3.6.a Launch Vehicle Mass Properties

1.4 ORION System Overview

1.4.1 Introduction

ORION was a multipurpose launch system that would be able to achieve a high mission success rate while providing a low cost launch option over the entire mission lifetime of the program. ORION incorporated modular staging for both the manned and unmanned missions. This section will illustrate ORION in its different configurations.

1.4.2 Vehicle Components

The components of the system are a primary launch module, an upper stage, and a manned spacecraft capable of dynamic reentry. The ORION spacecraft was designed to support a crew of six astronauts for up to fifteen days in low earth orbit (LEO.) The spacecraft was a delta winged vehicle capable of gliding to a horizontal landing on a runway. Its primary landing site was Kennedy Space Center. It was 21 m in length with a height of 4.1 m and a wingspan of

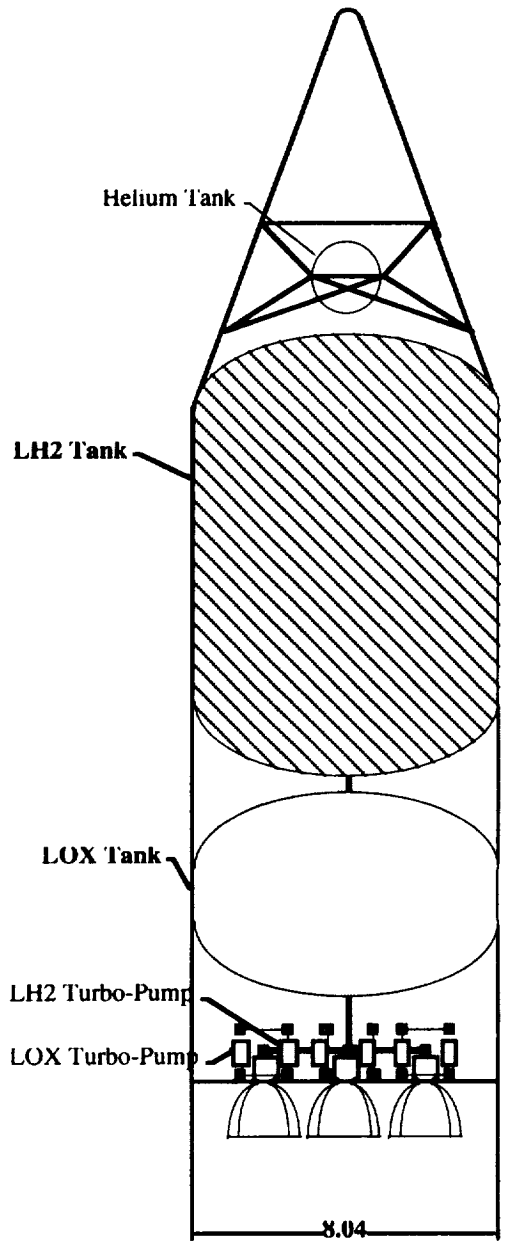

Figure 1.4.2.b Launch Vehicle Module

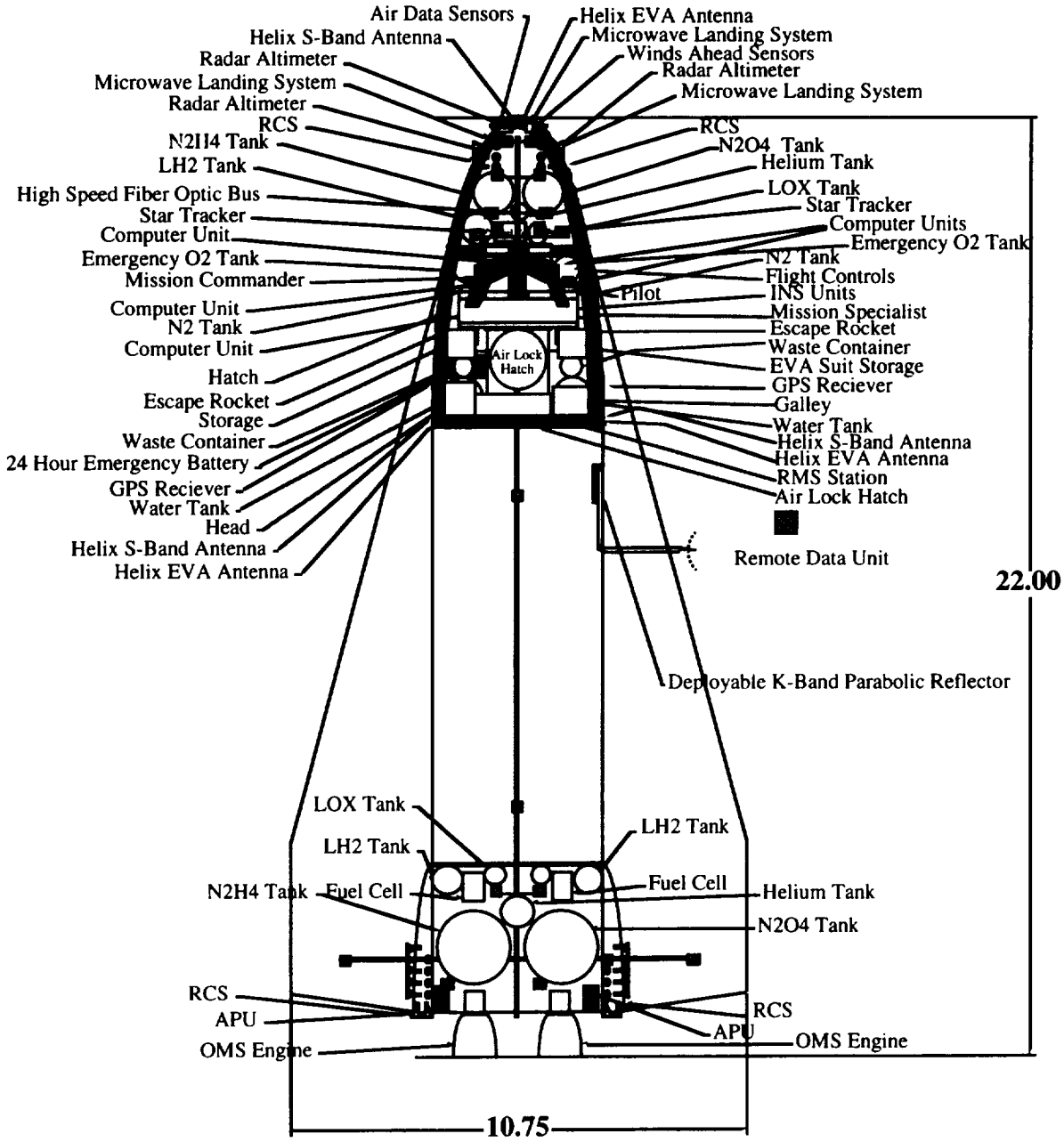

ORION Spacecraft

Figure 1.4.2.a ORION Spacecraft

10.75 m. Primary control surfaces for landing were located on the winglets of the wings. It was equipped with three sets of landing gear arranged in a tricycle configuration.

The primary modules used a liquid oxygen (LOX) liquid hydrogen (LH_2) propellant system with three engines. The modules were 22.4 m in length with a diameter of 8.0 m. They had a wet mass of approximately 28,000 kg. The upper stages also used a LOX/LH2 system with only one engine. The upper stages were 19.5 m in length with a diameter of 4.4 m. They had a wet mass of approximately 8700 kg.

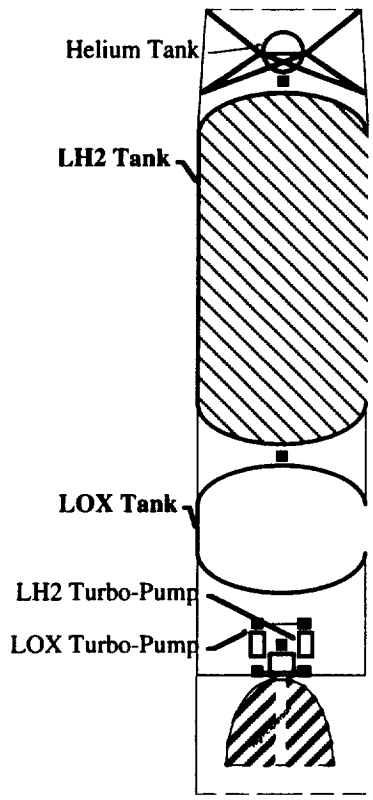

Figure 1.4.2.c Launch Vehicle Upper Stage

1.4.3 Vehicle Configurations

There were two configurations of the ORION system. The first configuration was a manned system designed to perform reference missions 1 and 2. The three stage launch vehicle used two primary modules as its first stage (stage 1m), one primary module as its second stage (stage 2m), and one upper stage as its third stage (stage 3m). The first stage was not used as a booster stage, but was fired independently of the other stages. The second stage was not ignited until after the burnout and separation of the first stage modules. The spacecraft sat on top of the stack and was attached to stage 3m. The launch

vehicle was capable of boosting approximately 50,000 kg of payload into low earth orbit in this configuration.

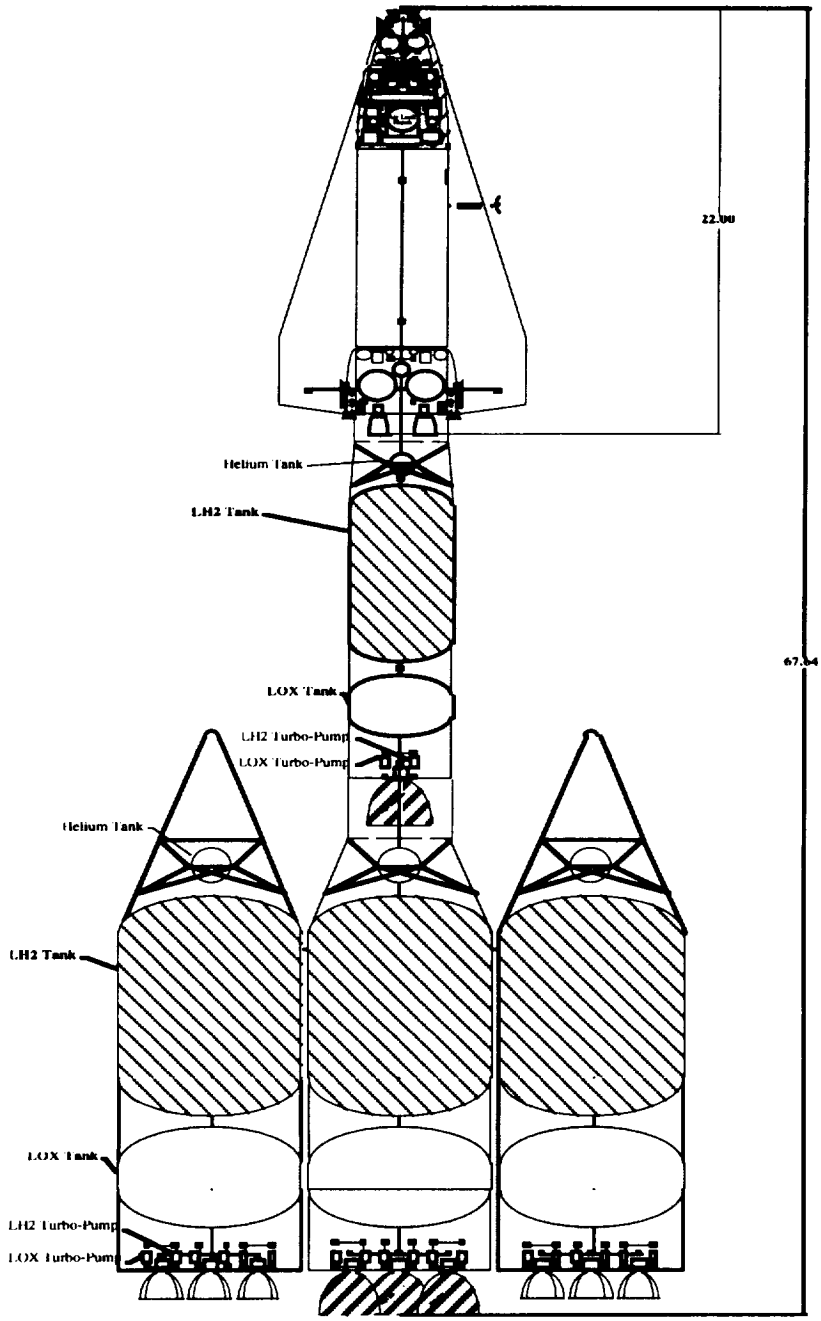

Figure 1.4.3.a ORION Manned Configuration

The second configuration was an unmanned two stage vehicle designed to perform reference mission 3. The launch vehicle was a two stage system. The first stage (stage 1u) used one primary module and the second stage (stage 2u) used one upper stage. The spacecraft was not used since the mission was not required to be manned. In its place, mounted on stage 2u, was a payload

shroud designed to protect the satellite during launch. The launch vehicle was capable of taking approximately 7,800 kg of payload to GEO in this configuration.

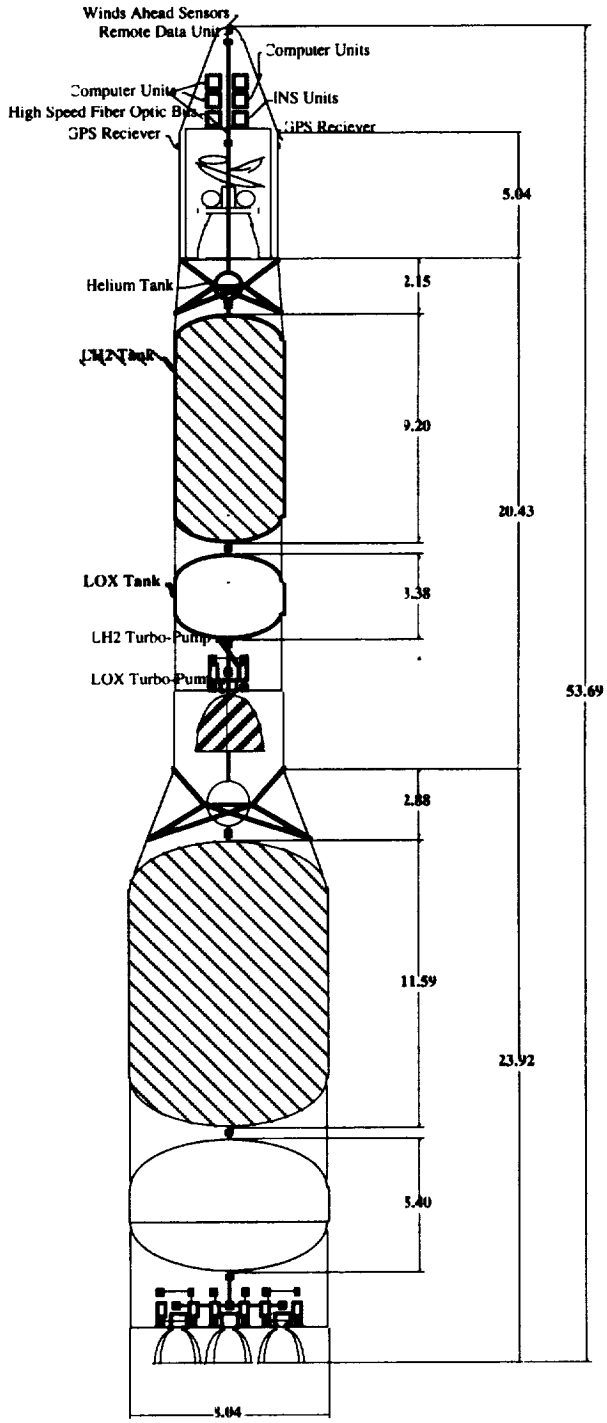

Figure 1.4.3.b ORION Unmanned Configuration

1.4.4 Heavy Lift Capability

The modularity of the ORION launch vehicle was successful not only in reducing cost but also in customizing the vehicle for a specific mission. It would be able to accomplish missions far more demanding than the reference missions by using additional modules. With two more modules as an additional stage, the four stage launch vehicle would be able to place the spacecraft into geosynchronous orbit. This ability would be valuable for possible geosynchronous satellite service missions. The same configured vehicle would be able to deliver 51000kg bulk cargo into GEO, and 84000kg to the space station. With a more ambitious configuration (four more modules as an additional stage), the launch vehicle would be able to place the spacecraft with over 30000kg payload into a hyperbolic orbit. The same configuration would deliver 80000kg into GEO, and 117000kg into LEO. This configuration far surpassed the capability of all pre-existing launch systems.

Configuration One: two modules as an additional stage			
Desired Orbit	**ΔV Required (m/s)**	**Max Payload (kg)**	**Possible Applications**
Space Station	9500	84,000	Deliver large payload and crew
GEO	10,600	57,000	GEO satellite service
Hyperbolic	11,200	46,300	Interplanetary mission

Table 1.4.4.a Heavy Lift Capability in Configuration One

Configuration Two: four modules as an additional stage			
Desired Orbit	**ΔV Required (m/s)**	**Max Payload (kg)**	**Possible Applications**
Space Station	9500	117,000	Deliver entire modules
GEO	10,600	80,000	GEO satellite replacement
Hyperbolic	11,200	65,700	Interplanetary mission

Table 1.4.4.b Heavy Lift Capability in Configuration Two

2.0 Mission Analysis

2.1 Introduction

The launch trajectories, orbital and rendezvous maneuvers, and the reentry trajectory were all designed to fulfill the mission requirements given in section 1.2. Both the unmanned and manned configurations used Kennedy Space Center as their launch site. The spacecraft used the runway at Kennedy Space Center as its primary landing site. The Space Station Freedom missions were assumed to have a seven day duration, and the Hubble Satellite Servicing missions were assumed to have a twelve day duration.

2.2 Launch Trajectory Analysis

2.2.0 Symbols used in Section 2.2

$X =$ Downrange of vehicle

$t =$ Time

$V =$ Velocity

$\gamma =$ Flight Path Angle

$T =$ Thrust

$\psi =$ Thrust Angle with respect to the horizontal

$C_D =$ Drag coefficient

$m =$ Instantaneous mass

$m =$ Payload mass (Section 1.3.4)

$\rho =$ Density

$A =$ Maximum Vehicle cross sectional area at time t

$R_e =$ Radius of the Earth

2.2.1 Purpose

The launch trajectory analysis was used as a tool to verify the launch systems capability to deliver the payload into the desired orbits. The three orbits that the launch system was designed to support are detailed below.

Mission	Altitude	Inclination	Circular Velocity
International Space Station	500 km	52°	7612 m/s
Hubble Space Telescope	520 km	28.5°	7601 m/s
Geosynchronous Satellite Deployment	36000 km	0°	3067 m/s

Table 2.2.1.a Orbit Summary

Besides satisfying these constraints the launch system also had to comply with additional requirements. The Structural requirements stated that the dynamic pressure during the flight may not exceed 80000 Pa. The Human Factors requirement was that the vehicle's acceleration may not exceed 4 g's. With these requirements acceptable trajectories were characterized as having the following qualities:

- Achieving given altitudes and inclinations.
- Near zero flight path angle at the desired orbit.
- Sufficient velocity the maintain a circular orbit over the mission duration.
- Maintain all Structures and Human Factors requirements.

Once an acceptable trajectory was found the ΔV lost due to drag and due gravity were determined. With the information regarding the drag losses and the gravity losses the trajectories were tuned to minimize these losses. Details of the program that was used to calculate the results seen in this section can be seen in Appendix A.2.2.1.

2.2.2 Vehicle Model

The Vehicle model is shown below.

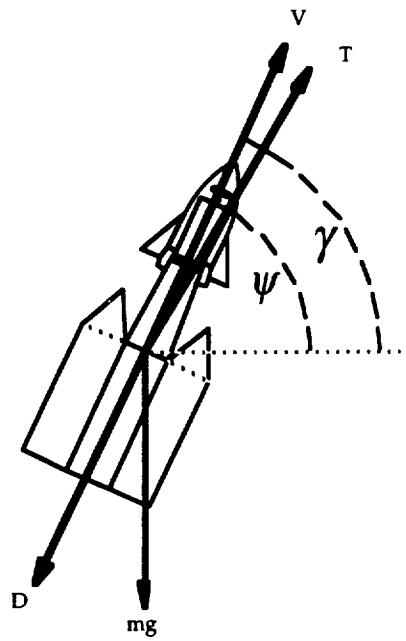

$$\frac{dX}{dt} = V\cos\gamma$$

$$\frac{dH}{dt} = V\sin\gamma$$

$$\frac{dV}{dt} = \frac{T}{m}\cos(\psi-\gamma) - \frac{C_D}{2m}\rho V^2 A - \left(g - \frac{\dot{X}^2}{R_e - H}\right)\sin\gamma$$

$$V\frac{d\gamma}{dt} = \frac{T}{m}\sin(\psi-\gamma) - \left(g - \frac{\dot{X}^2}{R_e - H}\right)\cos\gamma$$

Figure 2.2.2.a Free Body diagram of the vehicle and equations of motion*

*Note: The vehicle pictured does not represent the actual dimensions of the vehicle. Further the vehicle is shown rotating about the yaw axis despite the fact that all rotations mentioned in this section are pitch rotations.

The equations above are composite equations constructed from models listed in two different texts (Sutton, pp. 128, and Weisel, pp. 208). Both sets of equations were good but they did not contain all of the information that needed to be modeled so a composite set was formulated and rederived to confirm the composite sets validity. From the above equations several things become apparent. First, the model does not have a lift term in the flight path angle equation. Second, the altitude and the downrange equations are centered at the vehicle reference frame, which negates the need for a change of reference frames. Third, the gravity term includes a spherical earth so that gravity turn trajectories could be investigated, but neglects the change of gravity with altitude. And finally, the model neglected roll and yaw changes in the flight path. All of these assumptions and conditions will be discussed in the following sections.

2.2.2.1 Lift and Drag

The lift was modeled out of the vehicle because the structures group discouraged the idea of the vehicle flying at some angle of attack. To model out the lift means that the vehicle cannot be allowed to make any rapid changes in the flight path angle inside of the sensible atmosphere, and these

requirements influenced the choice for the pitch program equation, which will be discussed in a later section.

The drag seen on the vehicle during the flight was idealized as a modified V2 rocket. The drag coefficient versus Mach number for the V2 was available so it was used. The equations for the drag coefficient versus Mach number can be seen below.

$$C_D = 0.11(1 + e^{-(1-M)^2}) \text{ for } M < 1$$

$$C_D = 0.11(1 + e^{-(3-M)^2}) \text{ for } M > 1$$

Without a vehicle model to test in a wind tunnel, it was impossible to know how applicable these equations would be to the vehicle. However, Dr. Mark Lewis, an aerospace engineering professor at the University of Maryland at College Park, provided the equations and verified their usefulness.

2.2.2.2 Altitude and Downrange

The altitude and downrange equations are fixed to the vehicle and referenced to the surface of the earth. This means that the earth is not properly treated as a rotating body and the vehicle does not need to change to a space based reference frame during the flight. The rotation of the earth was neglected because the simulation was designed to verify capability. The earth's rotation aids in getting the vehicle into orbit, provided that the vehicle is launched to benefit from this rotation. Launches from KSC benefit from these rotations, so if the rotating earth was modeled it would only enhance the vehicles capability.

2.2.2.3 Gravity Turns and Pitch Functions

Two major categories of trajectories were investigated, gravity turns and a trajectory that involved choosing a pitch function that the vehicle would be forced to follow.

To use a gravity turn, the thrust vector of the vehicle must be deflected from the velocity vector momentarily to initiate a slow torque free rotation of the velocity vector, so that eventually at some altitude the vehicle would have zero flight path angle. However, iterating to find an acceptable gravity turn trajectory is long and tedious. Further, since gravity turns are an open loop, error-ridden, and inefficient way to get into orbit, the approach was dropped in favor of a more elegant solution.

The pitch function is the more elegant solution. The function that would dictate the path of the vehicle during its ascent phase had to be carefully

chosen to reflect both the previously mentioned requirements, and to be easily modified to accommodate different destinations. With these considerations in mind an exponential decay function was chosen, as shown below,

$$\gamma_o = \gamma e^{\frac{-t}{At_b}}$$

where t is the time since the beginning of the flight, t_b is the maximum unthrottled burn time of the rocket, and A is some constant that was determined from the boundary conditions of the trajectory. Using boundary conditions that specified the initial flight path angle (90°) and the final flight path angle (0°), the constant A was found to have a value of 0.177. This value for A was used for only one of the trajectories. The value of A was modified to maximize the vehicle's performance for each of the other two missions.

Mission	A
International Space Station	0.185
Hubble Space Telescope	0.180
Geosynchronous Satellite Deployment	0.177

Table 2.2.2.a Values of A for the different missions

2.2.2.4 Yaw and Roll

Yaw and roll were not modeled due to the fact that all of the required course changes could be implemented in the pitch plane. Although some of these changes may require the vehicle to rotate, it was assumed that the vehicle could be forced to rotate without any difficulty.

2.2.3 Results

The missions all follow the same basic trajectory. It was found that the vehicle is best off "circularizing" at a lower orbit, (actually flying tangent to the lower orbit), with excess velocity equal to that of the first burn of a Hohmann transfer. For the manned missions the upper stage is reignited to provide the impulse required for the second burn of the Hohmann transfer at the desired orbit. After this maneuver the upper stage has approximately 4500 kg of fuel left. For the unmanned mission the apogee kick motor is used to provide the imulse needed. Below are the statistics for the three different orbits, including an illustration that defines the points used in the tables.

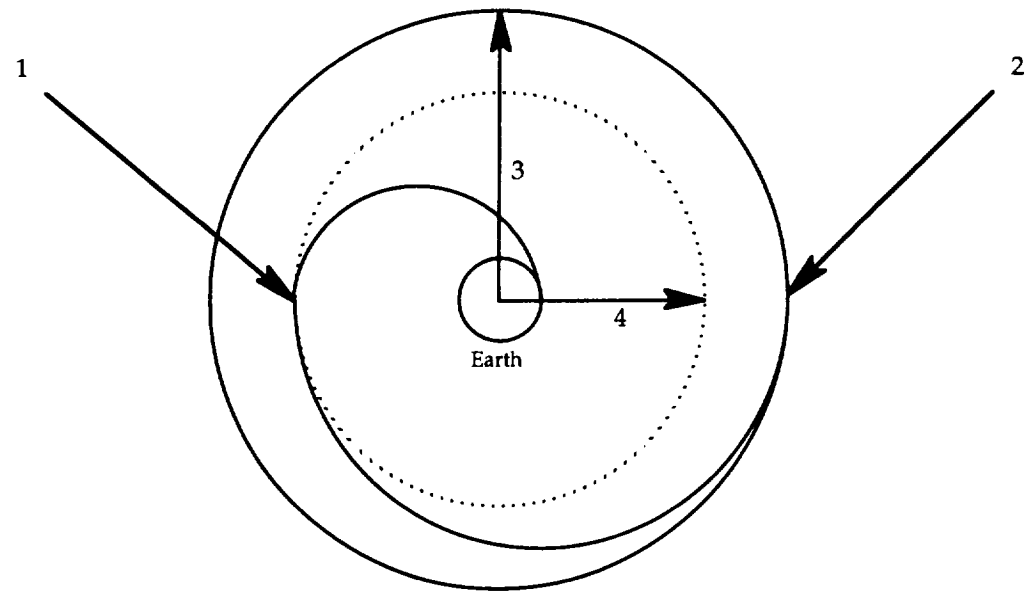

Figure 2.2.3.a Critical points along the trajectory. (Number three is the desired orbital altitude as seen in Table 2.2.3.a)

Mission	ΔV required to bring Flight path angle to zero at point 1	Altitude at burnout (point 4)
International Space Station	38 m/s (0.3°)	100 km
Hubble Space Telescope	165 m/s (2.35°)	143 km
Geosynchronous Satellite Deployment	90 m/s (1.21°)	150 km

Table 2.2..3.a Critical values along Flight Path

2.2.4 Drag and Gravity Loss Determination

To fully evaluate how the launch system performed during launch, the ΔV lost due to drag and gravity had to be determined.

The ΔV lost to drag is the energy that was expended along the flight path as the drag force retards the motion of the fuselage of the launch vehicle. This energy lost was set equal to the kinetic energy of the payload that would have resulted if this energy had been used to accelerate the payload, as shown below.

$$\frac{1}{2}m\Delta V^2 = \oint_{\text{Flight Path}} D(s)ds$$

To allow the simulation software to reconstruct the lost ΔV from the existing columns of data, the above equation was modified such that the integral term was approximated as a sum along the path. The modified equation is shown below.

$$\Delta V = \left(\frac{2\sum D_i \sqrt{(X_{i+1} - X_i)^2 + (H_{i+1} - H_i)^2}}{m} \right)^{\frac{1}{2}}$$

Each of the missions followed different paths through the atmosphere and their individual drag losses are listed below.

Mission	ΔV lost due to drag
International Space Station	827 m/s
Hubble Space Telescope	852 m/s
Geosynchronous Satellite mission	803 m/s

Table 2.2.4.a Mission Drag Losses

The ΔV lost due to gravity was reconstructed from the equations of motion. The portion of the equation that was used is shown below. This technique seemed to be valid because this portion of the velocity equation had already influenced the flight of the vehicle. To reconstruct this influence may involve some numerical error, but the general approach seems sound.

$$\Delta V = -\left(g - \frac{\dot{X}^2}{R_e + H} \right) \sin\gamma$$

Below are listed the ΔV losses encountered due to gravity for each mission. The interesting result is that the Space Station mission, as expected, has the most significant gravity loss for the manned missions. This is due to the fact that the inclination change was modeled into the gravity term, assuming that the centripetal acceleration would be reduced by the magnitude of the inclination change thus making the perceived gravity larger during the flight. Had a rotating earth been modeled the inclination change would have been modeled inside the rotating earth term, so the ΔV lost due to the inclination change is an just an approximation.

Mission	ΔV lost due to gravity
International Space Station	740 m/s
Hubble Space Telescope	497 m/s
Geosynchronous Satellite mission	908 m/s

Table 2.2.4.b Mission Gravity Losses

2.2.5 Conclusions

The vehicle has the capability to achieve the desired orbits within requirements with fuel to spare. The spare fuel for the geosynchronous mission is near zero but for the other missions namely the Hubble Space Telescope mission the spare fuel is about 4500 kg. This left over fuel makes the system more robust and enhances it's capability to respond to all of the disturbances that where not modeled within the simulation.

Mission	ΔV (km/s)	Altitude(km)
International Space Station	9.2	500
Hubble Space Telescope	8.9	520
Geosynchronous Satellite mission	10.6	36,000

Table 2.2.5.a Mission Characteristics

The following are plot of the accelerations and the dynamic pressures. Note that the geosynchronous launch vehicle sees the greatest accelerations and dynamic pressures during the launch. The maximum accelerations for the geosynchronous launch vehicle are about 9 g's, this violates the human factors requirements, but since it is an unmanned mission this requirement is irrelevant. The structure has been designed to withstand these accelerations.

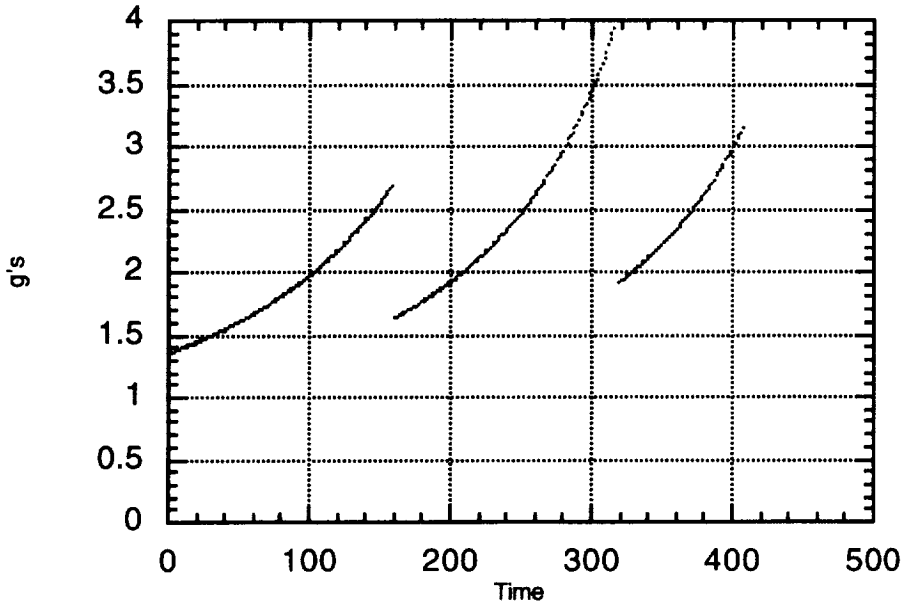

Figure 2.2.5.a Accelerations for the Space Station mission

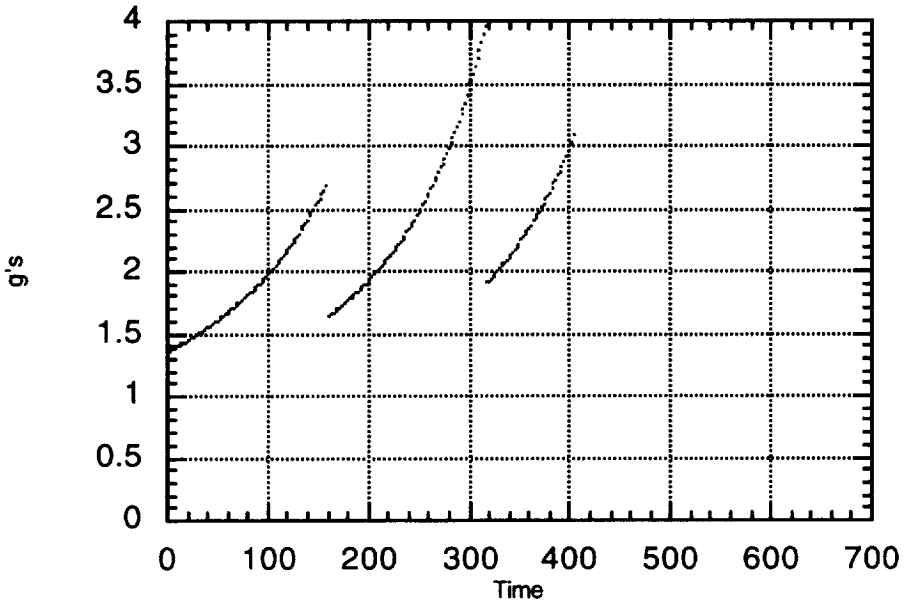

Figure 2.2.5.b Accelerations for the Hubble Space Telescope mission

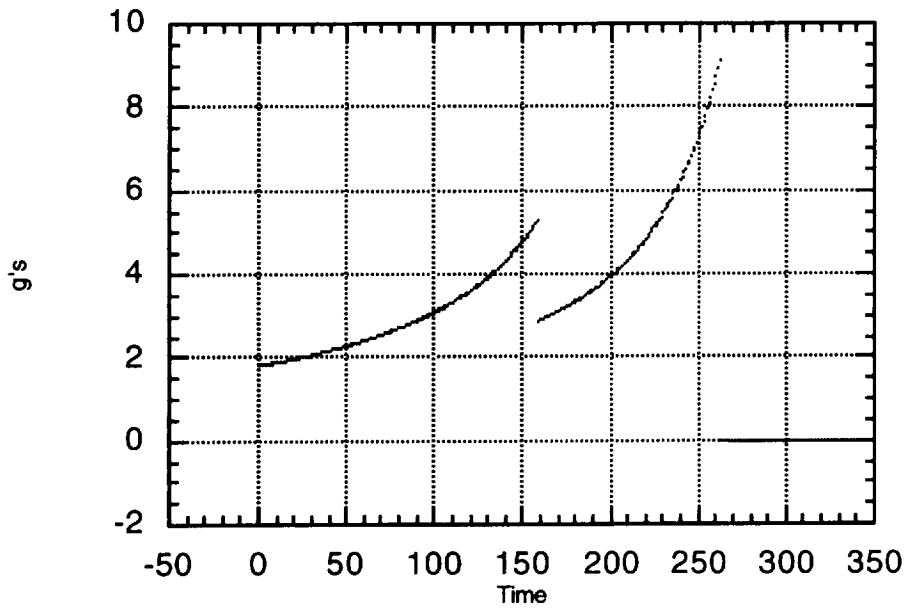

Figure 2.2.5.c Accelerations for the Geosynchronous Launch Vehicle

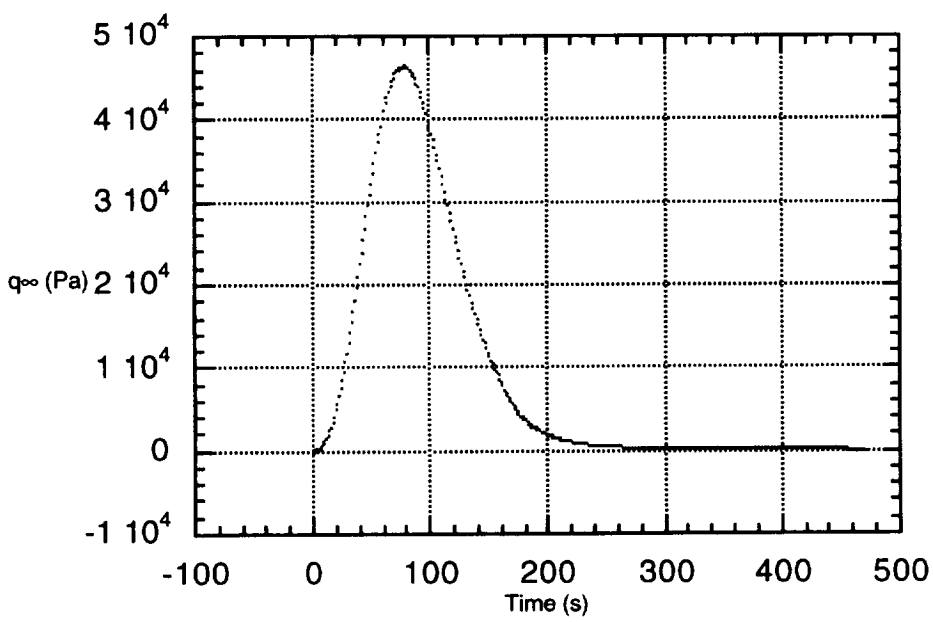

Figure 2.2.5.d Dynamic Pressures for the Space Station mission

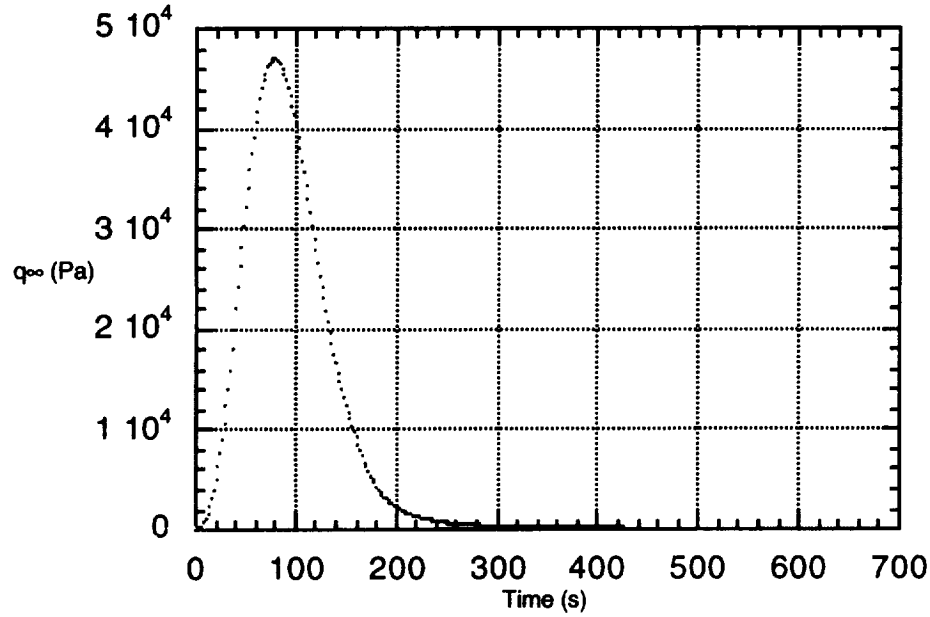

Figure 2.2.5.e Dynamic Pressures for the Hubble Space Telescope mission

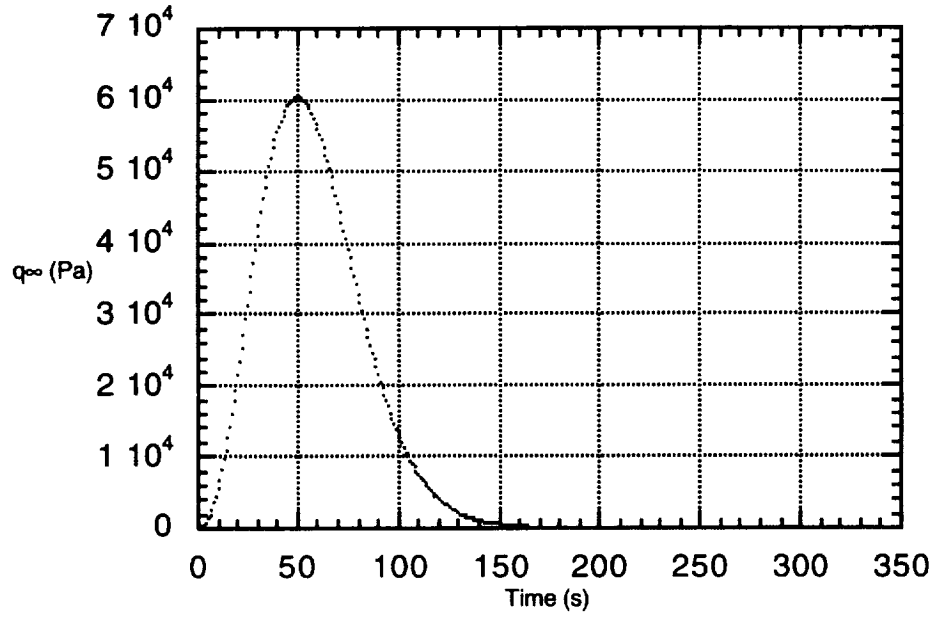

Figure 2.2.5.f Dynamic Pressures for the Geosynchronous Launch Vehicle

2.3 Orbital Analysis

2.3.1 Rendezvous Maneuver Sequence

The rendezvous sequence is initiated following insertion into the target orbit, which is determined by each specific mission. Refer to Table 2.2.1.a for descriptions of each target orbit. Rendezvous operations need not be considered for the third mission, deployment of a geosynchronous communications satellite. The rendezvous sequence ends with the first braking maneuver which places the spacecraft in a stationkeeping orbit approximately 120 meters from the target. This point in the approach is referred to as Proximity Operations (or PROX OPS) and involves a different set of procedures.

It is assumed that the target spacecraft will have receivers for the Global Positioning System (GPS) and that the spacecraft will be able to monitor their positions via groundlink communication. Before the rendezvous maneuver sequence is initiated, absolute GPS will be used to determine the orbit of the target spacecraft, and then relayed to the spacecraft.

Following the release of the last booster stage the spacecraft will be left in a coplanar orbit 18.5 km below the target. The star tracker will be used to follow the target at this range, prior to the first onboard targeted maneuver. This range was chosen to allow for flexibility in lighting conditions for achieving star tracker acquisition of the target.

When the spacecraft is 12.2 km behind and about 240 m above the target it will reach the transfer initiate (Ti) point. It occurs at about orbital noon, halfway through the daylight portion of the orbit. The standard maneuver at this point will raise the perigee of the spacecraft's orbit and place it on a intercept course with the target spacecraft. If no maneuvers are made, the spacecraft will move below and ahead of the target, with very little risk of collision. Alternately, a circularizing burn (called a Ti delay) would place the spacecraft in a stable standoff position relative to the target, allowing time for further analysis or observation. Starting at Ti, the star tracker is replaced with Relative GPS (RGPS) data, because the RGPS system can be used in darkness.

Midcourse corrective maneuvers will be performed as necessary to ensure a correct intercept trajectory. On-board computers will determine the maneuvers, and the data will be verified by ground computers. Depending on the magnitude of the errors, it may be necessary to recompute an intercept trajectory for the desired offset position of the target. The actual burn will be executed either automatically or manually. A crew member will perform the manual burns at the aft control station in the crew cabin, looking up through

the top window through a sextant-like device called a Crew Optical Alignment Sighter (COAS).

The end of the rendezvous maneuver sequence occurs with a series of burns called braking gates which match the velocity of the spacecraft and the target spacecraft at intercept. This part of the rendezvous must be performed in daylight. The braking gates establish a line-of-sight (LOS) velocity at a distance from the target using the RGPS information, and by keeping the target centered at LOS with the aid of the COAS. Onboard targeting software is used to compute burns for braking. Prior to the braking gates, the spacecraft is about 600 m from the target, below and slightly ahead of it. At the end of this sequence it has reduced the distance to about 300 m, still ahead and slightly below the target, with the payload bay oriented towards the target. At this point, the PROX OPS mode is initiated.

2.3.2 Proximity Operations

Proximity operations take the spacecraft from the final, stable position which follows rendezvous maneuvers to a desired position for payload deployment, remote manipulator system capture of a payload or docking/berthing. PROX OPS include transitions to specified offset position, station keeping, approaches, and after the mission is completed a separation of the spacecraft to a specified position. At this stage in the rendezvous, the effects of orbital mechanics are weaker and the influence of the spacecraft on the target are greater-rocket pulses (known as plume impingement) could disturb the target craft or its instruments, or radar pulses could disturb its electronics. PROX OPS will be performed to eliminate as much plume impingement as possible and still keep low RCS fuel usage. Maneuver targeting will be accomplished either by visual targeting or software assisted targeting. Visual targeting will require a crew member to maintain a target in a specified relative position, velocity and distance using COAS and a hand controller.

A transition will be used to move from a final stationkeeping position following the rendezvous maneuver sequence to a position where a final approach will be made. A transition will be made to the target's V-bar while maintaining a 300 m range to the target with the spacecraft's -Z axis (the axis that points out of the overhead window) pointed toward the target at all times.

The spacecraft begins transition below and ahead of the target at a range of 300 m. The +Z axis is pointed toward the center of the earth. The spacecraft is now in position to maneuver to +V-bar. Primary Reaction Control System (RCS) thrusters are used to translate. Vernier thrusters will be used when zero translation is required. Without translating the target should be centered in COAS using the hand controller. The tail of the spacecraft must be slowly pitched downward either manually or automatically while

translation occurs at the same time to keep the target centered on the COAS. RGPS is used to keep the 300 m range and zero relative velocity. This procedure moves the spacecraft to intercept the target's V-bar.

The V-bar approach begins by establishing an initial closing velocity toward the target of 300 m/s. This is in accordance with the "0.1% rule," which dictates, at close range, that the velocity must be less than or equal to 0.001 times the range to the target. A retrograde burn is used to initiate the closing rate, and causes the spacecraft to fall below the target, used in conjunction with the radial burns to position the spacecraft at V-bar. The final closing velocity is adjusted using small braking gates. During this maneuver, as the spacecraft closes in on the target, the RCS thrusters are limited in their use so as to prevent plume impingement within 150 m of the target. The range rate should be below 30 m/s at 60 m, going from a "0.1% rule" to a ".05% rule."

At less than 30 m, the RGPS is abandoned and all the maneuver operations are conducted manually using the overhead window, hand controller and cameras mounted in the payload bay and on the Remote Manipulator System (RMS). Once the spacecraft is within 10 m of the target, the RMS is used for either capture (in the case of the Hubble Space Telescope) or berthing (in the case of the space station resupply).

After deploying, retrieving, or service mission is complete, the spacecraft moves away from the space station or space telescope to a range of 300 m, where it initiates deorbit. This is achieved via a reverse V-bar. When the spacecraft has reached this safe distance it may move out of orbit and prepare for reentry.

2.4 Reentry

2.4.1 Introduction

In designing the spacecraft one of the major designing factors was reentry. The shape of the vehicle would determine its flight characteristics and loads on the vehicle during reentry. In this section the trajectory will be discussed.

2.4.2 Reentry Trajectory

2.4.2.1 Trajectory Selection

When choosing a reentry trajectory it is important that the loads on the vehicle not become adverse so that the vehicle or its contents may become damaged. the major considerations in the selection of the reentry trajectory are covered in Appendix A.2.4. The initial conditions of the selected trajectory are in table 2.4.2.a. From these initial conditions a simulation was

run to calculate the rest of the trajectory. See Appendix A.2.4 for the explanation of the reentry model.

Atmospheric Interface	150 km
Velocity	8000 m/s
Ballistic Coefficient	225 kg/m^2
L/D	1.43
Pitch Angle	-1.5°
Roll Angle	0°
Yaw Angle	0°

Table 2.4.2.a Initial Conditions of Reentry

The increase in altitude at approximately 400 seconds after start was due to an increase in lift. When the vehicle first enters the atmosphere the drag is very low due to the low density. Because there was very little drag the vehicle picked up velocity which helped it have a greater lift when the density increased.

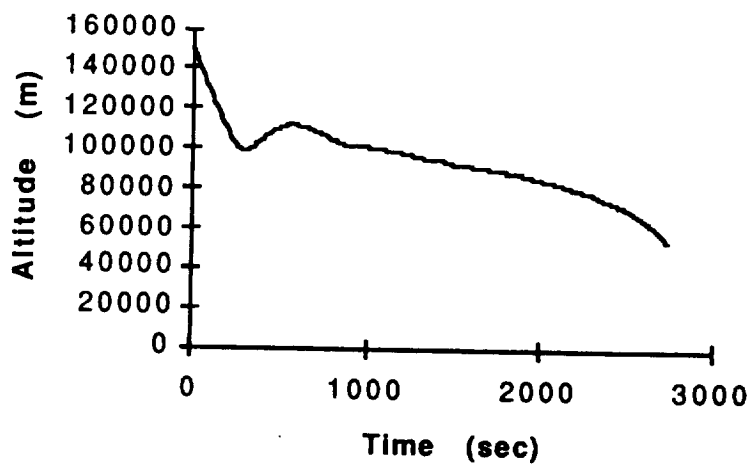

Figure 2.4.2.a Altitude vs. Time

This was corrected for in part by energy bleeding maneuvers but not entirely. When the vehicle reached about 100 km it initiated a turn upward. This was when the maximum heating and temperature occurred.

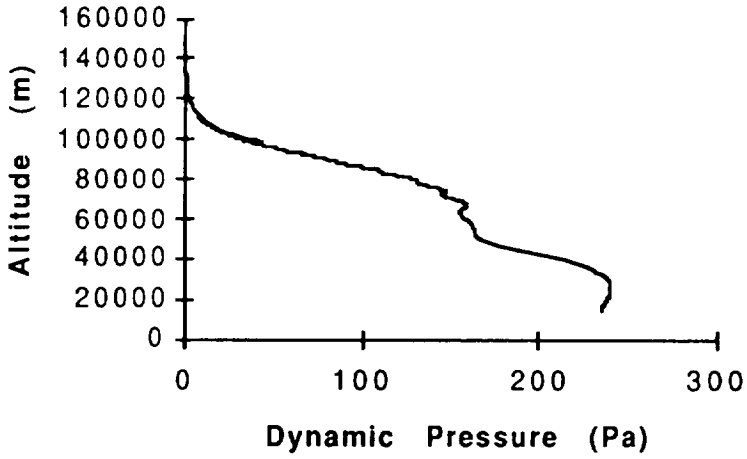

Figure 2.4.2.b Dynamic Pressure vs. Altitude

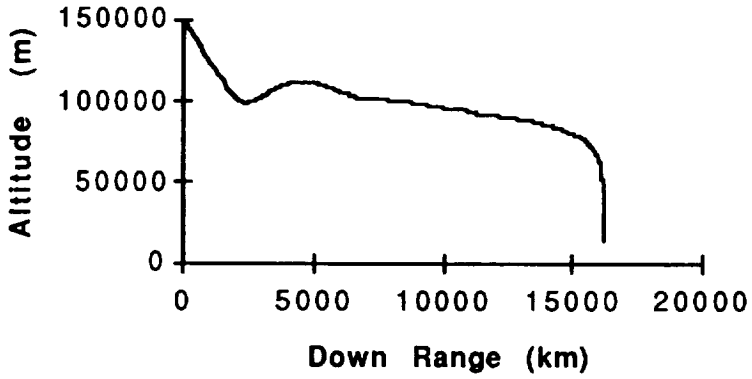

Figure 2.4.2.c Down Range vs. Altitude

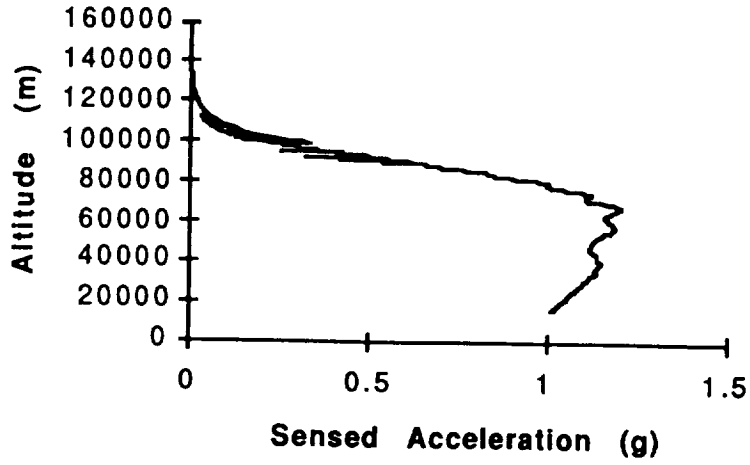

Figure 2.4.2.d G Forces vs. Altitude

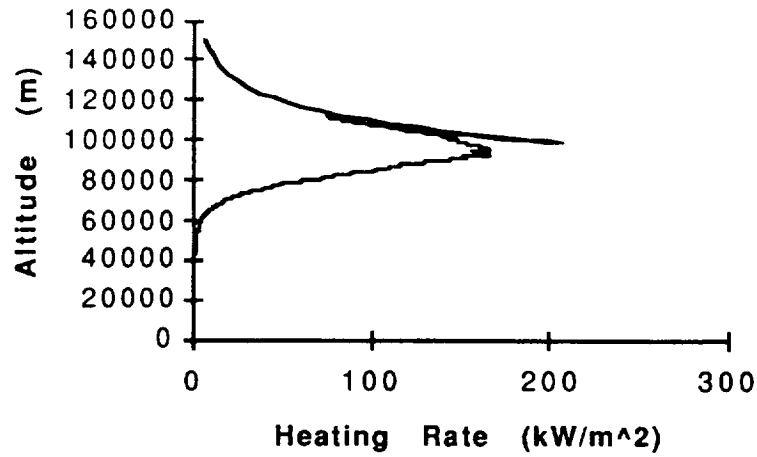

Figure 2.4.2..e :Heating Rate vs. Altitude

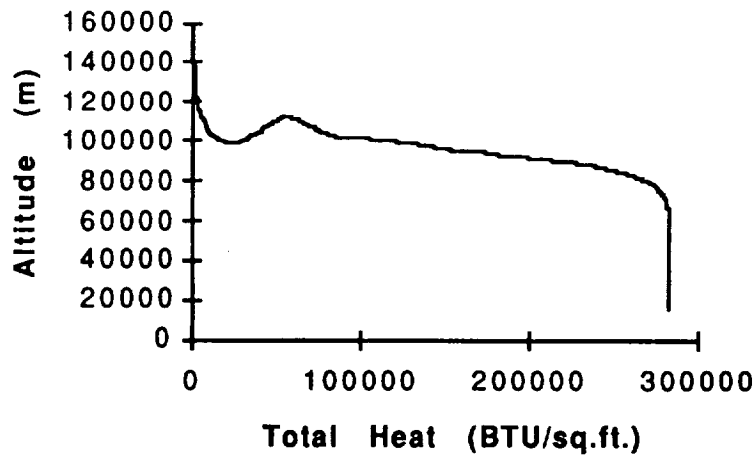

Figure 2.4.2.f Total Heating at Stagnation Point vs. Altitude

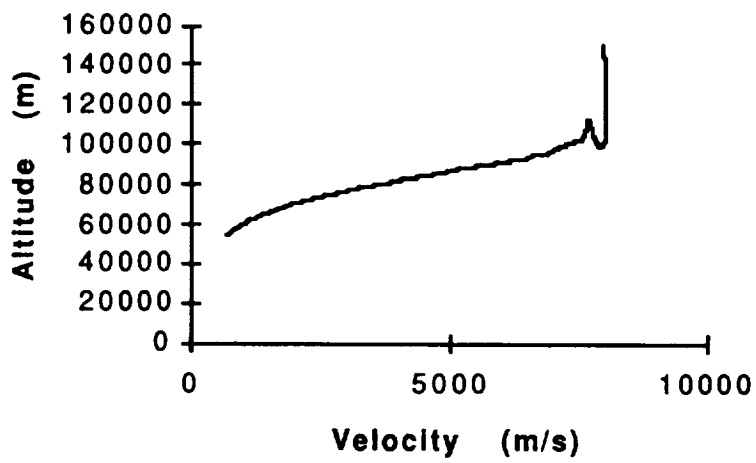

Figure 2.4.2.g Velocity vs. Altitude

The dynamic pressure curve as well as the sensed acceleration curve peaked at a lower altitude than the heating rate and temperature curves. This was due to the fact that pressure was density dependent, the drag was a function of the dynamic pressure, and the sensed acceleration was a function of the drag and the density.

2.4.2.2 Energy Bleeding Maneuvers

As the vehicle was coming down in the upper atmosphere it picked up velocity due to the low drag. As the density increased the vehicle started to climb. To compensate for this the vehicle needed to be rolled so that the energy could be used to go left or right instead of upward. This gave the benefit of reducing the total heat load by shortening the time of flight.

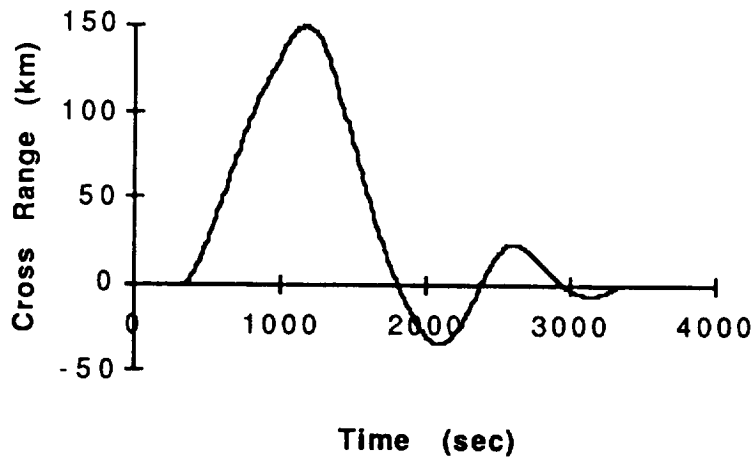

Figure 2.4.2.h Cross Range vs. Time

The goal of the s-turn was to bleed off energy without getting too far off course.

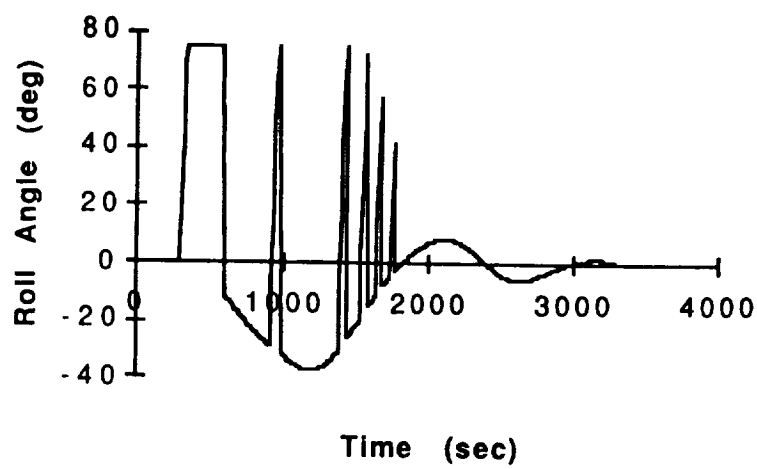

Figure 2.4.2.i Roll Angle vs. Time

The spikes in figure 2.4.2.i were due to the algorithm used to generate the roll angle. When the vehicle started to pull up the algorithm compensated by initiating a roll of $\phi_i = \phi_{i-1} + d\phi$, where $d\phi$ is 2° / second. This is the large flat topped segment peaking out at 75° roll angle. The max. roll angle was set at 75° because if it were higher it increased the sensed acceleration beyond the limit set by human factors. the oscillatory section of the roll angle plot was when the vehicle was going down and the only concern was to get the back toward zero cross range. This was done by incrementing the roll angle to be a function of the distance off the flight path or zero cross range.

2.5 Programmatics

2.5.1 Spacecraft Programmatics

The total number of spacecraft needed to complete the missions given in the mission model was determined by analyzing the turnaround time. The turnaround time was defined as the time needed to prepare the spacecraft for the next launch. The turnaround time was assumed to be four months at the beginning of the program. As the program progressed, the turnaround time was assumed to decrease by one quarter of a month (approximately one week) every two years. This decrease continued until the turnaround time reached two months in the year 2016. This analysis also assumed that the Hubble servicing mission had a two week duration and the Space Station resupply mission had a duration of one week. Three spacecraft were necessary to complete the mission model with this turnaround time.

The first spacecraft was built for the two manned developmental flights occurring in 1999. The second spacecraft, built in the year 2000, marked the beginning of the actual program. The manufacture of a third spacecraft was necessary in the year 2005 to complete the program. When they were retired in the year 2020, the first spacecraft had completed 74 missions and the second spacecraft had completed 72 missions At the end of the program in 2024 the third spacecraft had completed 81 missions. The total number of manned missions was 227.

Year	Turnaround Time (months)	Number of Spacecraft Needed
1999	4	1
2000 – 2001	4	2
2002 – 2003	3.75	2
2004	3.5	2
2005	3.5	3
2006 – 2007	3.25	3
2008 – 2009	3	3
2010 – 2011	2.75	3
2012 – 2013	2.5	3
2014	2.25	3
2015	2.25	3
2016 – 2017	2	3
2018 – 2019	2	3
2020 – 2024	2	1

Table 2.5.1.a Number of Spacecraft Needed

2.5.2 Launch Vehicle Programmatics

The launch vehicle was required to perform a total of 393 missions, including the three developmental flights in 1999. The 227 manned missions used three modules and one upper stage per mission. The 166 unmanned missions used one module and one upper stage per mission. The total number of modules needed was 847, and the total number of upper stages was 393.

Time Interval	Modules per Year	Upper Stages per Year	Total Modules for Interval	Total Upper Stages for Interval
1999	7	3	7	3
2000 – 2004	23	11	115	55
2005 – 2009	33	15	165	75
2010 – 2014	44	20	220	100
2015 – 2019	49	23	245	115
2020 – 2024	19	9	95	45
Total			**847**	**393**

Table 2.5.2.a Launch Vehicle Modules and Upper Stages

2.5.3 System Reliability

The target system reliability was 99%. The number of expected failures for the system was determined by the following equation:

$$P(f) = \sum_{m=0}^{n} \frac{n!}{(n-m)!m!} P^{(n-m)} (1-P)^{m} = 0.5$$

where n was the number of missions, m was the number of failures, and P was the reliability. When the aggregate chance of failure reached 0.5, the value of m at that time was the number of expected failures.

The value of n for the manned missions was 227 with a reliability of P=0.99. The number of expected failures was two. If the system reliability was as low as P=0.97, the number of expected failures increased to six.

Reliability (P)	Number of Failures
0.99	2
0.98	4
0.97	6

Table 2.5.3.a Manned Mission Reliability

The total number of unmanned missions was n=166. The unmanned mission reliability differed from the overall system reliability There were only two modules used in the unmanned missions, whereas the overall system was composed of four modules. The word module here referred to the modules as well as the upper stage of the vehicle. The reliability of the individual modules, P(module), was $P(\text{system})^{1/4}$. The reliability of the unmanned missions was $P(\text{module})^2$. With a system reliability of 0.99 the number of expected failures was zero for the 166 unmanned missions. If the reliability dropped to 0.97 the number of expected failures increased to two.

Reliability (P)	Number of Failures
0.995	0
0.990	1
0.985	2

Table 2.5.3.b Unmanned Mission Reliability

For the total 393 missions the system was expected to perform the total number of failures was two for the target reliability of 99%. This would require the manufacture of eight additional modules and possibly two additional spacecraft. The number of failures increased to eight when the

reliability dropped to 97%. This would require the manufacture of twenty eight additional modules and possibly as many as six additional spacecraft. The number of additional spacecraft needed depended on whether or not the spacecraft survived the failure.

Bibliography

Oberg, James E., "Rendezvous in Space," Air & Space. August/September 1993, pp. 44-52.

Price, Charles R., Telerobotic Activities at Johnson Space Center. NASA, Houston.

Schuck, Daryl, EVA Checklist STS-61 Flight Supplement. November 4, 1993. NASA, Houston.

Sedej, Dan and Clarke, Steve, Rendezvous/Proximity Operation Workbook. March 1, 1983. NASA, Houston.

3.0 Spacecraft

3.1 Spacecraft Configuration

3.1.1 Introduction

The ORION spacecraft was designed to transport a crew of six and up to 5000 kg of payload into low earth orbit and back. Specifically, it had to be capable of carrying out missions #1 and #2 of the ORION program.

Mission #1 was a space station crew transfer and re supply. The ORION spacecraft had to transport four space station replacement crew members and a 5000 kg logistics module to the space station and return a similar payload. As the returning crew members were not allowed to participate in flight operations, the ORION spacecraft was operated by an additional two crew members. Upon orbital insertion, the ORION spacecraft would rendezvous with the space station. Crew transfer would take place through a docking module attached to the airlock. The logistics module would be moved from the cargo bay by the spacecraft's RMS. The return crew and the used logistics module would be transferred to the spacecraft in a similar manner. The spacecraft would then separate from space station, de-orbit, and land.

Mission #2 was a repeat of STS 61, the Hubble Repair Mission. To carry this out, the spacecraft had to have extensive EVA facilities as well as a payload bay large enough for the Hubble repair equipment. Upon reaching orbit, the spacecraft would rendezvous under the control of the mission commander and the pilot. The other four crew members would be EVA trained. The pilot and mission commander, upon completion of the rendezvous, would grapple Hubble using the ORION spacecraft's RMS. Then, over a series of days, the EVA trained astronauts would participate in two-person EVA's to repair and service Hubble. Upon completion of the repairs, HST would be released, and the spacecraft would return to Earth.

The ORION spacecraft was located atop the launch vehicle stack which placed it into orbit. ORION was capable of orbital maneuvers, rendezvous, and de-orbit using its own Orbital Maneuvering System. It carried a Remote Manipulator System for grappling satellites. ORION had extensive airlock and EVA facilities for on orbit repair and servicing of spacecraft. Upon

completion of a mission, the spacecraft conducted a lifting body reentry and glided to a landing. Its primary landing site was Kennedy space center.

3.1.2 Spacecraft Layout

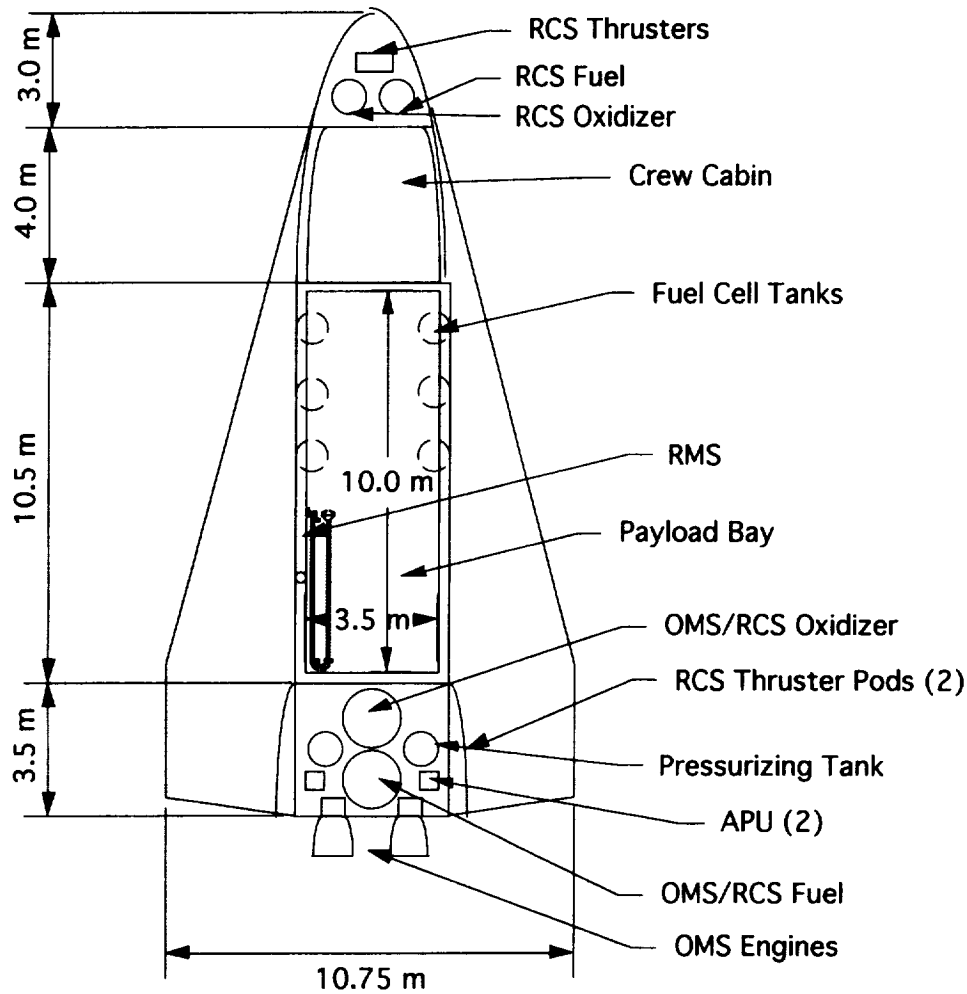

Figure 3.1.2.a Spacecraft Layout

The ORION spacecraft was 21m overall length with a wingspan of 10.75m. The fuselage diameter was 4.0m. The spacecraft's main component was the payload bay, which was 3.5m in diameter and 10m in length. The crew cabin was located forward of the payload bay to reduce cross section and provide for good visibility. The main propulsion was located aft of the payload bay. The wings were designed for reentry and a glider-like landing.

3.1.2.1 Forward Fuselage

The forward fuselage consisted of all spacecraft components forward of the payload bay. It included the crew cabin, forward RCS, forward landing gear,

avionics, and attitude sensors. The crew cabin was the largest component in the forward fuselage. It was 3.5m in diameter and 4.0m in length. It provided for all life support and other crew support facilities. It could support a crew of up to six astronauts for 15 days. It was designed so that part of the crew cabin could be ejected and carry the crew to safety in the event of an emergency. The crew cabin had an airlock that exited into the payload bay. Windows were provided forward for flight control and aft for RMS/EVA operations. All life support, with the exception of the oxygen supply, was located within the crew cabin. Oxygen was bled off the fuel cells, which were located in the mid fuselage. Avionics were also located within the crew cabin pressure vessel. Located forward of the crew cabin was the Forward RCS. It provided for attitude control in conjunction with the Aft RCS. The nose landing gear and attitude sensors were also located forward of the crew cabin.

3.1.2.2 Mid Fuselage

The mid fuselage extended from the beginning of the payload bay back to the engine compartment. Its primary component was the payload bay. The payload bay was 3.5m in diameter and 10m in length. It was sized to carry a docking module and logistics module or Hubble repair equipment. Payload attachment fixtures and power supplies were located throughout the bay. The airlock entrance was at the forward end of the payload bay. The RMS was mounted on the left side of the payload bay. The three fuel cells and supporting reactant tanks were located underneath the bottom of the payload bay between the support frames. The mid fuselage also provided the main support for wing loads.

3.1.2.3 Aft Fuselage

The aft fuselage housed the Orbital Maneuvering System, the Aft RCS, and supporting APU's. The OMS and RCS were bi-propellant systems, using the same propellant and oxidizer, simplifying the tanks, fuel lines, and valves. The OMS had two engines, which were gimbaled by the APU's. The OMS was used for orbital insertion, maneuvering, rendezvous, and de-orbit. The aft RCS was used with the forward RCS for attitude control.

3.1.2.4 Wings

The wings primary function was to provide lift through reentry to landing. They also housed the aft landing gear. Vertical stabilization was provided by winglets located on the edge of the wing.

3.1.3 Mass Breakdown

The spacecraft mass was determined by a component level bottoms up review (see Appendix A.3.1.3). Since no component level masses were calculated for

the spacecraft, empirical formulas were used (see Appendix A.3.6). The spacecraft's structure included the fore, mid, and aft fuselages, wings, vertical stabilizers, and landing gear. Wet loading included RCS propellant, LOX and LH2 for the fuel cells, crew, payload, emergency oxygen, and crew supplies.

Loading	Mass [kg]
Dry	29,929
Wet	50,926

Table 3.1.3.a Mass summary of spacecraft

Below is a dry mass breakdown of the spacecraft.

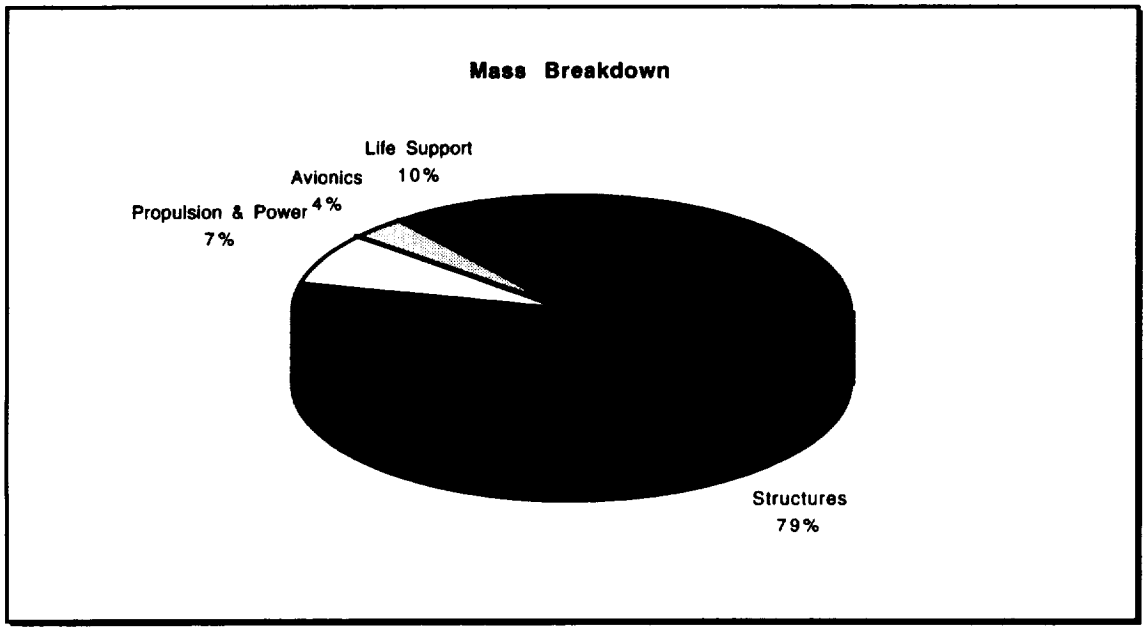

Table 3.1.3.a Dry mass breakdown of the spacecraft

3.2 Center of Gravity

The center of gravity was shown for two different configurations: orbital insertion, with full propellant load and post-deorbit burn when a majority of the propellant had been expended. Both assumed an 8000kg mass in the center of the payload bay. The distance given was the distance back from the nose.

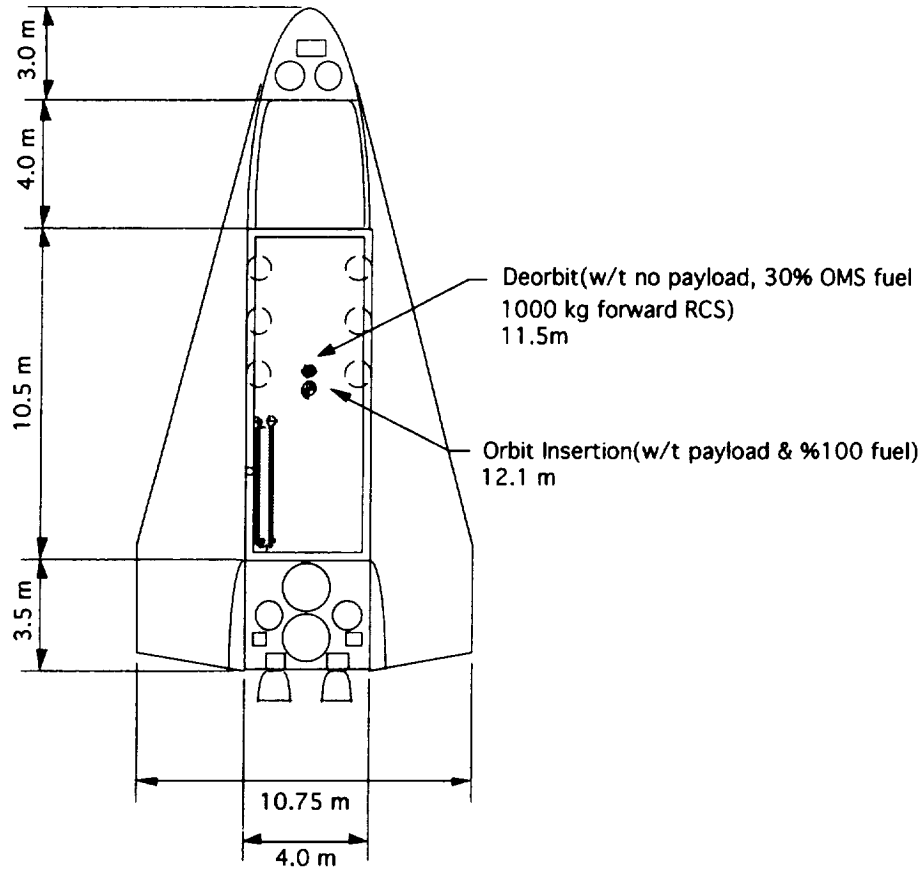

Figure 3.2.a Spacecraft Center of Gravity

3.3 Crew Cabin

3.3.1 Introduction

The purpose of the launch system was the delivery of humans to space at a low-cost. One of the key facets of getting humans in space was ensuring their survivability, comfort and performance. This meant that the crew cabin had to provide the astronauts with their basic needs and protect them from the harsh environment of space, while allowing them to perform all their tasks with a minimum of difficulty.

3.3.2 Requirements

3.3.2.1 Temperature

The productivity of the crew of a spacecraft was strongly influenced by their comfort and health, both of which were strongly influenced by the ambient temperature. At temperatures above 30°C, mental activities began to slow down, errors in judgment began to appear, and complex performance began

to deteriorate. At temperatures above 25°C, physical labor began to become fatiguing. At temperatures below 10°C, physical stiffness in arms and legs began to appear. For optimum performance with humidity in the range of 30-50%, the temperature should be about 21°C.

3.3.2.2 Humidity

The humidity of the cabin atmosphere was closely linked with the cabin temperature, but some guidelines can be made. Humidities in excess of 90% were generally considered intolerable. At humidities of 15% or less, external body fluids began to evaporate. Humidities in the range of 30-40% were considered comfortable. Figure 3.3.2.a shows human tolerance to temperature with respect to humidity.

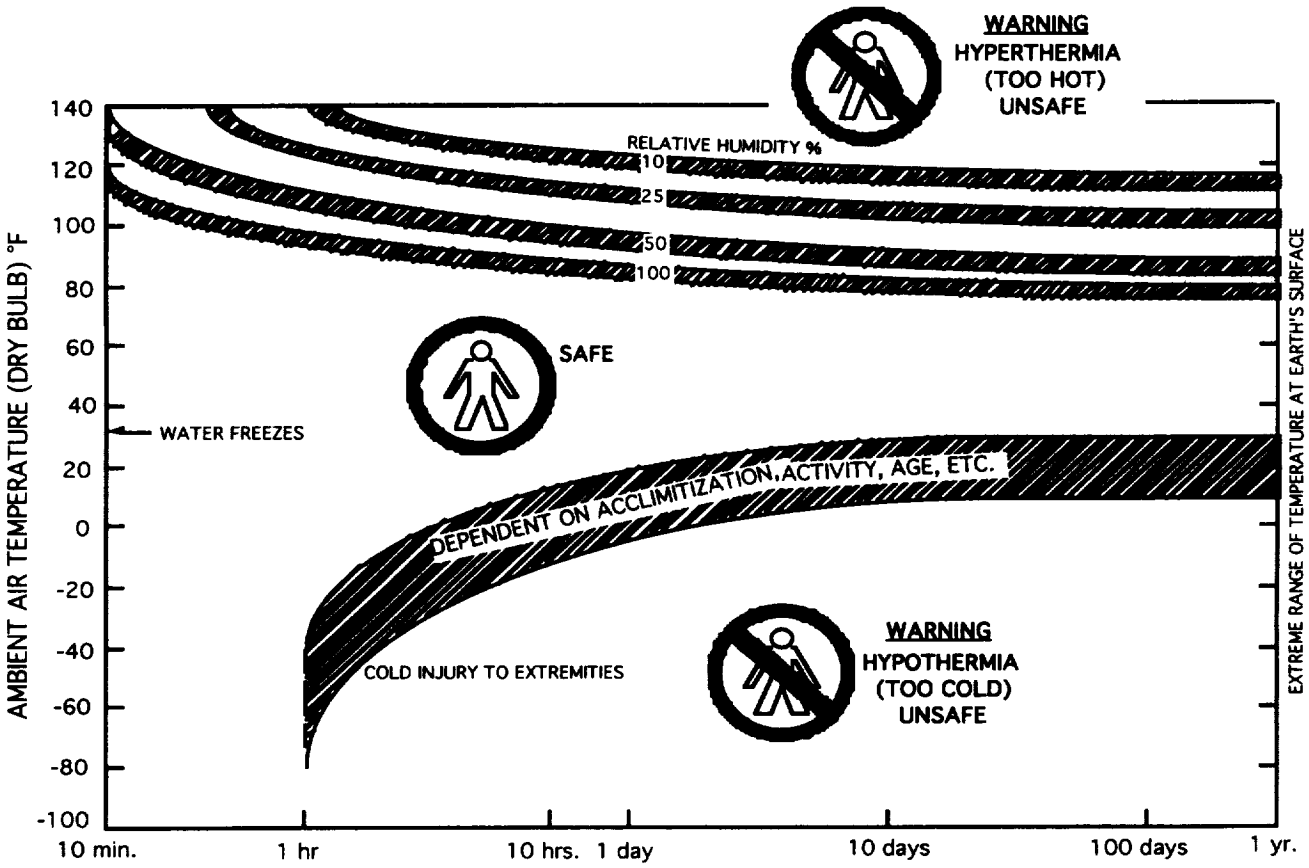

Figure 3.3.2..a Human Tolerance to Temperature with Respect to Humidity from Stine, Harry Handbook for Space Colonists, Holt, Rinehart and Winston 1985.

3.3.2.3 Atmosphere

An average-sized person consumed approximately 1.5 kg of oxygen per day-as such, a system designed to provide an artificial atmosphere had to be able to replenish at or faster than this rate. With respect to crew comfort, the optimal

atmosphere would have contained oxygen and nitrogen in the same proportions as the earth's atmosphere. The earth's atmosphere, in terms of pressure, was composed of 21 percent oxygen, 70 percent nitrogen and one percent trace contaminants.

However, humans were capable of surviving on far less atmosphere. Oxygen had to be present in the atmosphere at a pressure of at least .20 atm, referred to as the alveolar pressure, to allow its transfer across the alveoli in the lungs. The nitrogen did not need to be present for humans to function. However, to safely enter an atmosphere of reduced pressure and breathe it required prebreathing, a slow acclimation from the standard atmosphere. This allowed nitrogen to slowly leave the bloodstream-otherwise the nitrogen became soluble and bubbled, causing decompression sickness. To enter an atmosphere of 100% oxygen required about two hours of prebreathing. Higher concentrations of oxygen required less time prebreathing. For instance, going from a standard atmosphere to an atmosphere of .6 atm required about an hour.

Conversely, there were upper limits to the amount of oxygen present in the atmosphere. At partial pressures above .27 atm, hyperoxia could have occured, which could have caused inflammation of the lungs, respiratory disturbances, blindness, heart conditions or even loss of consciousness. In addition, higher pressures of oxygen could have caused a serious flame or explosion hazard.

In addition to oxygen, a major factor in establishing the requirements for the cabin atmosphere was the removal of toxic substances. Carbon dioxide (CO_2) was a natural byproduct of humans' consumption of oxygen and could have been extremely dangerous if not controlled. For safe and unimpeded crew performance, CO_2 should not exceed 1.0% of the cabin atmosphere. If it was allowed to rise to a greater concentration, the crew members risked suffering from respiratory acidosis, which could seriously impair their judgment, and then acute CO_2 toxicity, which could have more serious consequences.

The atmosphere also needed to be kept free of excessive concentrations of contaminant gases. Standards existed within industry concerning the maximum concentrations of toxic compounds. These standards can be found in Appendix A.3.3.2.3.

3.3.2.4 Acceleration

Acceleration was a serious consideration during launch and reentry. The acceleration loads experienced during the phases of the mission could have seriously impacted the operational ability and health of the crew. During the on-orbit and flight phases of the mission, the acceleration loads encountered

were extremely low and did not significantly influence the crew's health or performance.

A variety of factors influenced humans tolerance to acceleration, including duration, rate of onset and decline of the applied force, direction, body position, physical condition, and previous experience and training. For a positive linear acceleration, defined as into the chest, it was possible for many people to withstand accelerations several times that of gravity. Appendix A.3.3.2.4 gives an overview of acceleration guidelines, factors affecting human tolerance, and human responses.

The acceleration requirements established for the mission set the maximum nominal linear acceleration at four g's (four times the acceleration of gravity on earth's surface). This limit allowed for crew participation during launch and for a wide variety of astronaut candidates. In emergency abortive situations, the acceleration was required to be kept to within 14 g's to maintain the astronauts' consciousness, and within 30 g's to keep them alive.

3.3.2.5 Interior Volume

Studies performed for NASA by General Electric in 1971 determined the optimum amount of living volume as a function of duration. As the mission duration increased, crew members tended to feel cramped, and this psychological effect could have adversely affected crew performance. Figure 3.3.2.b shows optimal volume as a function of mission duration, and also shows the minimum amounts of tolerable and nominal performance cabin volumes.

The longest duration for the ORION spacecraft was the Hubble repair mission, at 12 days plus a three day safety margin. A fifteen day mission corresponded to an optimal volume of 6.8 cubic meters per person. The spacecraft crew cabin had an interior volume of 41 cubic meters and six astronauts, which reduced to 6.83 cubic meters per person, just above the optimal volume.

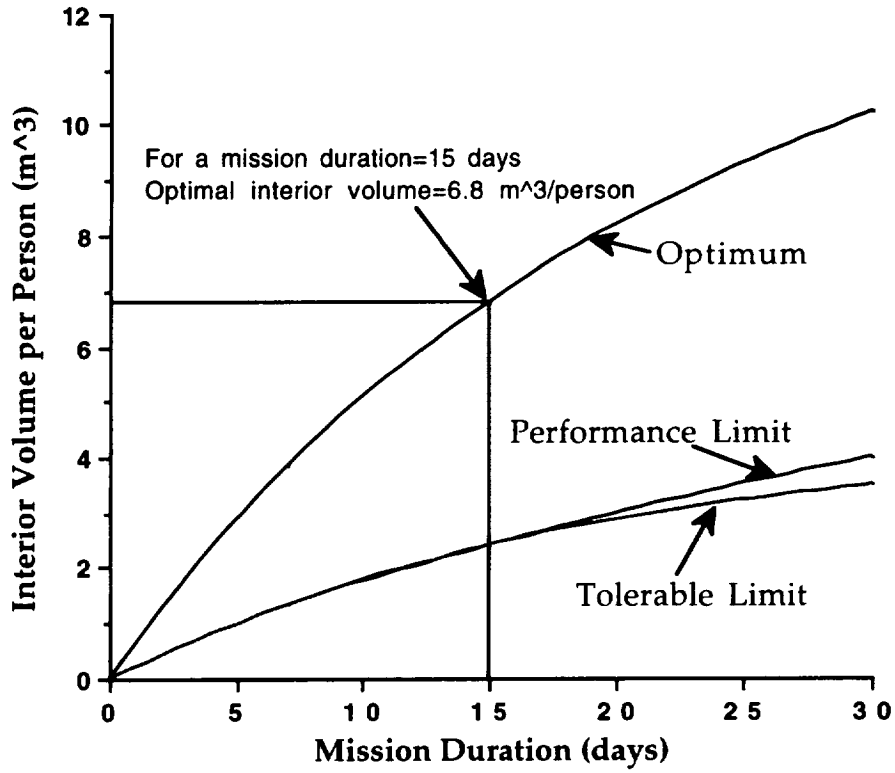

Figure 3.3.2.b Interior Volume vs. Mission Duration from NASA CR-1726: Handbook of Human Engineering Design Data for Reduced Gravity Condition, 1971

3.3.2.6 Acoustics

Spacecraft crewmembers were required to be provided with an acoustic environment that would not cause injury or hearing loss, interfere with communication, cause fatigue, or in any other way degrade crew performance. Although the human ear had a range from 2500 Hz to 2500 MHz, care needed to be taken to ensure that noise levels stayed within defined limits and did not exceed the durations for not damaging the ear. High noise levels were expected during launch and reentry, and were required to be monitored to reduce the interference with intercom and radio communication, and to prevent hearing loss. During the on-orbit and flight phases, which were customarily much longer, sound levels from all the various spacecraft subsystems were required not to exceed limits. Table 3.3.2.a shows the performance effects of noise on humans. As a systems requirement, the maximum sound environment the crew were required to be exposed to was set at 115 dB for a duration of two minutes over 24 hours; Hearing protection was required to be used if exposed to sound at 85 dB or

greater for a long period of time; the total sound exposure over a 24 hour period was required not to exceed an average of 80 dB.

Performance	Conditions of Exposure		
	Sound Pressure Level (dB)	Spectrum	Duration
Reduced ability to balance on a thin rail	120	Broadband	
Chronic fatigue	110	Machinery noise	8 hr
Reduced visual acuity, stereo-scopic acuity, near-point accommodation	105	Aircraft engine noise	
Vigilance decrement; altered thought processes; interference with mental work	90	Broadband	Continuous
Fatigue, nausea, headache	85	1/3-octave @ 16 kHz	Continuous
Degraded astronauts' performance	75	Background noise in spacecraft	10-30 days
Performance degradation of multiple-choice, serial-reaction tasks	90	Broadband	
Overloading of hearing due to loud speech	100	Speech	

Table 3.3.2.a Performance Effects of Noise on Humans from NASA STD-3000 Man-Systems Integration Standards

3.3.2.7 Vibration

The human body was especially sensitive to vibrations from 1 to 30 Hz. These vibrations ranged from reduced comfort (i.e. a slight irritation) to exposure limits (i.e. vibrations to the point of pain). Care was required to be taken to avoid such vibrations. The frequency range from .1 to .63 Hz was generally associated with those symptoms indicative of motion sickness, such as pallor, dizziness, nausea, vomiting and complete inability to function. Vibrations were required to be controlled such that they did not cause personal injury, degrade task performance or induce fatigue.

3.3.2.8 Illumination

The lighting in the spacecraft cabin was required to be such that viewing conditions were optimized during all conditions. This ranged from gross visual necessity, such as the light required to move about, to critical visual tasking, such as the light required to accurately observe precise data displays. The general illumination throughout the cabin was required to be around 108 lux. Illumination for reading was required to be at least 538 lux, and illumination for general functions within a workstation was required to be at least 323 lux. Emergency illumination was required to provide at least 32 lux.

3.3.2.9 Clothing

The crew clothing were required to provide enough comfort to allow the crew member to move comfortable about the crew cabin, and provide enough thermal comfort to prevent any degradation in performance due to a sensation of coldness. Approximately two kg of clothing were required to be provided per person per day, some of which could have been laundered with the allocated sanitation water.

3.3.2.10 Food and Water

The food provided to the astronauts was required to meet the United States Recommended Daily Allowance nutritional requirements as established by the United States National Research Council. This was between 2,000 and 3000 Calories (1.5-2 kg) per day. Additional nourishment was required to be provided for crewmembers who were undertaking EVA tasks that day. Approximately 3 kg of water was required to be provided per day for rehydration and drinking.

The food and water were required to be stored out of the way yet easily accessible. In addition, means for heating up food and water were required to be provided, to make the meals more appetizing.

3.3.2.11 Radiation

Radiation exposure was a serious consideration in manned space activities. Appendix A.3.3.2.11 outlines in detail the effect radiation has on humans. With respect to the actual requirements of the spacecraft, the radiation was required to be limited such that it caused neither a degradation in overall performance of the crew nor any long-term health effects. In low-earth orbit, the most serious radiation threat was due to trapped protons in the Van Allen belts, particularly over the South Atlantic Anomaly.

The threat posed by the trapped radiation was relatively low, however, compared to other orbits. The Van Allen belts shielded the astronauts from the more energetic and dangerous cosmic radiation and from most of the charged particles resulting from solar flare activity. Some of the more intense solar flares posed a minor threat to the astronauts, but enough lead time was often provided, in the form of visual identification of the flare before the charged particles arrive, to allow the astronauts to maneuver to safety, in this case performing an emergency landing.

The actual dose limits had been set by the National Council on Radiation and Measurement as no more than 25 rem per person over a 30 day period, no

more than 50 rem per person per year, and career limits set determined by the age of the astronaut:

200 + 7.5 (age - 30) rem for males, up to a 400 rem maximum

200 + 7.5 (age - 38) rem for females, up to a 400 rem maximum.

If the yearly limit had been exceeded, the astronaut was forbidden from space flight until enough time had passed to account for the excess. This allowed the astronaut's health to recover from the exposure.

3.3.3 Crew Cabin Configuration

3.3.3.1 Introduction

The crew cabin for the ORION spacecraft must be able to carry a crew and allow them to carry out their mission objectives. For ORION this meant being able to support a crew of six and provide necessary support for the two manned missions. This included provisions for docking with space station and providing the EVA facilities and spacecraft endurance for a mission similar to the HST repair mission.

3.3.3.2 Crew Cabin Design Philosophy

The crew cabin was designed with several basic guidelines to go by:

1. Cabin Diameter based on the diameter of the logistics module which was 3.5m
2. Keep all crew members together during launch and reentry to provide for a crew ejection capsule/abort system
3. Must have a view of payload area for RMS operation and EVA coordination
4. Fit a two person airlock in the crew cabin
5. Fit avionics into pressurized crew cabin
6. Provide space for Waste Control System, Food Preparation, general stowage, consumables, and trash

These guidelines addressed the mission requirements that the crew cabin design must meet. The requirements were as follows:

1. Cabin Diameter of 3.5m. The payload bay diameter was determined through a trade study on required volume for the missions. To minimize cross-section and vehicle size, the crew cabin was placed along the flight axis of the spacecraft and was not larger than the payload bay diameter.

2. All crew kept together for launch/reentry. The mission requirements specified that the crew have a 99.9% chance of survival of any mission. During examination of abort systems it was found that a major problem with the current shuttle was that the crew cannot be ejected because of their

separation. Earlier systems such as Mercury, Gemini, and Apollo had the crew in a small capsule which could easily escape. Keeping the crew together provided the ability to incorporate either ejection seats or an escape capsule concept. A escape capsule was chosen to provide for escape.

3. Have a view of payload area: A key requirement for any RMS or EVA activity was the ability to view and coordinate it. All RMS operators had to be able to see the RMS in operation and all EVA's had a coordinator who was inside the spacecraft and could see all the operations.

4. Fit a two person airlock in the cabin: Both missions required the use of an airlock, either for crew transfer or for EVA operations. As detailed in section 3.2.6, this was determined to be two person airlock.

5. Fit avionics inside crew cabin: It was determined that due to outgassing and other factors, the majority of the avionics had to be pressurized. Placement in the crew cabin also allowed for easy access for component replacement.

6. Provide space for life support systems: The crew cabin needed to have the space for the necessary life support systems for the given crew size and composition and the mission duration.

3.3.3.3 Crew Cabin Layout

3.3.3.3.1 Upper Deck

The upper deck was the location for nearly all of the crew's activities. During launch and reentry, the mission commander and pilot were seated in the forward two stations. The other four crew members were not involved in operations and were located on the bench aft. This bench was designed to fold up when not in use. Ingress and egress was through the hatch to the immediate left of the mission specialist's bench.

Aft of the flight stations were the systems for orbital operations. The airlock entry hatch was located on the floor, immediately aft of the mission specialist flight station. To the right side of the airlock hatch was the EMU storage, which held two EMU/PLSS. To the left was storage for personal belongings, clothing, and other items. Furthest aft was the RMS station. To the right of that was the galley, to the left, the Waste Control System.

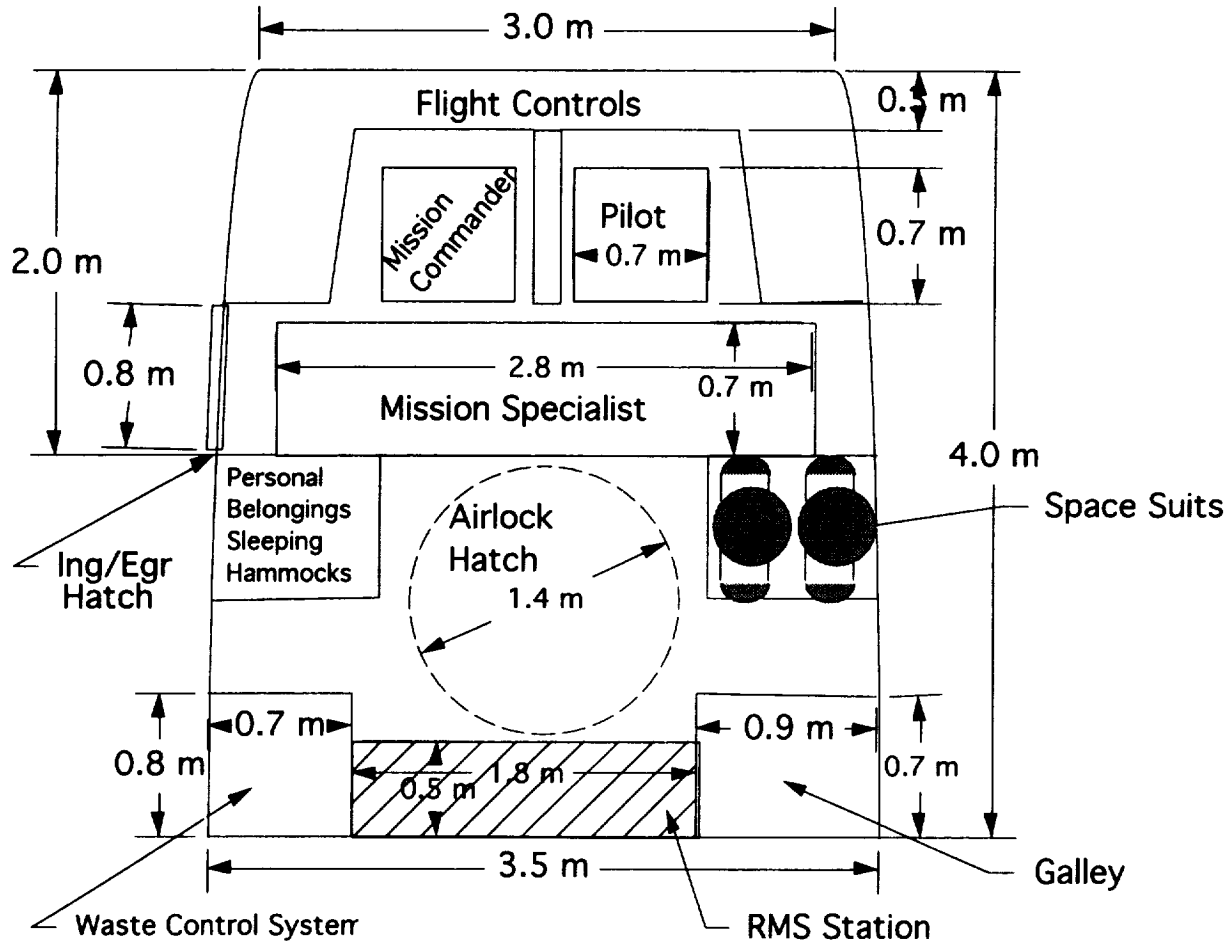

Figure 3.3.3.a Crew Cabin Upper Deck

3.3.3.3.2 Lower Deck

The lower deck contained the airlock and the support systems for the crew cabin. Immediately forward was the avionics bay. Directly beneath the avionics bay was the thermal control system. The emergency oxygen and nitrogen supplies were located forward. The escape rockets for propelling the upper deck escape capsule were located at the middeck point. The water supplies and waste tanks were located aft on both sides of the airlock. The airlock was aft and center. The egress hatch of the airlock passed through the crew cabin's aft bulkhead to the payload bay.

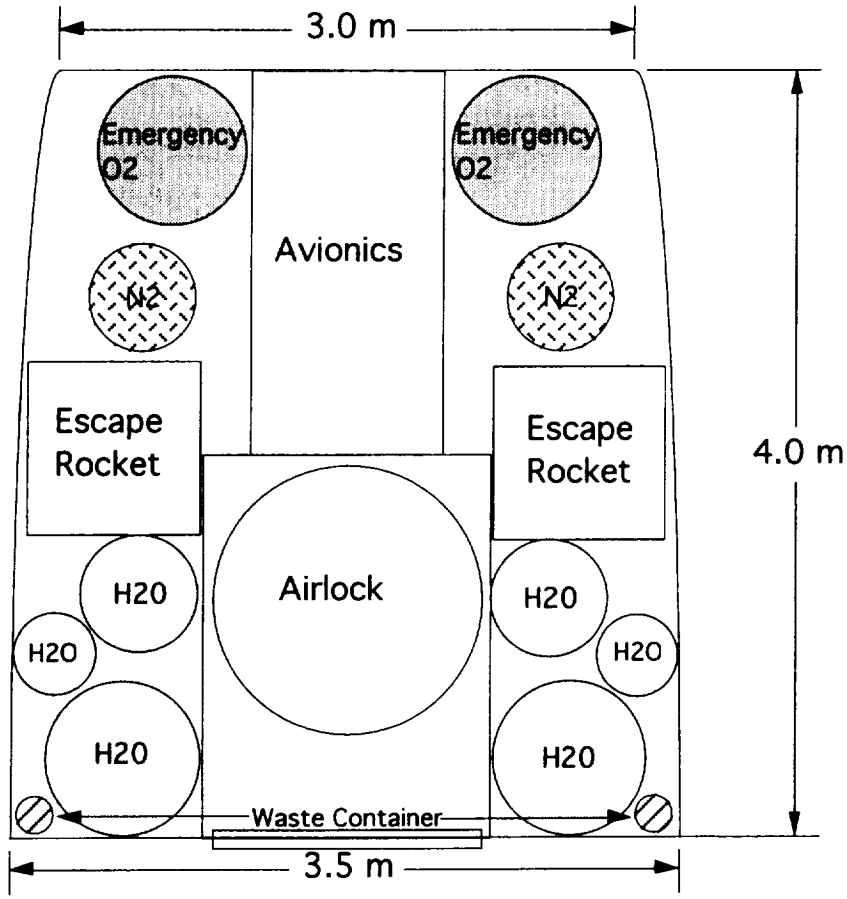

Figure 3.3.3.b Crew Cabin Lower Deck

3.3.3.3.3 Side View

This side view shows the vertical relationships of the various systems. The flight controls and crew launch/reentry positions were forward on the upper deck for visibility. The aft crew station was removable. Located under the crew flight station was the avionics bay. This allowed for easy access and for easy connection to the flight controls. The RMS station was located aft on the upper deck with a window capable of viewing the entire payload bay. The airlock's position in the lower deck was aft. Its ingress hatch was designed to open into the upper deck by swinging forward. Escape rockets were in the middle of the crew cabin, attached to the separable upper deck. The thermal control equipment was located under the avionics, which was the largest heat load.

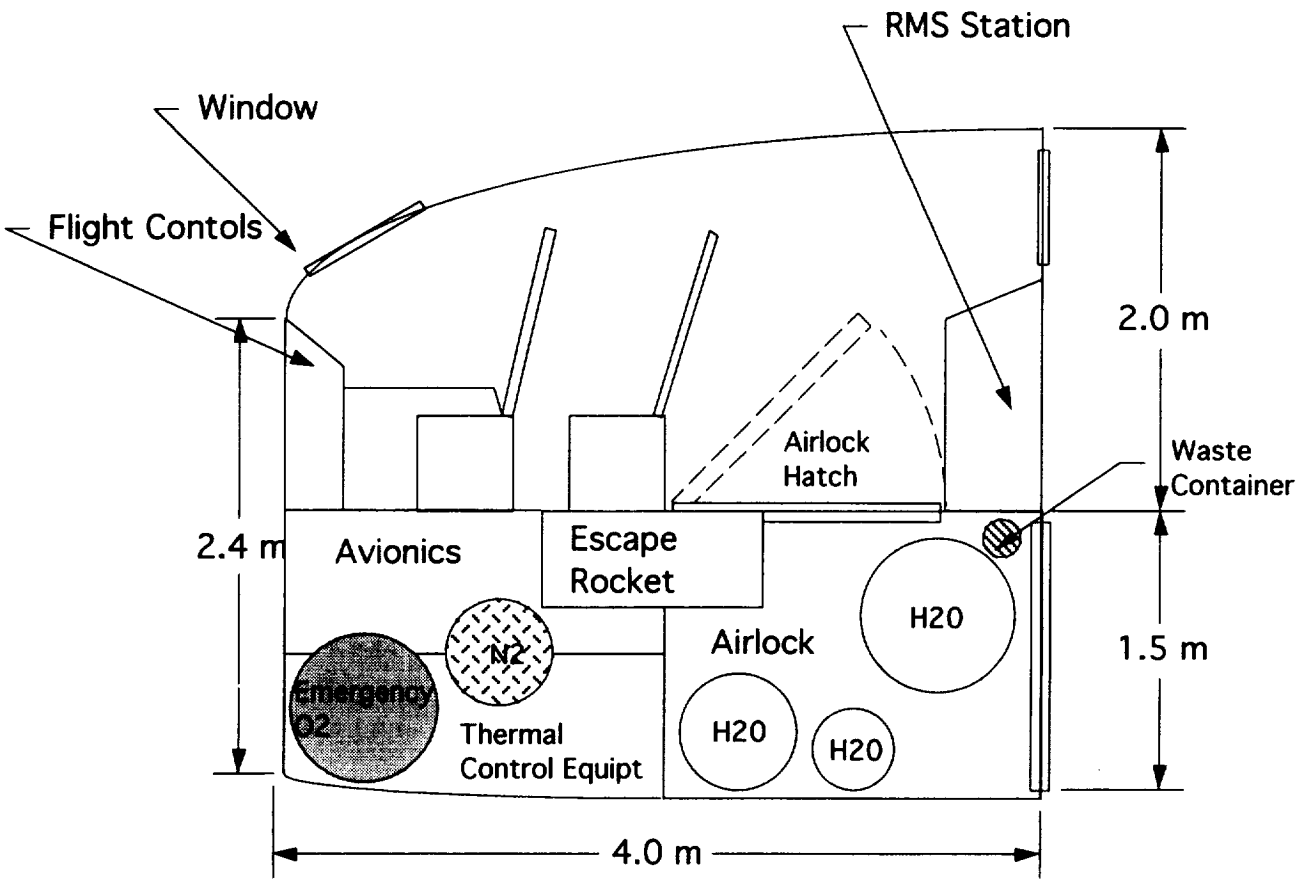

Figure 3.3.3.c Crew Cabin Side View

3.3.4 Life Support Systems

3.3.4.1 Introduction

The purpose of the life support systems was to provide an environment in which the astronauts could perform their mission tasks and attend to their personal needs for the duration of the mission. In addition, the environment should not hinder them in their of their work, allowing maximum performance in a comfortable environment.

3.3.4.2 Atmosphere Control

3.3.4.2.1. Introduction

The atmosphere control system provided a breathable atmosphere for the astronauts which was free of excessive contaminants or carbon dioxide. It also provided a means for cooling the cabin atmosphere to an optimum temperature and transferring that heat to the exterior of the spacecraft.

3.3.4.2.2 Oxygen and Nitrogen

The crew cabin contained air and nitrogen mixed and pressurized to .68 atm (10 psi). Diatomic oxygen was present at a partial pressure of .24 atm (3.5 psi), slightly above the alveolar pressure required for oxygen transfer in the lungs. The remaining partial pressure of .44 atm was diatomic nitrogen. The benefits of the reduced atmospheric pressure included less structural load, less fire hazard, and less time for prebreathing before EVA. Refer to the Structures section for a description of the structural analysis. The advantage of a reduced cabin atmosphere with respect to prebreathing was because the EVA suits were pressurized to only .27 atm (4 psi) to reduce the physical exertion required of the astronauts when they performed tasks in space. The process of transferring from the cabin atmosphere to the reduced pressure of the EVA suits meant that the nitrogen must be gradually dissipated from the bloodstream to prevent decompression sickness. A change from .68 atm to .27 atm only required about an hour of prebreathing. This was an important factor with respect to Mission #2, the Hubble repair. In this mission, five days of EVA requiring two astronauts per day were planned, with three days of margin to cover any contingencies. Given this degree of EVA, it was advantageous to reduce the time required for prebreathing as much as possible.

The diatomic oxygen was supplied to the atmospheric control system by the liquid oxygen fuel cell. The liquid oxygen passed from the cryogenic fuel cells into a high pressure regulator which reduced the pressure to the point of boiling, at which point the gaseous oxygen passed into the pressurized volume and into another regulator to reduce the pressure to .24 atm. From this point it went into the atmosphere control panel which regulated the oxygen content of the atmosphere automatically, allowing more oxygen in as necessary. Refer to the section on Safety Equipment for information on the emergency oxygen supply.

The diatomic nitrogen was stored in two pressurized tanks within the pressurized volume of the crew cabin. Refer to the section on Crew Cabin Configuration for more details on the location of the nitrogen vessels. Each vessel was .56 m in diameter and pressurized to 204 atm to contain 23.5 kg of nitrogen, which was enough to pressurize the cabin assuming a leak rate of .25% of the total volume per week, plus a 15% margin to account for the cycling of the airlock. The nitrogen was regulated into the atmosphere control panel which maintained it at a partial pressure of .44 atm.

3.3.4.2.3 CO_2 Removal

The removal of carbon dioxide took place via a lithium hydroxide (LiOH) scrubber which reacted with the carbon dioxide to produce water and lithium carbonate. The air in the cabin was ventilated through an air contaminant

removal loop which combined the lithium hydroxide scrubber with the activated charcoal filter (see next section). Approximately 1.1 kg of LiOH per person per day was consumed. The maximum quantity of LiOH taken aboard occured during the Hubble repair mission, when the fifteen day, six-person mission required 102 kg. A trade study analyzing various methods for CO_2 appears in Appendix A.3.3.4.2.3.

3.3.4.2.4 Contaminant Removal

A majority of unwanted contaminants in the cabin atmosphere were removed via an activated charcoal air filter system. This system absorbed a majority of organic contaminants which might be produced inside the crew cabin due to body odor (refer to Section 3.3.2.3 and/or Appendix A.3.3.2.3). Table 3.3.4.a lists the degree to which particular organic materials were adsorbed out of the air. The air was passed through the adsorber in the same contaminant control loop where the lithium hydroxide removed the carbon dioxide from the atmosphere. A loop diagram showing that process appears in Figure 3.3.4.a.

30% or More	15%	8% or Less
Acetic acid	Acetone	Low-weight amines
Butyric acid	Acrolein	Ammonia
Dichloroethane	Bacteria	Formaldehyde
Essential oils	Butyraldehyde	Hydrogen chloride
Indole	Carbon disulfide	Hydrogen flouride
Lubricating oils	Chlorine	Sulfur dioxide
Mercaptans	Ethylamine	Nitric oxide
Nitromethane	Ethylene oxide	
Putriscin	Formic acid	
Skatole	Freons	
Sulfuric acid	Hydrogen sulfide	
Toluene	Nitric acid	
Benzene	Phosgene	
Methanol	Sulfur trioxide	
Ethanol		

Table 3.3.4.a Absorption of Materials by Charcoal (percent adsorbed by weight) from Faget, et al "Manned Spacecraft Design," 1964

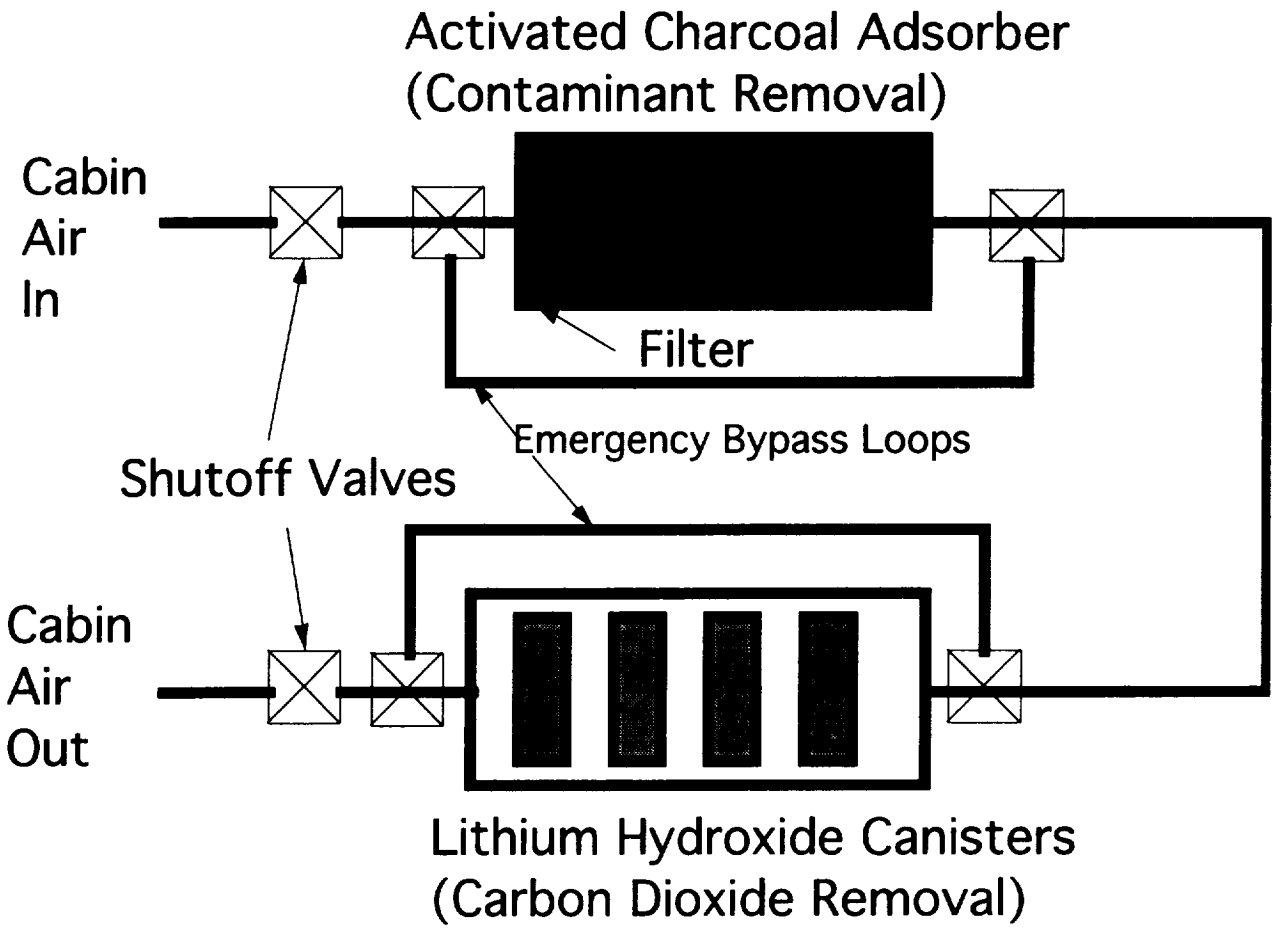

Figure 3.3.4.a Air Contamination Control Diagram

3.3.4.3 Thermal Control

The spacecraft utilized dual loop heat-rejection system to transfer accumulated heat from the crew cabin to the exterior of the spacecraft. A heat transfer loop ran through the crew cabin using water as a working fluid. Atmosphere was ventilated over heat exchangers located in the rear of the crew cabin. The water continued on through the avionics bay located in the front of the crew cabin and continued to accumulate heat. The water was circulated through the bay via modular "cold boxes" which utilized thermal interfaces.

The modular "cold boxes" were used because the of the reduced atmospheric pressure of the cabin; the reduced pressure meant the air did not have a sufficiently high coefficient of specific heat (with volume held constant) to adequately cool the avionics. Hence, a water cooling system was used. A diagram of the thermal system loop appears in Figure 3.3.4.b.

The main advantage of using water in the cabin heat-transfer was its safety. Water leaks were non-toxic and relatively easy to detect. Although a toxic refrigerant was used in the radiator fluid loop, its presence in the pressurized cabin was minimal, entering just to receive heat at the exchangers located in the rear of the cabin.

The radiator fluid loop received heat at the heat exchangers in the pressurized volume of the crew cabin and transferred it to space via radiators located in the doors of the payload bays. Freon-12, chemically known as dichloro-diflouromethane, was chosen as an optimal refrigerant. A trade study justifying the use of Freon-12 appears in Appendix A.3.3.4.3.

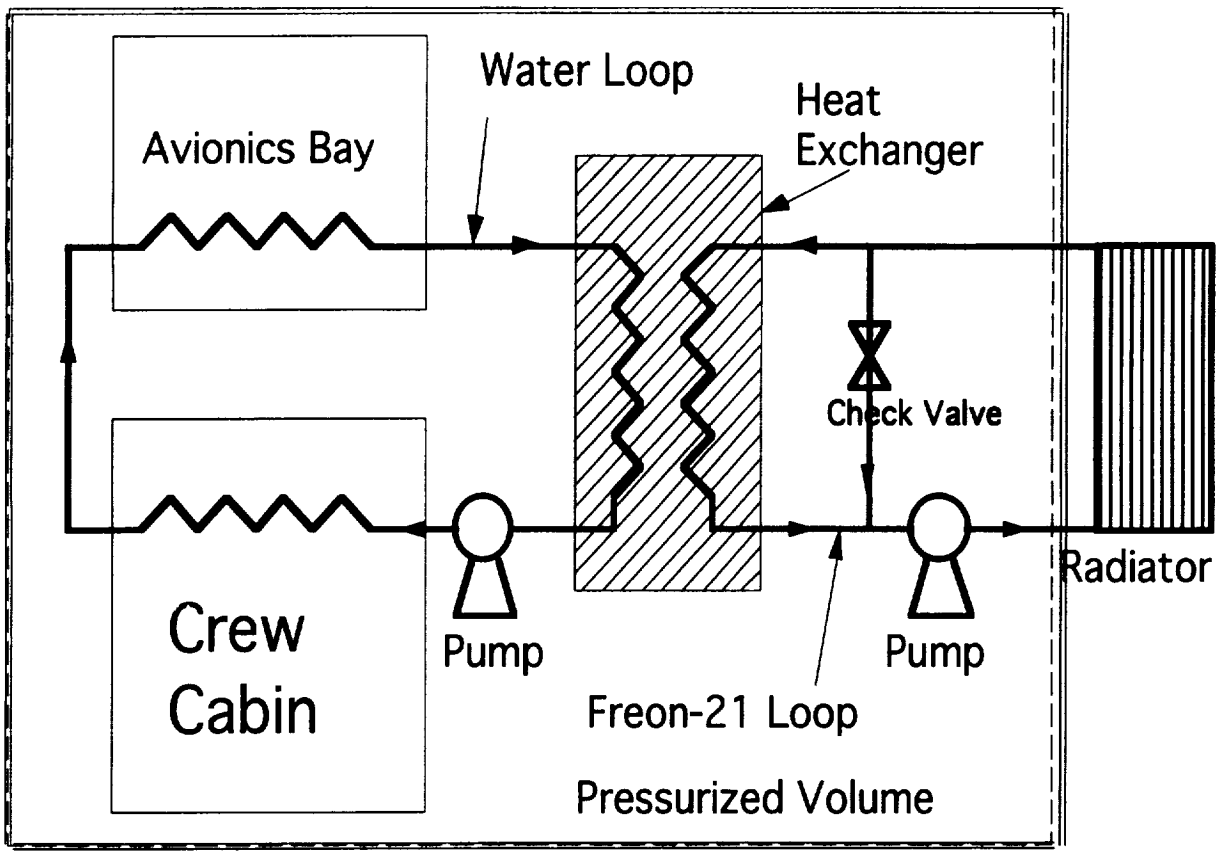

Figure 3.3.4.b Thermal System Loop Diagram

In a traditional two-phase system, the radiator fluid was heated to the gaseous phase by the heat exchangers with the assistance of the evaporators, and then was pumped into the condensers where it transmitted its heat to the vacuum of space and restarted the cycle. A problem with such a system was that inherently it took a large amount of energy to run the system. It was possible to use a single phase radiator fluid.

The radiators were designed for ΔT = 25 degrees Kelvin and T=300 degrees Kelvin. The radiators covered 80% of the inner surface of each payload door. The total radiator surface was 38.5 m^2. The energy radiated from the doors was related to the area of the radiating surface by the Stefan-Boltzmann equation:

$$E = (1/2) \bullet s \bullet T^4 \bullet A$$

where E = the energy radiated per unit time per unit area
s = the Stefan-Boltzmann constant = 5.6697×10^{-8} $W/m^2 \bullet K^4$
T = the temperature in degrees Kelvin
A = the area of the radiating surface

From this equation, E = 8.814 kW. This, in turn was related to the mass flow by the following equation:

$$E = (\Delta m/\Delta t) \bullet C_V \bullet \Delta T$$

where E = the energy radiated per unit time per unit area
$\Delta m/\Delta t$ = the mass flow through the pumps
C_V = the coefficient of specific heat with respect to constant volume
ΔT = the total change in temperature across the radiators

From this equation, the mass flow ($\Delta m/\Delta t$) was determined to be .20 kg/sec. This was the amount of refrigerant that must pass through the pumps.

3.3.4.4 Food & Galley

Food requirements were provided for by a meal system which consisted of microwaved or heated food in prepared meals. These meals were designed to meet the nutritional requirements. They came prepackaged for each meal. Parts of the package were microwaved as specified by the meal. The meal was placed on a tray that was reused for each meal. The meals had breakfast, lunch, and dinner varieties. In addition, snacks were provided, particularly for EVA missions which were demanding physically.

The galley provided storage of meals, preparation facilities, and sanitation facilities. Meals were provided for a crew of six for fifteen days. One crew member was assigned for preparation. They removed the meals from storage as specified by the mission meal plan. They placed the necessary meal components in the microwave for heating while placing the other components on the tray. In addition, they prepared the beverages. The hand washing facility was placed so that the other crew members may reach it without disturbing the crew member preparing the meal. A meal was able to be prepared in 30 minutes or less. Trash was disposed of and compacted in the galley system.

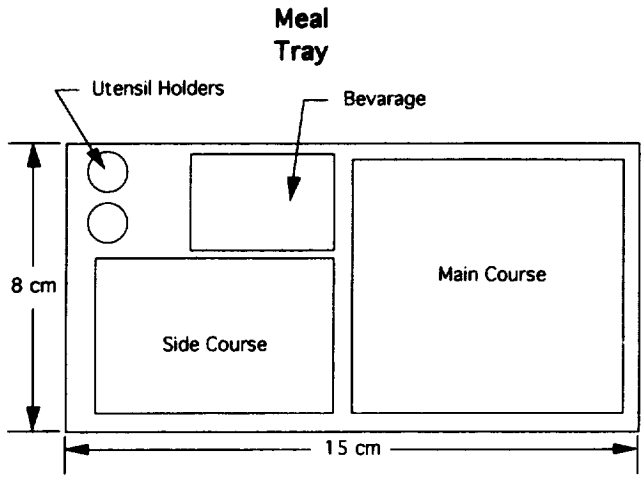

Figure 3.3.4.c Meal Tray

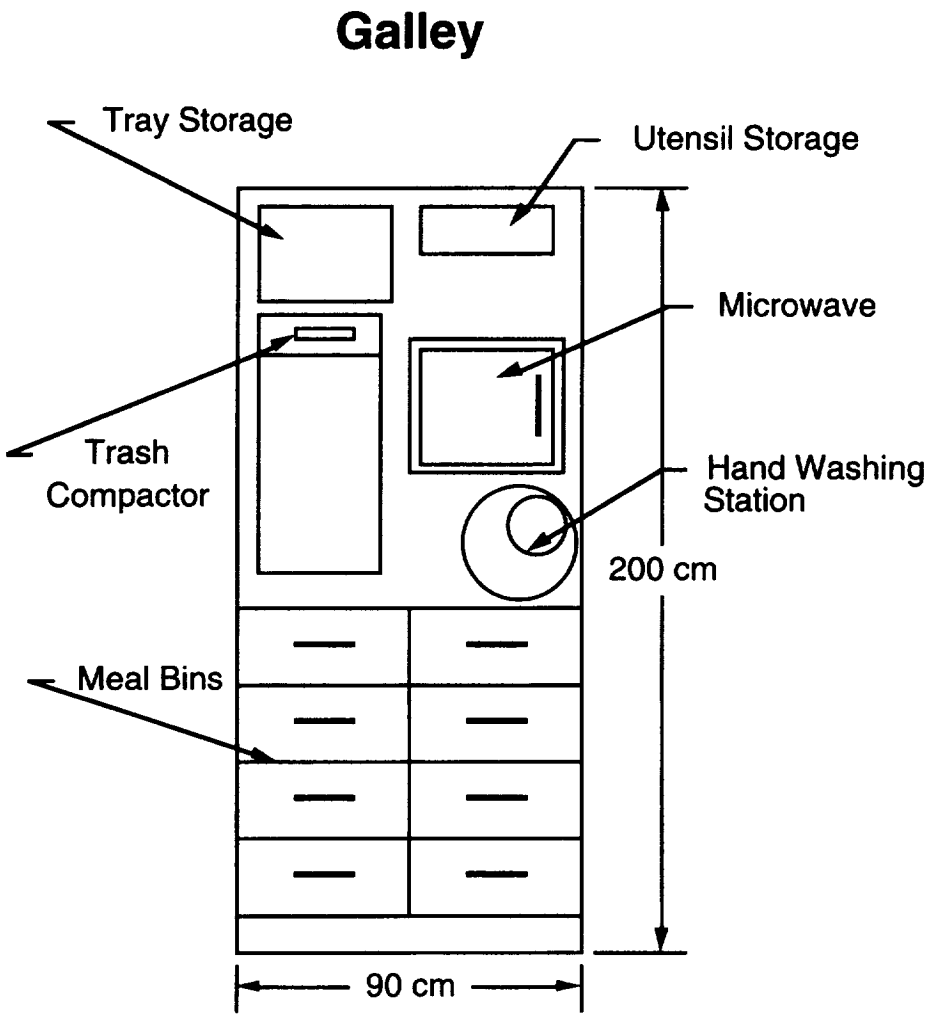

Figure 3.3.4.d Galley

3.3.4.5 Waste Control System

The Waste Control System was responsible for the safe disposal of human waste matter from the crew cabin. It was located in the rear left side of the upper deck. The station was 70 cm wide, 80 cm deep, and 2 m high. The system was similar to the current shuttle/space station systems. It used a suction process to evacuate waste matter and a centrifuge to separate liquid and solid waste. Solid waste was stored and returned; liquid waste was ejected on orbit. The system was designed for use by both genders and for all sizes of astronauts. The astronauts entered the waste control station and attached themselves to available restraints prior to use. Adequate sanitation facilities were provided in the station and air circulation was used to reduce unpleasant odors. The waste control system had storage tanks to support a crew of six for 15 days.

3.3.4.6 Personal Hygiene

Personal Hygiene was important for crew cleanliness and morale. Several different stations and facilities were provided in the crew cabin for personal hygiene. A hand-washing facility was located in the galley. This was used by all crew prior to and after all meals. It was also available for use at any other time a crew member needed or desireed to use it. The Waste Control Station had sanitation facilities as well. In addition, the station also had general hygiene supplies as well as the crew's personal toiletries kits. This included facial wipes, towels, shaving equipment, soap, and other items. Finally, the crew was provided with facilities for taking sponge baths as desired. These supplies were also located in the Waste Control Station.

3.3.5 Escape Capsule

The escape capsule was designed to provide a safe escape during a critical emergency. The system was designed to meet the requirement set forth by Human Factors section 3.3. The results of the design are shown in Table 3.3.5.a. The mass of the cabin loaded includes the electronics, crew, addition structure, explosive bolts, etc.

Escape Capsule (14 G's x,z)	Calculated
Mass Cabin/Loaded	2,400 kg
Thrust Needed	1,240,429 N
Isp	275 s
Ue	2,698 m/s
mdot	460 kg/s
Burn Time	3 s
Fuel Mass	1,379 kg
Casting Mass	10 kg
Thrust Structure Mass	316 kg
Subtotal Mass	4,105 kg
+ 10% margin	411 kg
Total Mass	4,516 kg
Mass Added to Vehicle	**2,416 kg**

Table 3.3.5.a Escape Capsule Masses

The trajectory that the escape pod follows for a pad abort is show in figure 3.3.5.a. The velocity during the flight is shown in figure 3.3.5.b. The acceleration is shown in figure 3.3.5.c. The flight path is similar for the assent abort, but the avionics package will determine the best abort trajectory and make modifications to the base line trajectory (i.e. for a landing abort, rockets only need to be fired in the vertical direction).

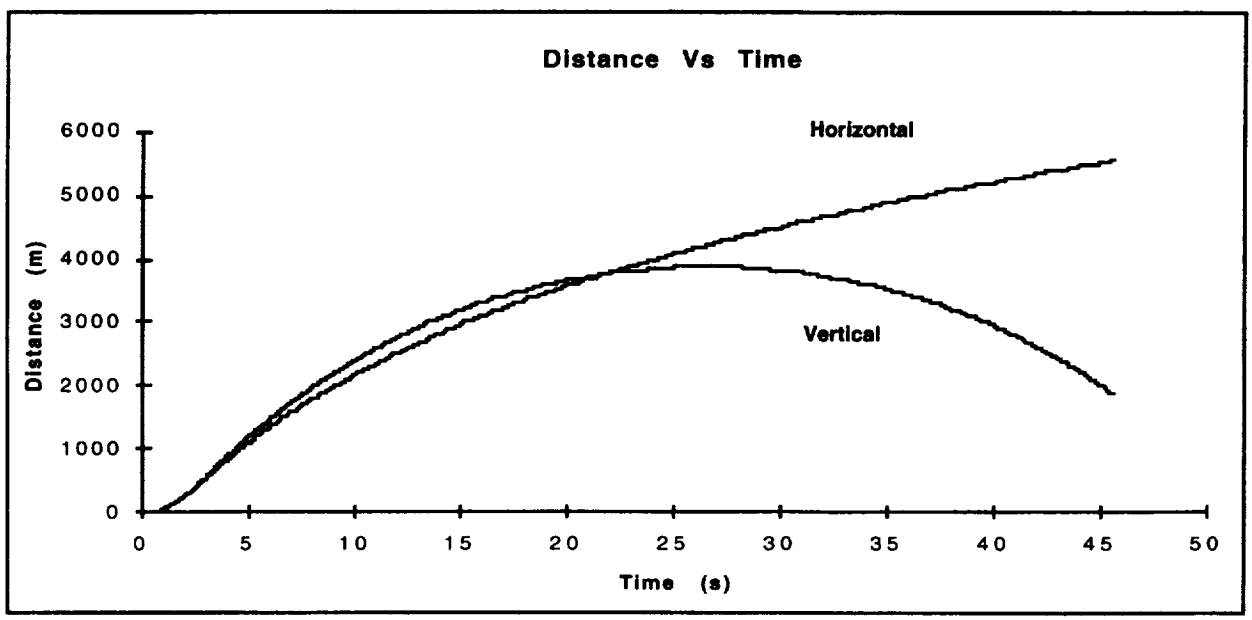

Fig. 3.3.5.a Escape Pod Trajectory

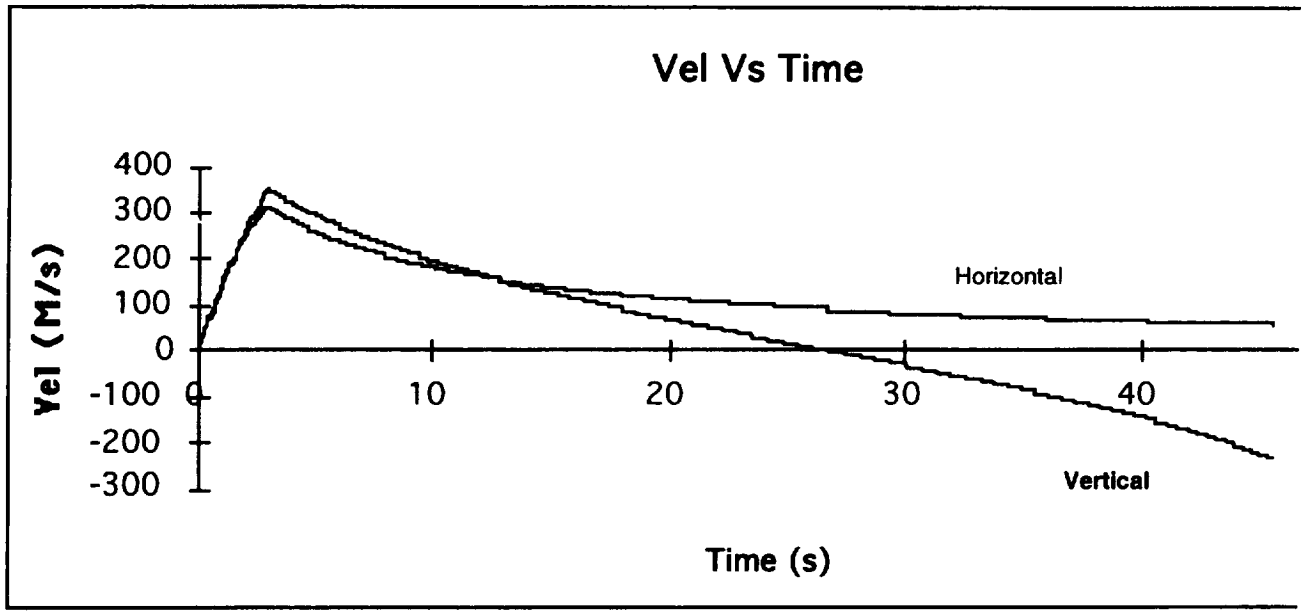

Figure 3.3.5.b Escape Pod Velocity During Flight

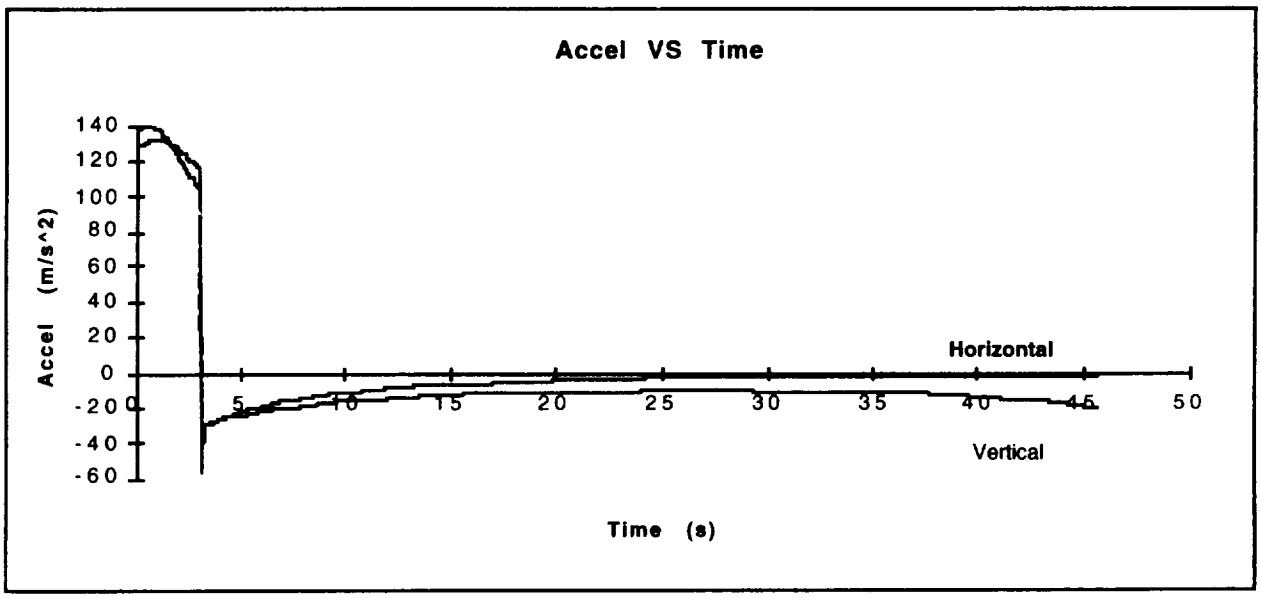

Figure 3.3.5.c Escape Pod Acceleration During Flight

After 20 seconds into the abort mode the drogue chute will be deployed followed by the main chute. The graphs do not show the deceleration phase. Based on the mass of the vehicle and its characteristics, a ring sail parachute 33.5 meters in diameter was selected to lower the Space Vehicle to the Earth (decent rate of 9.1 m/s). To absorb some of the force during impact, airbags will be used on the bottom of the structure. To further attenuate the impact energy, a honey comb structure will also be used on the bottom of the

structure. Appendix A.3.3.5 contains a mass analysis, as well as details of the equations used and the raw data obtained.

3.3.6 Safety Equipment

3.3.6.1 Introduction

Essential to any design of a technical device which supported humans was the integration of safety features. In the case of any sort of accident which threatened the health of the humans, safety features provided a means of either removing the threat or removing the crew from the threat. Section 3.3.5 addresses the problem of aborting the mission and escaping from the spacecraft. In this section, the means provided to either remove a threat or to function despite it are discussed.

3.3.6.2 Emergency Oxygen

In the case of some sort of failure of the primary oxygen supply, emergency oxygen in the form of pressurized gas was carried on board, with the pressurized nitrogen in the crew cabin. Two vessels pressurized to 204 atm, each with a diameter of .2 m and carrying 4.5 kg of diatomic oxygen, were used to supply emergency oxygen via closed loop air masks kept at the atmosphere control panel in the rear of the crew cabin. The crew was able to manually control and regulate the nitrogen content. Keeping the emergency air supply at the same nitrogen content as the crew cabin prevented nitrogen toxicity when the crew first donned the emergency masks.

Other instances which necessitated the use of the emergency oxygen system included failure of either the carbon dioxide scrubber system or the contaminant control system. Enough emergency oxygen was contained on board for six crew members for one day. That was assumed to be enough time to safely return to earth.

3.3.6.3 Fire Suppression

The spacecraft was equipped with a photoelectric smoke detector located near the intake of the contaminant control system. As all the cabin air was ventilated though this system, this was an ideal location. Once smoke particulates tripped the smoke detector, it emitted a loud sound which all crew members were able to hear, and accordingly respond to the fire hazard.

The spacecraft was equipped with two halon fire extinguishers, one per deck. Halon was the optimal choice for a space-based fire extinguishers because it effectively quenched electrical and chemical fires and did not damage equipment. Unfortunately, halon presented a mild health hazard to the crew.

The halon was kept to a low concentration, allowing the crew to don emergency air masks. The cabin atmosphere was slowly bled into space to remove the halon, and then the cabin was repressurized.

3.3.6.4 Emergency Lighting

In case of an emergency which caused failure of the main lighting system, an emergency system was activated which provided 32 lux of illumination, enough to effectively discern the equipment in the spacecraft. The power for the lighting was supplied by a battery independent of the main electrical system. This emergency lighting allowed the crew to return to earth.

3.3.7 EVA & RMS Requirements

3.3.7.1 Introduction

One of the primary mission requirements was that the spacecraft must be able to support a Hubble Repair Mission. This required the spacecraft to have adequate EVA facilities to accomplish that task. In addition, a crew transfer with the space station must be accomplished for mission #1. This involved use of the airlock for docking with the space station.

3.3.7.2 EVA Mission Requirements

There were several EVA requirements for carrying out the Hubble Repair Mission. They were:

1. Two person EVA teams were the smallest allowed
2. Five days of EVA by two person teams were required
3. A RMS system was needed to grapple Hubble and to move Astronauts during EVA

3.3.7.3 EMU/PLSS

The ORION system used the current shuttle Extra-vehicular Mobility Units and Personal Life Support Systems with evolutionary upgrades. The alternative was to use the 8 psi Space Station suits currently under development. Shuttle type EMU's had several advantages. They had no development cost, were proven, and were smaller and lighter than the 8 psi suits. The primary advantage to the 8 psi suit was that it required much less pre-breathing time. It was determined that this was not worth the additional cost for two reasons. First, the crew cabin atmosphere was designed to be 10 psi which meant lower pre-breathe times for a shuttle type EMU. Secondly an analysis was done that showed that even with a savings of several hours of pre-breathing, it would not be possible to do more than one EVA/day. On a space station the crew had many activities it could work on instead of

spending time pre-breathing. ORION, on the other hand, would be flying a dedicated EVA mission, where such extra time was much less useful.

The Shuttle type EMU/PLSS that ORION used have a mass of 122.7kg. It provided life support for up to 8 hours of EVA. Suits were individually sized requiring that a suit be carried for every crew member that was to go EVA. An additional backup suit was also carried that could be made to fit, although poorly, any crew member. For non-EVA missions, such as a space station resupply, two suits were carried for emergency EVA's. A Hubble Repair Mission required five suits (4 EVA crew + 1 backup).

3.3.7.4 Airlock Design

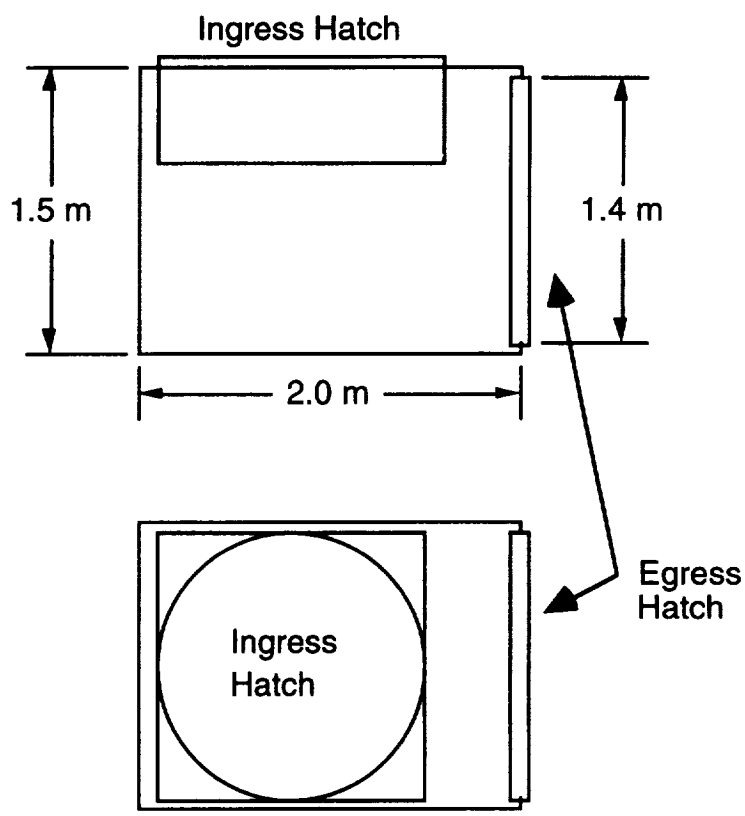

Figure 3.3.7.a Airlock System

The ORION spacecraft had two different requirements for an airlock system. The Hubble Repair Mission required that two Astronauts be able to cycle through at a single time. This was required for safety reasons. The airlock door, once open, was never shut while an astronaut was EVA. This

prevented an astronaut from being trapped outside if the airlock failed to cycle.

The Space Station Resupply required a crew transfer from the ORION spacecraft to the Space Station. Typically, a docking module was attached to the airlock. Thus the airlock did not need to be larger than required for one person to pass through.

A trade study was conducted to determine the feasibility of equipping the ORION spacecraft with a small airlock capable of crew transfer and attaching a larger two-person airlock for EVA missions. The results of the study appear in Appendix A.3.3.3.7.4. The study showed that this would save mass on the Space Station Resupply, and overall would cost less. However, it required that more mass be carried for the Hubble Repair Mission. It was decided that the airlock would be a two person version for several reasons. Safety was an important reason. As stated above, it was possible that if a one person airlock was used for a two person EVA team, a crew member could be trapped outside the crew cabin. If an emergency EVA was required during a non-EVA mission, it would mean exposing the crew to even greater danger. Another problem was that one of the major drivers of the spacecraft size was the payload bay dimensions. By taking up space with an external airlock, the payload bay would have to be larger. The Hubble Mission was already the driver on the payload bay size. An external airlock would also drive up the Hubble mission payload mass. The primary advantage was a 10 million dollar savings. This savings occurred if only one two person airlock was procured. If a second was needed, there was no cost savings. Given the safety and payload bay requirements, it was determined that an internal two-person airlock was the optimum design.

3.3.7.5 RMS Design

The spacecraft was equipped with a Remote Manipulator System (RMS) which provided a means to move and orient large objects as the mission required. The largest object the RMS needed to manipulate was the Hubble Space Telescope on Mission #2. Hubble measured 11,340 kg. The RMS had to be able to grab Hubble and position it in its servicing housing. In addition, the RMS had to be able to serve as a "cherry picker" for one of the EVA astronauts working on Hubble. A final mission of the RMS was to transfer the Pressurized Logistics Module (PLM) during Mission #1. The PLM measured 5000 kg.

An analysis was performed to determine the optimum configuration for the RMS. The RMS consisted of two links, each five meters long. It was fixed halfway down the longitudinal length of the payload bay, and it was stored with one link folded down on top of the other.

The RMS had seven degrees-of-freedom (DOF), which were arranged anthropomorphically such that the arm was similar to a human arm. The shoulder joint had three DOF, oriented in a yaw-pitch-roll configuration. The elbow joint had two DOF, pitch and roll. The wrist joint had 3 DOF, pitch, yaw and roll.

The main brakes needed to be able to grab Hubble moving at 5 cm/s or less and slow it down to a velocity of zero over .457 m (18 inches), requiring a maximum torque of 620 N-m.

An analysis of materials was performed to decide which material to use in the arm links and how much of it. Graphite/Epoxy was determined to be the optimum material, with a very high stiffness meaning that a rather small moment of inertia was required, and hence a small cross-sectional area and reduced mass. Each link was pipe-shaped and had an inner diameter of 60 cm and a thickness of 1 cm. The mass of each was approximately 568 km.

The end effectors needed to be able to hold onto the manipulated object while the Reaction Control System was firing in the case of a stability correction. The RCS could fire with a force up to 2000 N. Thus, the end effector needed to be able to provide a holding force of 2000 N. Data produced during the RMS analysis appears in Appendix A.3.3.7.5.

3.4 Avionics

3.4.0. Introduction

The avioincs system was divided into three areas: data management; navigation, guidance, and control; and communcations. The data management sub-system was composed of five modular computer units in a functionaly distributed architecture. Information was carried over a high speed fiber optic network. Primary navigation was performed by a tightly intergrated Internal Navigation System and a Global Positioning System. During landing, the spacecraft also employed a radar altimiter and a Microwave Landing System. All on-orbit communications were routed through TDRSS (Tracking and Data Relay Satellite System). Together, these components were responsible for performing 16 flight critical functions.

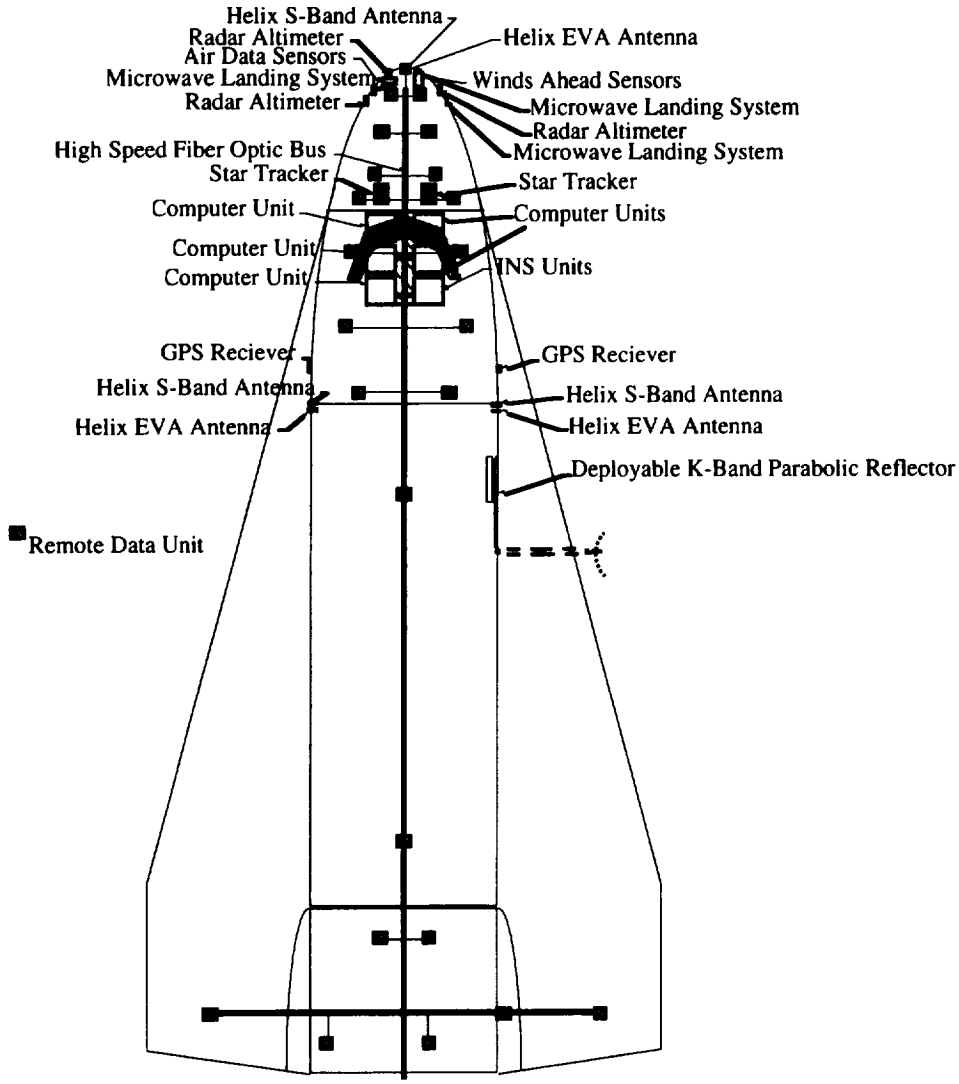

Figure 3.4.0.a Placement of avionics components

3.4.0.1. Functional Decomposition

The three reference missions were decomposed into 16 top level functions as shown in Table 3.4.0.a These functions were tasks that needed to be performed during the missions and were each composed of several sub-functions which are listed in Appendix A.3.4.0.1

3.4.0.2. Functional Allocation

The responsibility for performing each function was allocated to the crew, the computer, or a combination of both. The functions were allocated on the basis of performance using a Fitts Matrix (see Appendix A.3.4.0.2). The matrix listed the functions, Vs, the attributes of the crew and the computer. Then the designer rated the crew and computer on how well their attributes

matched the attributes needed to perform each function. The one with the higher rating was awarded responsibility for the function. If the rating of the crew and computer were close (approximately five points), the function could be allocated to a combination of the two. Functional Allocations are listed below.

Function	Allocation
Navigation	Computer
Guidance	Computer - Software
Control	Combination
Avionics System Management	Computer - Software
Winds Ahead Determination	Computer
Propulsion Control	Computer
Fluids Management	Computer
Power Management	Computer
Fire Control Management	Computer
Life Support Management	Computer
RMS. Control	Crew - Computer Assisted
Thermal Control	Computer
Stage Separation	Computer
Communications	Computer
Sensor Processing	Computer
Abort Control	Combination

Table 3.4.0.a Top level functions and their allocations.

Responsibility for the control function was dependent upon the maneuver to be executed. This function along with navigation and guidance functions are discussed in more detail in section 3.3.2. The responsibility for abort control (initiation and execution) depended upon the nature of the emergency that initiated the abort. If the emergency required faster than human reaction times or the crew became incapacitated, the computer was allocated the abort control. At other times the crew was allocated the abort control.

3.4.0.3. Requirments

The avionics systems were required to meet three requirements which were to acheive .9975 system level reliability, to reduce ground operations, and to standardize components so that they might be used on both the crewed and uncrewed vehicle configurations.

3.4.0.3.1. Reliability

A mission reliability of 99% was stated in the mission requirements. To define the reliability of the Avionics system, an approximate reliability budget was modeled assuming equal reliability among the four major subsystems.

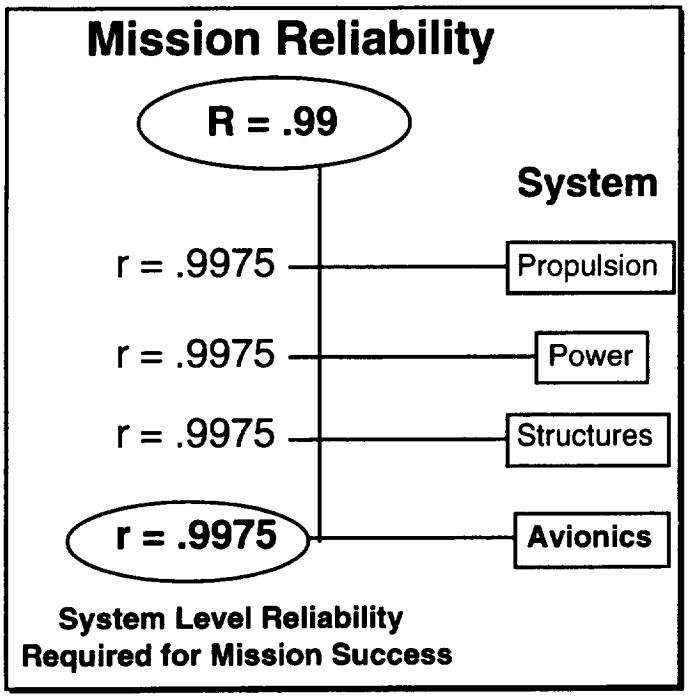

Figure 3.4.0.b Estimated system-level reliability.

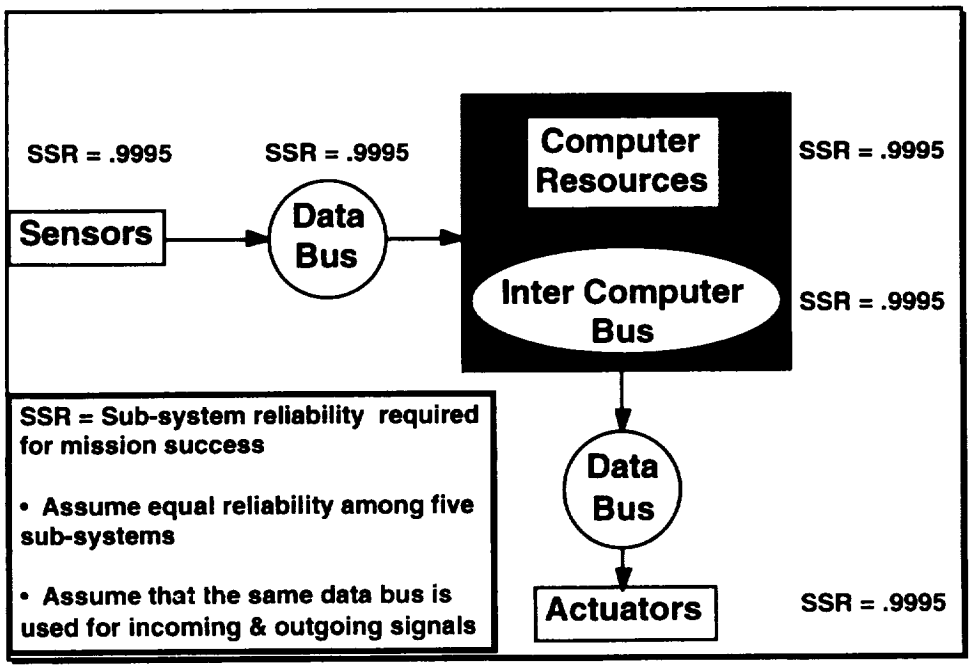

Figure 3.4.0.c Estimated Avionics sub-system reliability

The avionics system level reliability was then divided equally among the avionics subsystems.

3.4.0.3.2. Reduced Ground Operation Costs

Ground operation costs contributed a significant amount of expense to the overall life cycle cost, up to 80% percent in some cases[37]. The Mission Analysis Team identified reducing ground operation costs as a major cost saving strategy. The data management sub-system reduced these costs by imposing the following requirements:

- Reduce maintenance
- Simplify maintenance and/or installation procedures
- Simplify pre-flight testing procedures
- Transfer mission control functions from to ground to launch system creating a more autonomous control

These four requirements were based on trends in modern avionics system that were trying to lower the cost of avionics ownership.

3.4.0.3.3. Transferability

Transferability was the ability to use the same components in both the crewed and un-crewed configurations of the launch system. The Systems Integration Team requested that the avionics be transferable in order to lower R&D and recurring costs. So, the data management sub-system components used the same hardware and tried to use as much of the same software on both mission configurations.

3.4.1. Data Management and Processing

The data management sub-system was divided into two areas: the computer resources area and the vehicle network area.

The vehicle network gathered information from sensors and other devices (man-machine interfaces, communication receiver,etc.) then delivered this information to the computer resources. The computer resources processed the information and returned command signals or telemetry back to the network for distribution to the proper actuators/effectors and other devices. The computer resources area was divided into two sub-areas; hardware and software.

[37] Ricks, Allen (1994). Weekly Reports

The requirements and trade studies of each area are discussed below and the integrated data management sub-system design is presented at the end. The three areas were coupled together requiring an iterative design process. Due to time constraints, this design was iterated once and may not be the optimum design.

3.4.1.1. Computer Resources

This section describes the computer resources requirements for both the hardware and software sub-areas. The hardware included the computer units while the software included the operating system and the application programs. Trade studies on computer system architecture and computer type are also presented in this section.

3.4.1.1.1. Computer Resources Requirements

The computer resources requirements consisted of: reliability requirements, physical placement of components, failure modes, extent of computer control, and amount of processing power needed. The requirements were as follows:

- Reliability of .9995
- Physically centralized architecture
- Graceful degradation
- Autonomous Control
- Perform 16 top level functions
- Peak throughput ≈ 39 MIPS
- Average throughput ≈ 10 MIPS

The systems integration team decided to select the physically centralized architecture for lower recurring costs. Thus, this became a requirement and was not subject to trade. In the crewed missions, the physically centralized architecture allowed the computer units to be reused, lowering the recurring cost. This architecture also reduced maintenance and installation costs.

The maintenance costs on a physically centralized architecture were lower because components were located at a single easily accessible point. This principle also applied to installation. So, a physically centralized architecture complemented the requirement of reducing ground operation costs.

Graceful degradation was the ability of a system to continue to perform critical functions that were needed for survival in the presence of faults. The computer resources area was able to gracefully degrade to meet the 99.9 % reliability requirements for crew survival. The computers were responsible for performing most of the critical functions (see Table 3.4.0.a) aboard the

vehicle and thus ensured that the functions needed for crew survival were still met in the presence of a fault.

Autonomous or on-board control of the vehicle was selected as a requirement to reduce the ground costs. This requirement translated to less ground support during a mission but more sophisticated on-board software. The concept of using more complex avionics to reduce ground support costs was a growing trend in modern avionics systems and was considered a viable way to reduce overall life-cycle costs[38].

Computer throughput was the number of instructions executed by the computer per second and was a measure of computer processing power. The more throughput required to perform a function, the more computer processing power was needed. The throughput required for a function was also related the to the amount of software needed for that function. This relation was:

$$\frac{\text{Throughput}\left[\text{Instr.}/\text{sec}\right]}{\text{Frame Rate}\left[\text{sec}\right]} = \text{Instructions per Execution}$$

In this report, instructions per execution was approximated as lines of code. Lines of code for functions were referenced from existing software or approximated by analogy from similar software requirements. From this equation, the software requirements of each function were converted into throughput requirements (see Appendix A.3.4.0.1).

Since all functions are not performed for the entire mission, throughput was a function of the mission phase . The maximum amount of throughput was needed during the ascent phases. The average amount of throughput occured during the orbit phases.

The landing control function (a sub-function of the control function) could have been completely automated with a minimal increase in the total software costs, under 3%. This function was chosen not to be automated by the Systems Integration Team. It was decided to use a human controlled-computer assisted combination to keep with NASA's tradition of having a crew member "in the loop".

[38] Lala, Jaynarayan et el. (1990). Advanced Information Processing System (AIPS) - Based Fault Tolerant Avionics Architecture for Launch Vehicles

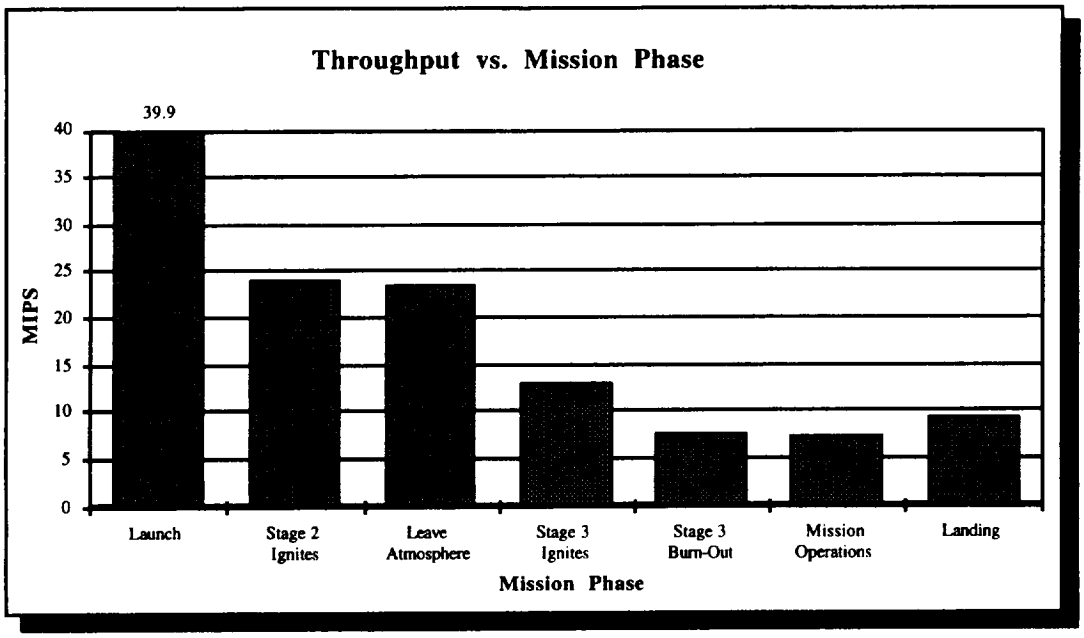

Figure 3.4.1.a Throughput vs. Mission Phase. Note: 10% margin on Throughput

The winds ahead determination function sensed wind gusts in front the vehicle during ascent. The computer used this information in a feed-forward loop to compensate for the wind disturbances. Normally, a wind profile was calculated on the ground and was up-loaded to the computers before launch. The software costs to perform this function on board was very expensive, 12% of the total software costs. Since winds ahead determination was still in the development phase, quantitative benefits of performing this function on board were unavailable. However, winds ahead determination was chosen to be performed by the on-board computers. This decision was made by the Mission Analysis Team who wanted a trajectory that was independent of wind profiles (i.e., wanted to neglect the effects of wind disturbances).

3.4.1.1.2. Computer Resources Trade Studies

Two trade studies were conducted to characterize the computer resources area. These were a functional architecture trade study and a computer unit trade study. The functional architecture type was the driving parameter in the computer resources area.

3.4.1.1.2.1. Functional Architecture Trade Study

This trade study examined five types of functional architecture. A functional architecture defined the structure of how the computer units were grouped together. This grouping affected reliability, cost, and performance of the computer resources area. It should be noted that a functional architecture was

different from a physical architecture. This trade study considered only functional architecture types.

3.4.1.1.2.1.1. Architecture Types Considered

The three main architecture types considered were centralized, federated, and distributed. Three different distributed architecture types were considered. These were the distributed, distributed-modular, and distributed-modular redundant.

3.4.1.1.2.1.1.1. Functionally Centralized

The centralized architecture was an older style architecture used until the 1970's. One main computer unit was used to perform the calculations for all the functions. The sensors, actuators, and other devices were connected directly with the main computer.

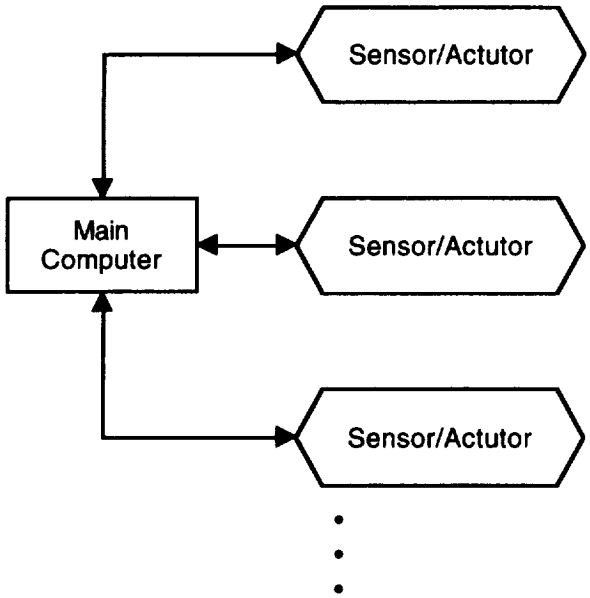

Figure 3.4.1.b Functionally centralized architecture

This architecture was ruled out because a single main computer could not meet the maximum throughput requirements.

3.4.1.1.2.1.1.2. Functionally Federated

The federated architecture was used on the Space Shuttle and was common aboard aircraft of the 1980's. Each computer was responsible for performing a specific function or a group of functions. For example: computer A performed propulsion control; computer B performed guidance, navigation, and control; computer C performed system health monitoring; and computer

D performed sensor processing. Each computer had its own data bus (or network) and shared information with other computers over an inter-computer data bus. Some architecture types used a main computer to process and control the information in the inter-computer network.

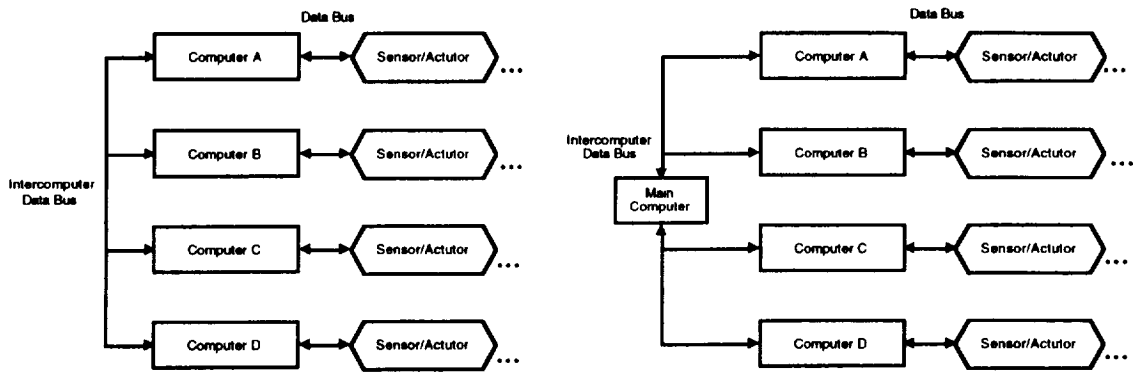

Figure 3.4.1.c Two versions of a functionally federated architecture. For example: computer A performs propulsion control; computer B performs guidance, navigation, and control; computer C performs system health monitoring; and computer D performs sensors processing.

In a federated architecture, the computer units along with the sub-systems they control were designed, built, and tested separately. The advantage of this was that the design of the sub-systems was easier since they were not interconnected. The disadvantage was that the sub-system parts were not interchangeable; increasing non-recurring and recurring costs.

3.4.1.1.2.1.1.3. Functionally Distributed

The distributed architecture was planned for use on the F-22 and other modern aircraft. In this architecture, any computer could perform any function. Responsibility for given function was allocated to a specific computer in real time by the systems executive software. For example: during launch computer 1 performed propulsion control; computer 2 performed guidance, navigation, and control; computer 3 performed system health monitoring; and computer 4 performed sensor processing. During orbit, computer 1 performed an automatic rendezvous maneuver; computer 2 performed system health monitoring; computer 3 performed sensors processing; and computer 4 was switched off-line to save power. So, a distributed architecture used the computer resources efficiently. All the computers shared information over a common network. If inter-computer communications required greater data rates than those supported by this common network an inter-computer data bus was required.

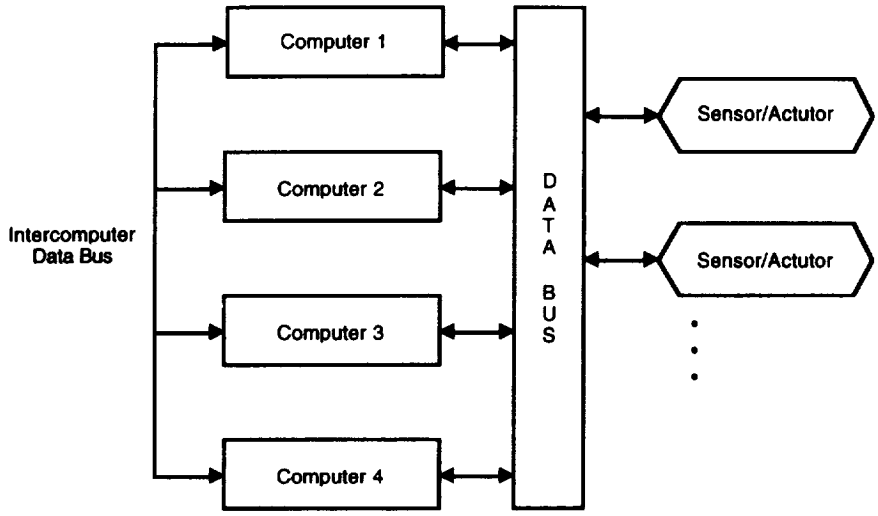

Figure 3.4.1.d Functionally distributed architecture

3.4.1.1.2.1.1.4. Functionally Distributed-Modular

The functionally distributed-modular architecture operated in the same manner as the functionally distributed architecture. However, the computer units in the distributed-modular architecture were composed of standard modules. A standard module was a circuit card that performed a certain task in the computer. Typical modules forming a computer unit included a processor module, a memory module, a power module, and an input-output module.

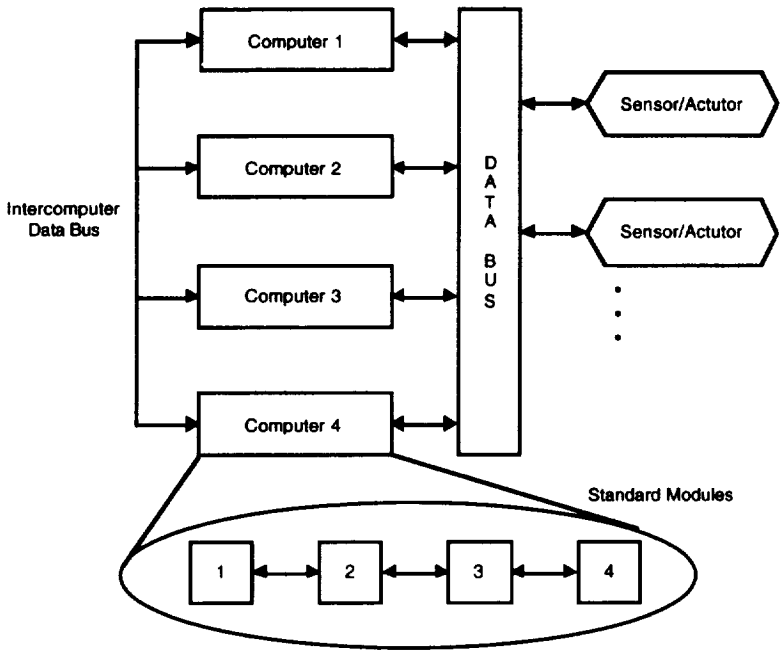

Figure 3.4.1.e Functionally distributed-modular architecture. Each computer unit is composed of standard modules.

The concept of the standard module was developed by the U.S.A.F.'s Pave Pillar program. These standard modules were the basic building blocks for any computer system and thus could be used in a wide variety of platforms. For example, the same modules found in the F-22 could be found in future space station. Using modules across a wide variety of platforms allowed these programs to share development and manufacturing costs.

Computer units using standard modules could isolate faults down to the module level. This ability allowed the faulty module to be replaced instead of replacing the whole computer unit which had to be shipped to a maintenance facility to locate the fault. Standard modules, often referred to as Line Replaceable Modules, replaced the concept of Line Replaceable Units or black boxes.

3.4.1.1.2.1.1.5. Functionally Distributed-Modular Redundant

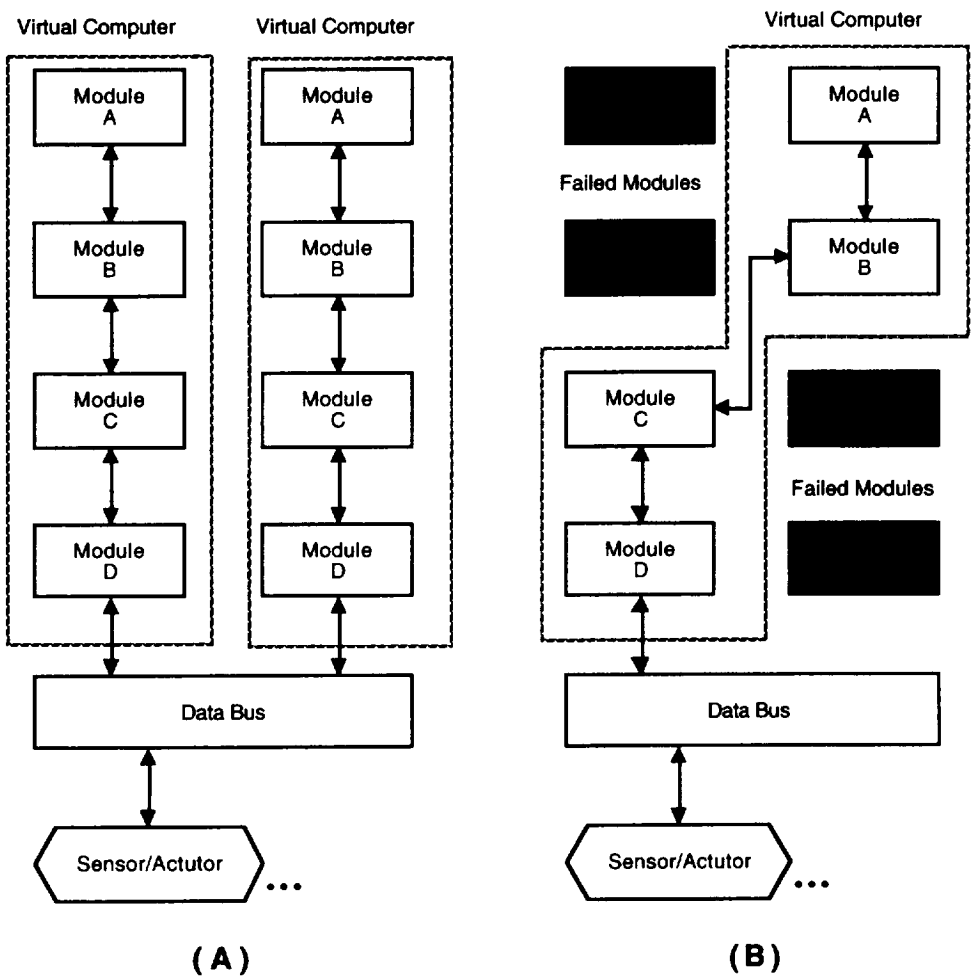

Figure 3.4.1..f (A) Functionally distributed-modular redundant architecture (B) Functionally distributed-modular redundant architecture operating in the presence of faults.

C-2.

The functionally distributed-modular redundant architecture was an advanced form of the functionally distributed-modular architecture because it could configure the connections of module to form virtual computers.

This architecture was not further considered because it was still experimental and did not meet the 1994 technology cut-off date.

3.4.1.1.2.1.2. Reliability Analysis

The purpose of this analysis was to determine how many redundant computer units were needed for each architecture type to meet the computer resources requirement of .9995. This requirement was divided evenly among the three main mission phases.

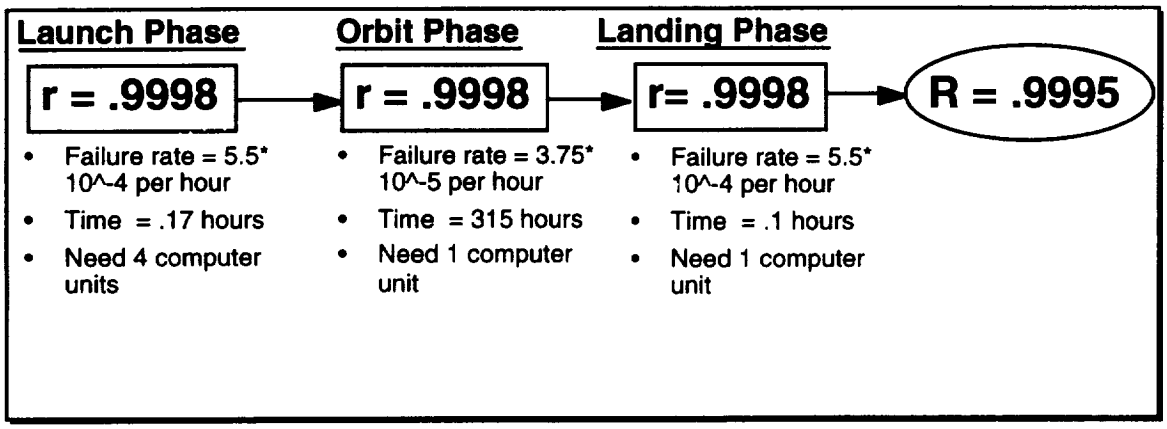

Figure 3.4.1.g Reliability Model as a function of mission phase.

The individual reliability of a computer unit was calculated from the failure rates and flight times. The results are as follows:

- Launch phase = .9999
- Orbit phase = .987
- Landing phase = .99993

The federated architecture used the following model to calculate the order of redundancy:

$$R = \left[1-(1-r)^n\right]^i$$

R = required mission phase reliability
r = computer unit reliability
n = order redundancy
i = required number of computer units

Since the distributed architecture could reallocate functions in the advent of a failure, a different model was developed:

$$R = \sum_{m=0}^{k} \frac{j!}{(j-m)!(m)!} r^{(j-m)} (1-r)^{m}$$

R = required mission phase reliability
r = computer unit reliability
j = number of computer units
k = number of faults tolerated. This equals number of computer units minus number of required computer units (j-i)

The result of this analysis indicated that a distributed architecture needed three less computer units than a federated architecture to achieve the same reliability requirements.

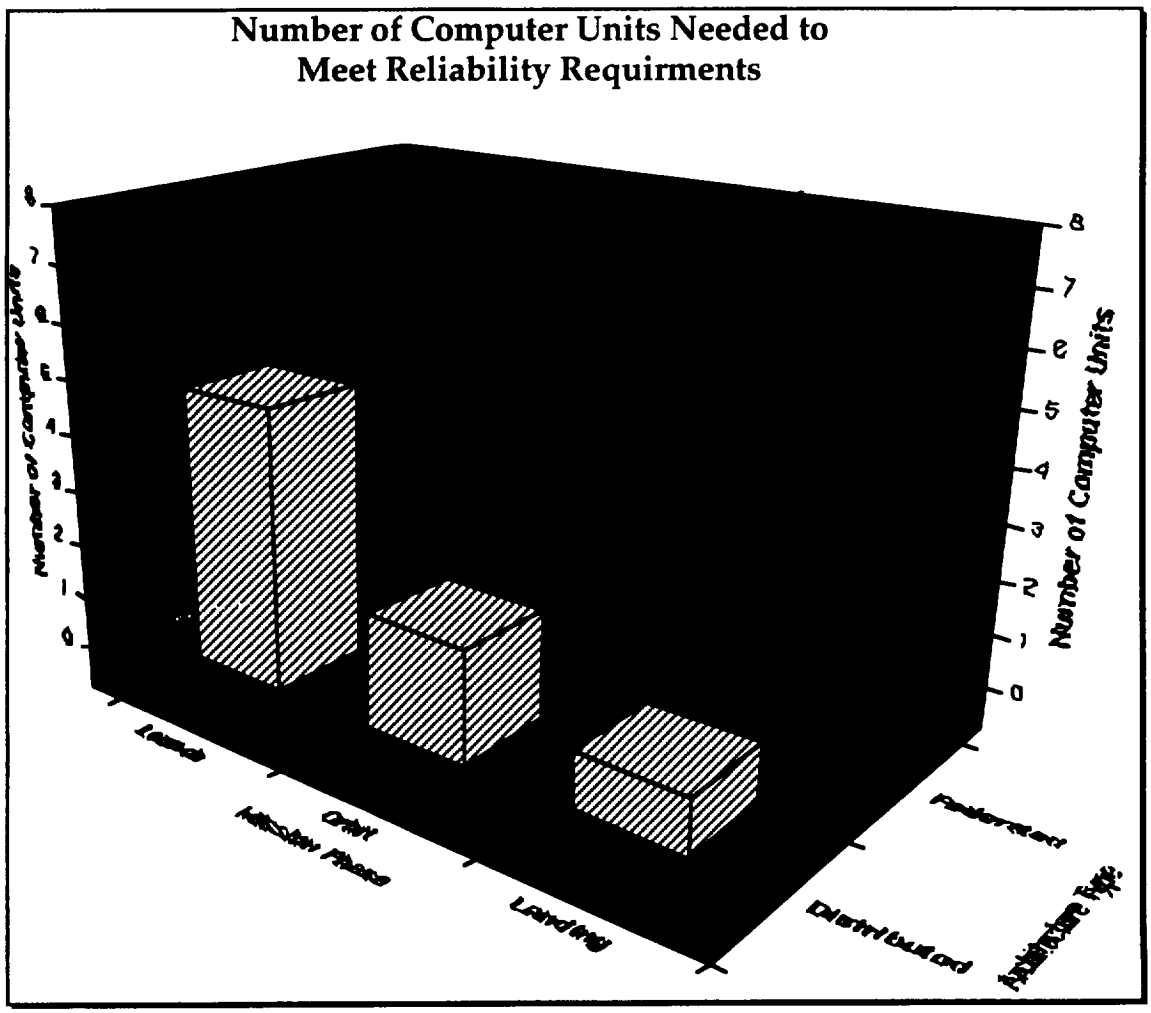

Figure 3.4.1.h Results of reliability analysis. Number of computer units needed is a function of mission phase and architecture type.

3.4.1.1.2.1.3. Cost Analysis

The purpose of this analysis was to determine the cost of developing and producing the different architecture types. The cost considered were research and development of the computer units (non-recurring), first unit production of the computer units (first unit recurring), and the cost of the additional software to manage a functionally distributed architecture. The non-recurring and recurring costs were estimated by empirical formulas based on the mass of the computer units. The distributed-modular architecture was modeled to receive a 50% reduction in non-recurring cost due to use of standard modules. The software costs were estimated from lines of code of similar software packages. The results are shown below:

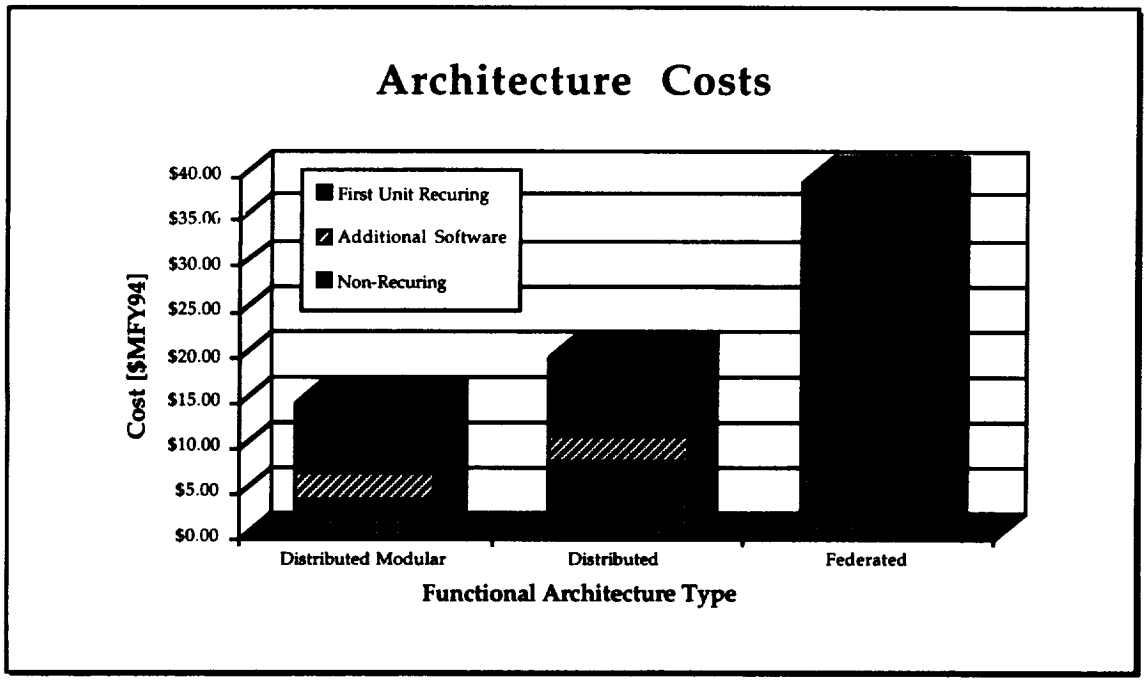

Figure 3.4.1.i Functional Architecture Type Vs Cost

3.4.1.1.2.1.4. Conclusion

A functionally distributed-modular architecture was chosen as the architecture for the entire Vehicle. The reduced costs and number of computer units along with other qualitative factors led to this decision. The table below summarizes the comparison of architecture types.

	Centralized	Federated	Distributed	Distributed -modular	Distributed -modular redundant
Feasible	No	Yes	Yes	Yes	Yes
Meets Technology Cut-off Data	Yes	Yes	Yes	Yes	No
Cost [$MFY94]	NA	39	20	15	NA
# of Computer Units	NA	8	5	5	NA
Grace Degradation	No	No	No	Yes	Yes
Development Risk	Very Low	Very Low	Low	Medium	High
Expandability	Difficult	Medium	Easy	Very Ease	NA

Table 3.4.1.a Summary of functional architecture trade study.

3.4.1.1.2.2. Computer Unit Selection

The decision to go with the functionally distributed-modular architecture required a modular computer unit. A computer unit, based on the Advance Fault Tolerant Processor was chosen because of its modular design. This computer unit had the following specifications:

- 32 bit RISC instruction set architecture
- 50 MHz
- 15 MIPS after processor overhead
- Mass = 13 Kg
- Power = 33 W
- Volume = .22 m^3

The computer unit was composed of the following nine modules:

- Inter Computer Interface Sequencer Module
- Shared Memory Module
- Memory Module (x 2)
- Computational Processor Module
- Input/Output Processor Module
- Power Module
- Input/Output Sequencer Module (x 2)

This computer was compared to other types of computer units to verify that a modular computer unit was the optimal choice. Computers based on Mil-STD 1750, RISC, and 80386 instruction set architecture (ISA) all had similar throughput, mass, and power specifications[39]. The RISC ISA seemed to be becoming the industry standard while the Mil STD 1750 and 80386 ISA was being phased out. Obtaining spare parts in the future could become expensive

[39]Larson and Wertz, (1992). Space Mission Analysis and Design

if an outdated ISA was selected. So, a computer unit based in the Advance Fault Tolerant Processor, with its modular design and RISC ISA, was chosen for the computer resources area.

To provide the required 39.9 MIPS at maximum throughput, four computers were needed. At average throughput (10 MIPS) one computer unit was needed. As a preliminary design procedure, the computer units used less than 70% of their useful throughput. The final design included five computer units to meet the reliability requirements.

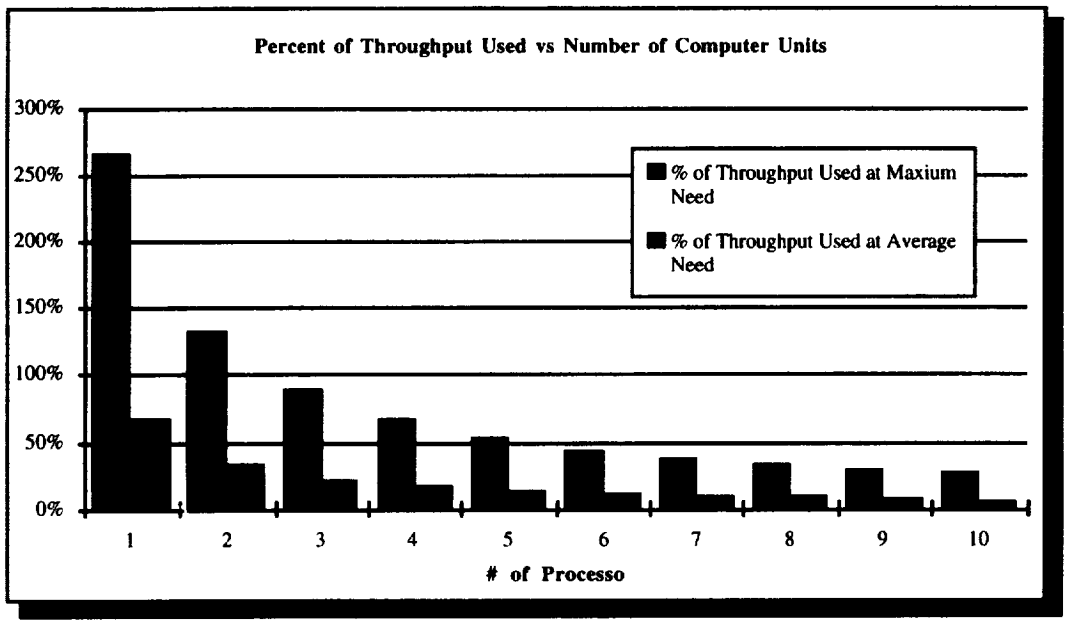

Figure 3.4.1.j Percent of throughput used Vs number of computer units for both maximum and average throughputs.

3.4.1.2.Vehicle Network

The vehicle network was composed of two major areas; the transmission medium and the remote data units. The Remote Data Units (RDUs) gathered the information from sensors or other devices (i.e. man-machine interfaces) and prepared this information for transmission. The RDUs also received information and prepared it for use by actuators or other devices. The transmission medium passed information between the computer units and the RDUs.

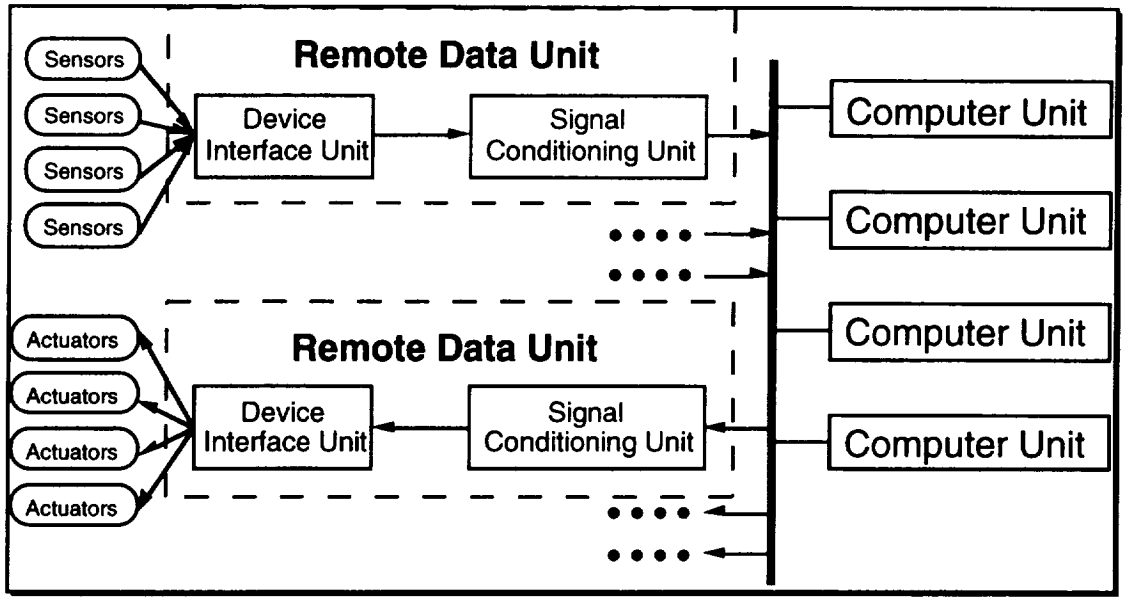

Figure 3.4.1.k Role of the remote data units

3.4.1.2.1. Network Requirements

The vehicle network had two main requirements. The first requirement was that the network must deliver the information in a timely manner. This requirement is stated as transmission rates. Transmission rates state how much information the network must handle. A transmission or data rate was calculated by the following equation:

Sampling Rate of Sensor [Hz] * Bits/signal [b] = Data Rate [b/sec]

Data rates were calculated for each sensor. A summary of the required transmission rates is shown below:

Functions	Transmission Rates [bits/sec]
Propulsion control (per engine)	553,900
Fluids management (per module)	20,000
G,N,&C	67,600
Life Support, Power, Thermal, etc.	23,000

Table 3.4.1.b Summary of transmission rates

All ground communications were routed through a computer unit via the vehicle network for processing. Using the vehicle network to carry ground communications, reduced the number of separate networks and thus reduced mass. However, the high transmission rates associated with ground communications required a high performance transmission medium that might have raised costs. The following ground communications would like to be routed through the vehicle network if it was cost effective.

Communications (voice)	≈ 192,000 b/sec
Communications (telemetry)	≈ 4 Mb/sec
Communications (Video)	≈ 1.55 Mb/sec
HDTV	≈ 100 Mb/sec

The second requirement was that the network must be able to interface with all sensors, actuators, effectors, and man-machine interfaces and have control over the flow of information. A remote data unit was used to meet this requirment. This remote data unit was composed of two sub-units. The signal conditioning sub-unit interfaces performed the byte-to-light and light-to-byte conversion. The device interface units controlled the flow of information, specifically it performed the following functions:

- Analog to digital or digital to analog conversion
- Implementation of the network protocol
- Support multiple devices
- Multiplexing and Demultiplexing of signals

3.4.1.2.2. Vehicle Network Trade Studies

Two trade studies were conducted to characterize the computer resources area. These were a network topology trade study and a transmission medium trade study. In order for the network to function properly, the network architecture and transmission medium were required to be compatible with each other.

3.4.1.2.2.1. Network Architecture Type Trade Studies

The network architecture determined how the terminals, the RDU's and computer units, were connected. The topology also drove the network protocol that controlled the flow of information.

3.4.1.2.2.1.1. Topologies Considered

The three architecture types considered were the token ring network, the token bus network, and the fiber distributed data interface network.

3.4.1.2.2.1.1.1. Token Ring Network

The token ring network connected the terminals in ring topology and allowed each terminal to transmit when it received the token. This was a common topology in local area networks (LANs) and supported both fiber optic and coaxial cable.

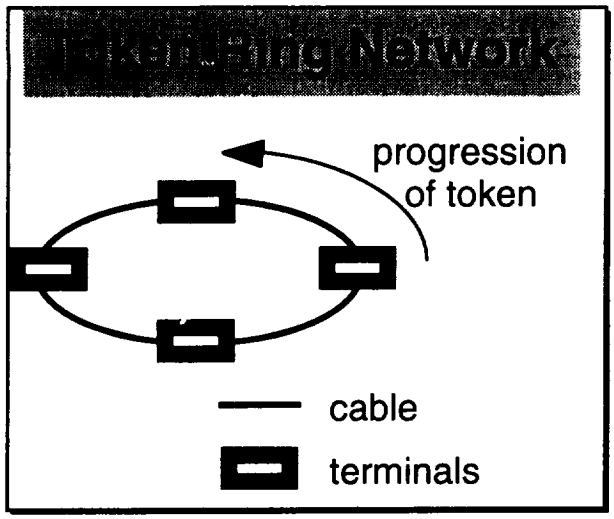

Figure 3.4.1.l Token ring network

In the token ring network, terminals could not be removed without breaking the ring and rendering the network inoperable. To use this topology, multiple rings were needed with each ring requiring a separate interface to the computer units.

3.4.1.2.2.1.1.2. Token bus network

This topology used the same token passing protocol as the token ring network. The major difference in the two networks was that terminals could be easily removed from the token bus network. This network supported coaxial cable and could support fiber optic cable over short distances using a combination of active and passive repeaters.

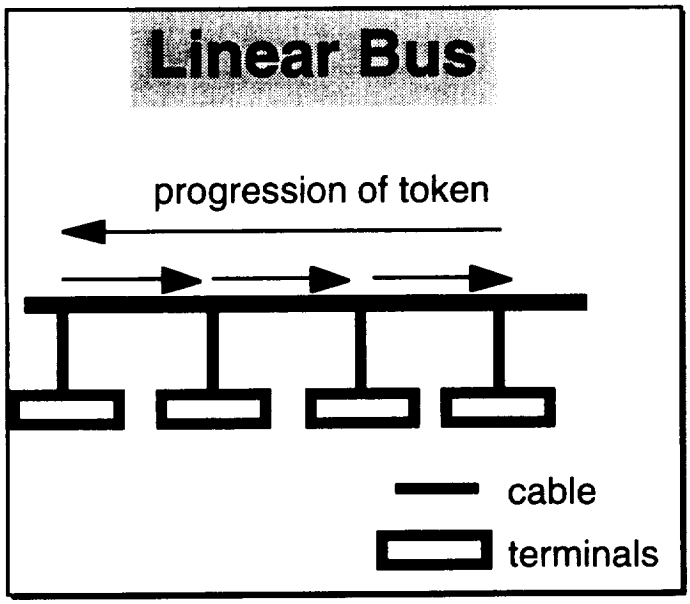

Figure 3.4.1.m Conceptual diagram of token bus network.

3.4.1.2.2.1.1.3. FDDI

This network used the token passing protocol and employed a dual ring topology. When a terminal received the token, it transmitted in the direction closest to the receiving terminal. If a terminal was removed, the network re-configured itself into a token ring topology.

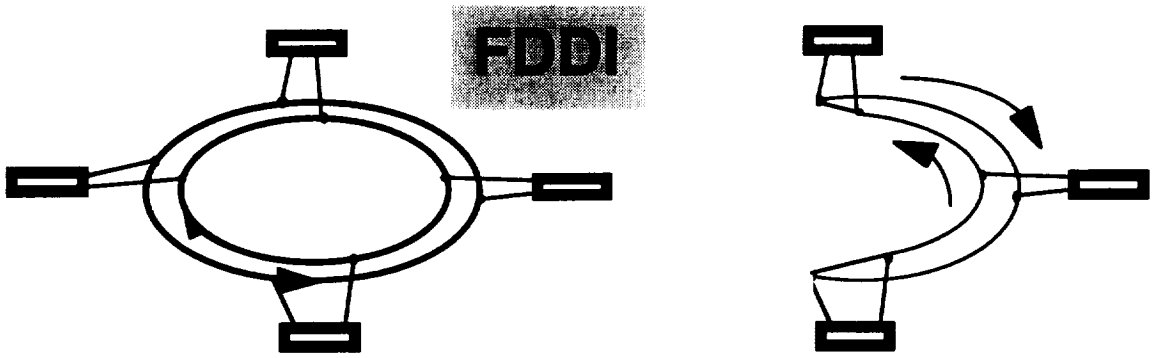

Figure 3.4.1.n Conceptual diagram of Fiber Distributed Data Interface, FDDI. On right, FDDI when a node is removed.

The token bus network was chosen for its ability to easily remove nodes and simpler design. The token bus network could support transmission rates as high as 50Mbit/sec. This allowed the network to meet all transmission requirements and all ground communications transmission rates except the HDTV data rate. So, all ground communications would go through the vehicle network. The RMS camera, which was high definition quality, would be a separate closed circuit camera.

3.4.1.2.2.2. Fiber Optics vs. Cable

Fiber optic cables offered increased performance, lower mass, and lower costs than coaxial cable. However, the remote data units and computer units needed the ability to convert between digital signals and light signals. The bit-to-light conversion circuitry increased the cost of a fiber optic network significantly. The Systems Integration Team opted for the fiber optic network for its reduced mass.

	Coaxial Cable	Fiber Optic
Cost ($/km)	5000	1000
Mass (kg/km)	1500	100
Spark Hazard	High	None
EM Interference	Low	None
Data Transfer Reliability	High	Very High

Table 3.4.1.d Fiber optic cable Vs coaxial cable

3.4.1.3. Integrated Data Management Sub-System

The data management sub-system was a state-of-the-arts avionics system. This system performed numerous functions on-board and supported high data rates: The features of this system included:

- physically centralized architecture
- functionally distributed architecture
- quad redundant high speed fiber optic data network
- 5 modular computer units using RISC ISA
- linear token bus network
- 82 remote data units each supporting 40 devices

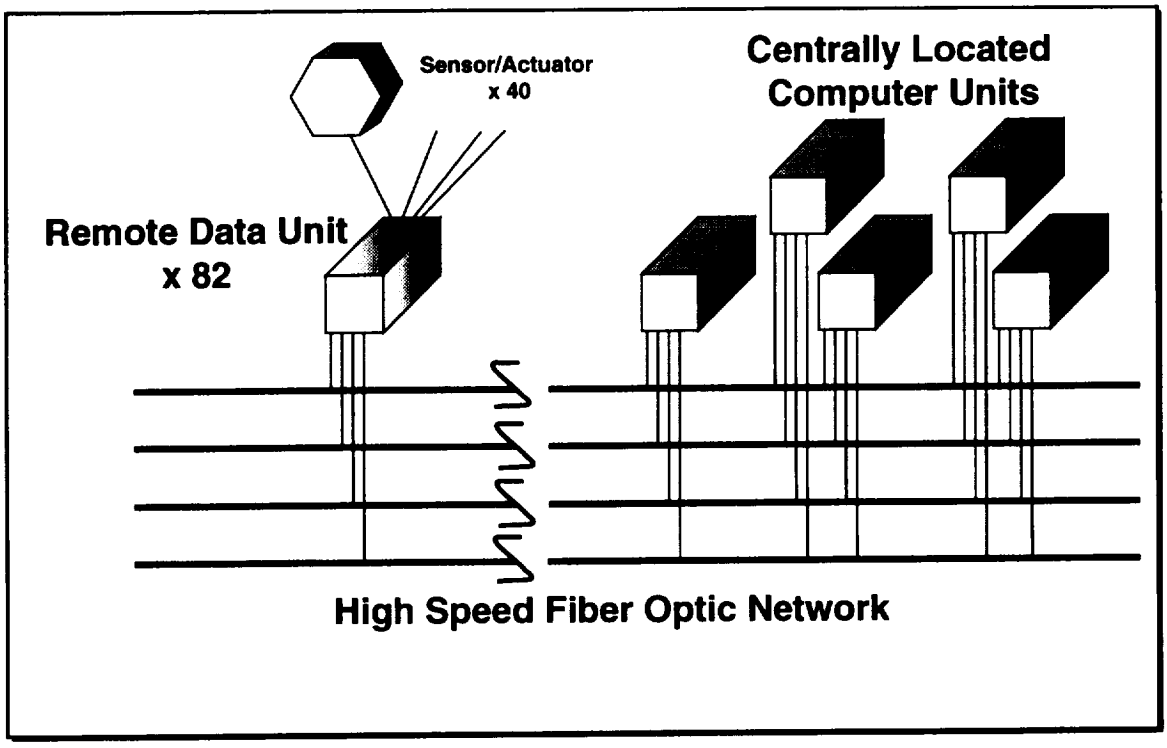

Figure 3.4.1.o Integrated Design of the data management sub-system

3.4.2 Navigation, Guidance, and Control - Manned Mission

3.4.2.1 Introduction

An autonomous integrated navigational system was proposed for the spacecraft using onboard Global Positioning System (GPS) and Inertial Navigation System (INS) measurements. The spacecraft carried all the NG&C system components. The launch vehicle received commands and

return feedback via an umbilical link. The accuracy requirements of NG&C are outlined in Table 3.4.2.a.

Because the accuracy of the inertial system degraded with time it had to be upgraded with Kalman filter by input data from GPS and Star Tracker. Configuration of the update sensors varied with flight phase. See Table 3.4.2.b.

Ascent Phase: Spacecraft received measurements from INS, GPS, and air data system for closed loop guidance to LEO.

On-orbit phase: The spacecraft used inertial navigation integrated with GPS to determine position and velocity. Attitude was updated by Star Tracker (ST).

Return Phase: Spacecraft performed return guidance. During radio blackout measurement was provided by INS. Post blackout phase reintroduced GPS navigational measurement. Air data measurement was initiated after 150 km.

Precision Landing phase: The Microwave Landing System (MLS) was released at the beginning of Terminal Area Energy Management (TAEM) interface which was assisted by Radar altimeter for approach and landing.

	Sensor					
Phase	km	IMU	GPS	ST	MLS	RA
	0					
Ascent						
	500,600					
On-orbit	500,600					
Entry Interface	120					
	100					
Radio Blackout						
	50					
TAEM Interface	21					
Landing Interface	3					
Groundsurface	0					

Table 3.4.2..b Sensor Configuration

Mission Phase	accur			accur
Ground Alignment,	180		Entry navigation positio	
azimuth, arc-sec, 3-sigma			at end of blackout	
			nmi, 3-sigma	
Ascent Navigation			RSS	9
performance, in plane, rms			Downrange	8.4
Position, ft	1300C		Crange	2.7
Velocity, ft/s	5		Altitude	1.1
Onorbit alignment	180		Landing, autoland	
(ST) arc-sec, 3-sigma			navigation position at	
			touchdown, ft, 3-sigma	
On-orbit navigation			Downrange	90
performance			Crossrange	40
Position, ft	220		Altitude	8
Velocity, ft/s	0.3			

Table 3.4.2.a NG&C Accur. Requirements

3.4.2.2 Primary Navigation System

GPS/INS was chosen as the primary navigation system. The system met all the positioning accuracy requirements during its implementation phases. With ST it achieved 13m accuracy, well within the most stringent accuracy requirement, on-orbit phase. Based on the fact that the spacecraft would be operating at no greater than 600 km in LEO, GPS was a practical candidate for navigation measurement. However, standalone GPS did not meet accuracy

nor reliability requirements in every phase of the mission. The following navigation systems were also considered.

MANS: Highest achievable accuracy was only 100 m, therefore not satisfying accuracy requirements. Information to accommodate system drivers was not available.

Pure INS: Failed in a cost and performance study to a GPS/INS system. A cost analysis by General Dynamics Space Systems Division of GPS/INS vs. pure INS over a 150 mission cycle claimed that there were substantial savings with integrated GPS/INS navigation (Maki 1990). A summary of the results are in Table 3.4.2.c

Integrated GPS/INS was chosen based on the following system drivers:

GPS Adaptability

- Reconfiguration to relative GPS for proximity and rendezvous operations (see section 3.3.4.6)
- In the future, use of GPS for attitude determination using additional techniques such as differential GPS, interferometric carrier phase processing, velocity, and attitude vector matching (Upadhyay 1993)
- Time Code (time synchronization of all systems)

Subsystem Savings

Integrated GPS/INS offered considerable cost savings over conventional pure INS based navigation systems. A study conducted by General Dynamics - Space Systems Division claimed that with integrated GPS/INS the overall performance was not compromised with a less accurate, cheaper INS component (see Table 3.4.2.c) (Maki 1990). A more detailed cost outline along with the specifications of the sensors used in the study is given in Appendix A.3.4.2.2. GPS/INS also offered substantial volume, weight, and power savings over pure INS based systems. A comparison to STS is provided in Table 3.4.2.d (Miller 1991). The subsystems savings over the shuttle amounted to the following:

volume savings	64%
mass savings	72%
power savings	3 1%

		GPS/INS	Pure INS
Production Cost		$229K	$493K
(Redundant shipset)			
Operations Cost		$3.5M	$15.9M
(150 missions)			
Performance		35 m SEP	1000 m rms
Measure		0.1 m/s	1 m/s

Table 3.4.2.c GPS/INS vs INS, Gen Dyn. Space Div. Itemized table given in Appendix A.3.4.2

	no.	vol (m^3)	m (kg)	pwr (watts)
Suttle orbiter				
AA	4	0.007646	4.536	14
RGA	4	0.047861	39.917	92
RAINS	3	0.08496	59.195	546
TACAN	3	0.035683	40.824	90
RA	2	0.002832	4.0824	8
ST	2	0.053242	11.431	44
MSBLS	3	0.045878	31.979	75
	Totals	0.2781	192	869
Proposed Design				
Sensor		Vol (m^3)	m (kg)	Pwr (Watts)
GPSR	2	0.004	4.54	6
INS	3	0.06	57	120
ST	2	0.06	26	33
MLS	3	0.045	32.1	75
RA	3	0.003	6.12	12
prox	2	0.003	6.12	12
RVR	2	0.003	6.12	12
	Totals	0.178	138	270

Table 3.4.2.d STS sensors by Honeywell Space Sys vs proposed spacecraft

Accuracy Capability

When configured with a Star Tracker, integrated GPS/INS achieved better positioning error estimation using Kalman filtering. An accuracy comparison by Toshiba Corporation, Space Programs Division was made from the following sensor configurations intended for the on-orbit phase (Harigae 1989) .

INS GPS
GPS/INS GPS/INS/STAR

SYSTEM	SENSOR	Qual.
INS	gyro	
	non g-sensitive bias	1.0 deg/h
	g- sensitive bias	1.0 deg/h
	accelerometer	
	bias	1E-2 m/s
	scale factor	< 0.1
GPS	1 ch. C/A code receiver	
	position error (1 axis)	40 m
		(1 sigma)
STAR	CCD type sensor	
	random error	1 arcsec
	quantization error	20 arcsec

Table 3.4.2.e Performance of sensors, Toshiba Corporation, Space Programs Division

		Static phase		Dynamic Phase	
System	pos (m)	Attit (deg)		pos (m)	Attit (deg)
GPS-INS-STAR	37	0.15		13	0.09
GPS-INS	348			98	0.09
INS-STAR	11km	0.42		235km	1.67
GPS alone	44			22	

Table 3.4.2.f Results of Toshiba Corp. Study

3.4.2.2.1 Navigation System Components

Navigation systems were based on off-the-shelf already existing hardware and software components to reduce non-recurring costs.

3.4.2.2.1.1 GPS

The GPS receiver (GPSR), coupled with the INS would determine position and velocity measurements. The receiver's implementation into the navigation scheme would be under the responsibility of the Kalman filter, discussed in section 3.3.4.2.1.3. GPS provided accurate measurement when there were four satellites available (it used the additional satellite as a cross check). When there were fewer than four, GPS accuracy degraded (Negast 1991). GPS degradation detection was handled by the Kalman filter, discussed further in section 3.3.4.2.1.3 . It was assumed that the spacecraft would not have access to selective availability, therefore the GPS receiver would only receive CA code. Carrier cycle slip detection and phase ambiguity was addressed in the receiver itself. A GPS-standalone mode was required to handle on-orbit navigation in the event of INS failure, but otherwise it would operate in cooperation with the INS tightly integrated by Kalman filtering.

The GPSR selected was a TANS II six channel continuous tracking receiver, providing three-dimensional positioning, velocity and time over dual digital interfaces. It was manufactured by Trimble Navigation Ltd.

Sensor	Type/Contrac	Quality	Accur.
GPS	TANS II	6 ch. CA code	
	Trimble	pseudo-range(pos	25m (3 sigma
	receiver	TFF	< 90 sec
	antenna	range-rate	.2m/s
		time	1ms

Table 3.4.2.g GPSR specifications, Jane's Avionics

GPS would purposely not be implemented into the navigation scheme during blackout phase nor the precision landing phase. During blackout it was assumed no reception of GPS signals was possible. During landing phase absolute GPS did not satisfy FAA type I, II or III landing standards nor Space Shuttle automatic landing requirements (Arnold 1991) (see section 3.4.2.5).

3.4.2.2.1.2 The Inertial Navigation System

The INS was required to make position, velocity, acceleration, and attitude measurements during all phases of the mission. Other than blackout and landing phases, it would be tightly coupled with GPS for determining position and velocity. INS - standalone had the ability to make accurate measurements in the event of GPS satellite dropout (Ward 1992) (see section 3.4.2.2.1.3). An interferometric fiber optic gyro (IFOG) with pendulous accelerometers was chosen due mainly to cost savings. The following inertial navigation systems were also considered.

Litton nondithered zero-lock laser gyro (ZLG)
Honeywell LINS
Hexad RLG

All of the above high precision INS systems met accuracy requirements, but were rejected due to their high costs, primarily operational costs.

The INS system selected was a Texas Instruments/Honeywell strapdown sensor consisting of three IFOGs and three solid state accelerometers. Because the IFOG, alone, did not achieve the high accuracies of the other candidate INS systems, much more burden was placed on the Kalman filter during normal integrated GPS modes, and especially during standalone INS mode (Ward 1992). Additional data of the INS is given in Table 3.4.2.h.

Sensor	Type/Contrac	Quality	Accur.
INS	Texas Instr		
GYRO (3)	Honeywell	Oper. Stability	.003 deg/hr
	IFOGS	Scale Factor error	10ppm
		Max angular rate	1,000 deg/sec
ACCEL(3)	solid state	Oper. Stability	10micro-g
		Scale Factor error	50ppm
		Max Accel	100g

Table 3.4.2.h INS specifications, Honeywell Inc

3.4.2.2.1.3 Kalman filtering for GPS/INS

Re configurability

Integration of sensor data was performed in Kalman filtering. A software package was necessary which would be capable of switching between Kalman filtering configurations in real time. The software must support the multimode kalman filter. Software sizing is listed in the appendix. The Kalman filter re configured to the following modes.

Integrated GPS/INS ---------- normal operations
Standalone GPS ---------- during INS failure
Standalone INS ---------- during blackout and GPS dropout
Relative GPS/INS ---------- during proximity and rendezvous operations

During the standalone modes the Kalman filter re configured to optimize for the particular standalone sensor, becoming more sensitive to the sensor's inherent error sources. i.e. gyro drift. The Kalman filter also contained software to disregard inputs from GPS in the event fewer than four satellites were available (Negast 1991). A 26 error state Kalman filter was chosen.

Measurement	Error	States	Error	St
Position	3	Baro bias		1
Velocity	3	Gyro bias		3
Attitiude	3	Gyro scale factor		2
Clock bias	1	Accel bias		3
Clock Freq	1	Accel misallign		4
Clock g Sensitive	2	Total		2 6

Table 3.4.2.i Kalman filter error states, Honeywell Inc

Integration Method for Error Determination

The fundamental role of the Kalman filter was to determine errors in sensor data. A full or tightly integrated method was chosen as the integration scheme for GPS/INS. Tight integration took raw data directly from the sensors, combining it in a single Kalman filter. The Kalman filter checked one measurement sensor against the other to determine the most accurate error possible (Negast 1991). The following integration methods were also considered.

Resetting INS parameters with GPS parameters - This was the most primitive integration method for GPS/INS sensors. Since the position and velocity parameters were simply replaced, there was more probability of faulty data being passed on (Upadhyay 1993).

Cascaded filter-driving-filter or loose integration scheme - Data from each sensor was processed in a separate Kalman filter and then combined in an integrating filter. Since GPS and INS data were time correlated, separate Kalman filtering resulted in filter stability problems (Negast 1991).

The tight integration scheme maximized the performance of both sensors using a closed loop scheme. Errors processed in the Kalman filter were sent forward to the sensor in the form of control signals to further reduce the output error (Negast 1991). Some preprocessing was necessary in the GPS receiver to handle for carrier cycle slip detection and phase ambiguity and detection of reduced satellite availability (Upadhyay 1993).

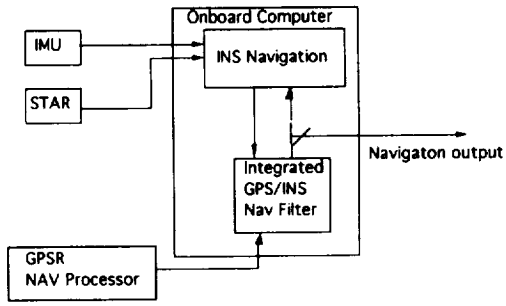

Figure 3.4.2.j Integration of sensors

3.4.2.2.2 Robustness of integrated GPS/INS navigation

During normal on-orbit operations, navigation data from the INS would help determine errors in GPS measurement and GPS data would determine INS errors. Because maximum performance required both sensors to be working effectively, analysis was conducted to insure a robust system overall. An IFOG Inertial Navigation system integrated with GPS was simulated against the General Electric Radio Tracking System (GERTS) by way of TRAJEX, a General Dynamics performance simulation (Maki 1990). The integrated GPS/INS with lower accuracy inertial sensors went through rigorous testing including deletion of accelerometers and GPS dropouts. Gyro drift rates were increased by an order of magnitude. The study showed that both INS and GPS could maintain accuracy standards to continue a mission under degradable conditions.

		Apogee Altitude	Apogee vel
		km	m/s
Nominal		656.8	5788
GERTS (3-sigma)		2.6	5.45
200 deg/hr gyro			
roll		-1.75	4.51
pitch		3.04	-2.35
yaw		1.83	-3.78
GPS dropout last 95 sec		0.455	-8.78
GPS cycle 10 sec on/off		-0.043	0
throughout			
GPS acq. at 250 sec		6.11	-5.67
20 deg/hr gyro			
roll		-0.016	0.076
pitch		0.209	-0.201
yaw		-0.016	0.03
GPS dropout last 20 sec		-0.32	-0.5

Table 3.4.2.k GPS/INS Robustness Analysis conducted by Gen. Dynamics Space Sys. Div.

3.4.2.3 Attitude Determination, Stabilization, & Control

Similar to navigation, the attitude determination sensors and control effectors were configured according to mission phase. The INS gyros measured attitude continually throughout the entire mission phase and were updated by star tracker, air data system, microwave landing system (MLS), and radar altimeter, depending on mission phase.

Ascent Phase: Guidance would perform attitude pitch and yaw a control by thrust vector gimbaling. INS gyros would measure attitude.

On-orbit Phase: INS would perform Attitude measurement by use of gyros and input from star tracker. Control would be accomplished by RCS system.

Return Phase: Return guidance would initiate prior to re-entry and terminate at terminal area energy management (TAEM). Control would be accomplished by RCS cold gas thrusters and phasing in of aerodynamic surfaces at 150 km. INS gyros would make attitude measurement. Air data system would be phased in as an additional sensor to make atmospheric measurements.

Precision Landing Phase: Atmospheric data would come from air data system. INS would measure attitude with respect to a glide slope provided by microwave scanning beam and ground mapping by radar altimeter. Control would be accomplished by aerodynamic control surfaces.

3.4.2.3.1 On-orbit Attitude Determination Sensors

In addition to the INS another sensor was required on board to provide an attitude reference and update the INS. The star tracker was chosen as the updating sensor due to its unmatched achievable accuracy of one arcsec. The sensors in Table 3.3.2.3.1.a were also considered. They were rejected due to not meeting accuracy requirements specified in Table 3.3.2.3.1.a, during their on-orbit implementation.

Sensor	Accur
Earth Horizon	1 arcmin
Sun sensor	6 arcmin
Magnetometer	30 arcmin

Table 3.4.2.l Other sensors considered (Nishimura 1990)

The star tracker chosen was an HDOS HD-1003 charged coupled device (CCD), manufactured by Hughes Danbury Optical Systems, Inc. The HD-1003 had six star tracking capability which allowed determination of attitude about all three orthogonal coordinate axis (Cassidy 1993).

Sensor	Type/Cont.	Quality	Accur.
		Max Accel	100g
ST	HD-1003S	CCD type image sensor	
	Hughes Danbury	Angle	60 arcsec
	Optical	FOV	8 deg X 8 deg
	Sys	Acquis. time	6 sec

Table 3.4.2.m Star Tracker specifications , Proceedings

3.4.2.3.2 Stabilization and Control System

The drivers of the automatic stabilization and control system were to provide maneuvering capability for orientation of the primary propulsion thrust vector and accuracy of control during velocity changes to optimize fuel

consumption. The automatic stabilization and control system could receive input from the attitude reference sensors, manual control, or from guidance commands. Attitude data was processed by the control function of the computer. If a maneuver was necessary, determined by deadband, the computer would initiate control commands to the effectors. A detailed functional block diagram of the automatic stabilization and control system is given below (Chambers 1964)

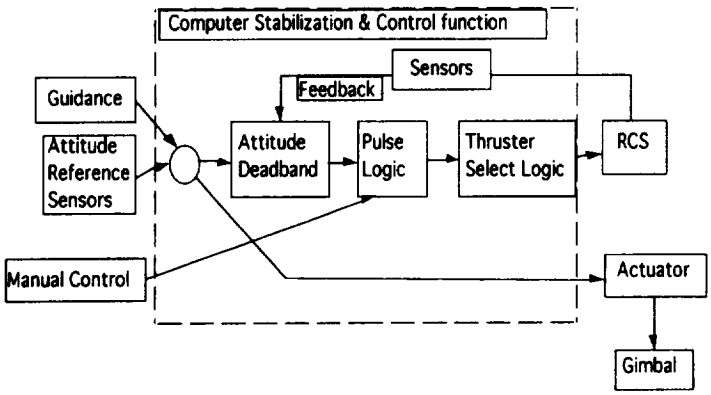

Figure 3.4.2.a Automatic Stabilization & Control System functional block diag.

3.4.2.3.2.1 Control Function of the Computer

The control computer processed measurements from the spacecraft rate (accelerometers) and position (GPS, ST) sensors, combined them with the desired maneuver position information obtained from the guidance system or within the stabilization and control system, and directed commands to the RCS and OMS systems. The control computer was responsible for translation of inertial-axis to body-axis conversions. The specific tasks of the control computer were selection of deadband and rate-to-attitude switching ratio, control and thruster selection switching logic, and stabilization augmentation (Chambers 1964)

3.4.2.3.2.1.1 Selection of deadband

Holding the vehicle to a certain attitude tolerance, deadband, would be dependent on mission phase. Activation of the control system required a breach of the deadband. Therefore, within the deadband no system torques would be produced. The deadband attitude was based on accuracy requirements during the particular mission phases shown below. An upper and lower limit of 5 deg/s was placed on the angular rate in order to initiate a correctional maneuver in a faster response time.

Mission Phase	Deadband Attitude
Coast Phases	(1 degree)
Mid course corrections	(.1 degree)
Rendezvous	(.1 degree)
Re-entry	(.1 degree)

Table 3.4.2.n Deadband Attitudes

3.4.2.3.2.1.2 Stability Augmentation

The Control computer provided spacecraft motion dampening by control feedback and selection of a rate-to-attitude mixing ratio. The rate-to-attitude ratio determined the slope of the switching lines, time when a thrust command was delivered. The rate-to-attitude ratio changed to compensate for changes in spacecraft inertias and disturbance torques. The control computer would determine the rate-to-attitude ratio or would use an averaged value (Chambers 1964).

3.4.2.3.2.1.3 Control Switching Logic

The control computer handled control switching logic by producing minimum impulses as output commands. The pulse width modulation (PWM) power driver was chosen because it allowed for a less than full on or off thrust impulse. The following types of switching logic were also considered.

ON/OFF (Bang-Bang method): The thruster "ON" time was dependent on component lags and hysteresis. System was not capable of optimal performance because it was restricted to either maximum or zero (Chambers 1964).
Logically controlled pulses: There was no optimization for small disturbances. Every disturbance, even small ones, must pass through the high-thrust mode first, before incrementing into the low-thrust mode (Chambers 1964).

The type of PWM was narrowed down to a pseudo-rate pulse modulation and pulse-ratio modulation modulators. Both were combinations of pulse-width and pulse-frequency modulation (Chambers 1964). Both offered the following advantages:

-Less than full-control acceleration could be produced
-Vehicle dampening was less sensitive to inertia changes
-Limit-cycle rates could be reduced until one minimum impulse is used to reverse the vehicle rate at each end of the deadband.
-Minimum impulse rates would reduce to below the rate sensor threshold. For low rates there was inherent damping.

-Effective control of disturbance torques by application of the theoretical minimum control torque.

It was decided that either type of PWM satisfied the control logic function.

3.4.2.3.2.1.4 Thruster-Select-Logic

It was the function of the control computer to determine which arrangement of thrusters was optimal to operate for a translational or rotational motion. Thruster-select-logic determined the least number of thruster operations for each control function.

3.4.2.3.3 Control/Effector Linkage

Linkage from the computer, guidance computer, or manual controller to the effector, was chosen to be fiber optic cable. Control information was distrubited by the vehicle's high speed fiber optic network. The fiber optic network, fly-by-light system, was a quad-redundant, digital system that offered significant mass savings to other control linkage methods. The following control linkage systems were also considered.

Manual-Proportional System: Complicated mechanical linkage was a severe mass and operations disadvantage. Did not provide suitable feedback and stick "feel" characteristics.
Fly-By-Wire System: More massive overall, compared to fly-by-light.

Fly-by-Light is discussed in more detail in the data handling and management section (3.4.1).

3.4.2.3.4 Control Actuators

Actuators were considered for gimbals and valves for both launch vehicle main engines and spacecraft OMS engines and. Additionally actuators were sized for RCS valves and servos for aerodynamic surfaces of the spacecraft. Electrical mechanical actuators (EMA) were chosen mainly due to their savings in operational costs and self check capabilities. All on board actuators were the electrical type.

Centralized Hydraulic Actuators and valves were also considered, but were rejected due to their operational costs. Launch operations costs in terms of work hours demonstrated how time consuming and expensive it was to service conventional hydraulic, fluid, pneumatic, propulsion, and RCS systems (Sundberg 1990).

		% Savings	
Atlas /Centaur	HRS	If EMAs used	Savings
Fluids	4929	10%	490
Hydraulics	2177	90%	1960
Pneumatics	5143	40%	2060
Propulsion	4616	20%	920
RCS	2333	8%	0
		Total	5340 HRS
STS Launch Ops			
Plumbing,vent	2880	20%	576
and drain			
Hydraulics	4236	90%	3812
Propulsion	27200	10%	2720
ACS	5654	8%	0
		Total	16378 HRS

Table 3.4.2.o Man-hour savings for STS and Atlas, NASA,Lewis

Advantages of Electromechanical Actuation

An Assured Shuttle Availability study, conducted by NASA, showed that retrofitting STS with electromechanical actuators and valves would improve STS by the following figures (Sundberg 1990).

- weight savings of 2300 kg
- 10% of total vehicle operational cost
- turn around time would be reduced as to allow at least one additional Shuttle flight per year.

EMAs offered easier access to inspection. Conventional hydraulic actuators required a labor intensive inspection that translated to man-hour and time waste. EMAs could be manually inspected with the use of a power source, but could also have the capability to implement and integrate automated, remote, self check-out through microchip built-in-test (BITE) (Sundberg 1990)

3.4.2.3.4.1 EMA Subsystem

The EMA subsystem consisted of the power source inverter, electric link, converter, control system, and the motor.

3.4.2.3.4.1.1 Inverter

Resonant inverters generated a single phase ac voltage. The high frequency ac system had advantages in redundancy management and voltage level shifting over a dc system as long as loads could be managed. This type of inverter had bi-directional power capability (Burrows 1992).

3.4.2.3.4.1.2 Electric Link

A 20 kHz electric link allowed the power conversion to be done at this high frequency instead of machine frequency (Burrows 1992).

3.4.2.3.4.1.3 Converter

The pulse population modulated converter (PPM) was chosen. The PPM selected individual pulses of the link voltage to produce a variable voltage, variable frequency wave form to drive the motor. The PPM was also bi-directional which was necessary since the actuation system would return energy that the motor would generate. The PPM performed switching at zero current, thereby eliminating switching loss. The PPM allowed frequency and voltage to be varied independently, which was critical for control (Burrows 1992).

3.4.2.3.4.1.4 Motor

The induction motor was chosen due to its rugged construction, high temperature tolerances, and high torque-to-inertia and torque-to-current ratios. Two currents were needed for the induction motor. One current went to the stator which established the flux. The second, torque producing current, was supplied to the rotor. Due to the absence of a permanent magnetic field, unlike a magnetic motor, the induction motor was more benign to failure (Burrows 1992).

3.4.2.3.4.1.5 Control

Field oriented control (FOC) was achieved by obtaining proper orientation of flux by maintaining the correct slip angle between the torque producing current and the flux producing current (Burrows 1992).

3.4.2.3.4.2 EMA Sizing

EMAs were chosen for all flight actuator purposes including gimbals, valves, and flight control servos. For gimbals it was assumed that two actuators were required for torque about the pitch and yaw axis. Both the launch vehicle main engines (10) and the spacecraft OMS engines (2) were taken into account. Actuators sizing for valves assumed that ten were needed for each engine of the launch vehicle and spacecraft OMS and two were needed per spacecraft RCS (40). EMAs were sized according to stall loads, dynamic loads, and reaction time required (Sundberg 1990).

		Stall Load	Dynamic Load	Act.Rte	Fluid Pres.	Response	PwrRq(ea)	Mass(ea)	PwrRq(tot)	Mass(tot)	R Costs	NR Costs
	Qty	(N)	(N)	(deg/sec)	(pascal)	(sec)	Watts	(kg)	(watts)	(kg)	$M94	$M94
Gimballing												
LVME	20	400320	266880	15	NA	NA	57750	20.455	1155000	409.09	18.82	18.823
S/C OMS	4	44480	33360	9	NA	NA	4620	4.5455	18480	18.182	0.508	0.5083
Servos									0	0	0	0
Flt Cntrl	20	80064					3080	4	61600	80	2.835	2.835
Valves									0	0	0	0
LVMe	100	NA	NA	NA	2068500	1	1617	1.5909	161700	159.09	6.293	6.2933
S/C OMS	20	NA	NA	NA	1379000	1	385	0.2273	7700	4.5455	0.102	0.1018
RCS	40	NA	NA	NA	1379000	1	192.5	0.0909	7700	3.6364	0.079	0.0786
								Totals	**1412180**	**674.55**	**28.6**	**28.64**

Table 3.4.2.p EMA sizing

3.4.2.4 Guidance Scheme

The overall function of guidance was to predict future path of vehicle from the measured state vector, derived from navigation, and evaluate the flight-path error (Chambers 1964). Guidance then calculated the correction to the present state vector required to correct the present flight path to the desired flight path. Guidance was implemented for ascent and return phases.

3.4.2.4.1 Ascent Guidance

Closed loop guidance, based on Spherical Atmospheric Linear Tangent guidance (Hanson 1992), would be initiated at lift-off and terminate after insertion into orbit. Trajectory was corrected for in an iterative guidance mode (IGM) numerically integrating the equations of motion. A numerical integration approach was selected over a closed-form to allow for modification of parameters, especially in the atmosphere, as they changed. Linear tangent steering, where the optimal thrust angle in terms of time with respect to a set of fixed coordinate axes, was solved for in both the pitch and yaw planes (Hanson 1992). Feedback was in terms of flight path angle and load relief. The ascent guidance scheme went as follows.

1) Vertical Liftoff, initiated closed loop guidance
2) At 15 sec into ascent wind parameter was phased into guidance profile. Angle of attack was held to zero.
3) At 45 sec wind was fully modeled. Angle of attack continued being held to zero.
4) At vacuum, guidance commanded precise control of velocity and position.
5) At orbit insertion, guidance commanded strict velocity control.
6) After orbit insertion, terminate guidance.

3.4.2.4.2 Reentry Guidance

The reentry guidance function was a prediction of azimuth to terminal area energy management (TAEM). Closed loop control was initiated at initial reentry maneuver. Steering was broken up into horizontal guidance and

vertical guidance. Guidance feedback was in terms of INS and GPS measurements. Atmospheric data was provided by air data system.

Sensor	Quality	Accur.
Air Flow Meas	dynamic press	.05 pa
Rosemnt 858	static press	0.05pa
	AOA	.1 deg
	Angle of sideslip	.1 deg
	Total Temp	.5 deg C
	Pressure Alt.	5 pa

Table 3.4.2.q Air Data Sys. specifications

3.4.2.4.2.1 Horizontal Guidance

Horizontal guidance controlled the spacecraft heading by steering according to roll angle (Buhl 1991). Horizontal guidance, using a predictive method, kept the vehicle in a desired heading error by maneuvering the spacecraft through a series of S-turns.

3.4.2.4.2.2 Vertical Guidance

Vertical guidance was an energy controller, adjusting range by varying the angle of attack and the commanded traveling altitude (Buhl 1991).

3.4.2.5 Precision Landing System for Spacecraft

The spacecraft was a lifting body requiring horizontal landing at a runway. A precision landing system was required to assist or completely automate the landing. GPS/INS and the air data system were responsible for navigation above a 10 km ceiling. Once the spacecraft had descended to 5 km MLS was activated. When the spacecraft had descended to 1.5 km, the radar altimeter was initiated into the precision landing scheme. Accuracy requirements for the horizontal landing return were based on STS orbiter autoland requirements (Braden 1990).

Space shuttle Autoland Rqmts (3 sig	
Sink rate	1.83 m/s
Pitch altitude	13.5 deg max
Energy reserve	5.0 sec min
Roll attitude	1.5 deg max
Heading wrt centerline	5.0 deg
Centerline position	12.2 m
Vertical position	2.4 m

Table 3.4.2.r Shuttle landing Rqmts, Honeywell Inc.

The following precision landing systems were considered.

GPS/INS standalone could only achieve vertical position estimation within 5 m, therefore it did not satisfy vertical position requirements set by the space shuttle.
ILS The scanning beam was limited to straight in approaches. ILS could not transmit beam at steep angles of slope, which would be required during return of spacecraft. ILS accuracy's vary depending on category of landing category, I, II, III (Arnold 1991).

MLS with RA could achieve accuracies of 1 meter independent of category landing. MLS scan beam volume allowed for curved or steep approaches. See Table 3.3.2.5.b. MLS was also accepted by FAA as a primary precision landing system (Arnold 1991) .

DGPS with RA in a NASA/Langley lifting body return vehicle experiment had achieved vertical position accuracy to within 2 m. DGPS was not, however, accepted by FAA as a primary precision landing system (Arnold 1991).

It was determined to use MLS over DGPS as precision landing system. DGPS was still in the experimental phase. MLS had been ruggedly evaluated and proven to be a robust precision landing system.

The MLS chosen for the spacecraft was the MLZ-900 microwave landing system receiver. The MLZ-900, manufactured by Honeywell, used in conjunction with a ground-based time reference scanning beam, permitted the spacecraft to approach at a glide slope up to 20 deg vertical (Janes Avionics). Additional information about the MLZ-900 is given in table 3.4.2.s.

The radar altimeter chosen for the spacecraft was the RA3003 radar altimeter manufactured by Smith Industries Aerospace & Defense Systems Ltd. Additional information is given in table 3.4.2.t

Sensor	Type/Cont.	Quality	Accur.
MLS	MLZ-900	Azimuth rnge	40 deg
	Honeywell	Elev rnge	.9-40 deg
	receiver	Azimuth	
	control unit	PFE	.1 deg
	antenna	CMN	0.06 deg
		Elevation	
		PFE	0.12
		CMN	0.06

Table 3.4.2.s MLS specifications, Janes Avionics

Sensor	Type	Quality	Accur.
RA	Pulse	range	1500 m
	Reflection	at 150 m	.6m

Table 3.4.2.t Radar Altimeter Specifications, Janes Avionics

3.4.2.6 Rendezvous and Docking Sensors

It was decided that rendezvous and docking would be controlled by a manual interface. It was assumed that the target vehicle would have receivers for GPS and that the spacecraft, chaser, would be able to monitor its position. Actual rendezvous maneuvers and strategies are discussed in Orbital Analysis, section 2.3. The sensors provided measurement of range, rate, and azimuth at errors less than .15 degrees and .1 deg/sec. The sensors required to rendezvous were configured according to distance to target. The implementation of each sensor is outlined below.

Absolute GPS was implemented before rendezvous phase began to determine orbit estimation of target vehicle. It was assumed that target vehicle navigation, by GPS, would be provided to the spacecraft by communication link.
Relative GPS (RGPS) would be implemented at beginning of rendezvous phase and assisted in navigation until 15 meters of target. RGPS measurements were the difference in GPS measurements of the target and chaser vehicles on the same satellites (Frezet 1991).
Rendezvous Sensors During final translation, inside 100m a medium range sensor (MRS) was used to update the RGPS with relative range and line of sight measurements. At 20 meters until docking, the short range sensor was activated. The short range sensor (SRS) was composed of a camera positioned near the spacecraft docking port directed at a pattern on the target docking port (Frezet 1991). The SRS made line of sight and relative attitude measurements.

3.4.2.7 System Reliability

Navigation, guidance, and control was required to meet .9995 system reliability. Component reliability was based on component mean time between failure (MTBF). The MTBF for each sensor is given in Table 3.4.2.u For the manned mission, 360 hours was assumed to be duration for the mission. Since reliability decreased with dependencies, component redundancy was figured for worst case scenarios. The spacecraft reliability analysis was conducted for the following sensor configurations.

GPS/INS/Star Tracker
GPS/INS
INS/MLS/RA

Sensor	MTBF (hrs)
GPS/INS	30,000
Star Tracker	57,000
INS-alone	15,000
MLS	20,000
RA	20,000

Table 3.4.2.u Sensor MTBF

GPS/INS/StarTracker and GPS/INS sensor configurations required dual component redundancy in order to maintain .9995 system component reliability. The landing phase (INS/MLS/RA) required triple component redundancy to meet .9995 system component reliability.

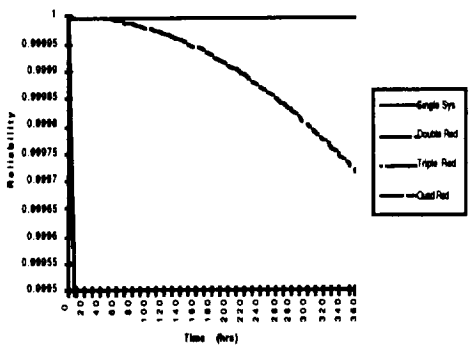

Figure 3.4.2.v Reliability curve for (GPS/INS/STAR). Dual component redundancy needed

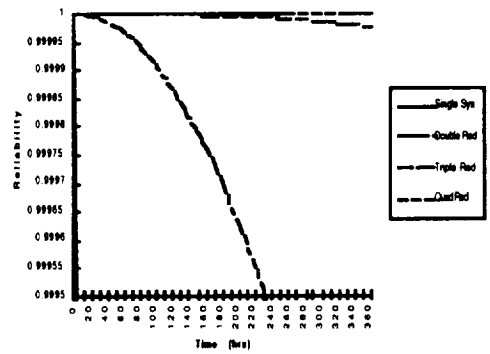

Figure 3.4.2.w Reliability curve for INS/MLS/RA . Triple component redundancy needed

3.4.2.8 Conclusion

A summary of the sensor mass, volume, power, and cost breakdown of the manned launch vehicle is given below.

					R	NR
Sensor	Qty	Vol (m^3)	mass (kg)	Pwr (Watts)	Cost($M93)	Cost($M93)
GPSR	2	0.004	4.54	6	0.85	5.96
INS	3	0.06	57	120	8.64	25.79
ST	2	0.06	26	33	4.21	16.37
MLS	3	0.045	32.1	75	5.10	18.49
RA	3	0.003	6.12	12	1.12	7.08
proximity	2	0.003	6.12	12	1.12	7.08
RVR	2	0.003	6.12	12	1.12	7.08
Totals		**0.178**	**138**	**270**	**22.15**	**87.86**

Table 3.4.2.x Volume, mass, power, and cost breakdown for spacecraft sensors

3.4.3 Communications

3.4.3.1 Overview

In order to increase chances for mission success, ORION had to be able to maintain contact with the ground for as much time as possible. Two systems currently exist which ORION was permitted to use, namely the Satellite Tracking and Data Network (STDN) and the Telemetry and Data Relay Satellite System (TDRSS). At an altitude of 600 km (maximum altitude set by human factors) ORION could expect to maintain contact for approximately 15% of each orbit using STDN and about 80% of each orbit through the TDRSS (these numbers can be found in just about any satellite communications book where TDRSS is mentioned). Therefore, the primary communications link for the manned ORION missions was through the TDRSS. A secondary back up link provided direct spacecraft to ground communications through the STDN in the event that the TDRSS link failed. The only regions where the TDRSS was ineffective were the polar regions, which did not affect ORION, and a small area above the Indian ocean, which did affect the ORION missions. The latter problem could be minimized if permission was obtained from the U.S. Air Force to use the Space Ground Link Systems (SGLS) Indian Ocean Tracking Station. Other supplemental links included spacecraft to astronauts in Extra-Vehicular Activity (EVA), Merritt Island tracking facility to launching vehicle, spacecraft to space station, and dumping recorded information. All links were digital, (except EVA where the lower frequencies limited the amount of data transmitted at any given time). Digital communications have decreased error rates and several sources of information could be multiplexed into a single link.

3.4.3.2 Frequencies

For the primary communications link, the frequencies had to be compatible with those of the TDRSS (See Appendix A.3.4.3.2). The frequencies were 2.1/2.25 GHz (uplink/downlink) for the S-Band link and 13.775/15.0034 GHz for the K-band link. For the back-up link through STDN, and the launch communications, the frequencies were the same as those for the primary S-Band link listed above. This was done to minimize the number of transceivers that were required. For the EVA communications the frequencies had to be compatible with existing shuttle EVA suits. The frequencies were 243/259.7 MHz. The Space Station Requirements Document did not list transmitting and receiving frequencies, but did state that its primary link would be through the TDRSS. This meant ORION could link to the Space Station using the same frequencies as it used for a link through the TDRSS for communications with the Space Station.

3.4.3.3 Data Rates

In order to increase the effectiveness of the link, it was advantageous to reduce the transmitted data rates provided quality was not compromised. Reduced data rates meant less chance of error (since less was being transmitted) and reduced power consumption (See Appendix A.3.3.3.3). The data rates calculated in this section were the maximum possible.

3.4.3.3.1 Telemetry, Data and Command

From Appendix A.3.4.2.1 (section on sensors), a data rate of 68.87 kilobits/second (kbps) was required to transmit all sensor data, excluding that of the launch (which was recorded and dumped). The data rate that was used in the link analysis was 105 kbps which included a safety factor of 1.5 for any increases that might occur as the project grows. This value was slightly less than the Space Shuttle's S-Band maximum telemetry and data rate of 128 kbps. The maximum data rates during a satellite repair mission were estimated at 10 Mbps based on the maximum possible payload data rates. The data rate for the command uplink was estimated at 8 kbps through the S-Band and 152 kbps through the K-Band. These rates were based on the Space Shuttles command links.

3.4.3.3.2 Voice

The standard methods for digitizing a voice signal and their corresponding data rates are listed below.

Method	Data Rates
Pulse Code Modulation (PCM)	64 kbps
Delta Pulse Code Modulation (ΔPCM)	56 kbps
Adaptive Differential Pulse Code Modulation (ADPCM)	32 kbps
Continuous Variable-Slope Delta Modulation (CVSD)	24 kbps
Code Excited Linear Prediction (CELP)	16 kbps

Table 3.4..3.a Voice Encoding Techniques

In the interest of keeping data rates as small as possible, PCM and ΔPCM were eliminated immediately as possibilities. ADPCM looked like a good possibility mainly because it was the method currently used by the space shuttle, however it had the highest data rate of the remaining methods. CVSD had a relatively low data rate, but was "plagued with bad quality and high delays" (Faidoon). CELP was just recently recorded as the standard method for 16 kbps voice compression by the Consultative Committee for International Telecommunications and Telegraphy (CCITT), a division of the International Telecommunications Union (ITU) and it provided "excellent

quality and minimal delay"(Faidoon). Thus, ORION used CELP for digitizing a voice signal.

3.4.3.3.3 Video

Several techniques for digitizing video signals and their subsequent required data rates are listed below.

Technique	Data Rate
Broadcast television	92.5 Mbps
Commercial television	44 Mbps
Broadcast television (compressed)	32 Mbps
Video Teleconferencing System (VTS)	1.544 Mbps

Table 3.4.3.b Video Encoding Techniques

VTS offered by far the smallest data rate of the listed possibilities. The compression techniques used in this process were interframe encoding and intraframe encoding. Since video signals contain redundant information these methods compared current frames with previous ones and only transmitted the pixels that changed. A *codec* was used in encoding and decoding the signal. It delivered thirty frames per second, which was virtually undetectable by the human eye, and was in full color. Thus, VTS one way transmission (teleconferencing from ORION to the ground, not reverse) was the method of video compression employed by ORION.

3.4.3.3.4 Downlink/uplink Summary

The data rates for downlinking from ORION to the ground are listed below. The voice links were based on two channels operating on the CELP method. When the antenna was positioned such that the K-Band was capable of transmitting successfully to the ground, all data was transmitted through the K-Band, and the S-Band was shut down. During launch, the rates were the same as those listed for the S-Band.

S-Band	Data Rates
Telem. & Data	105 kbps
Voice	32 kbps
Total	137 kbps

K-Band	Data Rates
Satellite Repair Data	10 Mbps
Same as S-Band	137 kbps
Video	1.544 Mbps
Total	11.68 Mbps

Table 3.4.3.c Downlink Data Rates

S-Band	Data Rates
Command	8 kbps
Voice	32 kbps
Total	40 kbps

K-Band	Data Rates
Command	152 kbps
Voice	32 kbps
Total	184 kbps

Table 3.3.3.3 b Uplink Data Rates

3.4.3.4 Antennas

3.4.3.4.1 K-Band Link

The high data rate that was transmitted via this link increased the power required. This increase, however, could be alleviated by using a smaller beamwidth (see Appendix A.3.4.3.3 and A.3.4.3.4.1). Parabolic reflectors were the most common directional (small beamwidth, high gain) antennae used. This narrow beam meant a steering device was required in order to maintain contact with the TDRSS. Therefore, a steerable parabolic reflector was chosen.

3.4.3.4.2 S-Band Link for TDRSS and STDN

Since it was important for the S-Band to maintain contact for a majority of the time, it would be far too complex to try to implement parabolic reflectors. This was because several reflectors would be needed, and implementing a steering system would be more work than needed. A simpler solution was found, which was to have several fixed antennae with large beamwidths. This was possible for the S-Band (unlike the K-Band) because the data rates were much lower thus the required transmitting power was smaller. In order to reduce the number of antennae needed, the same antennae were used for both the primary link through the TDRSS and the secondary link through the STDN.

3.4.3.4.3 Launch Antennas

These antennae were the same type used on the unmanned launch configuration, (see section 4.3). The main difference was that the two additional boosters both employed the omnidirectional microstrip antennae as well. The size of the antenna was 4.2 cm x 25m. The rest of the information on the microstrip antenna can be found in section 4.3.

3.4.3.4.4 Antenna Placement

There were a total of seven helix antennae for the S-Band communications, seven helix antennae for EVA communications, and one parabolic reflector for the K-Band communications.

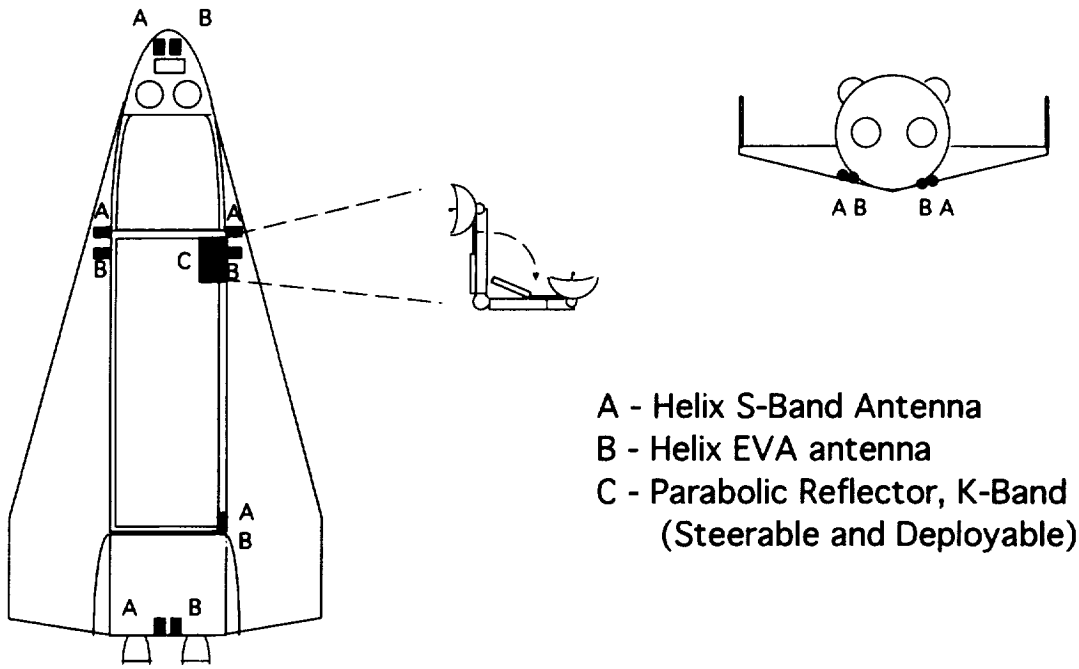

Figure 3.4..3.a Antenna placement on the Glider

3.4.3.5 Transmitting Beamwidths

3.4.3.5.1 K-Band Link

Parabolic reflectors were used primarily as highly directional antennas, thus the K-Band link required a small half-power beamwidth. Generally, the beamwidth was varied until a decent power and antenna diameter were achieved (see Appendices 3.4.3.3 and 3.4.3.4.1). This yielded a beamwidth of 1.4°.

3.4.3.5.2 S-Band Link for the TDRSS and STDN

For communications through the STDN, it was most advantageous to have a halfpower beamwidth spanning the entire earth, this ensured maximum contact time. The calculated value for this beamwidth was 132° (see Appendix A.3.4.3.5.2). The S-Band antennas had to be capable of maintaining contact with a TDRS at all possible times. Since steerable antennae had been ruled out, a large beamwidth was required. In order to ensure a decent link, the beams should cross over at some point between the transmitter and the receiver to eliminate any dark spots that may exist. Since these antennae would be used for the STDN link as well, the shortest distance concerned was 300 km (there was no reason to orbit below this altitude). The farthest distance two antennae could be placed from one another is 21 meters (the distance from nose to tail). The beamwidth(θ) required was calculated to be 90.004°, a beamwidth of 91° was used for safety.

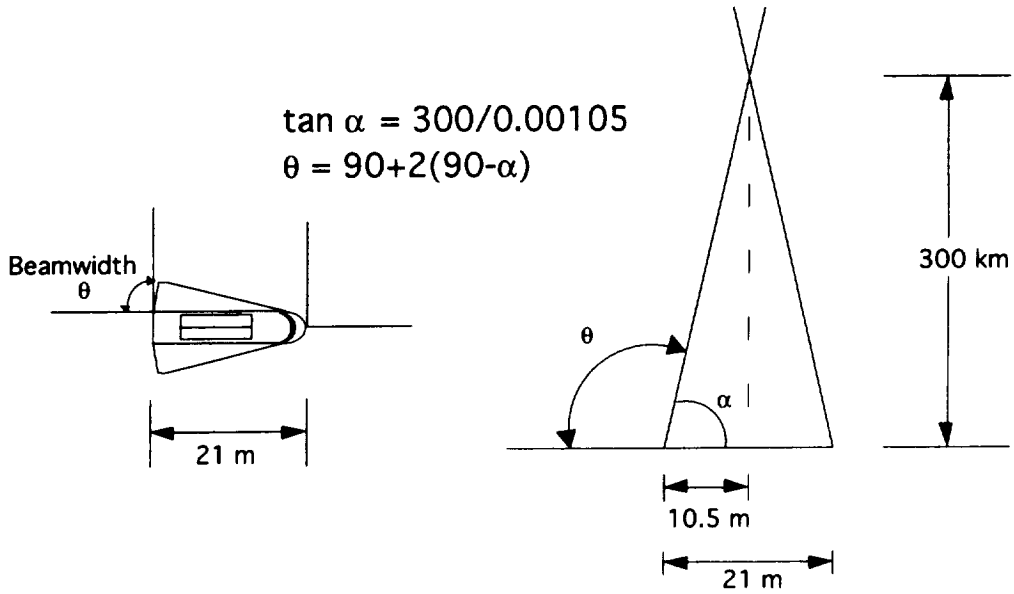

Figure 3.4.3.b S-Band Antenna Beamwidth (Not to Scale)

3.4.3.5.3 Launch Beamwidth

During the launch, omnidirectional antennae was used, thus the beamwidth was 360°. This allowed the vehicle to remain in contact with the ground no matter what orientation it was.

3.4.3.6 Propagation Distances

The link analysis was based on the worst case scenario. Therefore the distance used was the farthest that ORION would ever be from a TDRS. Basically, a TDRS was in geostationary orbit which was approximately 42,241 km from the center of the Earth. There were two operational TDRS's (one back-up) positioned 130° apart, therefore the maximum angle between a TDRS and ORION, corresponding to the maximum distance, was calculated as 115° with the center of the earth as the focus. Using the law of cosines, the maximum distance was calculated to be 45,631 km.

For the link to the STDN, the maximum distance was when the satellite was just at the horizon and at the edge of the receivers line of sight (LOS). This corresponds to the beamwidth calculated in section 3.3.3.5.2, it was the side of the triangle labeled S in Appendix A.3.4.3.5.2. Using simple trigonometry, the distance calculated for use in the link budget analysis was 2831 km. The maximum distance of EVA astronauts used was 2 km, there was no need for them to exceed this distance.

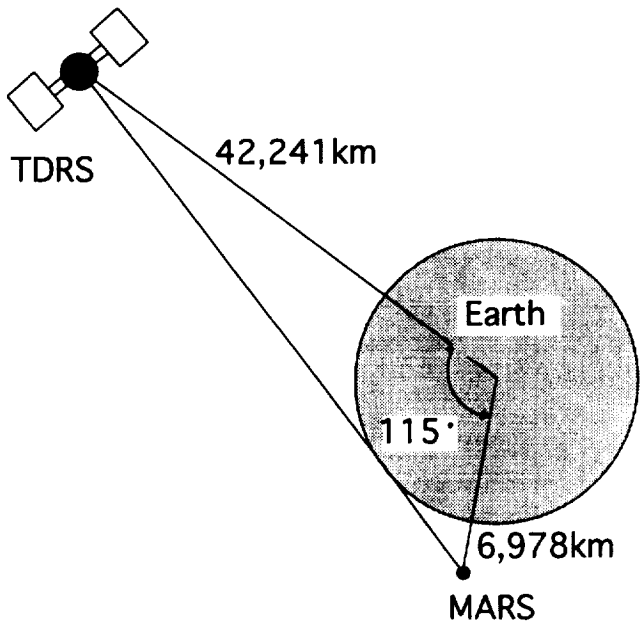

Figure 3.4.3.c Maximum Distance Between ORION & a TDRS (Not to Scale)

3.4.3.7 Link Budgets

A link Budget anaylsis was preformed for each connection. These link budgets are listed in Appendix A.3.4.3.7. A summary of the results are listed below:

Parameter	Downlink	Uplink	Units
f	2.25	2.1	GHz
P_t	50		W
D_t	0.036		deg
BER	10^{-5}	10^{-5}	-
Margin	5.4	7.1	dB

Table 3.4.3.d S-Band Link Budget Through the TDRSS

Parameter	Downlink	Uplink	Units
f	15.0034	13.775	GHz
P_t	5		W
D_t	1.0		deg
BER	10^{-5}	10^{-5}	-
Margin	12.0	32.8	dB

Table 3.4.3.e K-Band Link Budget Through the TDRSS

Parameter	Downlink	Uplink	Units
f	2.25	2.1	GHz
P_t	0.5		W
D_t	0.036		deg
BER	10^{-5}	10^{-5}	-
Margin	19.2	19.9	dB

Table 3.4.3.f S-Band Link Budget Through the STDN

Parameter	Downlink	Uplink	Units
f	2.25	2.1	GHz
P_t	1	1	W
D_t	N/A	9	deg
BER	10^{-5}	10^{-5}	-
Margin	8.2	6.6	dB

Table 3.4.3.g Launch Link Budget

Parameter	Downlink	Uplink	Units
f	259.7	243	MHz
P_t	0.5	0.5	W
D_t	0.21	0.01	deg
C/N_o	68.2	79.0	dB
Req. E_b/N_o	53.3	53.3	dB
Margin	14.9	25.7	dB-Hz

Table 3.4.3.h EVA Link Budget

3.4.3.8 Recorders

These devices were used primarily during launch and repair missions or any other time when the amount of telemetry and data information became too large to transmit at any one time. The excess information was stored on tape and delivered to the ground when possible. There were several companies that produced space-rated digital tape recorders, nominally Datatape Inc., Lockheed Electronics, and Odetics Inc..

	ORION 1600/2000	Lockheed 4400	Odetics 8500EC	Odetics 9500
Size (m^3)	0.044	0.0285	0.043	.115
Mass (kg)	29.9	11.3	33.3	85.3
Power Record	not available	30 W	144 W	166/170
Power Play	not available	40 W	235 W	255/259
Rate Record	3.3 Mbps	4-1500 kbps	10 Mbps	3-300
Rate Play	3.3 Mbps	4-1500 kbps	150 Mbps	150/300
Capacity	not available	1 Gbit	105 Gbit	1,000 Gbit
Record Time	not available	8.3 min-35 hr	174 min	4100/41 min

Table 3.4.3.i Space Rated Digital Tape Recorders

The time of launch was relatively short (i.e. less than an hour), so any of the listed recorders could handle that application. The maximum allowed time for the repair mission was eight hours a day for seven days. This meant that if the entire repair mission was to be stored and analyzed at the end of the mission, the recorder would have to have a maximum record time of at least 3360 min. The only model capable of handling this was the Odetics 9500, but because of its relatively large size and mass it was ruled out. The other option was to store the excess information on a smaller recorder and dump it to the ground when the opportunity arose. Assuming that the K-Band antenna was transmitting at full capacity, it would have to be dumped directly to the ground. The period of a 600 km orbit (calculated using Keplers third planetary law) was 1.61 hrs. Contact was possible for approximately 15% of this time or 0.24 hours. The worst case was assumed and it was determined that the recorder would be able to handle a record time of 1.37 hours (83 min) at a rate of 10 Mbps (see section 3.4.3.3 for data rate information). The only unit capable of handling this was the Odetics 8500EC. The video recorder chosen to record and dump information was the same one used during the Hubble repair mission. Because this recorder had only a 30 minute recording time, a rad hardened VHS analog VTR (video tape recorder) may be taken to record long term events to be viewed after ORION has returned.

3.4.3.9 Equipment Summary

A summary of all equipment needed is listed in Table 3.4.3.5. Extra transceivers were used for redundancy. The costs were estimated using cost relations. Only re-curring costs are listed since all of the equipment currently exists and little to no research and development needs to be done.

Component	Size (m)	#	Mass (kg)	Cost/Piece $FY94 (M)
Helix S-Band Antenna	0.06x0.036 Dia.	7	3	0.294
Parabolic Antenna	1.0 Dia	1	135	8.108
Omnidirectional Microstrip Antenna	0.042x12.57	1*	2	0.213
Omnidirectional Microstrip Antenna	0.042x25.13	2	4	0.369
Helix EVA Antenna	0.3 x 0.2 Dia.	7	3	0.294
VTR (Digital)	not available	2	22.73	2.054
Tape Recorder	0.33x0.38x0.34	2	33.3	2.890
K Band Transceiver	0.14x0.33x0.14	2	4.45	0.569
S Band Transceiver	0.17x0.34x0.09	4	6.87	0.840
L Band Transceiver	0.14x0.30x0.09	2	4.75	0.603

Table 3.4.3.j Component Information *- For the unmanned configuration as well.

3.5 Structures

3.5.1 Introduction

The masses of the individual structural componenets were found by using mass estimating relations from NASA CR 2420 (section 3.3). The two main structural components , the crew cabin and the wing, were analyzed in detail and are discussed in this section.

3.5.2 Crew Cabin

The analysis on the crew cabin structure was based on the following dimensions of the crew cabin as previously stated by human factors.

Diameter = 3.5 m
Length = 4 m
Internal Pressure = 10 psi

3.5.2.1 Material Selection

Several materials were looked at for the crew cabin structure. They were Aluminum 2024, Aluminum 7075, Aluminum 6061 and Titanium. An analysis was done comparing the thickness required using the different materials. The materials that required the least amount of mass from this analysis were Aluminum 2024 and Titanium. The difference in the required masses between these two materials was very small. Since Titanium costs four times more than Aluminum 2024, Aluminum 2024 was chosen. The

reason Aluminum 2024 had a low required mass was that it has a high strength (482×10^6 N) and a low density (2770 kg/m^3). The rest of the analysis was done using the chosen material Aluminum 2024.

3.5.2.2 Crew Cabin Loads

The load sources for the crew cabin were the ultimate load (P_{ult}) and the critical buckling load (P_{cr}). The ultimate load was found using the limit load, the moment (M), the radius of the cabin (R) and a factor of safety. The limit load (P_{lim}) was found by using a maximum gravitational force of 4. The following was the equation (Larson, 1992) used to find the ultimate load:

$$P_{ult} = 2*P_{eq} = P_{lim} + (2*M)/R$$

where: $P_{lim} = 2.0 \times 10^6$ N
$M = 4.5 \times 10^6$ Nm
$R = 1.75$ m
factor of safety = 2

The value of P_{lim} was calculated using the maximum gravitational force,as previously stated, and the total mass of the spacecraft. The value of M was calculated by using the given dimensions of the cabin. The value of R was a given dimension of the cabin. The factor of safety was determined by assuming that none of the structures have been built or tested as of yet. The result of the previous equation was an ultimate load of 14.3×10^6 N.

The critical buckling load (P_{cr}) was found by taking the cross sectional area times the critical buckling stress (Larson, 1992). The critical buckling stress was found using the radius of the crew cabin (R = 1.75 m), the thickness of the cabin and the modulus of elongation of the chosen material ($E = 72 \times 10^9$ N/m^2). Since both the cross sectional area and the critical buckling stress were functions of the thickness of the structure, the critical buckling load was also a function of the thickness. Therefore, an analysis was done by finding P_{cr} over a range of thicknesses.

For a structure to be adequate, the critical buckling load must be greater than the ultimate load. As shown in figure 3.5.2.a, an analysis was done showing the ratio of P_{cr}/P_{ult} over a range thickness, with P_{ult} equal to 14.3×10^6 N (as calculated previously). This shows the minimum thickness required for the structure to be adequate.

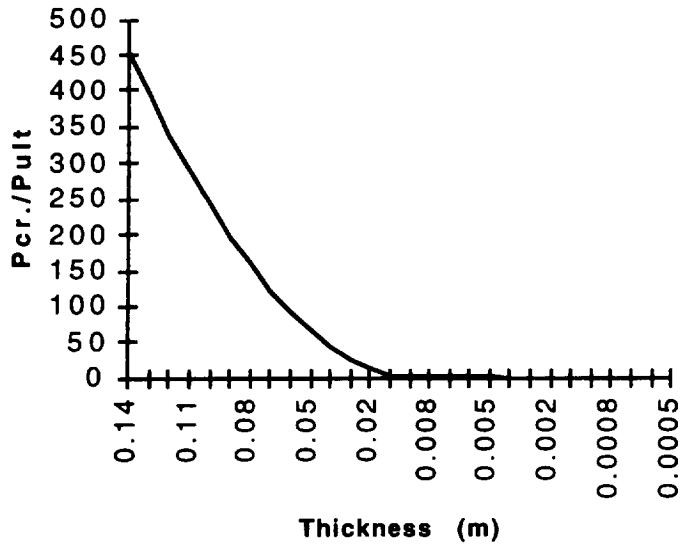

Figure 3.5.2.a Pcr/Pult versus thickness of structure.

From the figure, it was determined that the thickness required for the structure to be adequate was 0.004 m. This was the absolute minimum thickness that could be used for the structure.

3.5.2.3 Crew Cabin Stresses

Stresses on a structure can also affect the determination of the thickness of the structure. Since the crew cabin structure was cylindrical, the stresses that acted on the structure were hoop stress and longitudinal stress. Both hoop and longitudinal stress were a function of thickness. The following equations were used to calculate hoop and longitudinal stress:

hoop stress = (P*D)/(2*thickness)
longitudinal stress = (P*D)/(4*thickness)

where P is the internal pressure and D is the diameter of the crew cabin, which were given in the beginning of this section. As with critical buckling stress, an analysis was done to calculate hoop and longitudinal stress over a range of thicknesses. Since, by definition, hoop stress was twice that of longitudinal stress, determination of thickness was based on hoop stress. Figure 3.5.2.b, below, shows how hoop stress varies with thickness.

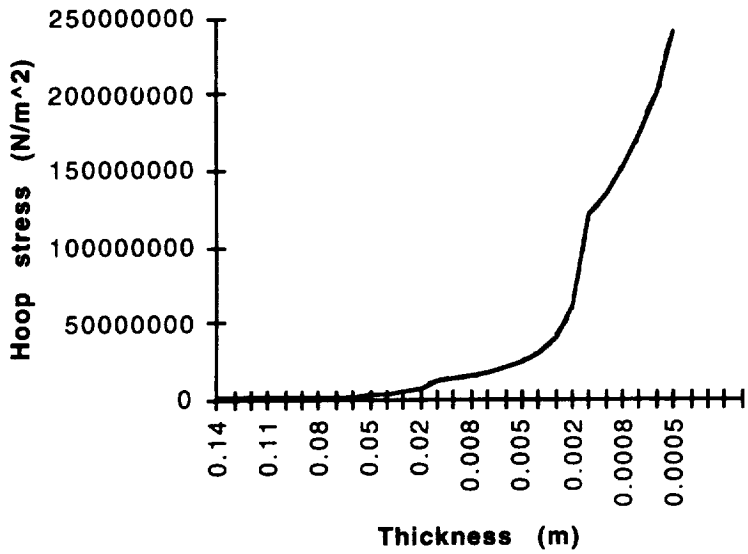

Figure 3.5.2.b Hoop Stress versus thickness of structure.

As seen in figure 3.5.2.b, the hoop stress started to increase rapidly after the thickness reached 0.01 m. For example, the hoop stress at 0.01 m was 12.1 x 10^6 N/m^2 and the hoop stress at 0.009 m was 13.4 x 10^6 N/m^2. Since 0.01 m was greater than 0.004 m, which makes the structure adequate, the thickness chosen for the crew cabin was 0.01m in order to keep the hoop stress low.

3.5.3 Wings

The shape of the wings was a single delta wing. It has tip chords at the bottom of the wings for the wing tips as shown in the pictures of the spacecraft in the beginning of the report.

3.5.3.1 Wing Size Selection

The selection of the wing size was based on an analysis done in the hypersonic region of reentry and on the desired wing performance for landing. For the hypersonic region, there were several desirable affects that changed with the size of the wings. The desirable affects were a low ballistic parameter, a high lift to drag ratio, and a low wing mass. In the analysis, shown in the spreadsheet in Appendix A.3.5.3.1.a, the wing size was varied by changing the wing span. The equations in Appendix A.3.5.3.1.a were based on a couple of factors. The area calculations were based on the geometry of the wings and the normal and axial component calculations were based on equations for reentry aerodynamics (Hankey, 1988).

Increasing the wing span had several different affects (see Appendix A.3.5.3.1). As the wing span was increased in length, the ballistic parameter deceased. This was a desirable affect. Figure 3.5.3.a, below, shows this affect.

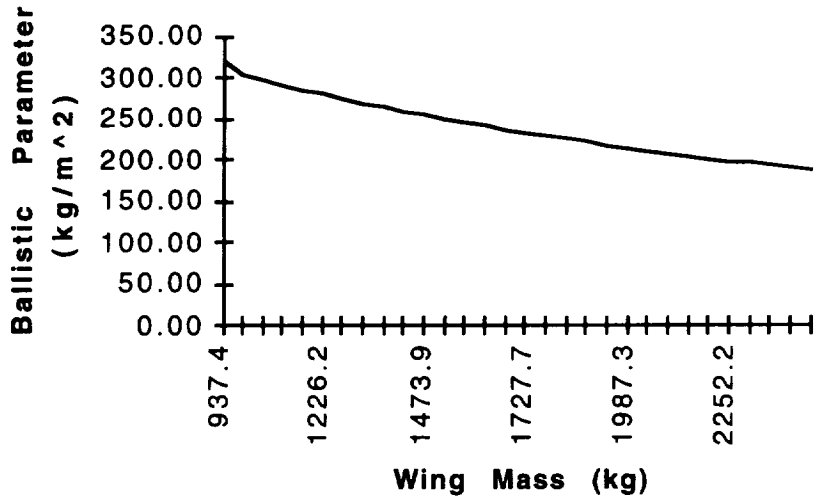

Figure 3.5.3.a Ballistic Parameter versus Wing Mass.

As the wing span increased, the wing mass increased linearly. This was not a desirable affect. When the wing span increased, the lift to drag ratio decreased. This was also not a desirable affect. Therefore, the only advantage, in the hypersonic region, of increasing the wing size was lowering the ballistic parameter. The ballistic parameter not only depended on the size of the wings, but it also depended on the coefficient of drag. The coefficient of drag also changed with the size of the wings. Both the coefficient of drag and the coefficient of lift decreased as the wing size increased. This was what caused the lift to drag ratio to decrease as the wing size increased. The landing mass of the spacecraft also increased as the wing size increased. This caused the ballistic parameter to increase.

From this analysis, the wing size that was chosen had a wing span of 10.75 m, a wing area of 88.06 m^2, a lift to drag ratio of 1.43 and a ballistic parameter of 265 kg/m^2. The values for lift and drag were calculated using an angle of attack of 30 degrees for reentry. This angle was determined in order to provide adequate lift in the hypersonic region.

3.5.3.2 Wing Performance

Before the wing size could be set, an analysis needed to be done for landing to make sure the spacecraft could land at a reasonable speed. For the subsonic region, the wings needed to have a low stall speed and a low wing loading. This also played a factor in determining the size of the wings. The value of

the stall speed (V_{stall}) was calculated using the landing mass of the spacecraft, the wing area, density at sea level and C_{Lmax} of the wings. The chosen C_{Lmax} was 1.4 based on airfoil data. Using the chosen size of the wings from the previous analysis and the landing mass of approximately 44000 kg, V_{stall} was calculated to be 75.6 m/s^2. This was well within reasonable parameters for landing.

The wing loading was also calculated using the chosen wing area from the previous analysis. The wing loading was equal to approximately 4900 N/m^2. This was also within reasonable parameters for landing. Therefore, the chosen wing size could be used on the spacecraft.

3.5.3.3 Calculation of Wing Mass

The mass of the wings was calculated using a hypersonic equation to find the weight of the wings as discussed by system integration. The following constants were used in the equation:

Wing area = 88.06 m^2
Wing span = 10.75 m
Root thickness = 1.5 m
Ultimate Load Factor (ULF) = 12

The wing span was chosen as discussed in the previous sections. The size of the wing span determined the given wing area. The root thickness was determined by the area needed to hold the landing gear inside the wings. The Ultimate Load Factor was determined by taking a maximum gravitational force of 4 and using a safety factor of 3. This safety factor was chosen to insure that the wings would survive any kind of situation. From these values, the mass of the wings was calculated to be approximately 1400 kg (the mass of the wings was a function of the total mass of the spacecraft).

3.5.3.4 Wing Tip Sizing

The total required area of both of the wing tip was determined by using the following equation (Raymer, 1989) for the area of the vertical tail:

$$S_{VT} = (C_{VT} * b_w * S_w) / L_{VT}$$

where C_{VT} was the tail volume coefficient, b_w was the wing span, S_w was the wing area and L_{VT} was the distance from the quarter chord of the tail to the cg of the spacecraft. C_{VT} was set equal to 0.07, which was the typical value for a jet fighter (Raymer, 1989). L_{VT} was determined to be 6.1 m using the approximate center of gravity location on the spacecraft of 12.4 m from the nose. The wing span and wing area were determined in the previous section.

When these values were put into the previous equation, the total area of the vertical tail came out to be approximately 10 m^2. Since there were two wing tips on the spacecraft, the area needed for each of the wing tips was 5 m^2. The calculated area for the wing tips can be seen in Appendix A.3.5.3.1.

Using the calculated area for the wing tips, the sizing was determined in order to fit that area. The tip chords of the wing tips were 4 m in length and the height of the wing tips were 2.5 m. Using the calculated area of the wing tips, it was determined that there was adequate area for the control surfaces.

3.5.4 Heating and Heat Transfer

3.5.4.1 Heat Transfer

The heating of the structure was calculated by breaking up the vehicle into several simple shapes and then analyzing the heating on these simple shapes. After the heating was known, then the heat transfer through the structure could be determined. All heating rates on the vehicle were increased by 25% as a safety factor.

The heat transfer model is shown in figure 3.5.4.a. The stucture was broken down into several small sections called laminates, where n and m were the laminate numbers in the material. Then the temperature difference across the laminates was calculated.

$$T_{X_{\lambda X_n}} = \left[\frac{T_{X_{(\lambda x-1)}} + T_{X_{(\lambda x)}}}{2} + \frac{T_{X_{(\lambda x)}} - T_{Y_1} \overline{\Delta b}_X}{\overline{\Delta b}_X + \overline{\Delta b}_Y} \right]_{n-1}$$

$$T_{Y_{1_N}} = \left[\frac{T_{Y_1} + T_{Y_2}}{2} + \frac{T_{X_{(\lambda x)}} - T_{Y_1} \overline{\Delta b}_Y}{\overline{\Delta b}_X + \overline{\Delta b}_Y} \right]_{n-1}$$

$$T_{ij_n} = \tfrac{1}{2}\left[T_{i_{(j-1)}} + T_{i_{(j+1)}} \right]_{n-1}$$

$$T_{Y_{(\lambda Y)_n}} = \tfrac{1}{2}\left[T_{Y_{(\lambda Y-1)}} + T_{Y_{(\lambda Y)}} \right]_{n-1}$$

$$\overline{\Delta b}_x = \frac{\Delta b_x}{K_x}$$

$$\overline{\Delta b}_y = \frac{\Delta b_y}{K_y}$$

Figure 3.5.4.a The Heat Transfer Model

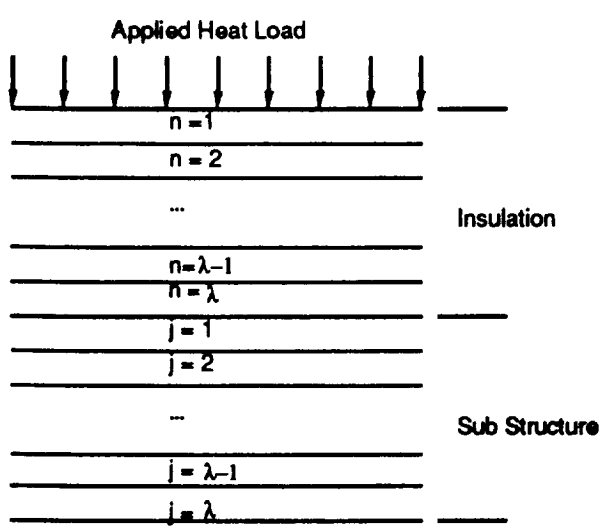

Figure 3.5.4.b The Heat Transfer Model

3.5.4.2 Component Heating

3.5.4.2.1 Nose Heating

The nose of the vehicle was the region subjected to the most severe conditions, as that was where the stagnation point was located. The stagnation point conditions were the design loading for the entire nose section. Due to the high temperatures carbon-carbon was selected as the nose cone material. The carbon-carbon heat shield was 9.6 mm thick with a titanium substructure 6.35 mm thick.

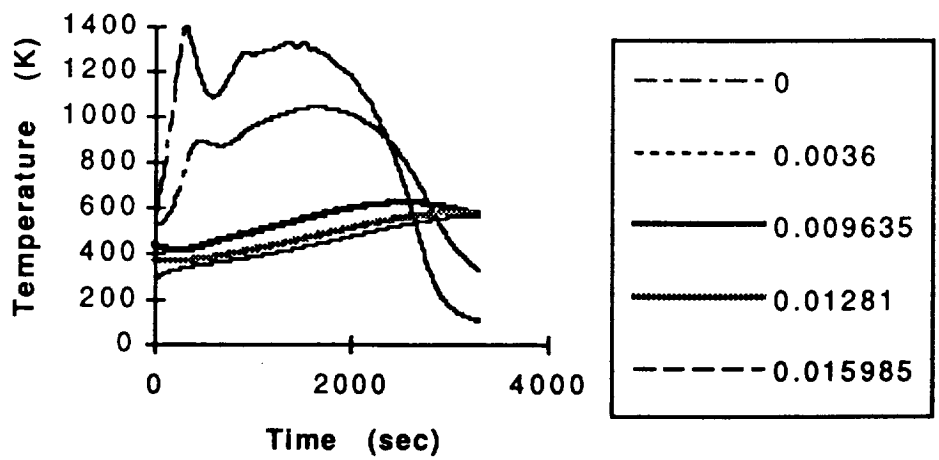

Figure 3.5.4.c Temperature vs. Time for Various Locations Inside the Nose TPS

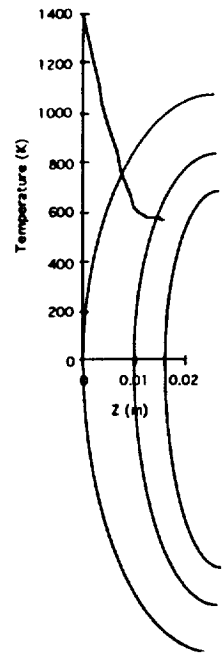

Figure 3.5.4.d Maximum Temperature Distribution Through the Nose TPS

3.5.4.2.2 Leading Edge Heating

$$\frac{\dot{q}(\Lambda)}{\dot{q}(\Lambda=0)} = \left[\frac{\rho_\Lambda \cdot u_\Lambda}{\rho_{ref} \cdot u_{ref}}\right]^{1-n} \cdot \left[\frac{\mu_\Lambda}{\mu_{ref}}\right]^{n}$$

$$\frac{\rho_\Lambda}{\rho_{ref}} = 1$$

$$\frac{u_\Lambda}{u_{ref}} = \cos\Lambda_e$$

$$\frac{\mu_\Lambda}{\mu_{ref}} = \sqrt{\frac{T_\Lambda}{T_{ref}}} = \sqrt{\cos^2\Lambda_e}$$

$$\frac{\dot{q}(\Lambda)}{\dot{q}(\Lambda=0)} = [\cos\Lambda_e]^{1-n} \cdot [\cos\Lambda_e]^{n} = \Lambda_e$$

$$\dot{q}(\Lambda) = \dot{q}(\Lambda=0) \cdot \Lambda_e$$

$$\dot{q}(\Lambda=0) = A(\rho_s \cdot u_s)^{1-n} \cdot \left(\frac{\mu_s}{x}\right)^{n}$$

$$\Lambda_e = \sin^{-1}(\sin\Lambda \cdot \cos\alpha)$$

$$\dot{q}(\Lambda) = A(\rho_s \cdot u_s)^{1-n} \cdot \left(\frac{\mu_s}{x}\right)^{n} \cdot \sin^{-1}(\sin\Lambda \cdot \cos\alpha)$$

Figure 3.5.4.e Leading Edge Heating Model

The leading edges of the wings were the second most severe heating area during reentry. Thus like the nose they were made of carbon-carbon. The temperature distribution through the leading edges was determined from the heating rates and is shown in figure 3.5.4.f.

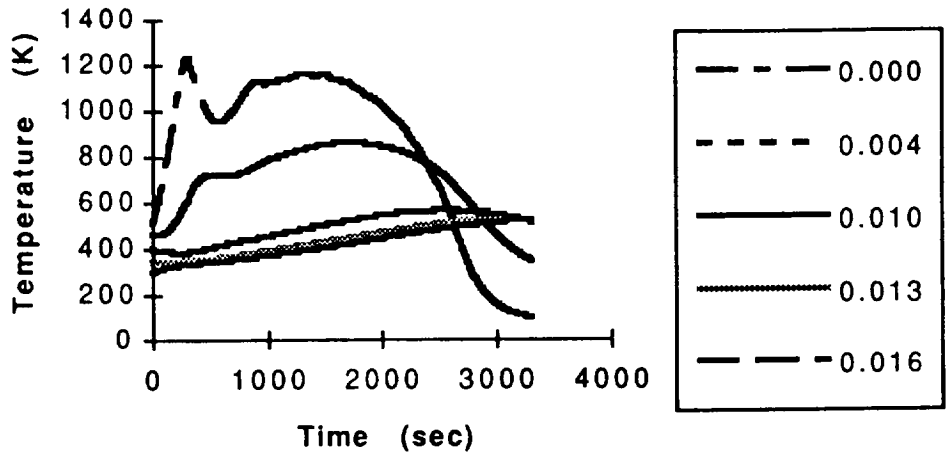

Figure 3.5.4.f Temperature vs. Time for Various Locations Inside the Leading Edge TPS

3.5.4.2.3 Lower Surface Heating

The lower surface did not experience the high heating of the nose and leading edge so an external insulation with lower performance was chosen. REI mullite was selected because of its low density and thermal conductivity.

$$\dot{q}_{\text{Flat Plate}} = \frac{K}{x^n} \cdot \left(\frac{V_\infty}{1000}\right)^3 \cdot \left(\rho_\infty \cdot Sin^2\alpha \cdot Cos\alpha\right)^{1-n}$$

Laminar Flow

$n = 0.5$

$K = 12.1$

Turbulent Flow

$n = 0.2$

$K = 4220$

Figure 3.5.4.g Flat Plate Heating Model

The temperature distribution along the lower surface was calculated from the heating rates. The temperature distribution for a location just after the nose cone where the Mullite insulation begins is shown in figure 3.5.4.h. These conditions were used for the rest of the vehicle. In further design the

thickness of the structure would have to be optimized for the entire vehicle to minimize the weight.

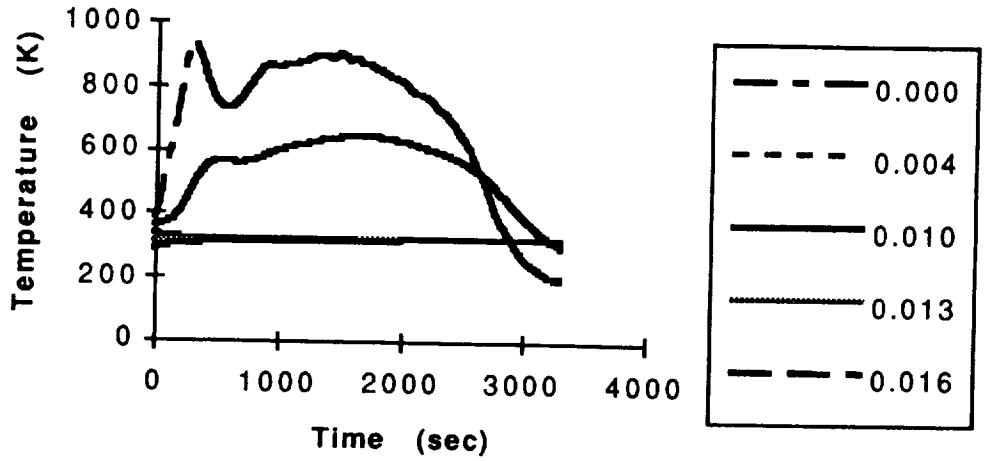

Figure 3.5.4.h Temperature vs. Time for Various Locations Inside the Lower Surface TPS

All of the heatings for the vehicle can be combined and then the maximum temperature for the entire underside of the vehicle is known.

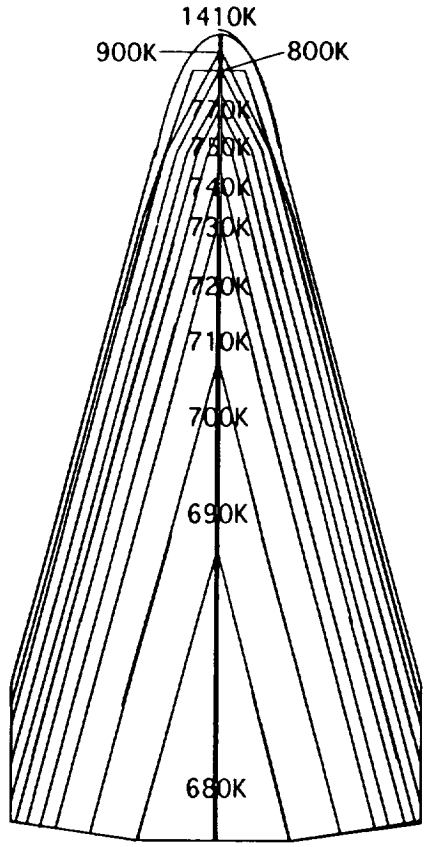

Figure 3.5.4.i Temperature distribution along bottom of heat shield

3.5.4.2.4. Mass Break Down

REI (Reusable External Insulation) Mullite	300 kg
Titanium Substructure	600 kg
Nose	30 kg
Leading Edge	1670 kg
Fasteners and Adhesives (20% of mass)	520 kg
Total	3120 kg

Table 3.5.4.a Mass Summary

3.6 Propulsion and Power

3.6.1 Orbital Maneuvering System

This section outlines the development of the orbital maneuvering system(OMS). A chemical propulsion system was chosen due to the ΔV requirement and reliability. Five different propellants are analyzed as well as propellant feed systems that the propellants require.

3.6.1.1 Requirements

In order to complete the missions a ΔV of 375 m/s is required. It was also required that the system be able to perform Hohmann transfer orbits in order to rendezvous with the space station or the Hubble Space Telescope(HST). The simplest system was designed to reduce both the mean time between failure and cost. A low mass system was the main factor in the designing of the OMS system, due to the direct relation between mass and cost.

3.6.1.2 Propellant Analysis

A comparison was made between cryogenic, hypergolic bipropellants, monopropellants and non-hypergolic bipropellants. Cryogenic propellants were not used due to complexity of the turbopump system needed to help the propellant to flow. Monopropellants also can not be used due to the low thrust that these systems produce. Non-hypergolic propellants were also ruled out due to the incredible difficulty in handling it due to its violent reaction with air. A detailed analysis of hypergolic propellants showed that although a fuel with a Beryllium additive saves on mass, the savings are only about 13%. Therefore a nitrogen tetroxide oxidizer and a hydrazine fuel were chosen.

3.6.1.3 OMS Parameters

Using the chemical properties of the propellants and the required ΔV set by mission analysis, the system was optimized based on the thrust coefficient (C_f) and the chamber pressure (P_c) , and found the point to be at approximately 689500 Pa and 7500 N. Table 3.6.1.a shows all other parameters derived.

3.6.1.4 OMS Size and Design

A standard cylindrically-shaped thrust chamber with a self-impingement injector plate was used. Five different nozzles were looked at for the design of the system. With the exception of the bell and the cone shaped nozzle, all

the other shapes are designed to compensate for changing atmospheric conditions with the trade off of complexity. However, since the system is constantly in a standard, no-atmosphere environment those shapes were ignored. The bell nozzle with a 15° half angle was chosen because it gave a 20% increase in efficiency compared to a cone nozzle.

Propellant	N2O4+N2H4	R (reac)	101
Isp(vac) (s)	343.8	R (prod)	101
Oxidizer/Fuel	1.42	Isp(thr. ch.) (s)	351
density (kg/m^3)	1220	Thr/Engine (N)	7500
Temp. (thr. ch.)	3266	Ue (m/s)	3373
c* (m/s)	1573	mass flow (kg/s)	2.22
Cf	0.512	γ	1.26

Table 3.6.1.a Nozzle and Thrust Chamber Parameters

The same design equations as the launch vehicle propulsion unit were used. Table 3.6.1.b shows the size of an OMS engine, and Figure 3.6.1.a shows a sketch of the engine.

Expansion Ratio	8	Throat Area	0.0212
Exit Diameter	0.465	Nozzle Length	0.567
Throat Diameter	0.164	Chamber Dia.	0.201
Exit Area	0.170	Chamber Length	0.304

Table 3.6.1.b Nozzle and Thrust Chamber Dimensions

In choosing the injector, a combustion process that will remain stable was desired. Nonimpinging, unlike-impinging, and like-impinging injectors are the main types of injectors that were looked at. Nonimpinging injectors could not be used due to the chemical properties of the propellant that would not allow proper flow through the injectors to insure stable combustion. Unlike-impinging injectors also cannot be used because of the phenomenon called reactive demixing. Reactive demixing occur because "hypergolic propellants usually have extremely short ignition delay and thus start generating gases before completion of the mechanical impact of the two streams. These gases add forces to the hydrodynamic ones and tend to separate the surfaces of the reactants." (Huang, 1992) Like-impinging injectors do not have reactive demixing problems because they spray fuel upon fuel and oxidizer on oxidizer which then proceed to mix in an overlap zone. Like doublet injectors are usually preferred due to the fast mixing time. Figure 3.6.1.a shows an injector plate as well as a like doublet injector. The OMS has a fast burning process in order to make the Hohmann transfers seem like impulsive burns.

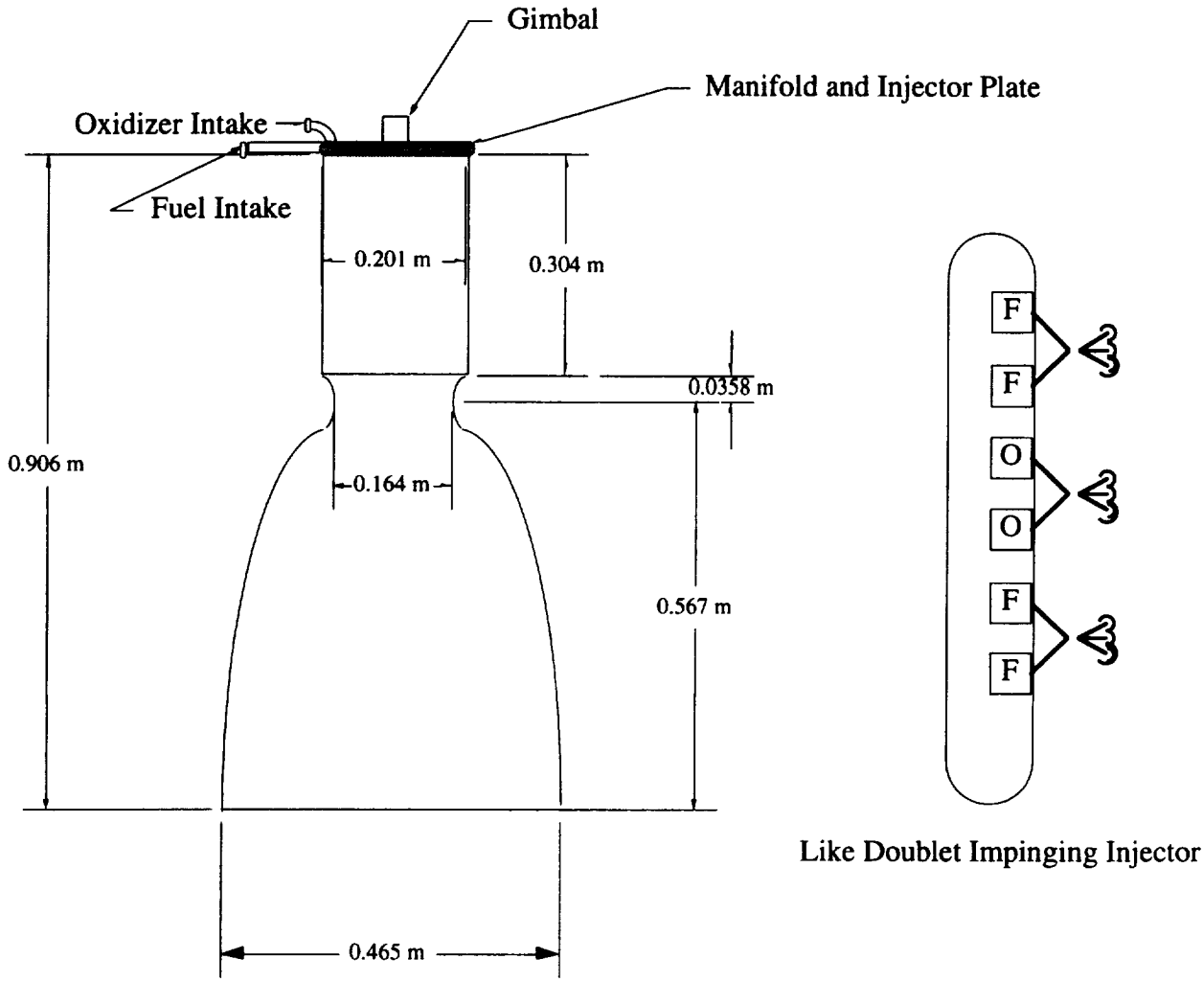
Gimbal
Manifold and Injector Plate
Oxidizer Intake
Fuel Intake
0.201 m
0.304 m
0.0358 m
0.906 m
0.164 m
0.567 m
0.465 m
F
F
O
O
F
F
Like Doublet Impinging Injector

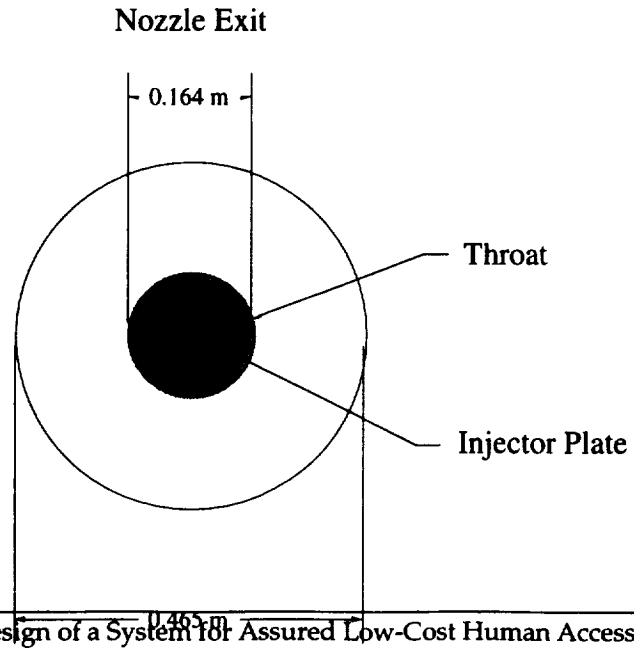
Nozzle Exit
0.164 m
Throat
Injector Plate
0.465 m

Figure 3.6.1.a OMS Engine and Injector Sketch

Four different types of cooling systems were explored: ablative, regenerative, radiative and film/transpiration. Ablative cooling entails too great of a loss in the thrust and the efficiency. Radiation cooling cannot handle the heat transfer problem for the amount time necessary for the burn. Film or transpiration cooling are used when a heat flux occurs, but heat flux was not taken into account for the design so is therefore not used as a design parameter. Regenerative cooling was thus the choice for the OMS cooling system. Fuel is bled off from the tanks and is injected into the walls of the nozzle, using a shower head (nonimpinging) injector, at approximately 298°K.

The final consideration taken into account for the OMS design was the thrust vectoring control(TVC) system. Four different types of TVC systems were analyzed:jet vanes, liquid side injection, auxiliary and gimbals. Jet vanes are rarely used due to the approximate 2% loss in thrust. Erosion of the vane is also another problem with this type of TVC. Liquid side injection requires a larger system to accommodate the extra pressure of a side injection as well as the possibility of contamination because the propellants are toxic. Side injection also requires extra fuel to inject into the flow and has a low angle for vectoring. Auxiliary thrusters are several small thrusters next to the main engine and are gimballed to provide directional control. The main problem with this system was that it required extra fuel, piping, nozzle and thrust chamber design, pressure feed, and two small gimbals. If a large electric powered gimbal is placed upon the thrust chamber then the system saves on those extra costs. But the system still needs power to run the gimbals. Two auxiliary power units(APU) provide the power necessary rotate the gimbals the full ± 15°. The APU's are powered the fuel of the OMS which only require an extra 2% of margined fuel.

3.6.2 Reaction Control System

3.6.2.1 Requirements

To determine the thrust (T in N) and total impulse (I_{total} in N•s) of the spacecraft two types of analysis were used. The first used a standard disturbance torque to back out a thrust, and then used that number to calculate the total impulse. However, the disturbance torques were not large enough to have any impact on the performance of the spacecraft. The second type of analysis is using the limit cycle analysis, which calculates the thrust and total impulse for a particular slew rate (Q in °/s). Given a particular slew rate, a thrust and total impulse for a principle axis can be found using the equation

$$I_{total} = \frac{(T \cdot dt)^2 \cdot L}{4 \cdot J \cdot \beta}$$ (Faget, 1964)

To find the information desired certain other parameters have to be found or calculated. These are the dead band width (b in ±°) which is the error that the spacecraft is allowed to oscillate at, the moment arm (L in m), the moment of inertia for a principle axis (J in kg•m^2), and the burn time (dt in s) which defines the pulse time width. Figure 3.6.2.a and Figure 3.6.2.b show how the total impulse and thrust vary with the slew maneuver. Definite slew rates could not be ascertained so an assumption of 1.5°/s was used. From these relationships the thrust and total impulse can be backed out. At 1.5°/s the thrust is 1000 N and the total impulse is 651000 N•s in the Ixx direction, 310000 N•s in the Iyy direction and 633000 in the Izz direction. The thrust is the same for all principle axis to reduce cost on the learning curve. From the total impulse the total propellant mass for the RCS can be calculated at approximately 2500 kg.

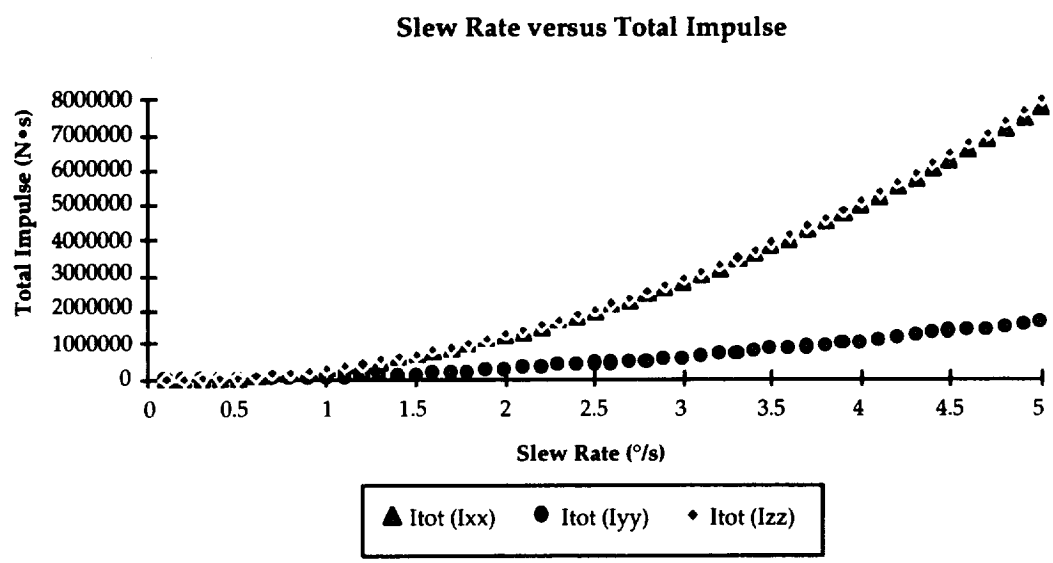

Figure 3.6.2.a Slew Rate Maneuver versus Total Impulse

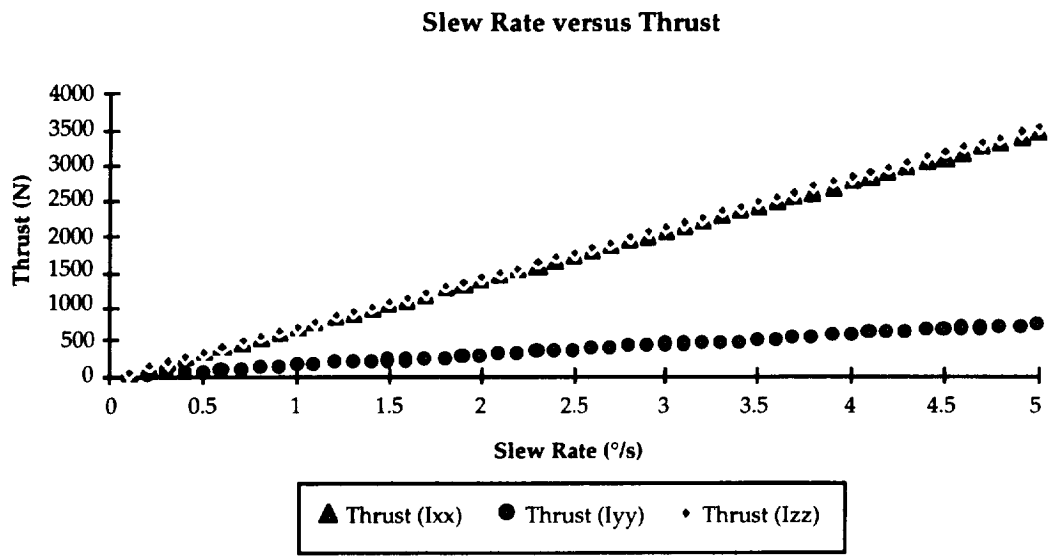

Figure 3.6.2.b Slew Rate Maneuver versus Thrust

3.6.2.2 RCS Size and Design

The thrust chamber for the thrusters are a standard cylindrical shape and the nozzle was a cone shape with a 15° half angle. The reason for the cone is that the same thruster was manufactured 31 times, and a simple design such as a cone would reduce cost. Also, since the propellants for these engines are the same for the OMS engines the same type of injector as well as design parameters and equations can be used. Table 3.6.2.a shows the parameters used to design the engine (Note: only the thrust and mass flow changed) and Table 3.6.2.b shows the design size of the engine.

Considering the small size and quantity of the thrusters needed, a regenerative cooling system would not be cost efficient. Film and transpiration cooling were used for the same reason as the OMS. Although radiation cooling is the simplest and most cost effective cooling system it was not chosen due to reliability reasons. If the OMS failed and could not return the spacecraft to Earth the RCS would have to be used as the maneuvering system. The time to complete a deorbit would sufficiently melt a radiation cooled engine. For this reason an ablative cooling system was used to cool the RCS engines. Figure 3.6.2.c shows a sketch of a RCS engine.

Propellant	N2O4+N2H4	R (reac)	101
Isp(vac) (s)	343.8	R (prod)	101
Oxidizer/Fuel	1.42	Isp(thr. ch.) (s)	351
density (kg/m^3)	1220	Thr/Engine (N)	1000
Temp. (thr. ch.)	3266	Ue (m/s)	3373
c* (m/s)	1573	mass flow (kg/s)	0.296
Cf	0.512	γ	1.26

Table 3.6.2.a Design Parameter for the RCS

Expansion Ratio	8	Throat Area	0.00283
Exit Diameter	0.17	Nozzle Length	0.211
Throat Diameter	0.06	Chamber Diam.	0.0735
Exit Area	0.0227	Chamber Length	0.156

Table 3.6.2.b Size of the RCS Engine

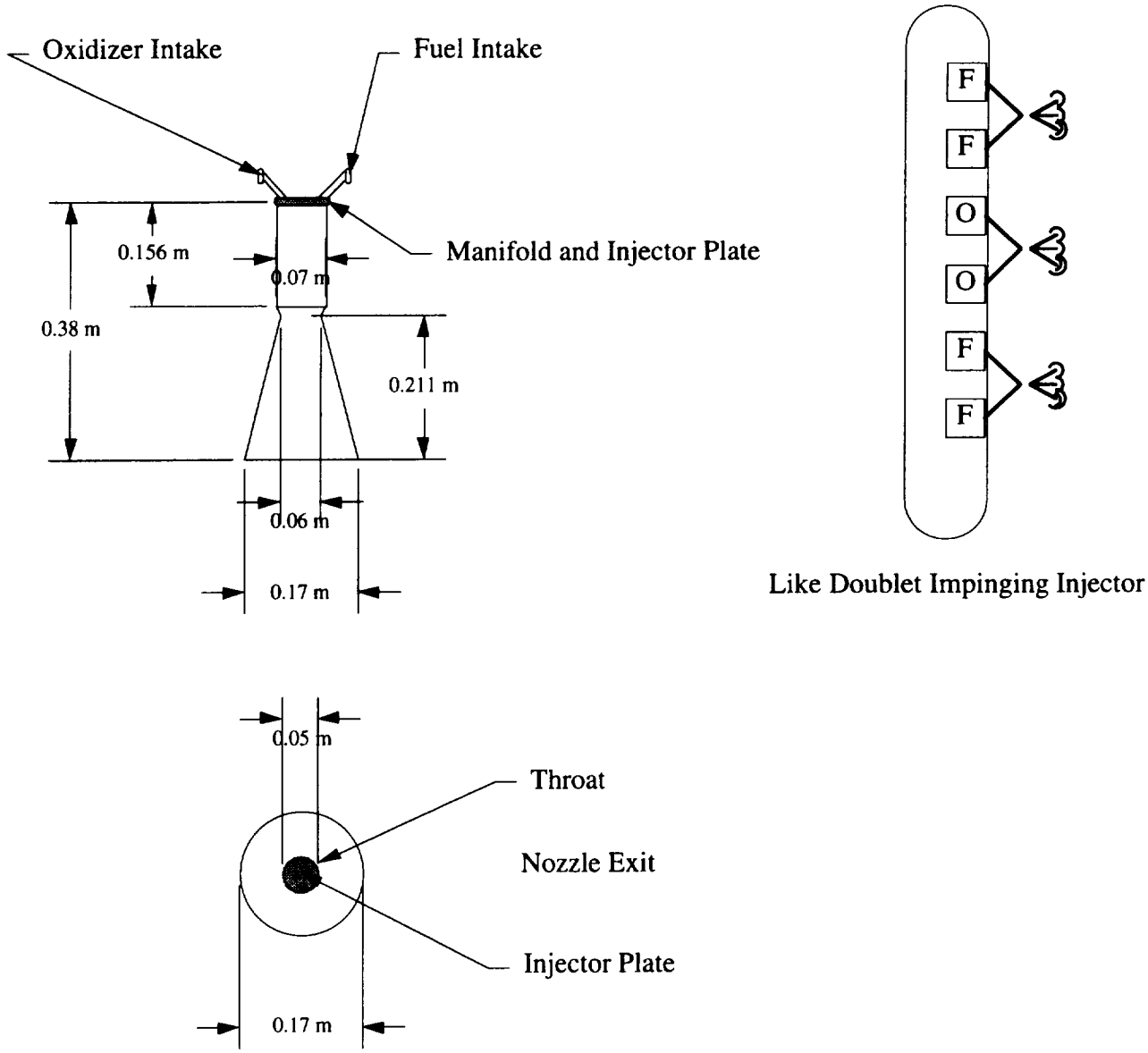

Figure 3.6.2.c RCS Engine and Injector Sketch

3.6.2.3 Propellant Feed System

There are two types of feed systems that were looked at in this design. The first was the turbopump feed system which is used to deliver the propellant into the thrust chamber at very high pressures. The fuel to be pumped to the engine only requires a pressure of .689 MPa which would not require a turbopump. Also, turbopumps are very complex and massive. The other type of feed system is the gas pressure feed system. This system essential uses an extra tank of some inert gas, which prevents reaction with the fuel or oxidizer, at very high pressures (usually between 10 and 20 MPa) to "blow down" the propellant into the engine. The tank pressures of propellant are slightly higher due to losses in the pipes, valves, regulators, and injectors that

may cause a pressure loss before the propellant reaches the engine. Table 3.6.2.c shows the size and mass of the tanks for the aft and forward RCS. The tanks for the aft system are used for both the RCS and OMS. The RCS and OMS aft system can be used in one or the other's place in case of a system failure (e.g. If a OMS failure occurred the RCS would be able to deorbit with enough fuel since it is directly connected to the fuel supply.). Extra piping was needed to complete this system. Figure 3.6.2.d shows a schematic diagram of the aft gas pressure feed system. The forward system is the same as the aft with the exception that OMS engines are not included.

3.6.2.4 Reliability and Redundancy

To increase the reliability of the RCS and OMS, a fully redundant system was used. The redundancy for both systems was based only on analogy from other systems. Quad check valves and pressure regulators are located after each of the tanks to prevent back flow and pressure loss (Figure 3.6.2.d). Two sets of piping stem from the propellant tanks to each system to prevent a total failure (i.e. an RCS and OMS failure). Also, a parallel isolation solenoid valve with pressure regulators setup is placed after the helium tank to ensure constant pressurized flow. Pressure relief valves are placed in front of each tank to prevent tank rupture. Each RCS pod is connected by intermediate piping increase reliability in case of a failure in the starboard or port piping. Finally, two isolation solenoid valves were placed in front of each RCS engine for fine torque control. Thruster redundancy is established by using groups of three for each pod in each axis direction. This gives a total of 36 thrusters. The number of thrusters in the aft system is 22 and 14 in the forward system.

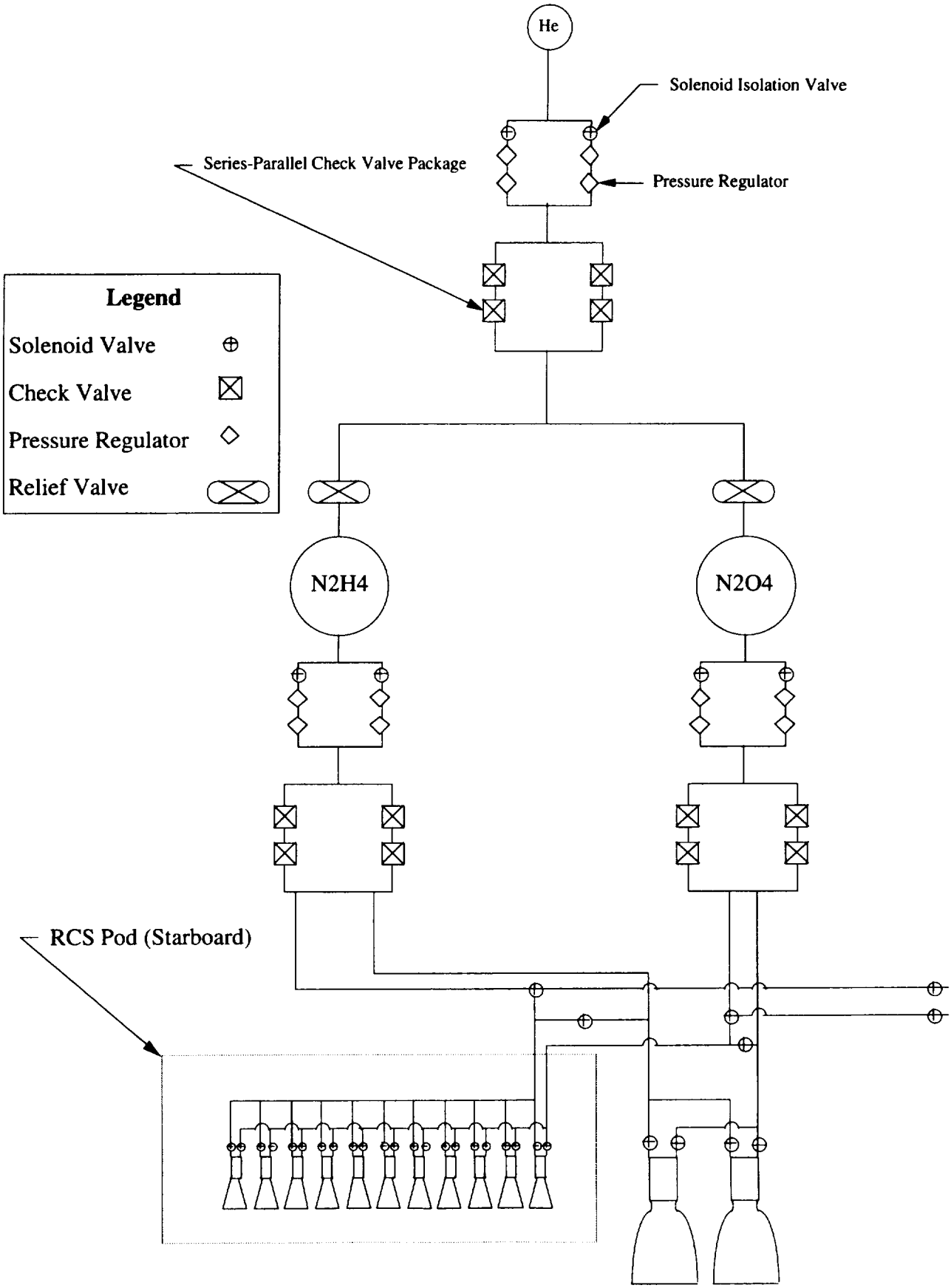
He
Solenoid Isolation Valve
Series-Parallel Check Valve Package
Pressure Regulator
Legend
Solenoid Valve
Check Valve
Pressure Regulator
Relief Valve
N2H4
N2O4
RCS Pod (Starboard)

Figure 3.6.2.d RCS and OMS Gas Pressure Feed System Schematic

Aft RCS and OMS		For RCS	
Fuel		**Fuel**	
N2O4 Prop. Mass (kg)	2794	N2O4 Prop. Mass (kg)	413
N2O4 Tank Material	Aluminum	N2O4 Tank Material	Aluminum
N2O4 Tank Press. (Pa)	1.45 M	N2O4 Tank Press. (Pa)	1.45 M
N2O4 Tank thick (m)	0.00563	N2O4 Tank thick (m)	0.00297
N2O4 Volume (m^3)	2.77	N2O4 Volume (m^3)	0.409
N2O4 Radius (m)	0.876	N2O4 Radius (m)	0.464
N2O4 Tank Mass (kg)	155.5	N2O4 Tank Mass (kg)	23
Oxidizer		**Oxidizer**	
N2H4 Prop. Mass (kg)	3967	N2H4 Prop. Mass (kg)	704
N2H4 Tank Material	Aluminum	N2H4 Tank Material	Aluminum
N2H4 Tank Press. (Pa)	1.24 M	N2H4 Tank Press. (Pa)	1.24 M
N2H4 Tank thick (m)	0.00482	N2H4 Tank thick (m)	0.00271
N2H4 Volume (m^3)	2.75	N2H4 Volume (m^3)	0.489
N2H4 Radius (m)	0.874	N2H4 Radius (m)	0.491
N2H4 Tank Mass (kg)	132.6	N2H4 Tank Mass (kg)	23.5
Pressurant		**Pressurant**	
He Prop. Mass (kg)	6.51	He Prop. Mass (kg)	1.5
He Tank Material	Aluminum	He Tank Material	Aluminum
He Tank Press. (Pa)	20 M	He Tank Press. (Pa)	20 M
He Tank thick (m)	0.0335	He Tank thick (m)	0.0188
He Volume (m^3)	0.221	He Volume (m^3)	0.0393
He Radius (m)	0.409	He Radius (m)	0.23
He Tank Mass (kg)	186.5	He Tank Mass (kg)	33.1

Table 3.6.2.c Tank Size, Volume, Mass of the Gas Pressure Feed System for the RCS and OMS

3.6.3 Power

Power for the spacecraft was defined by the power requirements for each subsystem. Human factors needed power for life support, airlock, galley, and the manipulator arm. Avionics required power for the main computer banks of the spacecraft. Secondary propulsion needed power for the actuators that control the valves and gimbals of the OMS, RCS, and flight controls.

3.6.3.1 Power Requirements

The following table shows each subsystem's power requirement, duration, power load, and usage.

Subsystem	Power (kW)	Usage	Duration (hrs)	Power Load (kWhr)
Lighting	0.25	Continuous	300	75
Ventilation & Fans	1	Continuous	360	360
Air & Water Pumps	1	Continuous	360	360
Airlock	0.5	Temporary	30	15
Manipulator Arm	1	Temporary	30	30
Galley	0.0125	Temporary	60	0.75
Electronics	1.5	Continuous	300	450
Communication	1.5	Continuous	300	450
Navigation	0.2	Continuous	360	72
OMS Gimbal Actuators	18.5	Temporary	5	92.5
OMS Valve Actuators	7.7	Temporary	30	231
RCS Valve Actuators	7.7	Temporary	15	115.5
Flight Control Servos	61.6	Temporary	7	431.2
Max Power	102.4625	Max Power Load		2682.95
Power Excluding EMA's	6.9625	Power Load Excluding EMA's		1812.75
Essential Power	5.45	Essential Power Load		1767

Table 3.6.3.a Power Requirements for Spacecraft

Since orbital maneuvers require a significant portion of the overall power needed, auxiliary power units (APU) were added to the primary power system to provide independent power to the OMS, RCS, and flight controls. These APU's should be fueled by the same hydrazine propellant as the OMS/RCS. Since the OMS and RCS are not used during the final part of the reentry when most of the flight controls are in use, the maximum power required for the APU's at any given time should be 61.6 kW. There should be two 65 kW APU's to provide a redundancy in case of an emergency.

To ensure a high reliability with minimal weight, the primary power system was designed with three separate power generators. Each power source should be able to supply 5.5 kW of power for the duration of the entire mission. This setup will provide a double redundancy for the essential subsystems required for a safe reentry. If one of the power sources fails, then the other two power sources should be able to provide 11 kW of power, which is more than enough to continue the mission. If two of the power sources fail, then the remaining power source should supply enough power for an emergency reentry.

A secondary power system should consist of a separate independent power source that can supply 5.5 kW of backup power just in case the primary power

system fails. The time to reach an emergency reentry window will not be longer than 24 hours. Therefore, the maximum power load of the secondary power system should not be greater than 131 kWhr.

3.6.3.2 Selection of Power Sources

In order to select a power source that satisfies the power requirements, a baseline model was developed. Four power sources were selected for the mass and cost trade studies: solar arrays, nuclear reactors, fuel cells, and batteries. The maximum power requirement was set at 7 kW.

The mass of solar arrays was based on silicon photovoltaic cells and nickel hydrogen secondary batteries. The mass of the nuclear reactors was based on the SNAP-2 compact nuclear reactors with 13,500 kg of shielding. The mass of the fuel cells was based on a scaled down version of the space shuttle fuel cells, liquid oxygen and hydrogen required to power the fuel cells, and the propellant tanks. The batteries were based on a group of large prismatic lithium thionyl chloride batteries.

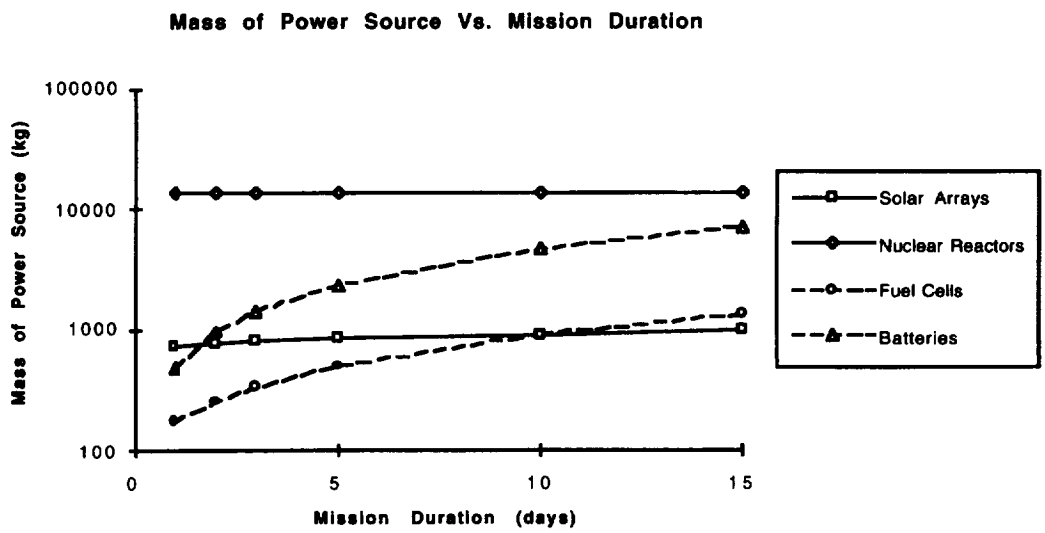

Figure 3.6.3.a Mass of Power Source Vs. Mission Duration

From the Figure 3.6.3.a, the main candidate for the primary power system was either fuel cells or solar arrays. The candidate for the secondary power system was either batteries or fuel cells. In order to eliminate choices of the various power systems, the cost of each power source must be looked at.

The costing model for each power source was based on the calculated cost per kg. The cost per kg was derived from specific power (W/kg) and specific cost ($/W) values found from various sources.

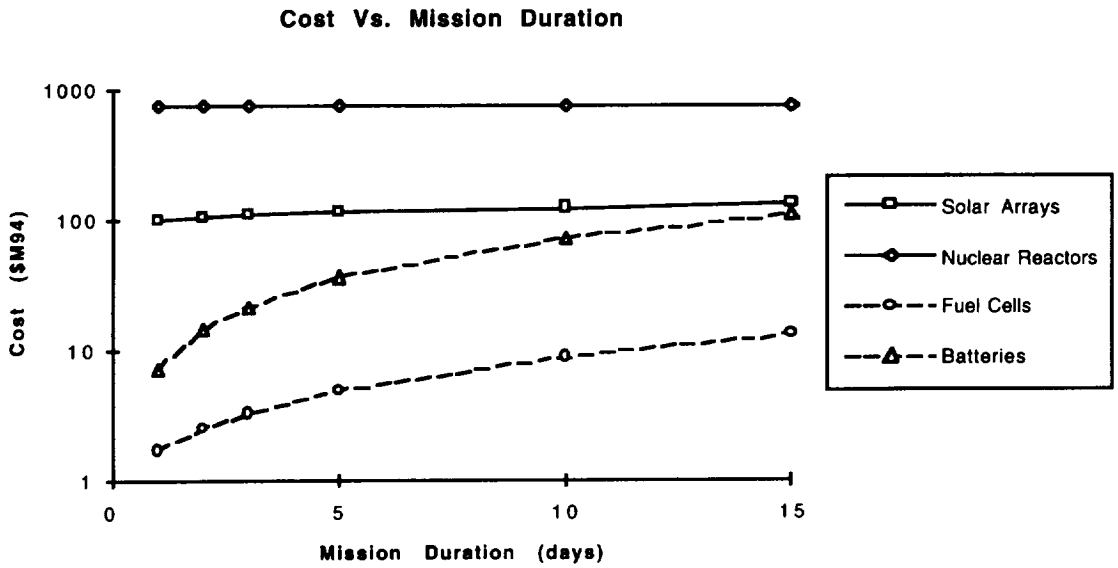

Figure 3.6.3.b Cost of Power Source Vs. Mission Duration

From Figure 3.6.3.b, the most cost effective power source was either fuel cells or batteries. Since mass is the main driver when designing the spacecraft and cost is the main driver of the project, fuel cells were selected over solar arrays to be the primary source of power. Because the secondary power system has to be independent from the primary power system, batteries were chosen for the secondary power system. A scaled down version of the space shuttle's APU's were selected for the spacecraft's APU's.

3.6.3.3 Mass Breakdown of Power Systems

The following table shows the mass of each power system and the mass of its components.

Mass Estimation for Power Systems		
	Mass (kg)	Basis
Fuel Cell #1 (5.5 kW)	72.67	Power Output = 5.5 kW
Fuel Cell #2 (5.5 kW)	72.67	Specific Power = 75 W/kg
Fuel Cell #3 (5.5 kW)	72.67	
24hr Backup Battery	373.71	Specific Power Load
for continuous power		= 350 Whr/kg
Wiring for Bus	200.00	Scale from STS
Prop for max power	815.74	0.45 kg/KWhr
O2 portion	*725.10*	16/18 portion
H2 portion	*90.64*	
O2 for cabin atmos	135.00	
O2 Tank#1	37.67	10% of prop mass
H2 Tank#1	3.02	
O2 Tank#2	24.17	
H2 Tank#2	3.02	
O2 Tank#3	24.17	
H2 Tank#3	3.02	
APU #1 (65 kW)	40.00	Scale from STS
APU #2 (65 kW)	40.00	
TOTAL	1917.53	

Table 3.6.3.b Mass of the Components of the Power Systems

The twenty-four hour backup battery was designed to provide a third redundancy for the essential components just in case the primary power system completely fails.

3.6.3.4 Electrical Power Distribution System

The electrical distribution system was designed to provide multiple redundancy in order to ensure a high reliability. The three fuel cells are fed by three separate pairs of propellant tanks. There are two sets of pipes connecting the tanks to fuel cells and the tanks to the redistributing pipes. The redistributing pipes were designed to feed the propellants from other tanks to any of the fuel cells if any of them should fail or any of the pipes should break. All three fuel cells are connected to a main power bus which in

turn is connected to a distribution bus by three separate relay switches. The backup battery is also connected to the main power bus in case the primary power source completely fails. The distribution bus supplies power to three separate sub-buses which in turn supply power to life support and avionics. The APU's, which are not shown on Figure 3.6.3.c, directly supply power to the OMS, RCS, and flight controls.

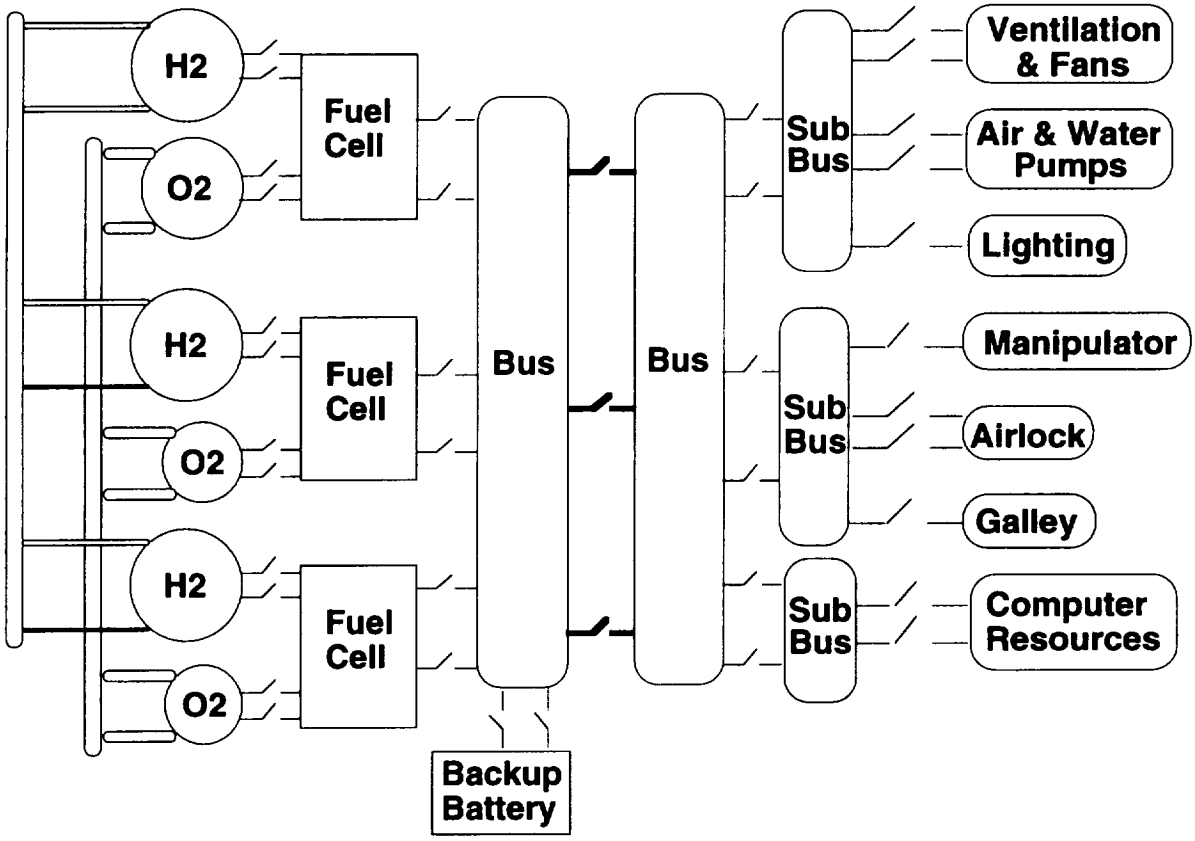

Figure 3.6.3.c Electrical Power System Schematic

References

Faget, Maxime, Purser, Paul, and Smith, Norman. Manned Spacecraft: Engineering Design and Operation, Fairchild 1964

Faidoon, Mazda (Ed.) Telecommunications Engineers Reference Book, Pp 56.3.2. 1993, Butterworth/Heinmann, London

Fortescue, Peter and Stark, John. Spacecraft Systems Engineering. Pp303-383. 1991, John Wiley and Sons Ltd., England.

Green, James Harry, The Business One Irwin Handbook of Telecommunications, Pp 458-459. 1992, Business One Irwin, Illinois

Jenkins, Dennis, Space Shuttle. Pp239-240. 1992, Motorbooks International. Wisconsin

Larson, Wiley and Wertz, James. Space Mission Analysis and Design. Pp503-551. 1992, Microcosm, Inc., Massachusetts.

NASA Cr-1726: Handbook of Human Engineering Design Data for Reduced Gravity Condition, 1971

NASA STD-3000 Man-Systems Inegration Standards

Prentiss, Stan. Satellite Communications Pp 271-272. 1987, Tab Books Inc., Pennsylvania

Stine, Harry. Handbook for Space Colonists. Holt, Rinehart and Winston 1985.

Wilson, Andrew (Ed). Interavia Space Directory Pp471-473, 513- 514 and 626-627. 1989, Interavia, Switzerland.

4.0 Launch Vehicle

4.1 Introduction and Overview

The goal of the ORION project was affordable human access to space. Therefore, reducing cost was the driving factor in the design of the launch vehicle. The resulting design had four major cost-reducing features.

1) The vehicle was customized for the manned and unmanned missions. For the manned missions, the vehicle would use all three stages. For the unmanned missions, the vehicle would use only the top two stages. This measurement was taken due to the fact that the manned and unmanned missions placed significantly different requirements on the performance of the launch vehicle.

2) A semi-modular design was chosen over the pure modular design and the conventional staging design with ideal ΔV distributions. This decision was made after extensive trade studies examined the launch vehicle cost per mission of these three cases. The resulting design consisted a custom top stage, one module for the 2nd stage, and two modules for the 1st stage.

3) Both the custom top stage and the modules would use the same LOX/LH2 engine with different expansion ratios. The top stage would use one engine and the modules would use three engines. Two nozzles were designed for the launch vehicle with different expansion ratios. For the manned missions, the top stage and 2nd stage module would use the nozzles with higher expansion ratio than the ones used by the 1st stage modules and for the unmanned missions the top stage would use the higher expansion ratio nozzle while the 2nd stage module would use the lower one. This design would require research, development, and testing of just one engine. No other launch system in the present or history had this characteristic.

4) The launch vehicle was expendable. This decision was made after careful studies comparing the cost per mission of the expendable and the reusable launch vehicle. It was determined that for the specific mission model and the configuration, the expendable vehicle had the cost advantage over the reusable one.

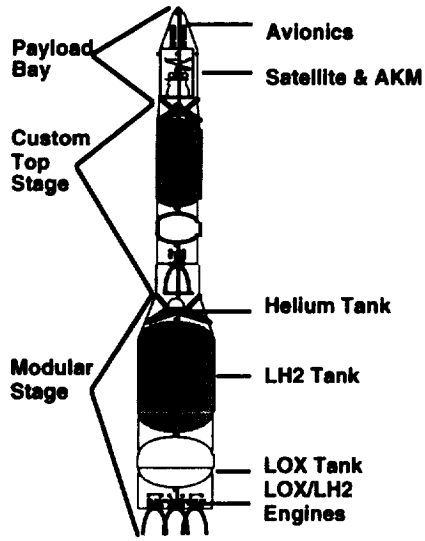

Figure 4.1.1 Launch Vehicle Overview (unmanned)

For the manned missions, the payload bay would be replaced by the spacecraft. Also, there would be an additional stage consisting of two modules.

4.2. Module Configurations

There were two configurations of the ORION system. The first configuration was a manned system designed to perform reference missions 1 and 2. The three stage launch vehicle used two primary modules as its first stage (stage 1m), one primary module as its second stage (stage 2m), and one upper stage as its third stage (stage 3m). The launch vehicle was capable of boosting approximately 50,000 kg of payload into low earth orbit in this configuration. The spacecraft sat on top of the stack and was attached to stage 3m.

The second configuration was an unmanned two stage vehicle designed to perform reference mission 3. The first stage (stage 1u) used one primary module and the second stage (stage 2u) used one upper stage. The launch vehicle was capable of taking approximately 7,800 kg to GEO in this configuration. The spacecraft was not used since the mission was unmanned. In its place, mounted on stage 2u, was a payload shroud designed to protect the satellite during launch.

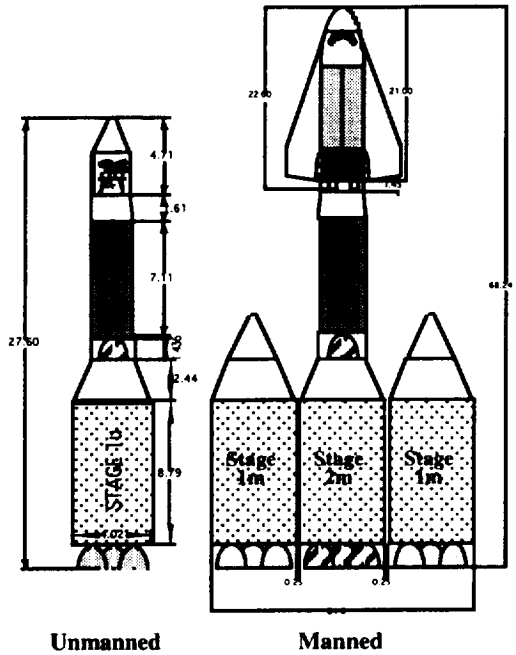

Figure 4.1.a ORION Manned and Unmanned Configurations

4.3. Mass and Center of Gravity Analysis

The mass breakdowns and center of gravity for the modules as well as the third stage are shown in Table 4.3.a and 4.3.b. Masses were calculated using one of three methods: analytically (such as for the tanks), from mass estimating relationships (Glatt, 1974), or by analogy to already existing systems or other similar systems that have been proposed. The mass breakdowns worksheet does not contain masses for avionics and the outer structure of the launch vehicle (i.e. the skin). For the modular stages (stage 1-2) the third column gives the structural masses as well as engine masses per engine per module. The fourth column gives the mass breakdowns for the three engines combined on the modules.

Based on the masses obtained, center of gravity calculations were performed for the modular stages and the third stage. Two possible configurations of the tanks were studied when the CG calculations were performed. Configuration 1 arranged the LOX tank on top of the LH2 tank while configuration 2 did the opposite. It was determined that with configuration 1 a significant shift in the CG would occur during the flight. This is obviously undesirable from a stability standpoint. This did not occur, however, when the second configuration CG calculations were performed. The second configuration therefore was chosen for the modules as well as the third stage. Figures 4.3.a and 4.3.b give the locations of the CGs of both vehicles.

Mass and Cost Breakdown Stage 1-2					
		1st Iteration			
		Mo			
Total Propellant Mass Mp=		218480			
Max Thrust-Liquid Engine @ a=1.3g		1940000			
O/F=		5			
Chamber Pressure=		16500000			
Area Ratio=		22			
		1st Run			
Components		**Masses 1**		**Config 2**	**C*G**
		Find Mo'		**CG LOC**	
LOX Mass		182067		6.35	1156125
LH2 Mass		36413		13.91	506505
LOX Tank		2647	SS	6.35	16808
LH2 Tank	??	11734	SS	13.91	163220
LOX Insulation		238	SS	6.35	1511
LH2 Insulation		755	SS	13.91	10502
Thrust Structure		495	OSS	3.65	1806
Res Prop. Mass		4370		10.00	43696
He Pressurant		100		22.47	2247
Helium Tank		55		22.47	1236
LV Strctrl Mass					
Intrstge Fairing		1212		22.40	27149
Intrtnk Fairing		285		9.00	2565
Nozzle Shroud		2816		3.65	10278
Other Inert Mass		646		4.24	2740
Engine Mass		1881	5642		
Chamber and Nozzle		658	1975	0.71	1402
Turbopumps		602	1806	3.22	5814
Piping		340	1021	3.22	3288
Injector		70	209	3.22	672
Gimbal Mass		60	180	2.11	379
Instruments, etc.		75	226	3.22	727
Other Inert		75	226	3.22	727
		1881	5642		
		Total Mass		wet cg	dry cg
		249475		7.85	9.57

Table 4.3.a Mass and CG of Modular Stages

Mass and Cost Breakdown Stage 3				
		Mo		
Total Propellant Mass Mp=		50200		
Max Thrust-Liquid Engine @ a=1.3g		1940000		
O/F=		5		
Chamber Pressure=		16500000		
Area Ratio=		22		
		1st Run		
Components		**Masses 1**	**Config 2**	**C*F**
		Find Mo'	**CG LOC**	
LOX Mass		41833	6.15	257275
LH2 Mass		8367	12.50	104583
LOX Tank		647	6.15	3979
LH2 Tank		3022	12.50	37775
LOX Insulation		98	6.15	603
LH2 Insulation		334	12.50	4175
Thrust Structure		495	4.4	2177
Res Prop. Mass		1004	9.00	9036
He Pressurant		100	18.2	1820
Helium Tank		14	18.2	255
LV Strctrl Mass				
Intrstge Fairing		262	18.7	4891
Intrtnk Fairing		285	7.85	2237
Nozzle Shroud		631	0.85	536
Other Inert Mass		646	10.00	6462
Engine Mass		1881		
Chamber and Nozzle		658	0.85	560
Turbopumps		602	3.20	1926
Piping		340	3.20	1089
Injector		70	2.10	146
Gimbal Mass		60	2.10	126
Instruments, etc.		75	2.10	158
Other Inert		75	3.22	242
		1881		
		Total Mass	wet cg	dry cg
		59618	7.38	8.30

Table 4.3.b Mass and CG breakdowns for third stage

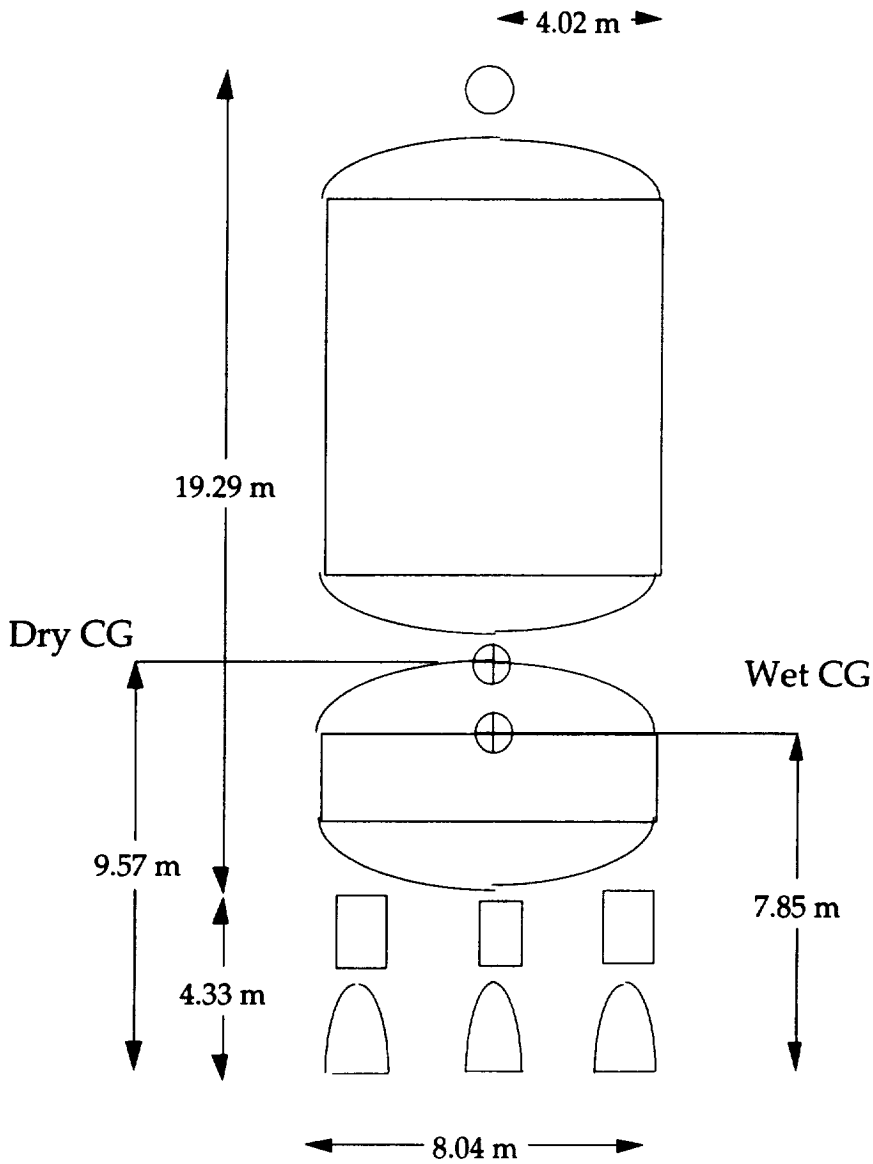

Figure 4.3.a. CG Location for the modular stages
Note: Fairings and support structure not displayed.
Avionics and skin structure not taken into account
in CG calculations.

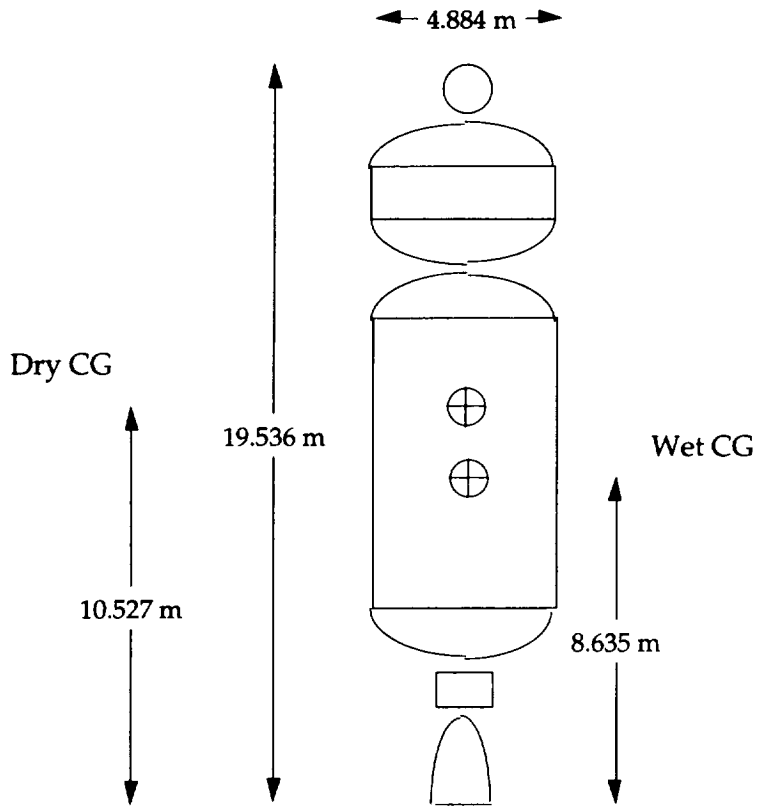

Figure 4.3.b. CG Location for the third stage.
Note: Fairings and support structure not displayed.
Avionics and skin structure not taken into account in CG calculations.

4.4. Avionics

4.4.1 Introduction

The avionics system was divided into three areas: data management; navigation, guidance, and control; and communications. The data management sub-system was composed of five modular computer units in a functionally distributed architecture. Information was carried over a high speed fiber optic network. Primary navigation was performed by a tightly integrated Internal Navigation System and a Global Positioning System. During landing, the spacecraft also employed a radar altimeter and a Microwave Landing System. All on-orbit communications were routed through TDRSS (tracking and data relay satellite system). The avionics' components and navigation, guidance and control are discussed in more detail in section 3.4

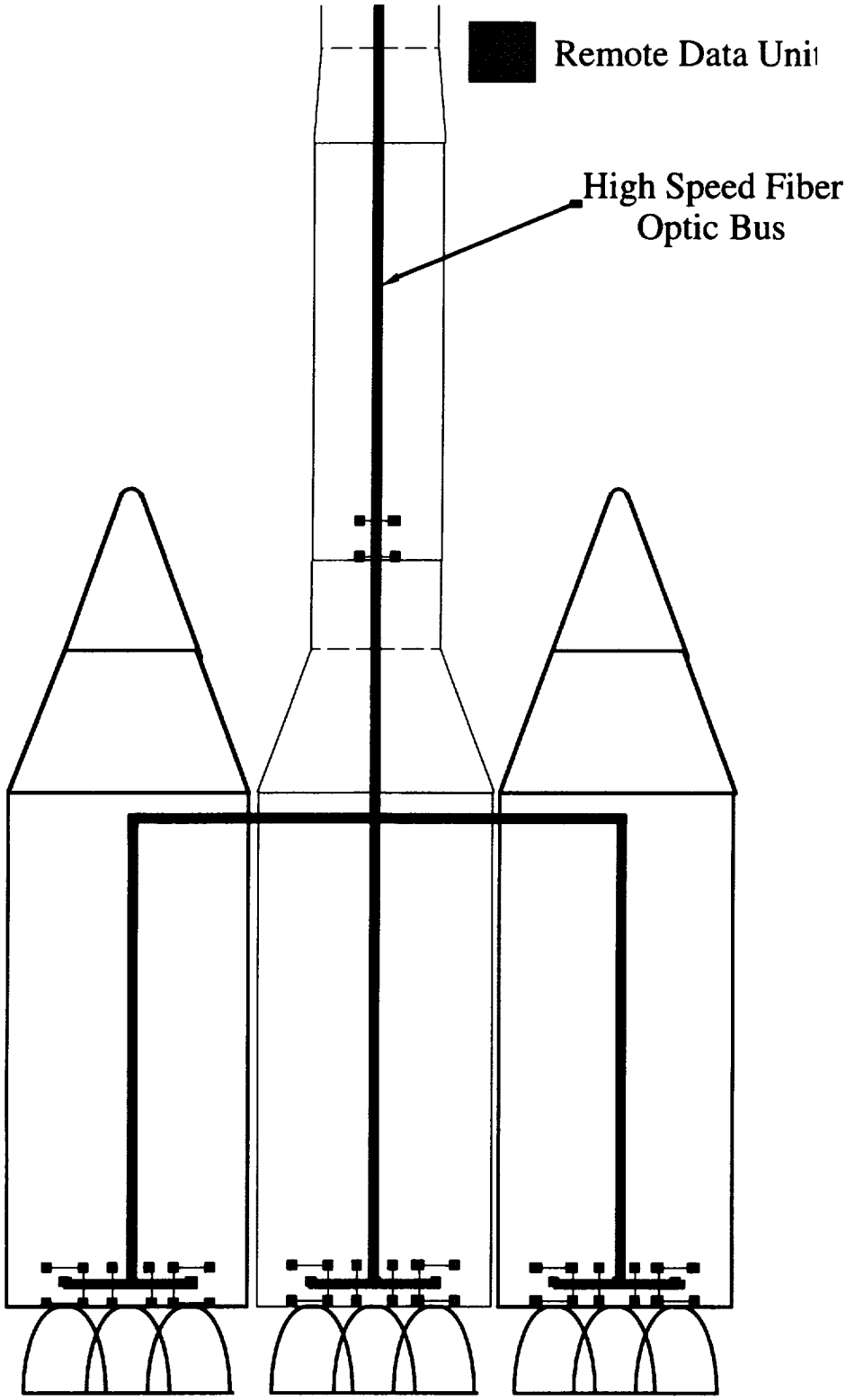

Figure 4.4.1.a Remote Data Unit Placement on Launch Vehicle

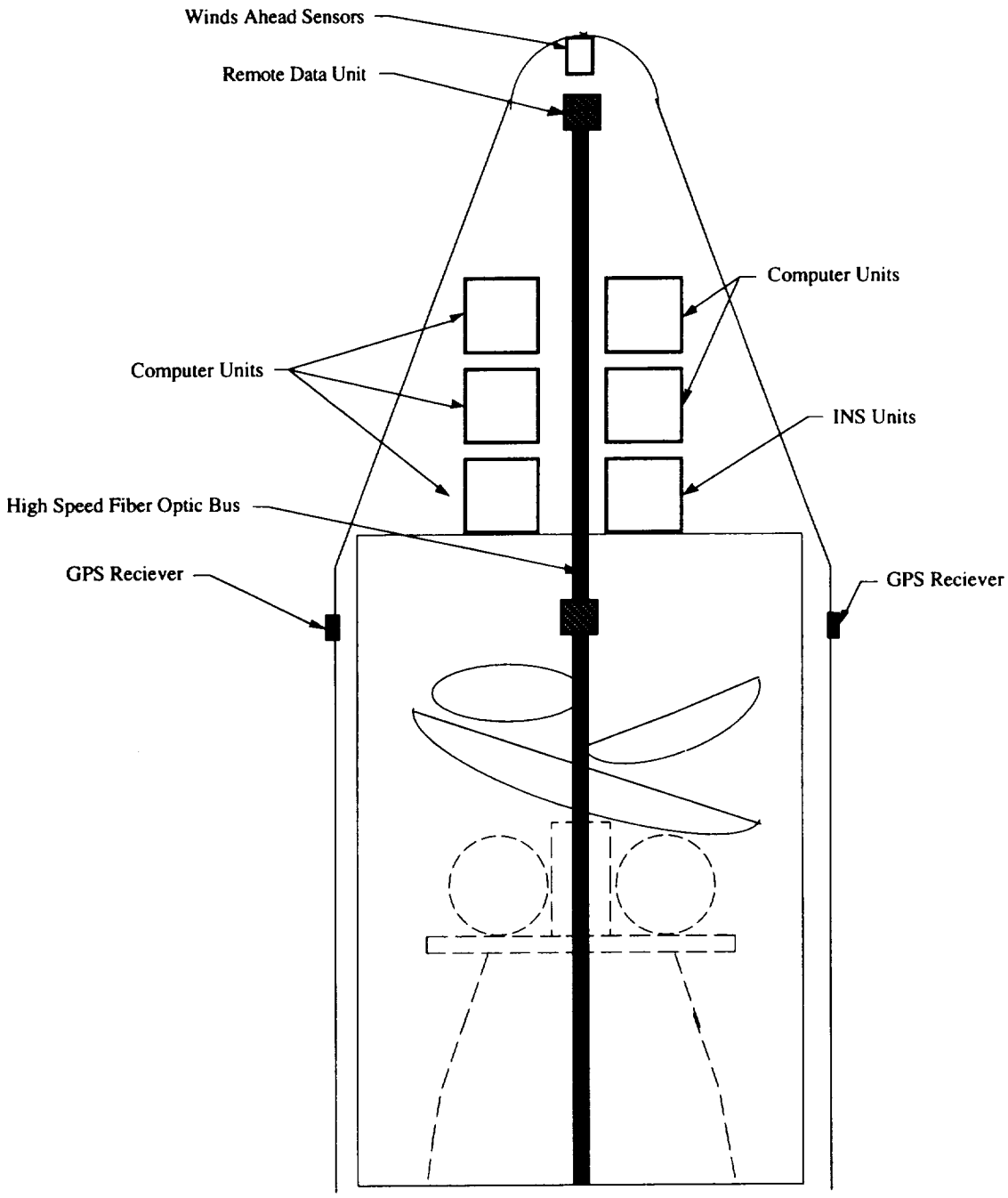

Figure 4.4.1.b Avionics Placement on Payload Shroud

4.4.2 Navigation, Guidance, and Control-Unmanned Mission

4.4.2.1 Introduction

The navigation, guidance, and control (NG&C) function for the unmanned mission was identical to the ascent phase of the manned mission, except all NG&C components were carried on board the launch vehicle. Since the

vehicle NG&C components have already been discussed in detail in section 3.3.2. only the differences will be discussed in the following sections.

4.4.2.2 Navigation Function

Navigation was accomplished by GPS and INS. The components were identical to the navigation components in the spacecraft, including the 26 state error Kalman filter. At approximately 200 km the apogee kick motor separated from the launch vehicle. The launch vehicle stayed within 200 km during entire mission phase so integrated GPS/INS was sufficient for maintaining pointing accuracy to carry out successful satellite separation. It was assumed that the launch vehicle's navigation, guidance, and control function for satellite insertion terminated at separation.

4.4.2.3 Reliability

Reliability for the unmanned launch vehicle was determined by the same methods as those determined for the spacecraft. Reliability was calculated over a mission duration of eight hours. It was determined that a single redundant sensor configuration was sufficient to maintain .9995 system reliability. A dual redundant configuration was ultimately decided on to reduce the probability of failure (see figure 4.4.2.a) . The cost of adding redundant sensors was determined to be worth the decreased risk of a NG&C catastrophic failure.

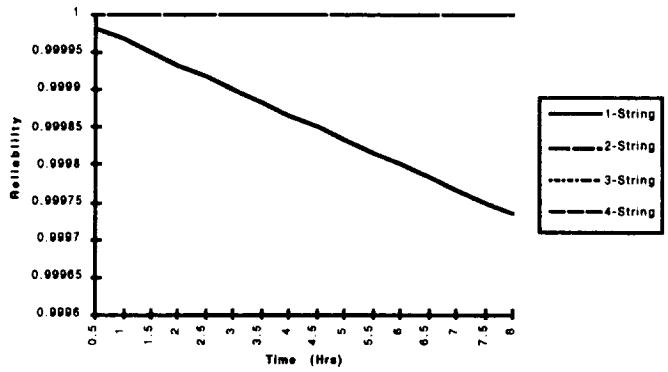

Figure 4.4.2.a Reliability curve for INS/GPS for Launch vehicle

4.4.2.3 Conclusion

A summary of mass, volume, power, and cost breakdown of sensors for NG&C of the un-manned launch vehicle is given in Table 4.4.2.a.

Senso		Qty	Vol (m^3)	mass (kg)	Pwr (Watts	Cost($M93)	Cost($M93)
GPSR		2	0.004	4.54	6	0.85	5.96
INS		2	0.06	38	120	5.96	20.39
Totals			**0.064**	**42.54**	**126**	**6.81**	**26.35**

Table 4.4.2.a Volume, mass, power, and cost breakdown for launch vehicle

4.4.3 Communications

For the unmanned missions, the only communications link required from the ORION launch system was tracking and telemetry. Once the payload was released, it was assumed that the payload would form its own telemetry and data link with the ground and would no longer have to go through ORION. From Table 3.4.3.c in section 3.4.3.3, the transmitted data rate was found to be 105 kbps. The antenna chosen for this process was an omnidirectional microstrip antenna. This was because it could remain flush with the sides of the launch vehicle thus greatly reducing the risk of being ripped off by the aerodynamic forces. Figure 4.4.3.a shows how it works.

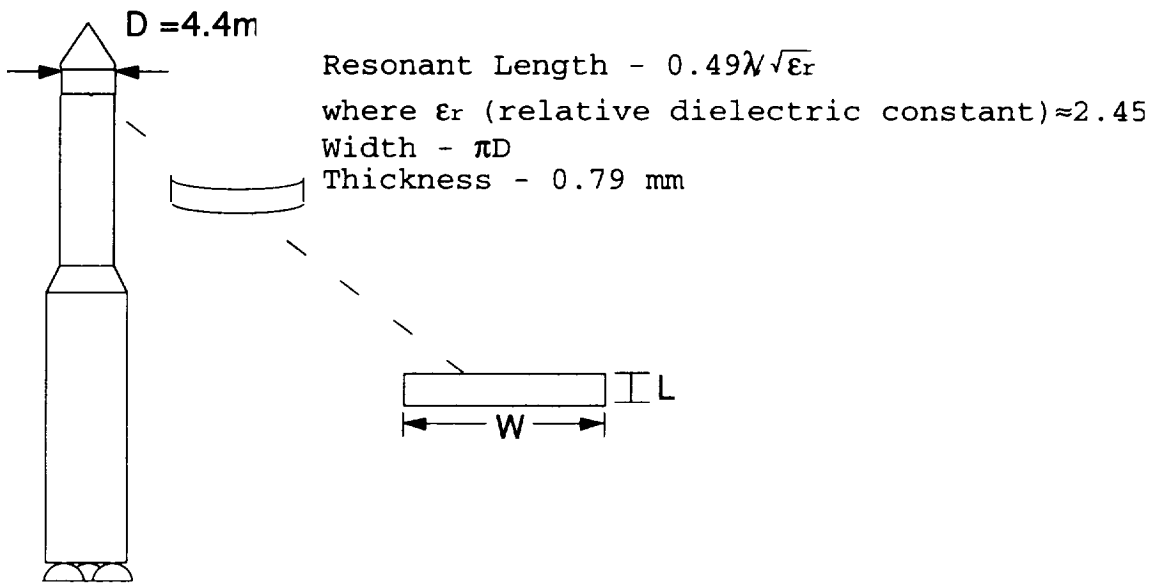

Figure 4.4.3.a Antenna for Launch Vehicle

Basically all of the link budget information can be found in section 3.4.3.7, the main difference being the smaller data rate. Since the transmission power remained the same, the link budget was as good as the one presented in section 3.4.3.7.4. Also, this configuration used only one antenna and one S-Band transciever.

4.5. Structures

4.5.1 Introduction

This section covers the structural design of the major launch vehicle components. This included: all the tank structures, the inter-stage and inter-tank fairings and nozzle shrouds. All analysis directly relating to the rocket engine and its supply piping was done by the propulsion and power team. The overall analysis was done by setting up a spreadsheet that calculated all the needed component thicknesses and masses. This spreadsheet incorporated all mass and aerodynamic forces into its calculations. Load factors were obtained from human factors. The first stages of this spreadsheet were used to determine material selection and tank end-cap geometries.

4.5.2 Design Margins and Load factors

In the design all loads and pressures were multiplied by factors of safety and by load factors. The factors of safety were included to ensure the vehicles structural integrity and to increase the reliability which was especially crucial for the manned mission. The load factors represented the multiple of g forces that the structure must endure.

The vehicle's mission requirements gave three separate overall trajectories that resulted in the following different launch accelerations: (1) the two manned missions had a 4 g load factor and, (2) the unmanned mission gave a 9 g load factor. Though the unmanned mission had a load factor 2.25 times larger than the manned missions the payload mass was 3.6 times lower. As a result the crucial load factors came from the manned missions.

Besides the steady state factors the vehicle was subject to transient accelerations that resulted from acoustic and engine vibrations. These values were found by analogy with the Atlas-II cryogenic launch system.

During launch the launch-vehicle experienced frequencies that resulted from engine oscillations and aerodynamic forces. To ensure that the vehicle did not have a matching natural frequency which would cause dangerous resonance of the structure, the structure's natural frequency was designed to be above the driving frequencies. The values were chosen by taking an upper bound analogy with other systems already operating.

These values were as follows:

Factors of safety were 1.6 for yield and 2.0 for ultimate.

Rigidity requirements were: Axial = 20 Hz, Lateral = 20 Hz.

The load factors are summarized in the following table.

Type	Steady State	Transient	Total
lateral	±4.0 g's[1]	±2.0 g's	±6.0 g's
axial	±4.0 g's	±3.0 g's	±7.0 g's

Table 4.5.2.a Steady State And Transient Load Factors

As a further margin in the design of the tanks, all propellant volumes were given an added 10%. This was to allow for ullage, cryogenic boiloff, and trapped-propellant which was residual propellant that remained in the tank's pipes and valves.

4.5.3 Material Selection and tank end-cap geometries

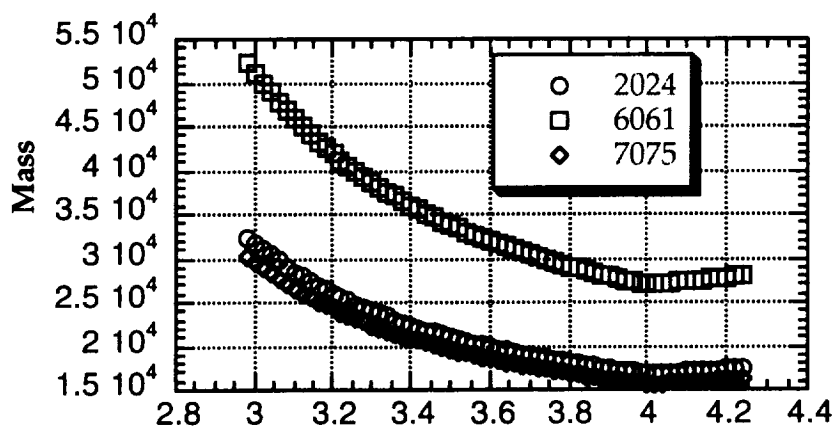

Figure 4.5.3a Material Selection for the Module

The choice of materials was chosen on the basis of cost and performance versus mass. After considering materials such as Titanium and Beryllium-Aluminum the choice was narrowed down to Aluminum. This still left several choices open. Among them were Al 2024, Al 6064, and Al 7075. Figure 4.5.3.a shows the resulting structural masses for the modules that result from using these materials. Even though this was done during the first stages of the analysis the general trends were used since the basic configuration remained unchanged. The results were similar for the third stage.

These results showed that Al 2024 and Al 7075 offered significant mass savings over Al 2024. Even though the graphs indicated that Al 7075 would be an optimum solution it was decided to use Al 2024 since Al 7075 was prone to

stress cracking from atmospheric corrosion which required cladding (which added to the overall mass and cost) or anodizing the material to prevent the problem. This was important since the stages were to be stored between manufacture and use. So to reduce costs and complexity it was decided to use Al 2024 for the stages. This material posed no problems with the cryogenic liquids that it stored.

Making the tank end caps hemispherical reduced the tank mass but did not necessarily reduce the overall stage mass. The geometries of the interstage, intertank and nozzle fairings all depended on the geometries of the tank end caps. By making the caps elliptical the end caps became shorter thus reducing the fairing lengths and their masses. At the same time the tank lengths had to be compensated to account for the change in volume for different end caps. Figure 4.5.3.b shows the results of a study of the effects of different ellipse shaped end caps. The results for both stages showed that using an ellipse with a ratio of semi-major to semi-minor axis of 2.0 gave the lowest overall masses.

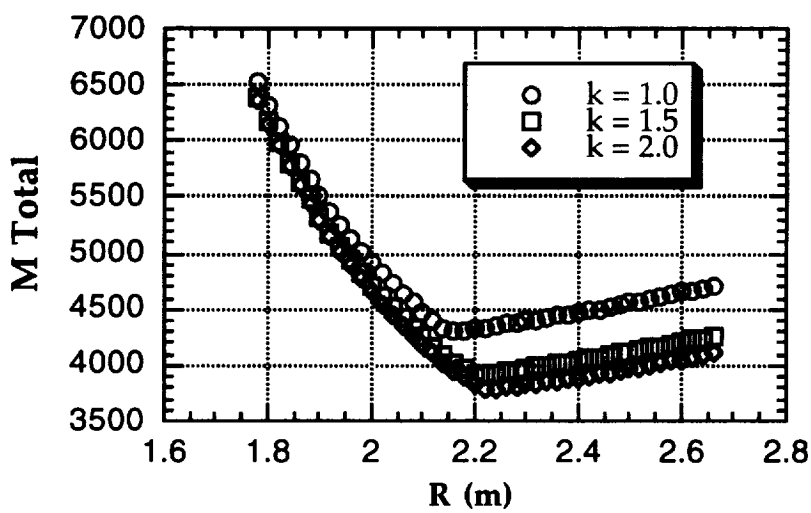

Figure 4.5.3.b Effects of different ellipse ratios on the overall mass.

4.5.4 Third Stage Masses and Dimensions

The masses and dimensions for the third stage were found from the spread sheet mentioned in the introduction (see Appendix A.4.5.4). It performed a top down design that calculated the loads exerted to the each part and then used these loads to determine the needed thicknesses of the part. Also the result of varying the radius of the structure was taken into account. The thicknesses were found from analyzing rigidity requirements, ultimate and yield stresses from equivalent loads, and hoop pressure stresses. The resulting structure was then checked to verify that the applied loads did not exceed the

critical loads of the part. The whole process was then repeated for the next part. Included in the calculations were estimations for the tank insulations.

The design of the helium pressurant tanks for the LO_X tanks was done separately. Results showed that the high pressures created a very massive part if conventional metals were used. Instead Kevlar-49 was chosen for its high hoop stress and for its gradual failure mode as opposed to the catastrophic failure mode of other composite materials.

Examination of figure 4.5.4a showed that the minimum stage mass occurred for a radius of 2.50 m. Since the design was frozen before these calculations at 2.22 m. which still gave good masses this result was used.

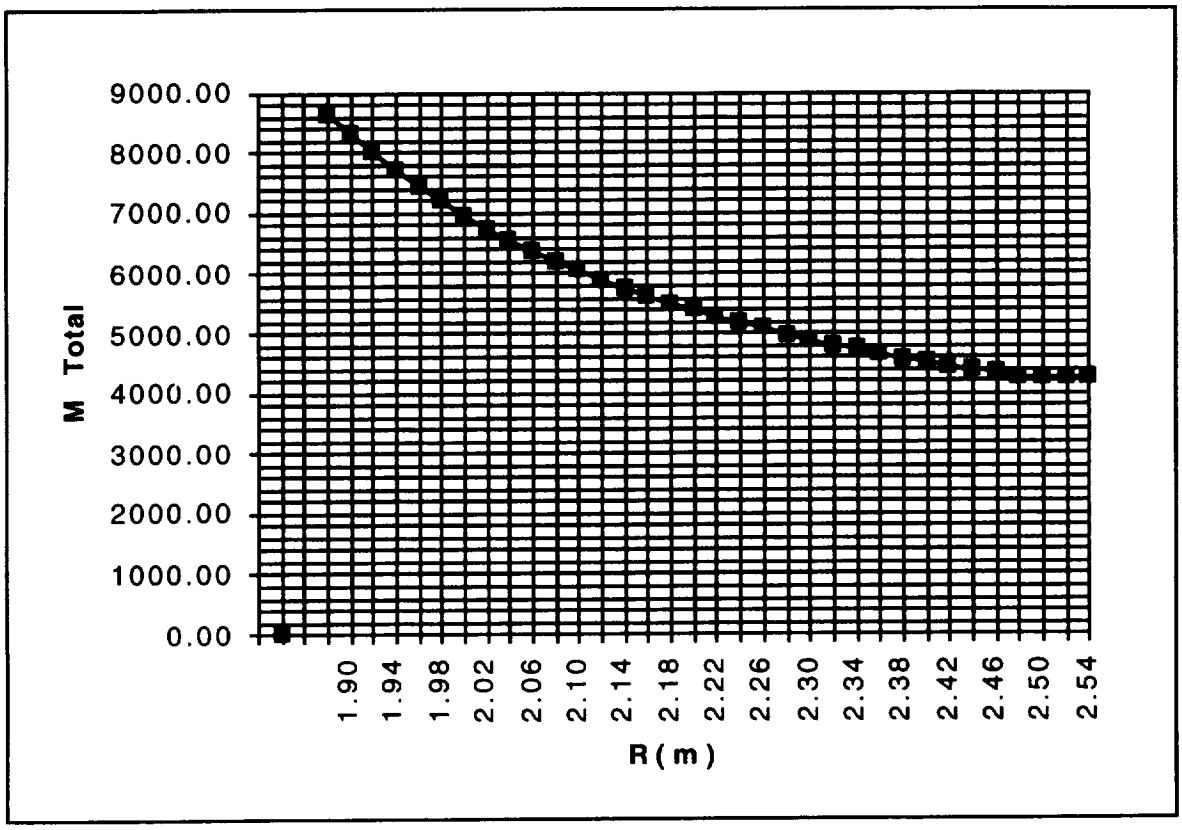

Figure 4.5.4a Mass Versus Radius For The Third Stage

The results of this analysis are shown in in figure 4.5.4b and summarized in Table 4.5.4a.

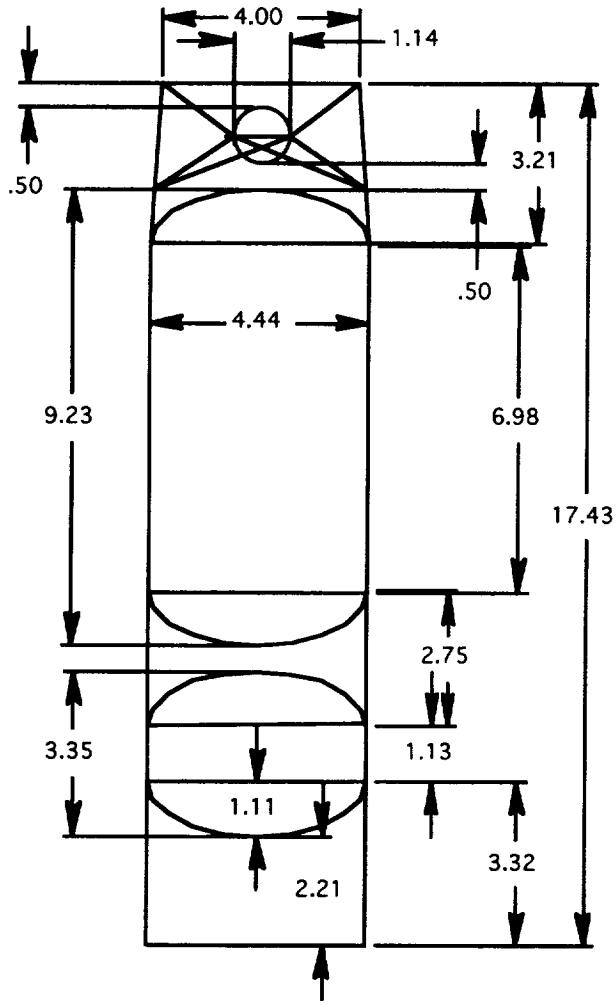

Figure 4.5.4b Dimensions of the Third Stage

Part	Thickness (mm)	Pressure (MPa)	Upper Radius (m)	Lower Radius (m)	Mass (Kg.)
Helium Tank	8.3	20	.57	.57	14
Interstage Fairing	2.16	-	2.22	2.22	261.54
Hydrogen Tank	7.47	.52	2.22	2.22	3022
Intertank Fairing	2.60	-	2.22	2.22	284.19
LO_X Tank	3.84	.45	2.22	2.22	647
Nozzle Shroud	4.73	-	2.22	2.22	631.06
Hydrogen Tank Insulation	-	-	-	-	334
LO_X Tank Insulation	-	-	-	-	98
Total	-	-	-	-	52778

Table 4.5.4.a Third Stage Mass and Dimension Summary

4.5.5 Dimensions and Masses of the Modules

The calculations for the module were similar to those for the third stage. The spreadsheet for the module mass calculations is in Appendix A.4.5.5. Figure 4.5.5.a gives the results of these calculations. The lowest mass occurred for a radius of 4.44 m. but due to the design freeze a radius of 4.02 m. was used. Figure 4.5.5.b shows the module's dimensions and Table 4.5.5.a gives a summary of these dimensions and of the masses.

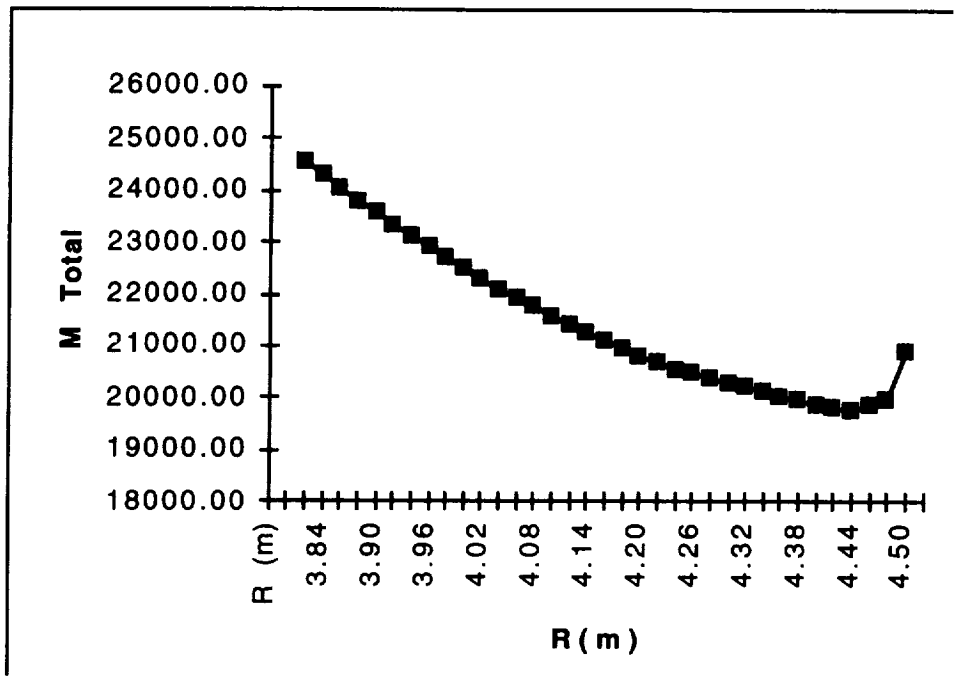

Figure 4.5.5.a Mass versus Radius for the Modules

Part	Thickness (mm)	Pressure (MPa)	Upper Radius (m)	Lower Radius (m)	Mass (Kg.)
Helium Tank	14	20	.94	.94	55
Interstage Fairing	4.22	-	4.02	4.02	1212
Hydrogen Tank	12.3	.52	4.02	4.02	11734
Intertank Fairing	8.72	-	4.02	4.02	284.19
LO_X Tank	6.05	.45	4.02	4.02	2647
Nozzle Shroud	9.26	-	4.02	4.02	2816
Hydrogen Tank Insulation	-	-	-	-	755
LO_X Tank Insulation	-	-	-	-	238
Total	-	-	-	-	22293

Table 4.5.5a Module Mass and Dimension Summary

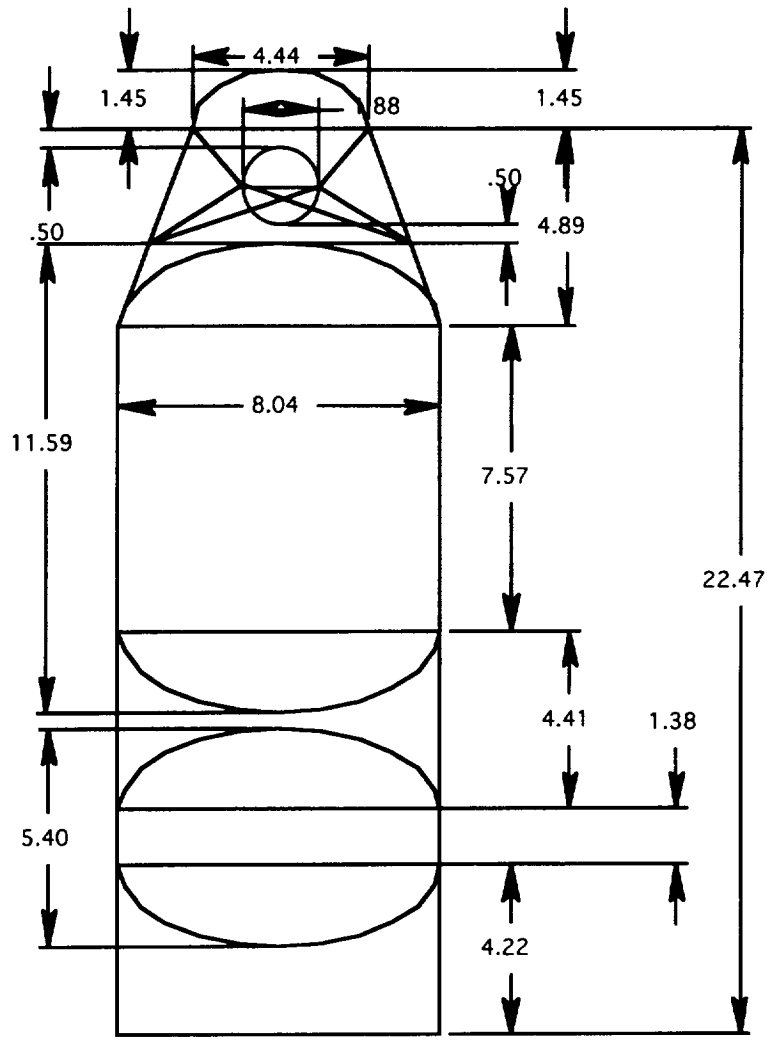

Figure 4.5.5b Overall Module Dimensions

4.6 Propulsion and Power

4.6.1 Introduction

The launch vehicle main propulsion system was based on cryogenic liquid hydrogen/liquid oxygen rockets engines with an Isp around 430 s. The main propulsion system consisted of combustion chambers, a feed system, propellant tanks, an injection system, an ignition system, thrust vectoring controls, and nozzles. Any power needed for the ignition system, valves, and gimbal actuators was provided by auxiliary power units located on the launch vehicle.

4.6.2 Engine Design

There were three stages to the launch vehicle (manned version); however, since the first and second stage were identical, the engines were also identical. Therefore, only two engine designs for the launch vehicle were needed: the modular engine and top-stage the engine. The modular engine and the top-stage engine were similar in design except for their dimensions.

4.6.2.1 Chamber Pressure

One of the main criteria of the design process was the selection of a chamber pressure. Several trade studies were performed to determine the effects of chamber pressure on the overall design of the engine.

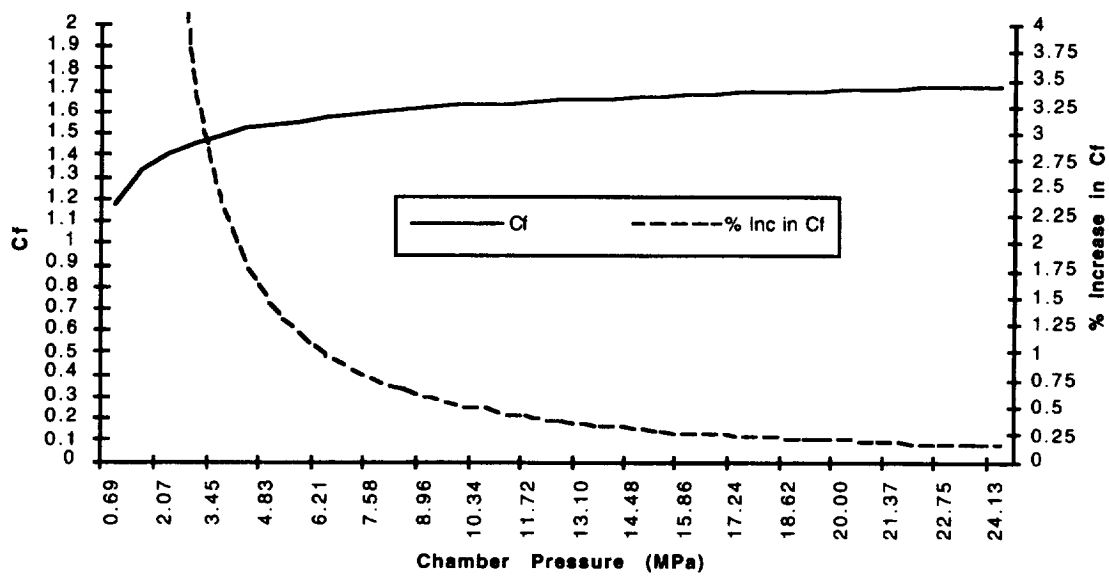

Figure 4.6.2.a Thrust Coefficient Vs Chamber Pressure

Given that the size of the launch vehicle was on the same magnitude as the space shuttle, any appreciable increase in thrust without a significant increase in weight was desired. From Figure 4.6.2.a, chamber pressures greater than 20 MPa were found to provide less than 0.25% increase in thrust; this was considered as the upper limit of the chamber pressure.

Even though higher chamber pressures increased the thickness of the combustion chamber walls, they also decreased the area ratio (see Figure 4.6.2.b). Smaller area ratios meant a smaller nozzle size, and a smaller overall mass of the combustion chamber and nozzle (See Appendix A.4.6.2.1.a for a detailed mass analysis). However, there was a direct relation between higher chamber pressure and higher manufacturing cost. By using current

technology, chamber pressures up to 16.5 MPa were attainable without a significant increase in cost (Akin 1994).

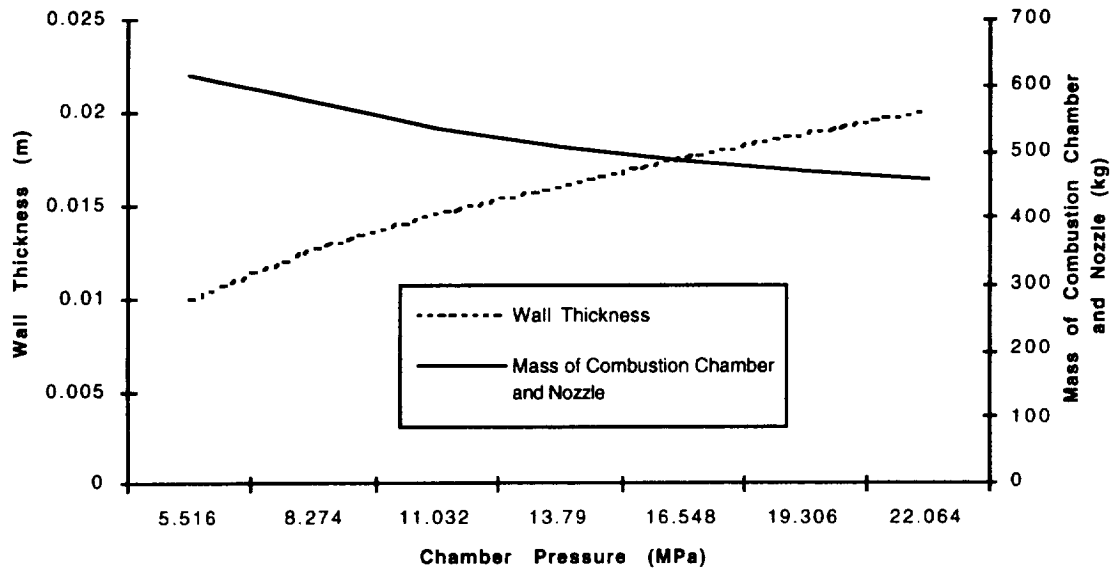

Figure 4.6.2.b Mass of Combustion Chamber and Nozzle Vs Chamber Pressure

4.6.2.2 Selection of Number of Engines

Due to the high reliability requirement, the number of engines for the modular stage had to be greater than one. A dual-engine modular stage avoided the single point failure; however, if one of the engines failed, the gimbal of the second engine would be under a lot of strain to counteract the torque created by the loss of the engine. A three-engine and a four-engine modular stage would avoid the single point failure and torque problem created by the loss of an engine. Having five or more engines per stage though added more mass to the launch vehicle and created more complexity for installation and maintenance (Huzel and Huang 1992). Since the mass of the avionics and the mass of propulsion system was a function of the number engines, the three engine per stage configuration was chosen to reduce the overall weight and cost.

4.6.2.3 Combustion Chamber and Nozzle Geometry

Using the formulas in Appendix A.4.6.2.3.a, the performance of the engine as well as the engine geometry was calculated. A single combustion chamber was designed for dual use in the modular stage as well as in the top-stage to reduce overall cost. The only difference between the modular stage and the top-stage engine was the expansion ratio. Even though the center modular stage operated at a higher altitude than the strap-on modular stages, the

nozzle for the center modular stage was identical to the nozzle for the strap-on modular stages. The reasoning behind identical nozzles was the research and development and production cost.

The following figures are scale drawings of the dual-use combustion chamber, modular nozzle, and the top-stage nozzle. See Appendix A.4.6.2.3.b. for detail specifications.

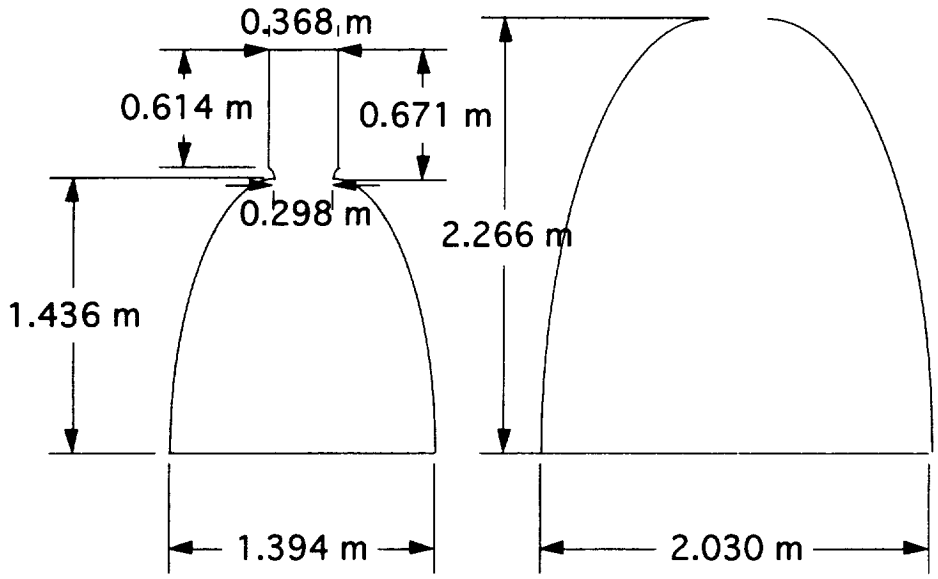

Figure 4.6.2.c Scale Drawings of the Combustion Chamber and the Two Nozzles

The next figures are the orientation of the engines with respect to the stages. To avoid impingement and gimbaling problems, the clearance between engines was one-half the diameter of the nozzles.

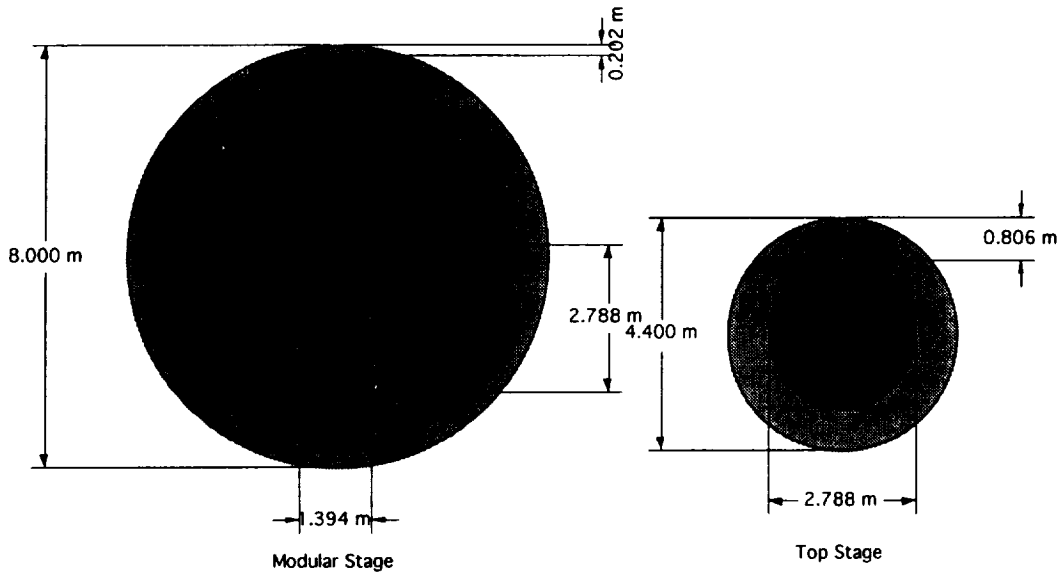

Figure 4.6.2.d Orientation of the Rocket Engines

4.6.3 Propellant Feed System

There were two primary methods of transporting the propellants from the tanks to the thrust chamber to provide the required chamber pressure: a gas pressure feed system and a turbopump system. Pressure feed systems required the propellant tanks to withstand much higher pressures (on the order of 10 to 40 times higher than turbopump systems). Pressure feed systems were, therefore, better for low propellant mass and low chamber pressure systems. In general, turbopumps were superior for long duration, non-impulsive, high chamber pressure applications. Since the ORION launch system was relatively massive and the engine thrust chambers required a high chamber pressure (16.5 MPa), a turbopump feed system had to be used.

4.6.3.1 Pump Cycle and Drive Arrangement

There were many different types of pump cycles and turbine-pump drive arrangements considered for the ORION launch vehicle. Appendix A.4.6.3.1.a lists the basic tradeoffs between these cycles and drive arrangements. From the list of pumping cycles in the appendix two cycles were chosen as primary candidates: the expander bleed cycle and the staged combustion cycle. Both of these cycles were very efficient closed cycle systems. The expander bleed cycle, however was not practical for high chamber pressure applications, since the turbine working fluid was not energetic enough to drive the turbines to provide the necessary power to the pumps. The staged combustion cycle was therefore chosen to provide the necessary

chamber pressure. Referring to Figure 4.6.3.a, the LH2 entered the fuel pump

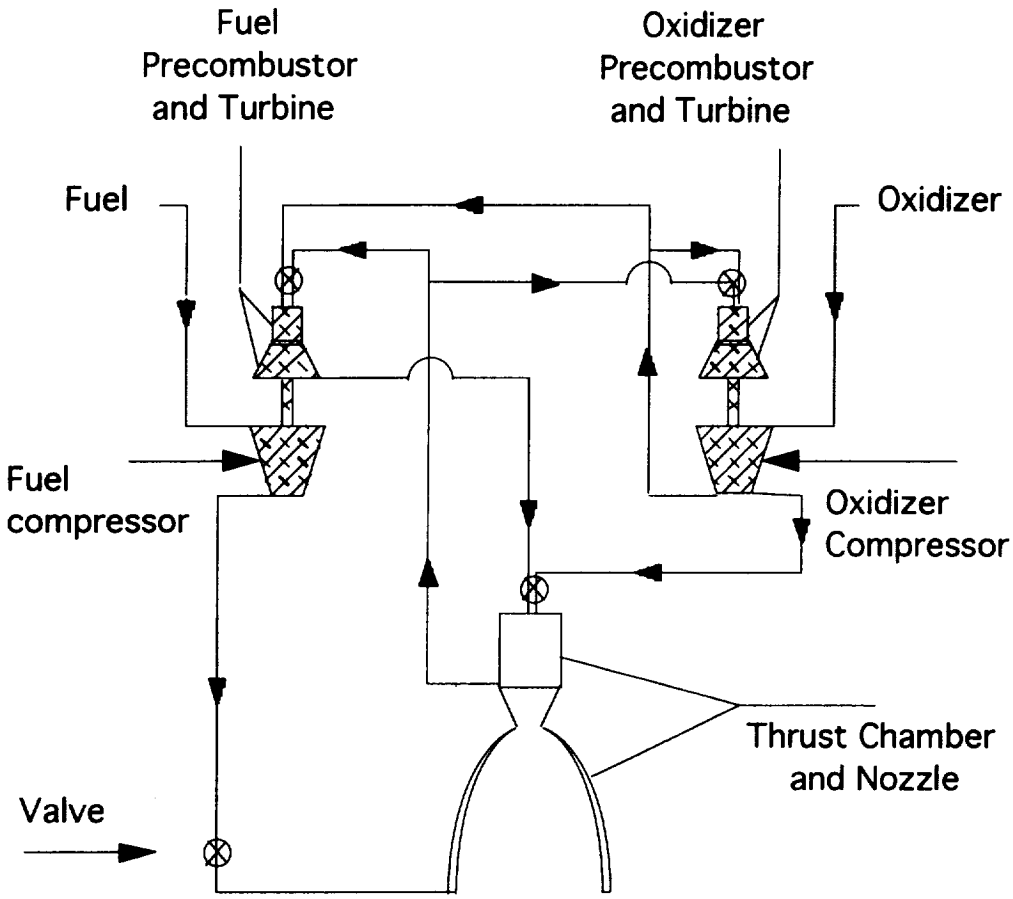

Figure 4.6.3.a Turbopump Cycle Schematic

and was then sent to the nozzle cooling jacket to cool the nozzle, where it gained thermal energy. It was then sent to the precombustor to be burned with the oxidizer. The LOX entered the oxidizer pump and the flow was then split with some of the oxidizer going directly to the main combustion chamber and some going to the precombustor. The precombustor burned all of the fuel with some of the oxidizer and thus had a different O/F ratio than the main combustion chamber. The precombustor supplied the high energy gases needed to run the turbines to provide the necessary pumping power. The gases were then sent to the main combustion chamber to be burned with the rest of the oxygen. This system could supply a very high chamber pressure as well as provide a high Isp. This system required an auxiliary power unit to start the pumps since the propellants were first pumped then used to drive the turbines. The APU was required until the pump power, propellant flows and shaft speeds of the pumps had reached steady state operating conditions.

The drive arrangement chosen for the turbopump system is also shown in Figure 4.6.3.a. The fuel and oxidizer pump were run by separate turbines

connected in parallel. Two turbines were chosen as opposed to one because the LH2 pump required a higher head rise (i.e. pressure rise) and operated at a much higher shaft speed than the LOX pump. Since the shaft speeds of the two pumps were so disparate (approximately 5800 rpm for LOX pumps and 34000 rpm for the LH2 pump), if only one turbine were used to drive both pumps a complex and inefficient gear reduction mechanism would be required.

4.6.3.2 Design Methodology

One of the main considerations behind the design of the turbopumps was to make sure that cavitation would not occur. Cavitation occured when the vapor pressure of the propellant was higher than the local static pressure. This caused the propellant to boil and could cause erosion of the compressor blades and pressure instabilities in the pumps. The pumps, therefore were designed such that the net positive suction head available or suction head above vapor pressure (i.e. the suction pressure of the pump minus vapor pressure at the pump inlet) was always higher than the net suction head required to suppress cavitation.

The pump pressure rise requirements were obtained by calculating the pump discharge pressure and subtracting the pump inlet pressure. First the discharge pressure of the LOX pumps was calculated from the following relation:

$$(P)_d = P_c + (\Delta P)_{loss}$$

where P_d was the pump discharge pressure, PC the thrust chamber pressure and ΔP_{loss} the pressure losses due to friction and injector pressure drop downstream of the pump. The injector pressure drop was assumed to be 20% and the friction losses were assumed to be 5% of the total chamber pressure. These values were obtained by examining the losses of similar engine systems and injectors. The pump inlet pressure was varied by varying the LOX storage pressure and thus a wide range of pump ΔP's were obtained. These ΔP's were then used to optimize the whole oxidizer feed system (tank and pump) by minimizing the system mass and size. Once an optimum range was found and the power requirements of the pump were determined, the turbine was characterized. A similar analysis was done for the LH2 pumps taking into account the losses in the cooling jacket (assumed to be about 25%) as well as the turbines, valves and lines.

4.6.3.3 Feed System Parameters

The results obtained from the optimization studies and analysis for the LOX and LH2 pumps as well as turbines , and tanks are shown in Tables 4.6.3.a-b. and Figures 4.6.3.b-c. From the optimization studies shown in Figures 4.6.3.b-c the propellant tank storage pressures were determined and the pump

characteristics were derived. The assumptions and equations used to derive the pump parameters are given in Appendix A.4.6.3.3.a and A.4.6.3.3.b

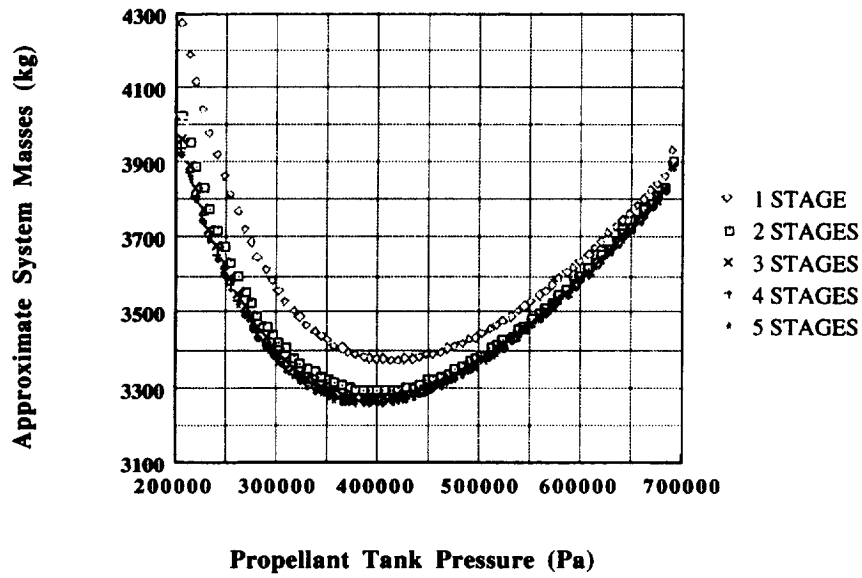

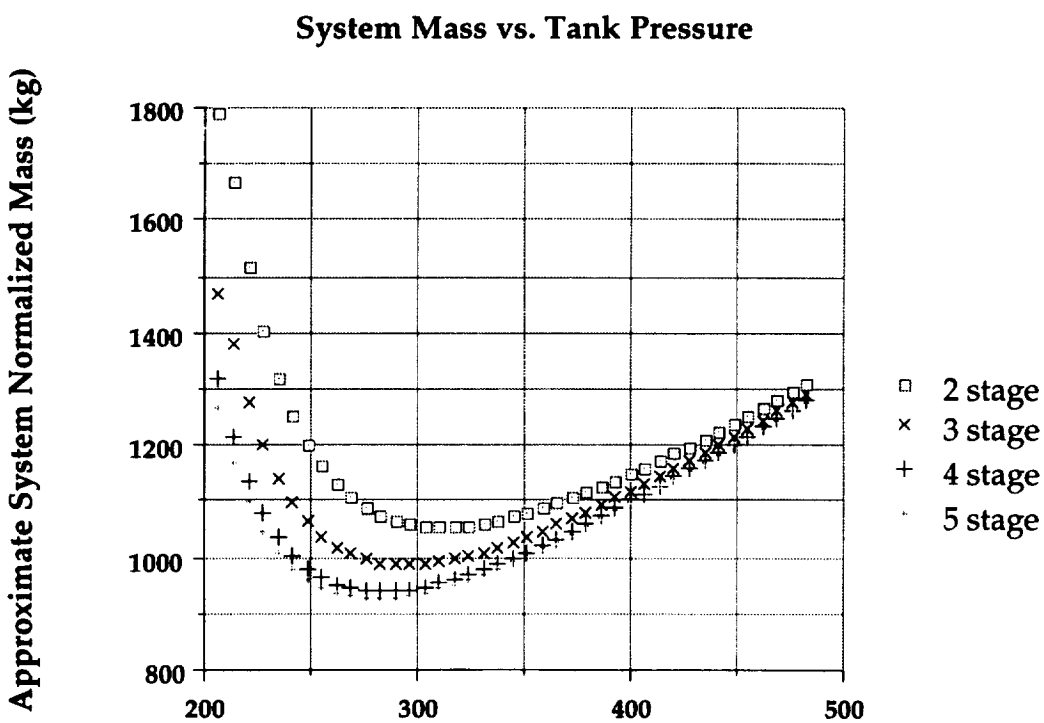

Figures 4.6.3.b and c Optimization of Turbopumps

ORION Engine Feed System	Pump Characteristics	
Designation	LOX Pump	LH_2 Pump
Type	Radial	Radial
No. of impeller stages	3	4
Impeller diameter (cm)	32.6	23.2
No. of inducer stages	1	1
Inducer diameter (cm)	16.2	12.5
Flow rate (kg/s)	382	78
Inlet pressure (MPa)	0.32	0.29
Discharge pressure (MPa)	22.3	32.66
Pump pressure rise (MPa)	21.9	32.36
Shaft speed (rpm)	5840	35840
Fluid power output (kW)	8203	35564

Table 4.6.3.a Pump Specs.

ORION Engine Feed System	Turbine Characteristics	
Designation	LOX Pump	LH_2 Pump
	TURBINES	TURBINE
Type	Low-reaction	Low-reaction
No. of stages	2	2
Flow rate (kg/s)	137	137
Inlet temperature (K)	811	811
Inlet pressure (MPa)	23.3	23.3
Pressure ratio	1.13	1.49
Shaft speed (rpm)	5840	35840
Turbine power (kW)	12594	54714
Mixture ratio (Precombustor)	0.79	0.79

Table 4.6.3.b Turbine Specs.

4.6.4 Propellant Tank Requirements

From the turbopump analysis the storage pressures of the propellants were determined. The LOX tanks were required to be pressurized to .386 MPa while the LH2 tanks were pressurized to .324 MPa. To pressurize the LOX tanks to the required value a helium pressurization system was used to maintain .386 MPa in the LOX tanks for expulsion of the oxidizer. The helium requirements for LOX tank pressurization are given in Table 4.6.4.a for the modular stages and the third stage. The LH2 tank on the other hand had to rely on self pressurization because it could not be pressurized by another fluid. Any fluid that came in contact with LH2 would be liquefied and thus rendered useless as a pressurizing gas. Since LH2 had a fairly high

vapor pressure as compared to oxygen, self pressurization was the only practical solution.

		MODULE HELIUM REQUIREMENTS			
LOX Mass	He Storage Temp.	He Storage Press	Mass of He Required	He Density	He Vol.
182067	295 K	20 MPa	101 kg	.034 kg/m^3	3.427 m^3
		STAGE 3 HELIUM REQUIREMENTS			
LOX Mass	He Storage Temp.	He Storage Press	Mass of He Required	He Density	He Vol.
41834	295 K	20 MPa	23.2	.034 kg/m^3	0.79 m^3

Table 4.6.4.a Helium Pressurant Requirements for modules and 3rd stage

4.6.5 Injection System

Injection of the propellants into the combustion chamber had to occur such that sufficient atomization and mixing of the propellants was achieved and a homogeneous mixture of propellants was burned. A non-impinging concentric "ring-groove" type manifold would be used to inject the propellants into the thrust chamber as well as into the precombustors. The injector elements consisted of hollow post and sleeve coaxial tubes. A schematic of the element and the manifold is displayed in Figure 4.6.5.a. This type of injector element provided very high performance and combustion stability for a gaseous fuel and liquid oxidizer. Since the fuel was burned prior to entering the combustion chamber this injector type was an obvious choice for the engine. In the coaxial element a central stream of LOX flowed through the inner tube of the element while gaseous hydrogen flowed through the outer tube of the element. Mixing and atomization was promoted by the shearing action of the gaseous hydrogen against the liquid oxygen. The area required for injection of LH2 was determined to be 115 cm^2 while the area required for injection of LOX was determined to be 58 cm^2 (for the main thrust chamber).

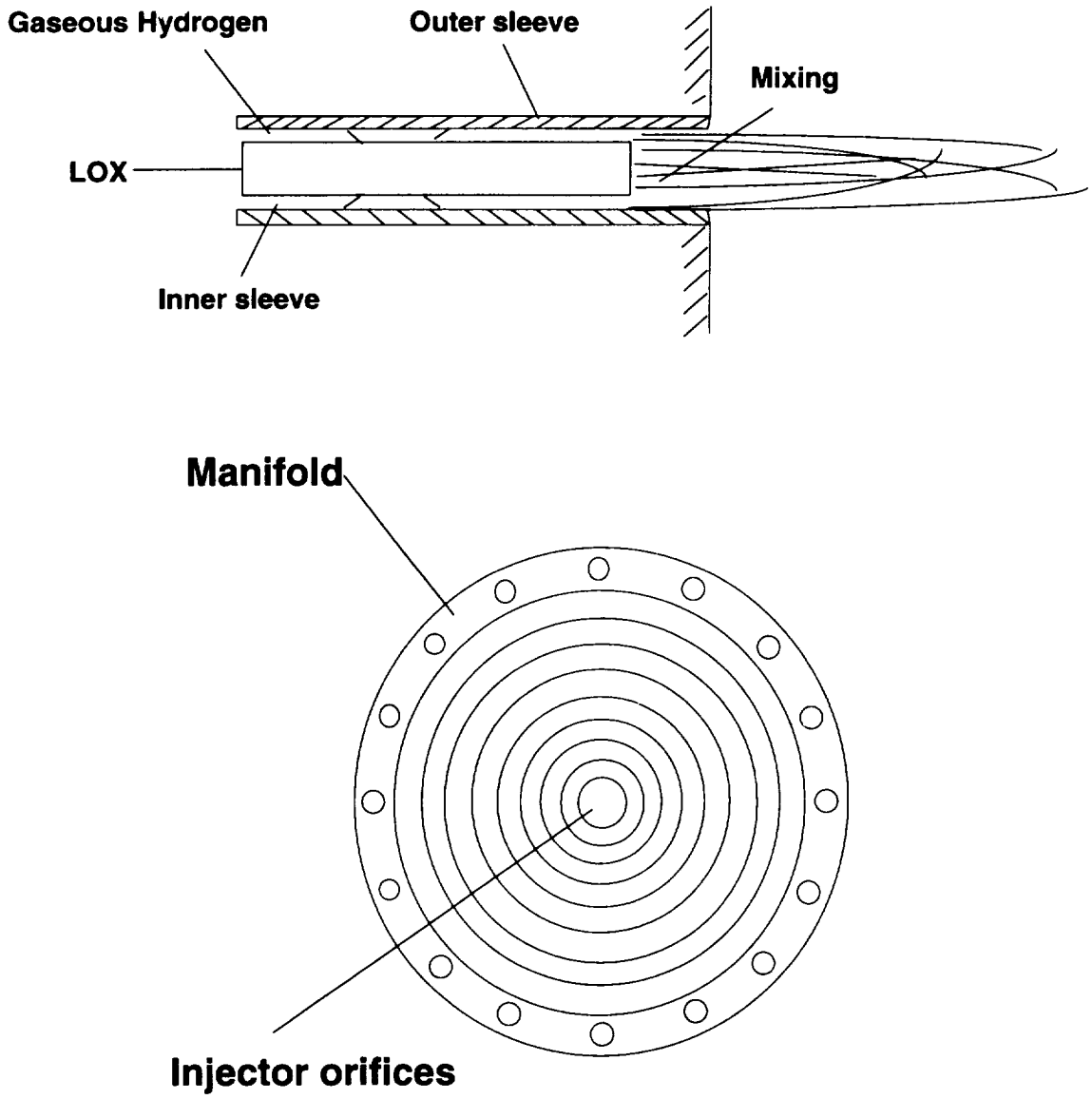

Figure 4.6.5.a. Injector element and manifold schematics

4.6.6 Ignition System

The ignitions system was required to rapidly and reliably combust the incoming propellant before any accumulation of the propellants occurred in the thrust chamber. Any accumulation of propellants could lead to the formation and detonation of explosive mixtures. Obviously, this was undesirable since it could lead to engine failure and loss of the vehicle.

Three types of ignition systems were investigated for the main engines: pyrotechnic igniters, hypergolics, spark plug igniters, and spark torch igniters. Hypergolics were ruled out because of their toxicity and they would require separate tanks and piping for storage and transport to the thrust chamber.

Spark plug igniters were ruled out because in order to obtain even combustion of the propellants multiple plugs would be required to be mounted to the injector face. This would be unnecessarily complex and there would also be a higher chance of failure with many plugs. Also, if multiple spark plugs failed, pressure spikes could occur in the thrust chamber because of the uneven combustion of the propellants that would result.

Pyrotechnic igniters were ruled out because they required redundancy due to the complex electro-explosive interfaces and components that were required. Also compared to spark torch ingiters they were larger systems. Spark torch igniters were chosen for the ignition system for the main thrust chamber as well as the precombustors. Spark torch igniters were relatively small systems ranging in diameter from .64 to 2.6 cm. In spark torch igniters, a small amount of fuel and oxidizer were admitted into the igniter combustor and spark ignited. The flame that resulted from this combustion was ducted to the rest of the injector face plate to ignite the rest of the propellants.

4.6.7 Thrust Vector Control

In order to provide for the maneuvers during takeoff and in order to attenuate disturbances imparted on the launch vehicle during takeoff the launch vehicle had to be equipped with a mechanism to control its thrust direction. Four systems were investigated for thrust vector control of the launch vehicle stages: gimbals, liquid side injection, jet vanes, and auxiliary thrust chambers.

Liquid side injection into the nozzle, while seemingly a simple concept, was ruled out because it would add complexity to the feed system and was only applicable to low vector angle applications. The additional plumbing that would be required to implement the design and the fact that the nozzle was regeneratively cooled (thus making it difficult to inject the fluid into the nozzle) would make it very tough to implement the design. Jet vanes were ruled out because of the loss in thrust and performance that would occur and also due to the fact that they tend to erode rather quickly in the nozzle. Auxiliary thrust chambers were ruled out because of the added weight and complexity of having extra chambers, nozzles, and piping leading to these components. Also these auxiliary thrust chambers would have to be hinged or gimballed to provide control which added even more complexity. Finally, because there were already three engines on the modular stages there would be very little room to implement the design and plume impingement would also have to be considered.

Gimbals were chosen for both the modules and the third stage because they were a reliable, proven technology and could provide for relatively large angular displacements (on the order of 15 or more degrees). Also, loss of thrust and specific impulse when the engines were gimballed was negligible.

4.6.8 Power

The following table shows the power requirement for gimbal actuators and valves on the launch vehicle.

	Power Required		Total Power
	Per Engine (kW)		Per Stage (kW)
Gimbal Actuators	115.5	Modular Stage	395.01
Valves	16.17	Top Stage	131.67

Table 4.6.8.a Power Requirements for Launch Vehicle

The power system for the modular stages consisted of four APU's similar to the APU's on the spacecraft except they supplied up to 135 kW each. Only three were necessary to operate all the actuators and valves; the fourth APU was used only in case of an emergency. Prior to launch, the same APU's supplied power to the turbines to start the pumping the fuel.

The top stage only needed one 135 kW APU. Emergency power was provided by the spacecraft's two 65 kW APU's.

5.0 Conclusion

5.1 Introduction

The overall masses of the vehicle and the overall vehicle cost are discussed in this section. This section shows whether or not we met the cost goals laid out in the first chapter. These goals were less than $100M per manned mission or less than $1000/kg bulk cargo.

5.2 Overall Mass and Center of Gravity

After the first design iteration, the spacecraft and the launch vehicle masses were obtained from either mass estimating relations or from the volume and the density of specific components. Please see appendix for detailed component level mass break down.

The spacecraft mass was calculated to be 39,681kg dry, and 50,936kg wet (with 10% margin).

The launch vehicle mass was summarized below:

	Inert mass	Propellant mass	Stage total
Top stage	10,124 kg	49,200 kg	59,324 kg
Modules	33,253 kg	214,110 kg	247,363 kg
Unmanned total	43,377 kg	263,310 kg	306,687 kg
Manned total	109,883 kg	691,530 kg	801,413 kg
Initial estimate			
Top stage	8,860 kg	50,200 kg	59,060 kg
Modules	38,560 kg	218,480 kg	257,040 kg
% difference			
Top stage	14%	2%	0.4%
Modules	-14%	-2%	-0.4%

Table 5.2.a Launch Vehicle Masses

The actual mass of the launch vehicle was quite close to the initial estimate. This would make the second iteration and subsequent design process easy.

To determine the center of gravity (cg)of the entire ORION system, the mass budget was used and locations were input. The system is assumed to have the cg centered in the directions perpendicular to the fuselage. The cg was determined for the individual first stage module, the second, upper stage, the spacecraft and the unmanned payload. From this data, the overall cg of the system was determined, along with the change in cg as fuel is consumed and stages are exhausted and jettisoned. Appendix A.5.2 shows the actual spreadsheet data, including cg analysis for each component. Table 5.2.a shows the relevant data from the spreadsheet.

ALL DISTANCES RELATIVE TO GROUND				
Unmanned Payload		Mass (kg)	CG Location (m)	
	GeoSAT	7800	47.77	
	Structure	1560	50.31	
	TOTAL	9360	48.1933333	
	Dry Mass (kg)	Dry CG (m)	Wet Mass (kg)	Wet CG (m)
Module	560566.035	16.86	2251454.02	9.1
Upper Stage	296991.121	29.33	1873450.52	31.53
Spacecraft	2039024.53	56.52	2690595.13	56.85
Unmanned Payload	9360	70.14	9360	48.19
Config 1-2	4017713.75	37.90958124	11318407.7	24.1637278
Config 3	866917.16	21.70726833	4134264.54	19.35
CG LOCATIONS				
		Config 1-2 (m)	Config 3 (m)	
Launch		24.16	19.4	
Stage 1 Burnout/Separation		31.67851988	28.2281896	
Stage 2 Ignition		34.11612809	31.6128217	
Stage 2 Burnout/Separation		43.219152	29.9062329	
Stage 3 Ignition		46.4566405		
Stage 3 Burnout/Separation		54.11428127		
Orbital Insertion Igntion		56.85		
After Deorbit Burn		56.52		

Table 5.2.a CG Data

To obtain a better understanding of the movement of the cg during flight, the cg locations were superimposed on drawings of the ORION system in the manned and unmanned configurations, as shown in Figures 5.2.b and 5.2.c.

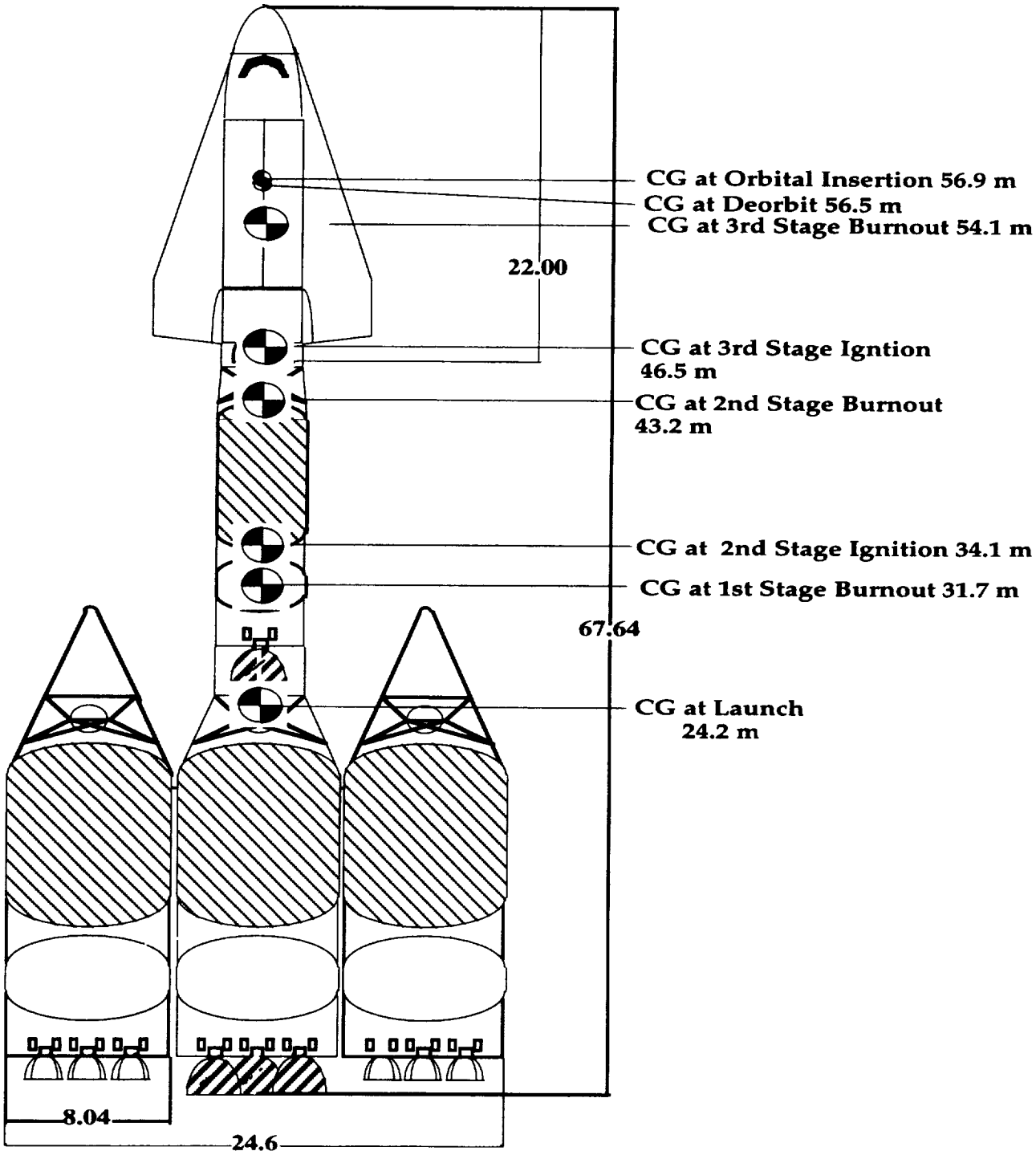

Figure 5.2.b CG Locations - Manned Configuration

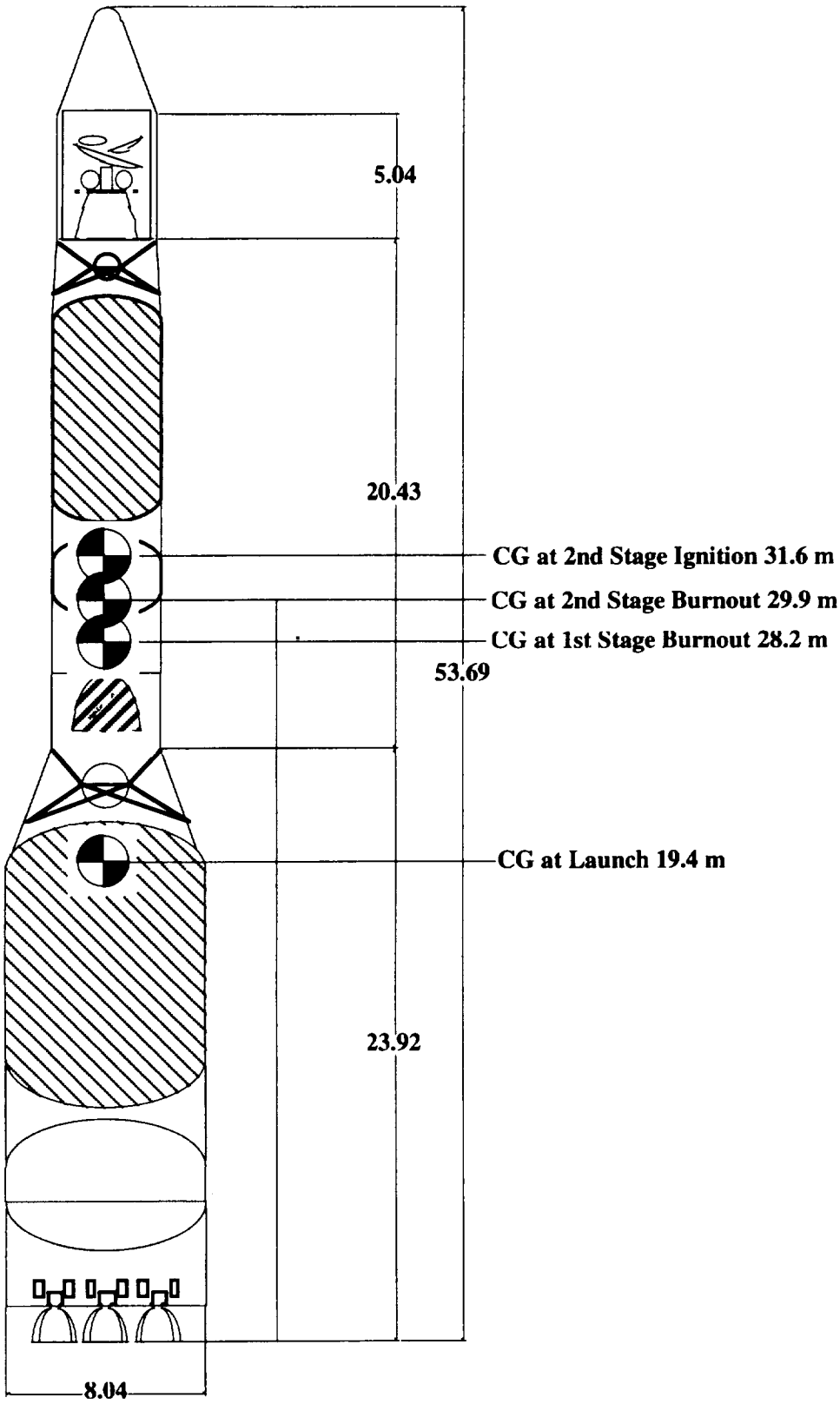

Figure 5.2.c CG Locations - Unmanned Configuration

5.3. Cost Estimation

A cost analysis was performed to estimate the cost per mission. The cost per mission was determined by setting the net present value of the total expenditures equal to the net present value of the total revenue. The total revenue is the cost per mission multiplied by the number of missions. Knowing the number of missions and the net present value of the total expenditures one can solve for the cost per mission. The total expenditures, which include research and development cost, ground operation costs, expendable parts cost, spacecraft costs, and spacecraft refurbishment costs are discussed below.

5.3.1. Research & Development

Research & development costs were approximated for each component using empirical formulas that relates costs to mass (Appendix 5.3.1). The total R&D costs were $1.5 billion FY94 dollars. The R&D also included the $393 M FY94 dollars for software development. The R&D costs were distributed linearly over six years.

5.3.2. Ground Operation Costs

Ground operation costs were estimated using empirical formula and were as follows:

Category	Developmental Cost [$M FY94]	Costs/Year [$M FY94]
Launch Operations	$130	$100.00
Recovery Operations	$4	$1.50
Facilities	$30	$0.40
Ground Equipment	$89	$4.60
Management		$1.50
Engineering Support		$14.50

Table 5.3.2.a Ground Operation Costs

5.3.3. Expendable Parts

Expendable parts were components that formed the expendable launch vehicle. Theoretical first unit costs were estimated from empirical formulas that related costs to mass (see Appendix 5.3.1). The parts and their respective costs were as follows:

Expendable Part	Theoretical First Unit Cost [$M FY94]
Module	$34.14
Upper Stage	$19.68
Engine	$45.28
Avionics Package	$16.20

Table 5.3.3.a Expendable Parts Costs

A learning curve factor was multiplied to the theoretical first unit cost of each additional unit produced. A learning curve was a mathematical technique used to account for productivity improvements as a larger number of units were produced[176]. This learning curve used is shown below:

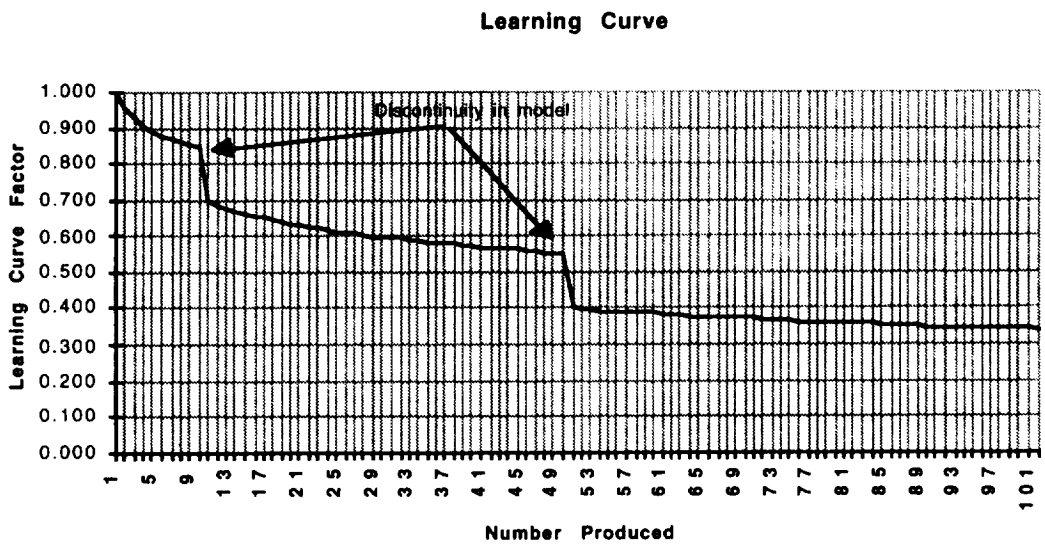

Figure 5.3.3.a Learning Curve

Discontinuities appeared in the model due to a change in a learning constant. This constant was .95 for the first 10 units produced, .90 for the next 40 units produced, and .85 for each additional unit produced.

176 Larson, W.J. and Wertz, J.R.,*Space Mission Analysis and Design*, 2nd edition, Microcosm, Inc. and Kluwer Academic Publishers,1992, pp.734

5.3.4. Spacecraft Costs

The total spacecraft cost was $429 M FY94 (see Appendix 5.3.4). Spacecraft refurbishment costs were estimated as 15% of the total spacecraft costs per flight.

5.3.5. Total Program Costs

The breakdown of program costs was as follows:

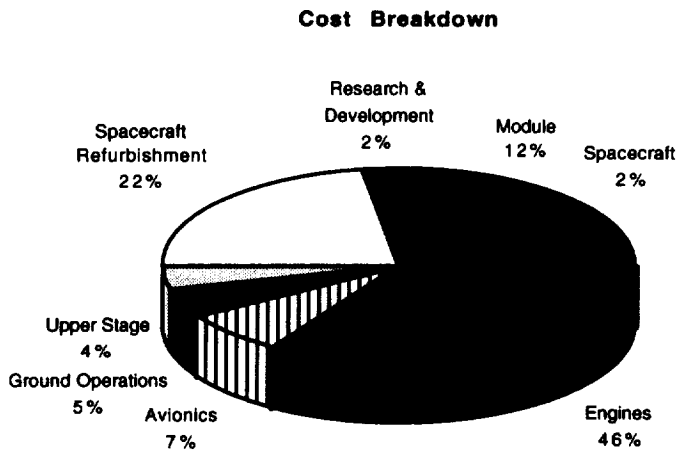

Figure 5.3.5.a Total Program Costs Breakdown

The net present value of the total expenditures equaled $16,276 billion FY94. The cost per mission of an un-crewed mission was scaled to .3 of the cost of a crewed mission. The cost per mission is as follows:

Mission	Cost $M FY94
Crewed	$ 283
Un-crewed	$ 85

Table 5.3.5.a Mission Costs

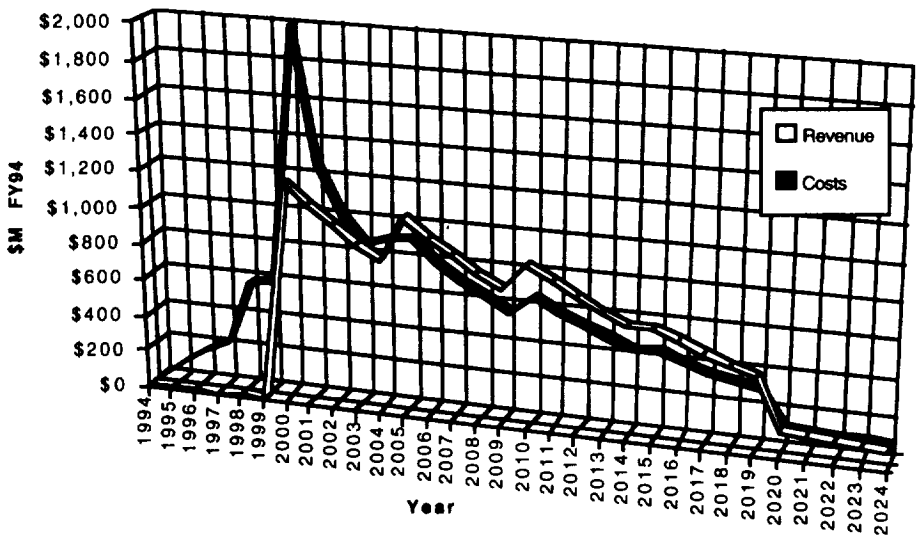

Figure 5.3.5.b Expenditure and Revenue vs Year

5.4 Final Conclusions

The ORION design failed to meet the cost goals laid out for the system. However, as this was only a preliminary design the cost hopefully would go down as more accurate cost and mass figures were determined. The vehicle managed to surpass the capabilities that were required of it through its versatility, modularity, and heavy lift capability.

Appendices

A.2.2.1	Details of the program used to calculate the trajectories
A.2.4.2.1	Reentry Trajectory Selection and Analysis
A.3.2.1	Component Level Mass Breakdown
A.3.3.2.3	Contaminant Standards
A.3.3.2.4	Acceleration Guidelines
A.3.3.2.11	Radiation
A.3.3.4.2.3	Carbon Dioxide Removal and Scrubbers
A.3.3.4.3	Thermal Control System Refrigerant
A.3.3.5	Mass vs Escape Option
A.3.3.7.4	Airlock Trade Study
A.3.3.7.5	RMS Trade Study
A.3.4.0.1	Mission sub-functions
A.3.4.0.2	Function Performance Levels
A.3.4.1.4.1.1	Sensor Data Rates
A.3.4.2.2	GPS/INS Comparison
A.3.4.3.2	General Information on TDRSS and STDN
A.3.4.3.3	Power vs. Data Rate
A.3.4.3.4.1	Power vs. Data Rate
A.3.4.3.5.2	Earth Coverage Beamwidth
A.3.4.3.7	Link Budgets
A.3.5.1	Mass Estimating Relations from NASA CR 2420
A.3.5.3.1	Wing Size Selection Spreadsheet
A.3.6.3.2	Mass and Cost Analysis on Various Power Sources
A.4.5.4	Third Stage Mass Spreadsheet
A.4.5.5	Module Mass Spreadsheet
A.4.6.2.1	Mass Analysis of the Combustion Chamber and Nozzle
A.4.6.2.3.a	Equations Used for Combustion Chamber and Nozzle Design
A.4.6.2.3.b	Specifications of Modular Engine and Top-Stage Engine
A.4.6.3.1	Turbopump Cycles
A.4.6.3.3	Turbopump Analysis
A.5.2	Center of Gravity Analysis Spreadsheet
A.5.3.1	Cost Estimating Relations
A.5.3.4	Raw Component Level Costs

A.2.2.1 Details of the program used to calculate the trajectories

The simulation was implemented in Microsoft Excel on an Apple Macintosh. The altitude, downrange, velocity, and flight path angle were generated using a fourth order Runge-Kutta for systems of equations. The atmoshpere was a standard exponential model, where density is exclusively a function of altitude. This approxiamation simplified calculations. The Mach number was generated using a lookup table that interpolated temperature at given altitudes.

Appendix A.2.4.2.1 Reentry Trajectory Selection and Analysis

Initially when selecting the reentry trajectory it was necessary to see the effects of different parameters on the reentry trajectory and the loads on the crew and the vehicle. One parameter was varied while the others were held constant. From this the effects of these parameters were learned and then parameters were set to design the reentry vehicle around.

Initial Flight Angle

The initial flight angle played and important part in determining what happened to the vehicle and the crew. if the angle was too steep (perpendicular to the earth's surface being the steepest) the vehicle would enter too fast and burn up to the high heating rates, and if the vehicle survived the crew would not due to extremely high G forces. if the initial flight angle were too shallow the vehicle would not reenter the atmosphere fully and would leave the atmosphere. this creates a reentry "window", which is the acceptable range of entry angles where the vehicle and the crew will survive. Once inside of the reentry window it is necessary to select an angle which is best for the crew and the vehicle. If the angle is too shallow and in the reentry window the total heat load is going to be to high due to the fact that the vehicle is going to be heated for much longer than if the initial flight path angle was steeper.

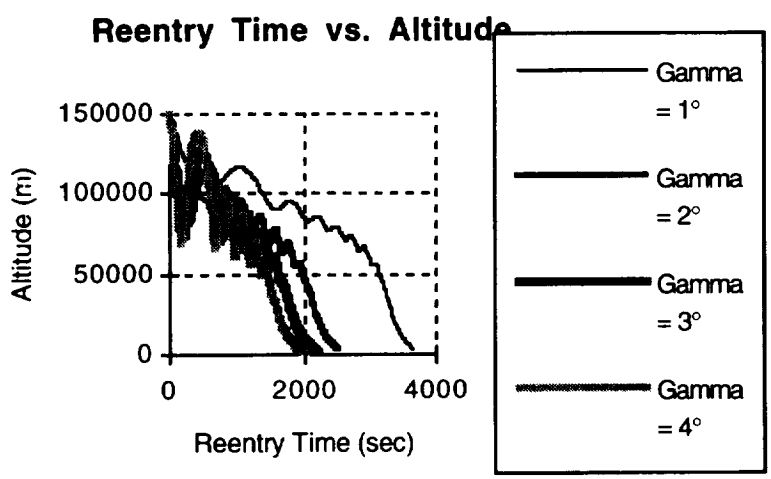

Figure A.2.4.2.1.a: Altitude vs. time for various entry angles

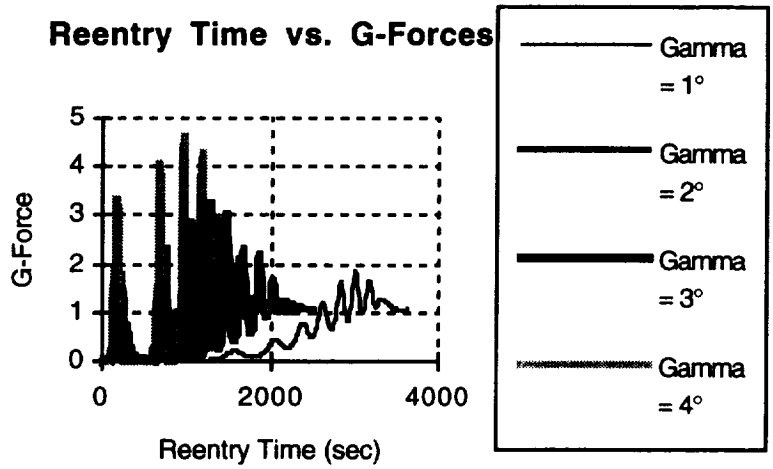

Figure A.2.4.2.1.b: Altitude vs. G-forces for various entry angles

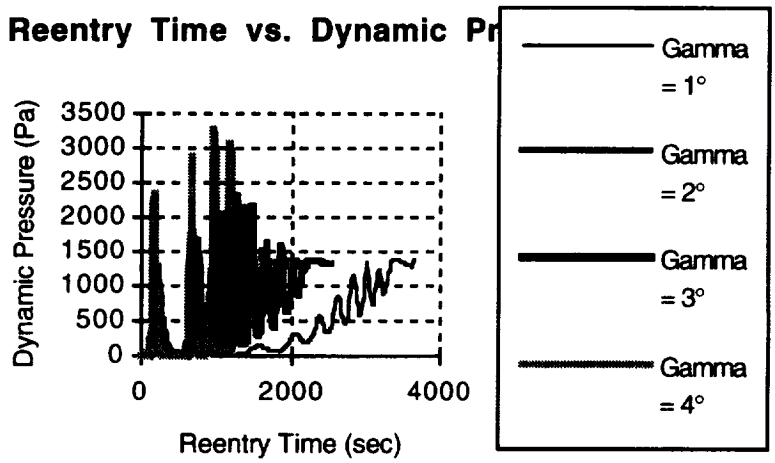

Figure A.2.4.2.1.c: Altitude vs. dynamic pressure for various entry angles

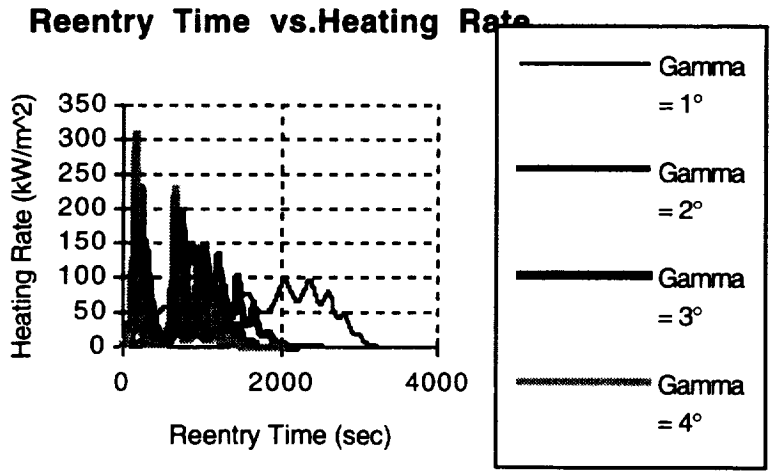

Figure A.2.4.2.1.d: Altitude vs. Heating Rate for various Entry Angles

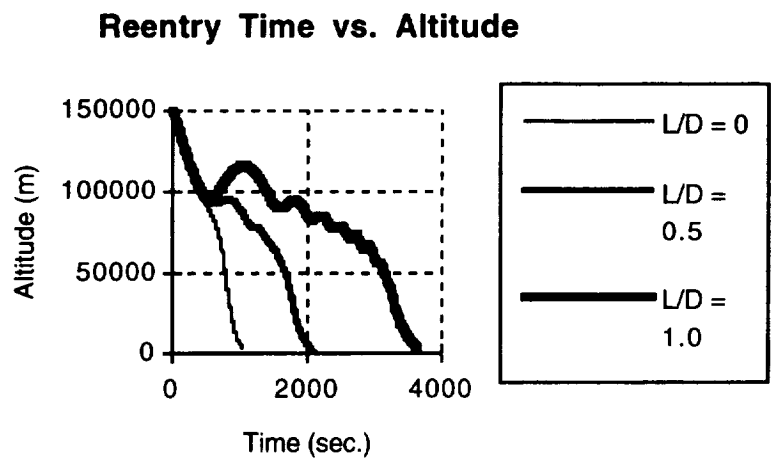

Figure A.2.4.2.1.e: Altitude vs. time for various L/D ratios

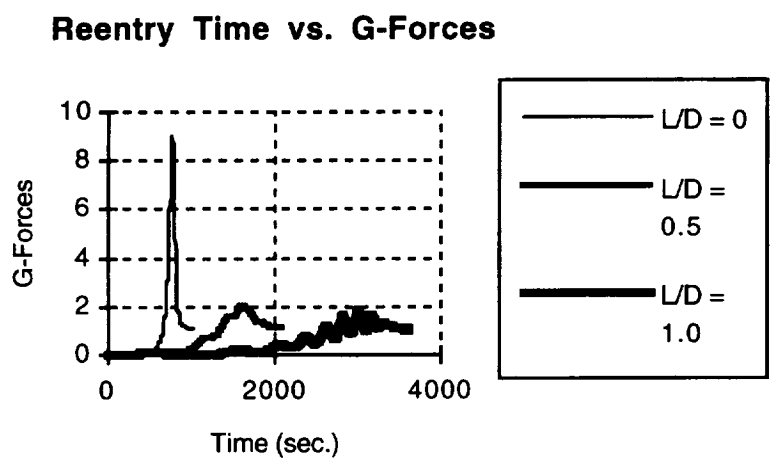

Figure A.2.4.2.1.f: **G-forces vs. time for various L/D ratios**

Lift to Drag Ratio

The lift to drag ratio effected how sharply the vehicle would start a phugoid oscillation, as well effecting the total reentry time. When the L/D was too high (approx. 3.0) the vehicle would become dynamically unstable and phugoid oscillations would begin. As well as making the total heat load on the vehicle too high. If the L/D were 0.0 then the vehicle would come in to fast and it acted as if the initial flight path angle were to steep.

Ballistic Parameter

The ballistic parameter, mass loading per unit area, effects the heating rate and the sensed acceleration. If the ballistic parameter is too high then the

vehicle enters too fast and the heating rate becomes very high and the sensed acceleration exceeds limits set by the human factor group.

Reentry Model

Velocity

$$V_i = V_{i-1} + \frac{\left(\kappa_{v1} + 2\cdot\left(\kappa_{v2} + \kappa_{v3}\right) + \kappa_{v4}\right)}{6}$$

$$\kappa_{v1} = \Delta t \cdot g \cdot \sin\gamma_{i-1} - \frac{\rho_{i-1}\cdot V_{i-1}^{\ 2}}{3.7\cdot \beta / C_{p0}}$$

$$\kappa_{v2} = \Delta t \cdot g \cdot \sin\left(\gamma_{i-1} + \frac{1}{2}\cdot\kappa_{a1}\right) - \frac{\rho_{i-1}\cdot\left(V_{i-1} + \frac{1}{2}\cdot\kappa_{v1}\right)^2}{3.7\cdot\beta / C_{p0}}$$

$$\kappa_{v3} = \Delta t \cdot g \cdot \sin\left(\gamma_{i-1} + \frac{1}{2}\cdot\kappa_{a2}\right) - \frac{\rho_{i-1}\cdot\left(V_{i-1} + \frac{1}{2}\cdot\kappa_{v2}\right)^2}{3.7\cdot\beta / C_{p0}}$$

$$\kappa_{v4} = \Delta t \cdot g \cdot \sin\left(\gamma_{i-1} + \kappa_{a3}\right) - \frac{\rho_{i-1}\cdot\left(V_{i-1} + \kappa_{v3}\right)^2}{3.7\cdot\beta / C_{p0}}$$

Altitude

$$Z_i = Z_{i-1} + \frac{\left(\kappa_{z1} + 2\cdot\left(\kappa_{z2} + \kappa_{z3}\right) + \kappa_{z4}\right)}{6}$$

$$\kappa_{z1} = -\Delta t \cdot V_{i-1}\cdot\sin\left(\gamma_{i-1}\right)$$

$$\kappa_{z2} = -\Delta t \cdot \left(V_{i-1} + \frac{\kappa_{v1}}{2}\right)\cdot\sin\left(\gamma_{i-1} + \frac{\kappa_{a1}}{2}\right)$$

$$\kappa_{z3} = -\Delta t \cdot \left(V_{i-1} + \frac{\kappa_{v2}}{2}\right)\cdot\sin\left(\gamma_{i-1} + \frac{\kappa_{a2}}{2}\right)$$

$$\kappa_{z4} = -\Delta t \cdot \left(V_{i-1} + \kappa_{v3}\right)\cdot\sin\left(\gamma_{i-1} + \kappa_{a3}\right)$$

Flight Path Angle

$$\gamma_i = \gamma_{i-1} + \frac{\left(\kappa_{a1} + 2\cdot\left(\kappa_{a2} + \kappa_{a3}\right) + \kappa_{a4}\right)}{6}$$

$$\kappa_{a1} = \Delta t \cdot \frac{g}{V_{i-1}} - \frac{V_{i-1}}{R_{\oplus} + Z_{i-1}} \cdot \cos(\gamma_{i-1}) - \frac{\rho_{i-1} \cdot V_{i-1} \cdot \frac{L}{D} \cdot \cos\phi_{i-1}}{3.7 \cdot \beta / C_{p0}}$$

$$\kappa_{a2} = \Delta t \cdot \frac{g}{\left(V_{i-1} + \frac{\kappa_{v1}}{2}\right)} - \frac{V_{i-1} + \frac{\kappa_{v1}}{2}}{R_{\oplus} + Z_{i-1}} \cdot \cos\left(\gamma_{i-1} + \frac{\kappa_{a1}}{2}\right) - \frac{\rho_{i-1} \cdot \left(V_{i-1} + \frac{\kappa_{v1}}{2}\right) \cdot \frac{L}{D} \cdot \cos\phi_{i-1}}{3.7 \cdot \beta / C_{p0}}$$

$$\kappa_{a3} = \Delta t \cdot \frac{g}{\left(V_{i-1} + \frac{\kappa_{v2}}{2}\right)} - \frac{V_{i-1} + \frac{\kappa_{v2}}{2}}{R_{\oplus} + Z_{i-1}} \cdot \cos\left(\gamma_{i-1} + \frac{\kappa_{a2}}{2}\right) - \frac{\rho_{i-1} \cdot \left(V_{i-1} + \frac{\kappa_{v2}}{2}\right) \cdot \frac{L}{D} \cdot \cos\phi_{i-1}}{3.7 \cdot \beta / C_{p0}}$$

$$\kappa_{a4} = \Delta t \cdot \frac{g}{(V_{i-1} + \kappa_{v3})} - \frac{V_{i-1} + \frac{\kappa_{v3}}{2}}{R_{\oplus} + Z_{i-1}} \cdot \cos(\gamma_{i-1} + \kappa_{a3}) - \frac{\rho_{i-1} \cdot (V_{i-1} + \kappa_{v3}) \cdot \frac{L}{D} \cdot \cos\phi_{i-1}}{3.7 \cdot \beta / C_{p0}}$$

Miscellaneous

Shield Temperature in °F

$$T = \left(\frac{229100580000 \cdot \dot{q}}{2}\right)^{.25} - 459.67$$

density

$$\rho_{\infty} = \rho_{sl} \cdot e^{\frac{-Z_i}{H}}$$

yaw angle

$$\psi_i = \psi_{i-1} + \frac{\rho_{i-1} \cdot g \cdot V_{i-1} \cdot \frac{L}{D} \cdot \sin\phi_{i-1} \cdot \Delta t}{2 \cdot \beta}$$

Cpo

$$C_{P0} = 1.35 - \tan^{-1}\left(\frac{1.96 \cdot (1 - M_i)}{\pi}\right)$$

Source:
Howard, Russell, University of Maryland, Space System Laboratory. Personal Interview/program, 1994.

Appendix A.3.2.1 Component Level Mass Breakdown

Component Level Mass Breakdown						
Inital Gross Mass Guess [lbs]	112407.407					
System/component	**Mass [kg]**	**M Spacecraft**	**M Module**	**M Stage 3**	**M Config 1-2**	**M Config 3**
Structures						
Module						
Module LOX Tank	2647		2,647		7,941	2,647
Module LH2 Tank	11734		11,734		35,202	11,734
Module LOX Insulation	238		238		714	238
Module LH2 Insulation	755		755		2,265	755
Module Thrust Structure	494.7		495		1,484	495
Module Helium Tank	55		55		165	55
Inter-Stage Faring/Nose Cone	1212		1,212		3,636	1,212
Module Inter Tank Faring	285		285		855	285
Nozzle Shroud	2816		2,816		8,448	2,816
Secondary Inert Mass	646		646		1,938	646
Upper Stage						
LOX Tank	647			647	647	647
LH2 Tank	3022			3,022	3,022	3,022
LOX Insulation	98			98	98	98
LH2 Insulation	334			334	334	334
Thrust Structure	494.7			495	495	495
Helium Tank	14			14	14	14
Inter-Stage Faring	262			262	262	262
Inter Tank Faring	285			285	285	285
Nozzle Shroud	631			631	631	631
Secondary Inert Mass	646			646	646	646
Wings	986	986			986	
Vertical Stabilizers	398	398			398	
Landing Gear						
Nose	394	394			394	
Main	1,446	2,893			2,893	
Fuselage	11,851	11,851			11,851	
Escape System	2400	2,400			2,400	
Secondary Structure	1,614	1,614			1,614	
Thermal Protection						
REI Mullite	300	300			300	
Titanium Sub-structure	600	600			600	
Nose	30	30			30	
Leading Edges	1670	1,670			1,670	
Fasteners and Adhesives	520	520			520	
Propulsion						
Main Engine						
Chamber & Nozzle	658		1,974	658	6,580	2,632
Turbopump LOX	301		903	301	3,010	1,204
Turbopump LH2	301		903	301	3,010	1,204
Piping	340		1,020	340	3,400	1,360
Injector	70		210	70	700	280
Gimbal Structure	60		180	60	600	240
Gimbal EMA	20.5		615	205	2,050	820
Valve EMA	1.6		480	160	1,600	640
Instruments, sensors, etc.	75		225	75	750	300
Secondary Inert Mass	75		225	75	750	300
Power Supply- Baterries	376		1,128	376	3,760	1,504
(350 W/kg;14000$/kg; 131KW)						
OMS Engine						
Chamber & Nozzle	100	200			200	
Gimbal Structure	25	50			50	
OMS Gimbal EMA	4.5	36			36	
OMS Valve EMA	0.3	12			12	
RCS Thruster						
Chamber & Nozzle	4	124			124	

Appendix A.3.2.1 Component Level Mass Breakdown

RCS Valve EMA	0.1	124			124	
RCS & OMS Feed System						
Forward Propellant Tank	24	48			48	
Forward Pessurant Tank	33	33			33	
Aft Propellent Tank	156	312			312	
Aft Pressurant Tank	187	187			187	
Power						
Fuel Cell	73	219			219	
24 Hour Back up Battery	374	374			374	
Electrical Bus Wiring	200	200			200	
LOX Tank	35	105			105	
LH2 Tank	3	9			9	
LOX Insulation	2	6			6	
LH2 Insulation	1	2			2	
Spacecraft APU	40	80			80	
Avionics						
Guidance sensors						
GPSR	4.5	9			9	9
INS	57.0	171			171	114
Star tracker	26.0	52			52	
Microwave landing system	32.1	96			96	
Radar Altimiter	6.1	18			18	
Proximity	6.1	12			12	
Rendezous Sensors	6.1	12			12	
Communications						
Helix S-Band Antenna	3.0	21			21	
Parabolic Antenna	135.0	135			135	
Omni. Micro. Ant. x12.57	2.0	2			2	2
Omni. Micro. Ant. x25.13	4.0	8			8	
Helix EVA Antenna	3.0	21			21	
VTR (Digital)	22.7	45			45	
Tape Recorder	33.3	67			67	
K Band Transceiver	4.5	9			9	
S Band Transceiver	6.9	27			27	
L Band Transceiver	4.8	10			10	
Stanard Modules						
Inter Comp. Interface Seq. Mod.	1.4	7			7	7
Shared Memory Module	1.4	7			7	7
Memory Module	1.4	14			14	14
Comp. Processor Module	1.4	7			7	7
I/O Processor Module	1.4	14			14	7
Power Module	1.4	7			7	7
I/O Sequencer Module	1.4	14			14	14
Remote Data Unit	4.5	108	81	32	383	113
Envirmental Housing (computer unit)	7	35			35	35
Envirmental Housing (RDU)	2	48	36	14	170	50
Fiber Optic Bus (module)	20		20		60	20
Fiber Optic Bus (upper stage)	20			20	20	20
Fiber Optic Bus (spacecraft)	20	20			20	
Flight Control EMA	4	80			80	
Human Factors						
EVA						
2 p Airlock	550.0	550			550	
4 Shuttle EMU	61.4	245			245	
RMS	1240.0	1,240			1,240	
Atmosphere						
E Ox Tanks	120.0	120.0			120	
Nit Tanks	249.0	249.0			249	
Filtering System	120.0	249.0			249	
Activated Charcoal	50.9	50.9			51	
Air System	20.0	20.0			20	
Thermal System	100.0	100.0			100	
Water supply						

Appendix A.3.2.1 Component Level Mass Breakdown

Water tanks	20.0	40			40	
Food						
Storage	5.0	5.0			5	
Preparation Unit	5.0	5.0			5	
Refrigerator	5.0	5.0			5	
Sanitation						
Trash Storage	75.0	75.0			75	
Toilet	20.0	20.0			20	
Waste holding tanks	10.0	10.0			10	
Safety Equipment						
Medical Equipment	4.0	4.0			4	
Fire Dectection/Suppression	2.0	12.0			12	
Emergency Breathing	1.0	6.0			6	
Crew Cabin						
Lighting	2.0	20			20	
Sleeping Berths	20.0	20			20	
Individual Lockers	5.0	30			30	
Dry Masses		29,929	28,883	9,120	125,697	38,225
Returning mass						
Res. Propellant			4,370	1,004	14,114	5,374
Retrun Payload	5500	5500			5,500	
Crew	510	510			510	
Emergency O2	135	135			135	
SUB TOTALS		36,074	33,253	10,124	145,956	43,599
Sub Total w/ 10% margin		39,681	36,578	11,137	160,552	47,715
Wet mass						
LOX		725	177,697	40,829	574,645	218,526
LH2		90	36,413	8,367	117,696	44,780
He			100	100	400	200
Hydrazine		4,600			4,600	
N2O4		4,600			4,600	
Nitrogen		50			50	
Water		810			810	
Food		380			380	
Payload		0			0	7,000
WET Totals		50,936	250,788	60,433	863,733	318,221
				Check	863,733	318,221

Appendix A.3.3.2.3 Contaminant Standards

To maintain a safe and comfortable working environment, the quantity of contaminants should be kept to a minimum. Industry standards have long been in place to regulate the quantity of dangerous exposure. The problem is made more critical in space due to the continuous exposure of crew to the cabin atmosphere. Table A.3.2.2.3.a shows the recommended maximum concentrations of atmospheric contaminants as set by the American Conference of Government Industrial Hygienists. The figures are based on a 40-hour work week with consideration of recovery during the off-hours. To apply these standards to space, multiply them by 1/3, to account for the disparity between an eight hour and 24 hour day.

Compound	Parts per Million	Approximate mg/M^3
Acetic Acid	10	25
Acetone	1000	2400
Acrolein	0.5	1.2
Ammonia	100	70
Amylacetate	200	1050
Amyl Alcohol	100	360
Benzene	25	80
Butyl Cellosolve	50	240
Carbon Disulfide	20	60
Carbon Monoxide	100	110
Carbon Tetrachloride	25	160
Cresol	5	22
Cyclohexane	400	1400
Dioxane	100	360
Ethyl Acetate	400	1400
Ethylene Diamine	10	30
Flourine	.1	.2
Formaldehyde	5	6
Hydrazine	1	1.3
Hydrogen Chloride	5	7
Hydrogen Flouride	3	2
Hydrogen Peroxide, 90%	1	1.4
Hydrogen Sulfide	20	30
Lithium Hydride	-	.025
Methyl Alcohol	200	260
Methyl Cellosolve	25	80
Nitrogen Dioxide	5	9
Methyl Ethyl Ketone	200	590
Ozone	.1	.2
Perchloroethylene	100	670
Phenol	5	19
Phosgene	1	4
Phosphine	.05	.07
Sodium Hydroxide	-	2
Sulfur Dioxide	5	13
Sulfuric Acid	-	1
Teflon Decomposition Products (as Flourine)	-	.05
Toluene	200	750
Trichloroethylene	100	520
Xylene	200	870

Table A3.3.2.a Recommended Maximum Concentrations of Atmospheric Contaminants from Faget, et al "Manned Spacecraft Design," 1964

Appendix A.3.3.2.4 Acceleration Guidelines

Space shuttle range is 1 to 3 +Gx during launch with a 4 +Gx spike at booster ignition and 1/2 =Gx during separation maneuvers

Acceleration Nomenclature

Linear Motion	Acting Force	Accel. Descrip.	Reaction Force	Verticular Descrip.
Forward	+ax	Forward accel.	+Gx	Eyeballs In
Backward	-ax	Backward accel.	-Gx	Eyeballs Out
Upward	-az	Headward accel.	+Gz	Eyeballs Down
Downward	+az	Footward accel.	-Gz	Eyeballs Up
To Right	+ay	R. Lateral accel.	+Gy	Eyeballs Left
To Left	-ay	L. Lateral accel.	-Gy	Eyeballs Right

Sample Acceleration Loads

Aircraft ejection seat firings - up to 17 +Gz
Crash landings - from 10 to greater than 100 G's (omnidirectional)
Orbiter crew compartment design loads for crash landing are 20 +Gx and 10 +Gz
Violent maneuvers - approx. 2-6 G's (omnidirectional)
Parachute opening shock - approx. 10 +Gz

Factors affecting human accelration tolerance

Magnitude of the applied force
Duration of the applied force
Rate of onset and decline of the applied force
Direction of the g vector
Types of g-protection devices and body restraints
The coupling between the crewmember and the vehicle via seats, couches, etc.
Body positioning, including specific back, head and leg angles
Environmental conditions such as temperature and lighting
Age of the crewmember
Emotional/motivational factors such as competitive attitude, fear, anxiety, self-confidence, confidence in equipment, and willingness to tolerate discomfort and pain
Previous acceleration training, techniques of breathing, straining, and muscular control
Human physical condition
Extent of microgravity adaptation and body fluid shift
Dietary habits, esp. w.r.t. quantities of fruits, fibers and fluids ingested

Subjective Effects of Linear Accelerations

Upward Acceleration Effects (+Gz, in seated posture)

2.5 Gz - difficult to raise oneself

3-4 Gz - impossible to raise oneself; difficult to raise arms and legs; progressive dimming of vision after 3-4 sec.; tunnel vision

4.5-6 Gz - blackout after ~5 sec.; hearing loss; unconsciousness

Downward Acceleration Effects (-Gz, in seated posture)

-2 - -3 Gz- headache; reddening of vision, hemorrhages

-5 Gz -five seconds tolerance limit

Forward Acceleration Effects (+Gx, in seated posture)

2-3 Gx - 2 Gx tolerable for at least 24 hours

3-6 Gx - loss of peripheral vision; difficulty in breathing and speaking; 4 Gx tolerable for at least 60 minutes

6 - 9 Gx - breathing difficult; tunnel vision; body, legs and arms cannot be lifted at 8 Gx; head cannot be lifted at 9 Gx

9 -12 Gx - severe chest pain; severe difficulty in breathing

15 Gx - extreme difficulties breathing and speaking; loss of vision

Backward Acceleration Effects (-Gx, in seated position)

Similar to forward accelerations; except breathing becomes easier

Lateral Acceleration (+/- Gy)

Little information is known; at +/- 5 Gy, 14.5 sec. exposure leads to external hemorrhage

Human Responses to Rotational Accelerations

Most subjects, without prior experience, can tolerate rotation rates up to 6 rpm in any axis or combination of axes

Most subjects cannot initially tolerate rotation rates in the region of 12 to 30 rpm and rapidly become sick and disoriented above 6 rpm unless carefully prepared by a graduated program of exposure

Human Responses to Impact Accelerations

Tolerance to impact and shock is usually based on skeletal fracture levels.

Damage to the vertebrae is most common, followed by head injury, which occurs more often at higher impact levels

The two main factors involved are total time of acceleration exposure and orientation of subjects' spinal axis and acceleration vector.

For linear impact accelerations, those applied at right angles to the spinal axis are better tolerated than those applied paralleled to this axis.

See Figure 5.3.2.4-1, Page 5-34, Man-Systems Integration Stds, Vol.1, NASA for impact survival experience.

Acceleration Design Limits and Requirements

See Figures 5.3.3.1-1 through 5.3.3.2-2 of NASA Man-Systems Integration Standards for Linear, Rotational, and Impact Accelerations for both Non-Preconditioned and Preconditioned crew members

Appendix A.3.3.2.11 Radiation

In space, humans are exposed to ionizing radiation at a much higher intensity than on earth, due to the lack of any protective atmosphere which absorbs most of the harmful high-energy particles. The radiation comes primarily from three sources: trapped radiation, galactic cosmic rays and solar cosmic radiation. The exposure to each depends on the type and duration of the spacecraft's orbit.

Trapped radiation refers to energetic protons and electrons which are trapped in the Van Allen belts, zones of either protons or electrons that exist because of earth's dipolar magnetic field. The trapped particles are concentrated in the equatorial zones; little intensity exists at the poles. The inner belt consists of high energy electrons located from peak altitudes of 2000-5000 km, to an outer limit of approximately 12,000 km altitude. Protons are located in a large region which extends from about 500 altitude (where the intensity of the radiation is low) to as far out as the magnetopause between 36,000 km and 67,000 km altitude. The peak of the proton belt intensity occurs between 1,000 km and 10,000 km. However, there is a region of high intensity protons of low altitude located slightly east of South America, referred to as the South Atlantic Anomaly (SAA). The center of the SAA is located at approximately 35°E longitude and 35°S latitude. For space vehicles with orbital inclinations of 30° or greater, there will be approximately five traverses through the SAA each day. A majority of the radiation which astronauts in low-earth orbit encounter is due to trapped radiation over the SAA, on average about .11 rem (see below for a definition of terms).

Galactic cosmic radiation originates outside the solar system and consists of atomic nuclei that have been ionized and accelerated to very high energies. A majority of these particles (about 85%) are hydrogen nuclei (protons). Most galactic cosmic radiation is either so energetic is passes right through the body without any appreciable side effects, or it gets trapped in the Van Allen belts and becomes trapped radiation. Only 5-10% of radiation exposure in space comes from galactic cosmic radiation.

Solar cosmic radiation is a result of solar flares, bursts of intense activity on the sun's surface which generates a powerful barrage of energetic charged particles. Even though most of the charged particles are captured in the Van Allen belts, some particles will get through and threaten the astronauts. However, the solar flares occur on an eleven-year cycle, so mission planners will have some idea ahead of time of how severe the radiation threat might be. Additionally, solar flares can be observed on earth before the dangerous particles reach the astronauts, giving them from 2 to 8 hours to react.

Radiation can be measured in a variety of ways; with respect to its effects on humans, it is quantified by rads and rems. A rad (radiation absorbed dose)

defines the dose of energy absorbed: one rad equals 100 ergs of energy per gram of material. The effect of the radiation is described by the rem (roentgen equivalent man). The product of the dose and the quality factor, Q, equals the rems absorbed. Q is an artificial factor which relates the biological effects due to different types of radiation. Q varies from a minimum of 1 for X-rays to a maximum of 20 for 1 MeV alpha particles. A majority of the radiation encountered in space results from energetic protons (on the order of .1 to 100 MeV), which relates to a Q in the range of 2 to 8.

Ionizing radiation breaks down chemical bonds in biological systems, leading to serious acute and latent effects. Low levels of ionizing radiation produces mostly small quantities of damaged molecules which the body replaces or recycles. However, it also damages DNA molecules, which is not repaired and can accumulate. Long-term exposure to low radiation levels can increase the possibility of dangerous mutations in offspring. High levels of ionizing radiation damage biological processes which can in turn lead to poisoning of the body, resulting in vomiting and nausea. Long-term effects include the disruption of the blood-forming cells in the bone marrow, which can seriously damage the body's immune system. Figure A.3.3.2.11.a describes the probable effects of increasing doses of radiation.

Dose in Rads	Probable Effect
0 to 50	No obvious effect, except, possibly, minor blood changes and anorexia.
50 to 100	Vomiting and nausea for about 1 day in 10 to 20 % of exposed personnel. Fatigue, but no serious disability. Transient reduction in lymphocytes and neutrophilis.
100 to 200	Vomiting and nausea for about 1 day, followed by other symptoms of radiation sickness in up to 50% of personnel; <5% deaths anticipated. A reduction of approximately 50% in lymphocytes and neutrophilis will occur.
200 to 350	Vomiting and nausea in 50 to 90% of personnel on first day, followed by other symptoms of radiation sickness, e.t. loss of appetite, diarrhea, minor hemorrhage; 5 to 90% deaths within 2 to 6 weeks after exposure; survivors convalescent for about 3 months.
350 to 550	Vomiting and personnel in most personnel on first day, followed by other symptoms of radiation sickness, e.g. fever, hemorrhage, diarrhea, emaciation. Over 90% deaths within 1 month; survivors convalescent for about six months.
500 to 750	Vomiting and nausea, or at least nausea, in all personnel within four hours from exposure, followed by severe symptoms of radiation sickness, as above. Up to 100% deaths; few survivors convalescent for about six months.
1000	Vomiting and nausea in all personnel within 1 to 2 hours. Probably no survivors from radiation sickness.
5000	Incapacitation almost immediately (several hours). All personnel will be fatalities within one week.

Figure A.3.3.2.11.a. Expected early effects of radiation from NASA STD-3000 Man-Systems Integration Standards

Standards detailing the maximum amount of radiation astronauts are exposed to during space activities were formally established by Scientific Committee 75 of the National Council on Radiation Protection and Measurement. The limits are outlined in Figure A.3.3.2.11.b. When considering safety levels for astronauts, one should also consider the following: the radiation should not impair the astronaut's health to the point where his or her performance capability is threatened, so as not to affect the overall performance of the mission; the dose of radiation received should not cause any serious long term health problems; and finally, the radiation exposure should be limited to avoid any possibly risk to the astronauts' offspring.

Exposure Interval	**Depth (5 cm)**	**Eye (0.3 cm)**	**Skin (0.01 cm)**
30 days	25 rem	100 rem	150 rem
Annual	50	200	300
Career	100 to 400[a]	400	600

Footnote:

a The career depth dose-equivalent limit is based upon a maximum 3-percent lifetime excess risk of cancer mortality. The total dose-equivalent yielding this risk depends on age at start of exposure. The career dose-equivalent limit is approximately equal to:
200 + 7.5 (age -30) rem for males, up to 400 rem maximum
200 + 7.5 (age -38) rem for females, up to 400 rem maximum.

Figure A.3.3.2.11.b Ionizing Radiation Exposure Limits from NASA STD-3000 Man Systems Integration Standards

Appendix A.3.3.4.2.3 Carbon Dioxide Removal and Scrubbers

The carbon dioxide scrubber is responsible for keeping the quantity of carbon dioxide in the atmosphere to a minimum of 1.5 percent by volume, as set by the systems requirements. In approaching the problem of reducing the carbon dioxide content of the atmosphere, the following systems were analyzed: scrubbers, molecular sieves, and electrodialysis.

Scrubbers remove carbon dioxide by exposing it to a chemical which reacts and produces a non-regeneratable byproduct.

Molecular sieves are similar to scrubbers in that they expose the CO_2 to a chemical that absorbs it, but the chemical byproduct is regenerated via a desorption process, usually either heating or the exposure to a vacuum. The drawbacks to molecular sieves are 1) the regenerating equipment is heavy, and 2) some type of dual loop must be used to allow for continuous CO_2 removal while some of the chemical byproduct is being regenerated.

The electrodialysis system is essentially a device containing ion-exchange resign which reacts with the atmospheric gases to remove carbon dioxide by forming carbonate ions. An electrical field causes the carbonate ions to move to a concentrating cell. This system is then connected to a Sabatier process-device which recycles the oxygen from the carbon dioxide. This system equipment is fairly massive, but there is very little byproduct.

Mass is the driving factor in the choice of a carbon dioxide removal system. Although the scrubbers produce a non-regeneratable byproduct, the scrubber systems are lighter than the other two systems. For shorter missions, the mass of the accumulated scrubber byproduct, which is linearly time dependent, does not exceed the heavy masses of the regenerating systems. For longer missions a regenerating system would be more mass efficient. For the planned missions, a maximum of 15 days are anticipated, and hence the scrubber is the optimal choice for a carbon dioxide removal system.

Four different scrubbers were investigated: soda lime, sodium hydroxide (NaOH), baralyme, and lithium hydroxide (LiOH). All have been investigated or used for carbon dioxide scrubbing in pressurized space and undersea environments, SCUBA decompression chambers, or mine safety applications. They were compared for mass per volume CO_2 absorbed, volume per volume CO_2 absorbed, minimum temperature and cost. The results are summarized in Table A3.3.4.a.

Characteristic	Soda Lime	NaOH	Baralyme	LiOH
Mass of Chemical for 400 L CO_2 absorption	3.4 kg	2.2 kg	5.8 kg	1.35 kg
Volume of Chemical for 400 L CO_2 absorption	4.2 L	3.0 L	6.0 L	2.6 L
Minimum Operation Temp.	0°C	-7°C	-10°C	-32°C
Refillable Canister Possible?	Yes	No	Yes	No
Cost per kg	$0.75-1.10	??	$1.50-2.20	$30-44

Table A3.3.4.a Carbon Dioxide Scrubbers Analysis

The cost of sodium hydroxide is unknown, because it is not available commercially, and at present is only manufactured in Germany for use in special long-duration breathing devices.

Given the general system requirement of minimal mass and volume, lithium hydroxide (LiOH) is the optimum choice.

One average-sized male astronaut requires approximately 1.1 kg of LiOH per day to adequately filter the atmosphere. It is assumed that the value for an average female would be the same or less. The LiOH reaction is as follows:

$$2LiOH + CO_2 \rightarrow Li_2CO_3 + H_2O$$

This is an exothermic reaction, and produces approximately 2035 kJ/kg per person-day. For a maximum mission-length of 15 days with six astronauts, 108 kg of LiOH is required.

Appendix A.3.3.4.3 Thermal Control System Refrigerant

A trade study was done to determine the refrigerant to use in the radiator fluid half of the dual loop heat-rejection system. The refrigerants were analyzed for compressor displacement, power consumption, condensing pressure, toxicity and flammability. After eliminating choices that were not even remotely close to being suitable for the spacecraft, three remained that could possibly be used. The results of the trade study are summarized in Table A3.3.4.a.

Coolant	Flammable?	Compressor Displacement (m^3*min/kg)	Power Consumption (W/kg)	Condensing Pressure @ 38°C (kPa)	Toxic @ <= 400 ppm?
Ammonia	Yes	.191	0.537	1426	Yes
Freon-12	No	.346	0.566	891	No
Freon-22	No	.215	0.572	1389	No

Table A3.3.4..a Refrigerant Trade Study

The chemical name of freon-12 is dichlorodiflouromethane, and the chemical name of freon-22 is chlorodiflouromethane. *Compressor displacement* is the volume rate required to produce a kg of refrigeration. It depends mainly on the latent heat of vaporization of the refrigerant and on the specific volume at suction pressure. Compressor displacement determines the size of the compressor necessary (the smaller the better). *Power consumption* is fairly straightforward. It describes the amount of power to process one kilogram of refrigerant. *Condensing pressure* is the pressure necessary to liquefy the refrigerant in the condenser. It is best to use a refrigerant with a low condensing pressure because higher pressure necessitates more mass in the compressor, piping, condenser and other components. *Toxicity* refers to whether the refrigerant is toxic when exposed to a standard male worker in a quantity of no more than 400 parts per million over the period of an eight-hour workday. This is an industry standard.

From the trade study above, it is apparent that Freon-12, dichloro-diflouromethane, is the optimal refrigerant to use. It has advantages over ammonia in that it is neither toxic nor flammable, and has a much lower condensing pressure at 38°C. Its power consumption is only slightly higher than that of ammonia. Compressor displacement is higher, but this disadvantage is outweighed by the other advantages. Dichloro-flouromethane has the advantage over chlorodiflouromethane (Freon-22) in that it has a lower condensing pressure, and requires less power to operate. Again, it fails to compare with respect to compressor displacement, but the savings in condenser mass should outweigh that.

PRECEDING PAGE BLANK NOT FILMED

Appendix A.3.3.5 Mass vs Escape Option

Ejection Systems			
(20 Kg per 45,000 N Thrust)			
Escape Capsule (14 G's y,z)			
	Mass Kg	Thrust N	
Crew	510		
Cabin	1,090		
Addit Sructure	600		
Elec.	300		
Misc.	200		
SubTotal	2,700	1,168,335	
Engine/Prop	1,558		
Total	4,258		
Mass Added to SV	2,158		
Open Ejection Seats (Crest M=3, 21 Km)			
Crew	510		
Mass Seats	1200		
Total	1710	51000	
Mass Added to SV	1200		
Encapsulated Ejection Seats (F 104 M=2, 30Km)			
Crew	510		
Mass Seats	10800		
Total	11310	200000	
Mass Added to SV	10800		
Entire Nose (14 G's)			
Subtotal	3,300	1,427,965	
Addit Struc.	500		
subtotal	3,800		
Enigne/prop	1,904		
Total	5,204		
Mass Added to SV	2,404		

Table A3.3.5a Ejection Systems Data

- **Escape Module Equations**

$$T = \dot{m}U_e$$

$$U_e = I_{sp} \bullet G$$

$$m_{fuel} = t_b \bullet \dot{m}$$

Solid Motor Casing

$$M(kg) = (.007) \bullet M_{propellent}$$

Trust Structure

$$M(kg) = (2.55E-4) \bullet T(N)$$

$$a = \frac{F}{M} \bullet Cos(\psi - \theta) - \frac{C_D \rho V^2 A}{2M} - g\sin$$

$$\rho = 1.752e^{-y/6700} kg / m^3$$

$$C_D = .075 \bullet [1 + e^{-3[1-M]^2}]$$

$$C_D = .075 \bullet [1 + e^{-[1-M]^2}]$$

Appendix A.3.3.5 - continued

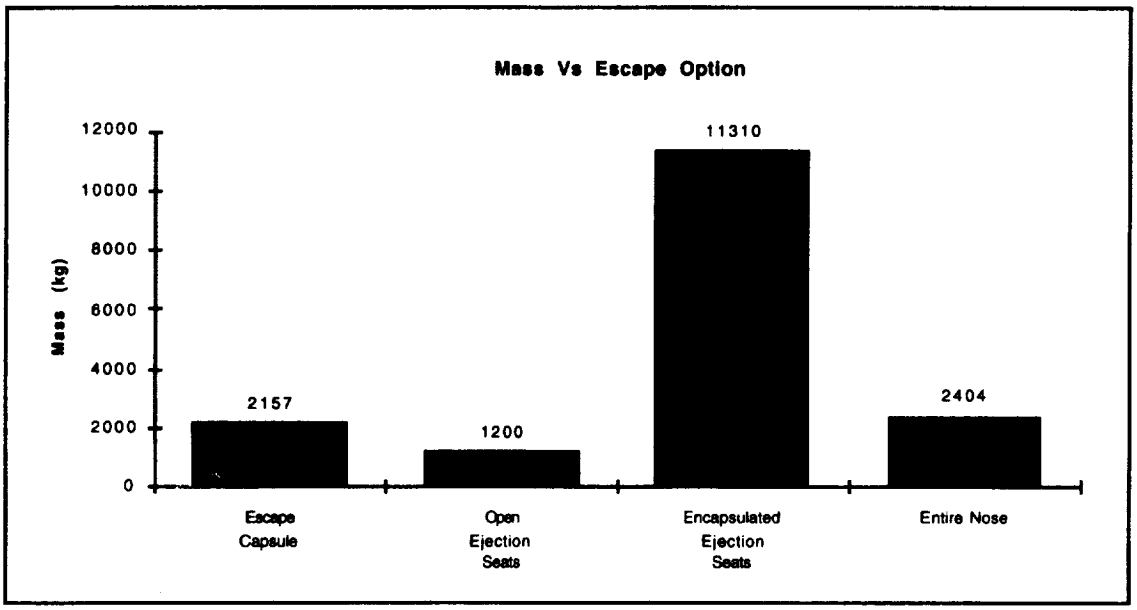

Appendix A.3.3.5

time	dy	dx	vy	vx	ay	ax
0.05	0.4796539	0.4796539	6.39538535	6.88588535	127.907707	137.717707
0.1	1.2812425	1.34251671	12.8254176	13.8056092	128.254176	138.056092
0.15	2.40640376	2.55322854	19.2884787	20.7550603	128.589858	138.367068
0.2	3.85668878	4.11303434	25.7828448	27.729881	128.914224	138.649405
0.25	5.63355588	6.02293401	32.3066746	34.725449	129.226698	138.901796
0.3	7.73836408	8.2836804	38.8579974	41.7368571	129.526658	139.122857
0.35	10.1723658	10.8957639	45.4346994	48.7588922	129.813427	139.311121
0.4	12.9366991	13.8593958	52.0345084	55.786014	130.086271	139.465035
0.45	16.0323785	17.1744911	58.6549782	62.8123357	130.344396	139.582968
0.5	19.4602858	20.8406504	65.293472	69.8316089	130.586944	139.663218
0.55	23.2211593	24.857141	71.9471463	76.8372154	130.812993	139.704028
0.6	27.3155831	29.2228785	78.6129355	83.8221669	131.021559	139.703612
0.65	31.7439745	33.9364092	85.2875384	90.7791192	131.211597	139.660183
0.7	36.5065723	38.9958936	91.9674068	97.700399	131.38201	139.571999
0.75	41.6034239	44.3990922	98.6487396	104.57805	131.531653	139.4374
0.8	47.0343721	50.1433549	105.32748	111.403898	131.65935	139.254872
0.85	52.799043	56.2256143	111.999321	118.169631	131.763908	139.023096
0.9	58.8968341	62.6423847	118.659718	124.866907	131.844132	138.741008
0.95	65.3269031	69.3897664	125.303908	131.487468	131.898851	138.407861
1	72.0881588	76.4634572	131.926941	138.023269	131.926941	138.023269
1.05	79.1792539	83.8587703	138.523718	144.466619	131.927351	137.587256
1.1	86.59858	91.5706589	145.089043	150.81031	131.89913	137.100282
1.15	94.3442655	99.5937478	151.617675	157.04775	131.841457	136.563261
1.2	102.414178	107.92237	158.104399	163.173069	131.753666	135.977557
1.25	110.805926	116.550609	164.54409	169.181215	131.635272	135.344972
1.3	119.516873	125.472341	170.93179	175.06802	131.485992	134.667708
1.35	128.544144	134.681284	177.26278	180.830233	131.305763	133.94832
1.4	137.884645	144.171043	183.532649	186.465532	131.094749	133.189666
1.45	147.53508	153.935157	189.737361	191.972508	130.853352	132.394833
1.5	157.491973	163.967141	195.87331	197.350619	130.582207	131.56708
1.55	167.751694	174.260529	201.937368	202.600135	130.282173	130.709764
1.6	178.310483	184.808908	207.926917	207.722057	129.954323	129.826286
1.65	189.164477	195.605953	213.839876	212.718039	129.599925	128.920024
1.7	200.309737	206.645454	219.674705	217.590297	129.220414	127.994293
1.75	211.742279	217.921337	225.430406	222.341522	128.817375	127.052299
1.8	223.458096	229.42769	231.106512	226.974793	128.392507	126.097107
1.85	235.453183	241.15877	236.70306	231.493498	127.9476	125.131621
1.9	247.723567	253.109022	242.220563	235.901259	127.484507	124.158557
1.95	260.265322	265.273081	247.659978	240.201869	127.005117	123.180446
2	273.074595	277.645781	253.022662	244.399232	126.511331	122.199616
2.05	286.147618	290.222159	258.310337	248.497317	126.005043	121.218203
2.1	299.48073	302.99745	263.525045	252.500112	125.488117	120.238149
2.15	313.070389	315.967094	268.669107	256.411593	124.962376	119.261206

Appendix A.3.3.5

2.2	326.91318	329.126727	273.745092	260.235696	124.429587	118.288953
2.25	341.005833	342.472182	278.75577	263.976291	123.891454	117.322796
2.3	355.345225	355.999482	283.704092	267.637169	123.349605	116.363987
2.35	369.928389	369.704836	288.593149	271.222027	122.805595	115.413629
2.4	384.752523	383.584635	293.426156	274.734458	122.260898	114.472691
2.45	399.81499	397.635444	298.206422	278.177946	121.716907	113.542019
2.5	415.113326	411.853999	302.937338	281.55586	121.174935	112.622344
2.55	430.645239	426.237198	307.622356	284.871455	120.636218	111.714296
2.6	446.408615	440.782097	312.264979	288.127868	120.101915	110.818411
2.65	462.401519	455.485905	316.86875	291.328125	119.573113	109.935141
2.7	478.622195	470.345974	321.437248	294.475135	119.050833	109.064865
2.75	495.069069	485.3598	325.974079	297.571701	118.536029	108.207891
2.8	511.74075	500.525012	330.482874	300.620518	118.029598	107.364471
2.85	528.712538	515.83937	336.484156	303.624179	118.064616	106.5348
2.9	545.828417	531.300757	339.391775	306.585181	117.031647	105.719028
2.95	563.195893	546.907178	344.430625	309.505926	116.756144	104.917263
3	580.727486	562.656755	347.734087	312.38873	115.911362	104.129577
3.05	597.990758	578.163124	345.382988	309.525915	-47.0219822	-57.2563019
3.1	615.168699	593.534468	343.645682	307.526819	-34.7461116	-39.9819068
3.15	632.259841	608.805906	341.909643	305.528668	-34.7207878	-39.9630236
3.2	649.264822	623.978763	340.185814	303.555783	-34.4765783	-39.4576938
3.25	666.184235	639.054241	338.473859	301.607014	-34.2391029	-38.9753997
3.3	683.032772	654.055816	337.04231	300.106511	-28.6309737	-30.0100519
3.35	699.81005	668.982912	335.616836	298.616424	-28.5094921	-29.8017421
3.4	716.516456	683.836256	334.199019	297.14067	-28.3563336	-29.5150819
3.45	733.15237	698.616552	332.78878	295.679008	-28.2047792	-29.2332261
3.5	749.718165	713.324495	331.38605	294.231244	-28.0546083	-28.955294
3.55	766.214215	727.960769	329.990759	292.797183	-27.9058061	-28.6812219
3.6	782.640888	742.526049	328.602842	291.376636	-27.7583569	-28.4109398
3.65	798.998547	757.021002	327.222229	289.969417	-27.6122449	-28.1443794
3.7	815.287557	771.446284	325.848857	288.575343	-27.4674549	-27.8814737
3.75	831.508274	785.802543	324.482658	287.194235	-27.3239717	-27.6221574
3.8	847.661055	800.090418	323.123569	285.825917	-27.1817803	-27.3663666
3.85	863.746251	814.310539	321.771526	284.470215	-27.040866	-27.1140386
3.9	879.764212	828.463529	320.426465	283.126959	-26.9012142	-26.8651124
3.95	895.715283	842.550001	319.088324	281.795983	-26.7628107	-26.619528
4	911.599807	856.57056	317.757042	280.477121	-26.6256414	-26.3772269
4.05	927.418123	870.525803	316.432558	279.170214	-26.4896922	-26.1381517
4.1	943.170569	884.416321	315.11481	277.875102	-26.3549496	-25.9022465
4.15	958.857479	898.242693	313.80374	276.591629	-26.2213998	-25.6694562
4.2	974.479182	912.005495	312.499289	275.319642	-26.0890297	-25.4397272
4.25	990.036007	925.705293	311.201397	274.058992	-25.957826	-25.213007
4.3	1005.52828	939.342646	309.910009	272.80953	-25.8277758	-24.989244
4.35	1020.95632	952.918106	308.625065	271.57111	-25.6988661	-24.7683878
4.4	1036.32045	966.432216	307.346511	270.343591	-25.5710845	-24.5503892
4.45	1051.62098	979.885516	306.07429	269.126831	-25.4444185	-24.3351998

4.5	1066.85824	993.278535	304.808347	267.920692	-25.3188557	-24.1227723
4.55	1082.03252	1006.6118	303.548628	266.725039	-25.1943841	-23.9130605
4.6	1097.14414	1019.88582	302.295079	265.539738	-25.0709916	-23.7060188
4.65	1112.1934	1033.10112	301.047645	264.364658	-24.9486666	-23.501603
4.7	1127.18061	1046.25819	299.806275	263.19967	-24.8273974	-23.2997694
4.75	1142.10607	1059.35753	298.570917	262.044646	-24.7071724	-23.1004754
4.8	1156.97007	1072.39964	297.341518	260.899462	-24.5879805	-22.9036793
4.85	1171.77291	1085.385	296.118027	259.763995	-24.4698103	-22.7093401
4.9	1186.51489	1098.3141	294.900395	258.638124	-24.352651	-22.5174178
4.95	1201.19629	1111.18739	293.68857	257.521731	-24.2364916	-22.3278729
5	1215.8174	1124.00536	292.482504	256.414697	-24.1213214	-22.140667
5.05	1230.37851	1136.76846	291.282148	255.316909	-24.0071298	-21.9557624
5.1	1244.87989	1149.47715	290.087452	254.228253	-23.8939064	-21.773122
5.15	1259.32184	1162.13188	288.89837	253.148617	-23.7816408	-21.5927096
5.2	1273.70462	1174.7331	287.714854	252.077893	-23.670323	-21.4144897
5.25	1288.02852	1187.28124	286.536857	251.015972	-23.5599428	-21.2384273
5.3	1302.2938	1199.77675	285.364332	249.962747	-23.4504905	-21.0644882
5.35	1316.50075	1212.22004	284.197235	248.918115	-23.3419561	-20.8926391
5.4	1330.64962	1224.61155	283.035518	247.881973	-23.2343301	-20.722847
5.45	1344.74069	1236.95169	281.879138	246.854219	-23.1276029	-20.5550796
5.5	1358.77421	1249.24088	280.72805	245.834754	-23.0217652	-20.3893055
5.55	1372.75046	1261.47953	279.582209	244.823479	-22.9168076	-20.2254936
5.6	1386.66968	1273.66803	278.441573	243.820298	-22.8127211	-20.0636134
5.65	1400.53215	1285.8068	277.306098	242.825117	-22.7094966	-19.9036352
5.7	1414.33811	1297.89623	276.175742	241.83784	-22.6071252	-19.7455298
5.75	1428.08782	1309.9367	275.050462	240.858377	-22.505598	-19.5892683
5.8	1441.78153	1321.9286	273.930217	239.886636	-22.4049064	-19.4348227
5.85	1455.41949	1333.87231	272.814965	238.922527	-22.3050419	-19.2821653
5.9	1469.00195	1345.76822	271.704665	237.965964	-22.2059959	-19.131269
5.95	1482.52915	1357.61669	270.599277	237.016858	-22.1077601	-18.9821072
6	1496.00134	1369.41809	269.498761	236.075126	-22.0103262	-18.8346538
6.05	1509.41875	1381.17279	268.403076	235.140682	-21.9136861	-18.6888831
6.1	1522.78163	1392.88115	267.312185	234.213443	-21.8178318	-18.54477
6.15	1536.09022	1404.54351	266.226047	233.293329	-21.7227553	-18.4022898
6.2	1549.34475	1416.16024	265.144625	232.380258	-21.6284488	-18.2614182
6.25	1562.54545	1427.73168	264.067879	231.474151	-21.5349045	-18.1221315
6.3	1575.69256	1439.25818	262.995774	230.574931	-21.4421147	-17.9844063
6.35	1588.7863	1450.74008	261.92827	229.68252	-21.350072	-17.8482196
6.4	1601.82691	1462.17771	260.865332	228.796842	-21.2587689	-17.713549
6.45	1614.81461	1473.5714	259.806922	227.917824	-21.168198	-17.5803722
6.5	1627.74963	1484.92149	258.753004	227.04539	-21.078352	-17.4486676
6.55	1640.63218	1496.2283	257.703543	226.17947	-20.9892238	-17.3184139
6.6	1653.46249	1507.49215	256.658503	225.31999	-20.9008063	-17.1895901
6.65	1666.24078	1518.71336	255.617848	224.466881	-20.8130924	-17.0621755
6.7	1678.96727	1529.89224	254.581544	223.620074	-20.7260753	-16.9361501
6.75	1691.64217	1541.02912	253.549557	222.779499	-20.6397482	-16.8114939

Appendix A.3.3.5

6.8	1704.26569	1552.12429	252.521852	221.94509	-20.5541042	-16.6881874
6.85	1716.83805	1563.17805	251.498395	221.116779	-20.4691367	-16.5662115
6.9	1729.35946	1574.19072	250.479153	220.294502	-20.3848391	-16.4455474
6.95	1741.83013	1585.16259	249.464093	219.478193	-20.301205	-16.3261764
7	1754.25026	1596.09396	248.453181	218.667789	-20.2182279	-16.2080805
7.05	1766.62006	1606.98511	247.446386	217.863227	-20.1359015	-16.0912418
7.1	1778.93974	1617.83633	246.443675	217.064445	-20.0542194	-15.9756428
7.15	1791.20949	1628.64792	245.445016	216.271382	-19.9731756	-15.8612661
7.2	1803.42953	1639.42015	244.450378	215.483977	-19.8927638	-15.7480948
7.25	1815.60004	1650.1533	243.459729	214.702171	-19.8129781	-15.6361122
7.3	1827.72122	1660.84766	242.473039	213.925906	-19.7338125	-15.525302
7.35	1839.79328	1671.50349	241.490276	213.155124	-19.655261	-15.4156481
7.4	1851.8164	1682.12106	240.51141	212.389767	-19.5773179	-15.3071346
7.45	1863.79079	1692.70065	239.536411	211.62978	-19.4999774	-15.1997459
7.5	1875.71662	1703.24252	238.565249	210.875106	-19.4232338	-15.0934668
7.55	1887.5941	1713.74693	237.597895	210.125692	-19.3470814	-14.9882822
7.6	1899.4234	1724.21414	236.634319	209.381483	-19.2715148	-14.8841773
7.65	1911.20473	1734.64442	235.674493	208.642426	-19.1965284	-14.7811375
7.7	1922.93826	1745.03801	234.718387	207.908469	-19.1221169	-14.6791486
7.75	1934.62417	1755.39516	233.765973	207.179559	-19.0482748	-14.5781965
7.8	1946.26266	1765.71613	232.817224	206.455646	-18.9749968	-14.4782673
7.85	1957.85391	1776.00117	231.87211	205.736678	-18.9022778	-14.3793474
7.9	1969.39808	1786.25052	230.930604	205.022607	-18.8301125	-14.2814234
7.95	1980.89537	1796.46441	229.992679	204.313383	-18.7584959	-14.1844822
8	1992.34595	1806.6431	229.058308	203.608958	-18.6874228	-14.0885109
8.05	2003.75	1816.78681	228.127464	202.909283	-18.6168884	-13.9934966
8.1	2015.10769	1826.89579	227.200119	202.214311	-18.5468876	-13.8994268
8.15	2026.41919	1836.97027	226.276248	201.523997	-18.4774156	-13.8062893
8.2	2037.68468	1847.01047	225.355825	200.838293	-18.4084675	-13.7140718
8.25	2048.90433	1857.01662	224.438823	200.157155	-18.3400387	-13.6227624
8.3	2060.0783	1866.98896	223.525217	199.480538	-18.2721243	-13.5323494
8.35	2071.20678	1876.9277	222.614981	198.808397	-18.2047198	-13.4428212
8.4	2082.28991	1886.83306	221.70809	198.140688	-18.1378205	-13.3541665
8.45	2093.32788	1896.70527	220.804519	197.47737	-18.0714218	-13.266374
8.5	2104.32084	1906.54454	219.904243	196.818398	-18.0055194	-13.1794327
8.55	2115.26896	1916.35109	219.007237	196.163732	-17.9401087	-13.0933318
8.6	2126.1724	1926.12513	218.113478	195.513328	-17.8751853	-13.0080606
8.65	2137.03132	1935.86688	217.222941	194.867148	-17.810745	-12.9236085
8.7	2147.84588	1945.57653	216.335602	194.22515	-17.7467833	-12.8399653
8.75	2158.61625	1955.2543	215.451437	193.587294	-17.6832961	-12.7571208
8.8	2169.34256	1964.90039	214.570423	192.95354	-17.6202792	-12.6750649
8.85	2180.025	1974.51501	213.692537	192.323851	-17.5577283	-12.5937878
8.9	2190.6637	1984.09836	212.817755	191.698187	-17.4956395	-12.5132797
8.95	2201.25882	1993.65063	211.946054	191.076511	-17.4340086	-12.4335311
9	2211.81052	2003.17202	211.077413	190.458784	-17.3728317	-12.3545326
9.05	2222.31895	2012.66274	210.211807	189.84497	-17.3121047	-12.2762749

Appendix A.3.3.5

9.1	2232.78425	2022.12296	209.349216	189.235033	-17.2518238	-12.1987488
9.15	2243.20658	2031.55289	208.489617	188.628935	-17.191985	-12.1219454
9.2	2253.58609	2040.95272	207.632988	188.026643	-17.1325846	-12.0458557
9.25	2263.92292	2050.32263	206.779307	187.428119	-17.0736187	-11.9704712
9.3	2274.21722	2059.66281	205.928553	186.83333	-17.0150836	-11.8957831
9.35	2284.46914	2068.97344	205.080704	186.242241	-16.9569756	-11.821783
9.4	2294.67881	2078.25472	204.235739	185.654818	-16.899291	-11.7484626
9.45	2304.84639	2087.50681	203.393638	185.071027	-16.8420262	-11.6758137
9.5	2314.97201	2096.7299	202.554379	184.490836	-16.7851776	-11.6038282
9.55	2325.05582	2105.92417	201.717942	183.914211	-16.7287416	-11.5324981
9.6	2335.09795	2115.08979	200.884306	183.34112	-16.6727148	-11.4618155
9.65	2345.09854	2124.22694	200.053452	182.771531	-16.6170937	-11.3917728
9.7	2355.05774	2133.3358	199.225358	182.205413	-16.5618748	-11.3223622
9.75	2364.97568	2142.41653	198.400005	181.642734	-16.5070548	-11.2535764
9.8	2374.85249	2151.4693	197.577374	181.083464	-16.4526303	-11.1854078
9.85	2384.68831	2160.49429	196.757444	180.527572	-16.3985979	-11.1178493
9.9	2394.48328	2169.49166	195.940196	179.975027	-16.3449544	-11.0508936
9.95	2404.23752	2178.46158	195.125611	179.4258	-16.2916966	-10.9845336
10	2413.95118	2187.40421	194.31367	178.879862	-16.2388212	-10.9187624
10.1	2423.62437	2196.31971	193.504354	178.337183	-16.186325	-10.8535731
10.1	2433.25724	2205.20825	192.697644	177.797735	-16.134205	-10.788959
10.2	2442.8499	2214.06998	191.893521	177.26149	-16.082458	-10.7249132
10.2	2452.4025	2222.90507	191.091967	176.728418	-16.0310808	-10.6614293
10.3	2461.91515	2231.71367	190.292963	176.198493	-15.9800706	-10.5985008
10.3	2471.38798	2240.49594	189.496492	175.671687	-15.9294242	-10.5361212
10.4	2480.82112	2249.25203	188.702535	175.147973	-15.8791387	-10.4742843
10.4	2490.2147	2257.98209	187.911074	174.627324	-15.8292112	-10.4129839
10.5	2499.56883	2266.68628	187.122092	174.109713	-15.7796386	-10.3522138
10.5	2508.88364	2275.36475	186.335572	173.595115	-15.7304182	-10.291968
10.6	2518.15926	2284.01765	185.551494	173.083503	-15.6815471	-10.2322405
10.6	2527.39579	2292.64512	184.769843	172.574851	-15.6330225	-10.1730254
10.7	2536.59338	2301.24731	183.990601	172.069136	-15.5848416	-10.114317
10.7	2545.75212	2309.82437	183.213751	171.56633	-15.5370015	-10.0561096
10.8	2554.87215	2318.37644	182.439276	171.06641	-15.4894997	-9.99839746
10.8	2563.95358	2326.90367	181.667159	170.569351	-15.4423333	-9.94117513
10.9	2572.99652	2335.40619	180.897384	170.07513	-15.3954997	-9.88443709
10.9	2582.0011	2343.88415	180.129934	169.583721	-15.3489962	-9.82817795
11	2590.96743	2352.33768	179.364793	169.095101	-15.3028203	-9.77239239
11	2599.89562	2360.76693	178.601945	168.609247	-15.2569693	-9.71707515
11.1	2608.78578	2369.17203	177.841373	168.126136	-15.2114406	-9.66222106
11.1	2617.63804	2377.55311	177.083061	167.645745	-15.1662318	-9.607825
11.2	2626.4525	2385.91032	176.326994	167.168051	-15.1213403	-9.55388194
11.2	2635.22927	2394.24378	175.573156	166.693032	-15.0767637	-9.50038692
11.3	2643.96847	2402.55364	174.821531	166.220665	-15.0324994	-9.44733501
11.3	2652.6702	2410.84001	174.072104	165.750929	-14.988545	-9.39472139
11.4	2661.33458	2419.10303	173.324859	165.283802	-14.9448982	-9.3425413

Appendix A.3.3.5

11.4	2669.9617	2427.34283	172.579781	164.819262	-14.9015565	-9.29079001
11.5	2678.55169	2435.55954	171.836855	164.357289	-14.8585176	-9.23946289
11.5	2687.10464	2443.75329	171.096066	163.897861	-14.8157791	-9.18855535
11.6	2695.62066	2451.92419	170.357399	163.440958	-14.7733387	-9.13806289
11.6	2704.09986	2460.07238	169.62084	162.986559	-14.7311942	-9.08798102
11.7	2712.54235	2468.19799	168.886373	162.534644	-14.6893433	-9.03830536
11.7	2720.94822	2476.30112	168.153983	162.085192	-14.6477837	-8.98903157
11.8	2729.31757	2484.38192	167.423658	161.638184	-14.6065133	-8.94015535
11.8	2737.65052	2492.44048	166.695381	161.193601	-14.5655297	-8.89167248
11.9	2745.94716	2500.47695	165.96914	160.751422	-14.5248309	-8.84357879
11.9	2754.2076	2508.49143	165.244919	160.311628	-14.4844148	-8.79587015
12	2762.43193	2516.48405	164.522705	159.874201	-14.4442791	-8.74854251
12	2770.62025	2524.45492	163.802484	159.439122	-14.4044217	-8.70159185
12.1	2778.77267	2532.40415	163.084242	159.006371	-14.3648407	-8.65501422
12.1	2786.88927	2540.33187	162.367965	158.575931	-14.3255338	-8.6088057
12.2	2794.97017	2548.23819	161.65364	158.147783	-14.2864992	-8.56296245
12.2	2803.01545	2556.12322	160.941253	157.721909	-14.2477347	-8.51748065
12.3	2811.02522	2563.98708	160.230792	157.298291	-14.2092383	-8.47235654
12.3	2818.99956	2571.82987	159.522241	156.876911	-14.1710081	-8.42758642
12.4	2826.93857	2579.65171	158.815589	156.457753	-14.1330422	-8.38316663
12.4	2834.84235	2587.45271	158.110822	156.040798	-14.0953385	-8.33909354
12.5	2842.71099	2595.23297	157.407927	155.62603	-14.0578951	-8.2953636
12.5	2850.54458	2602.99261	156.706892	155.213432	-14.0207102	-8.25197328
12.6	2858.34322	2610.73174	156.007703	154.802986	-13.9837818	-8.20891909
12.6	2866.10699	2618.45045	155.310347	154.394676	-13.9471081	-8.16619761
12.7	2873.83599	2626.14886	154.614813	153.988485	-13.9106873	-8.12380544
12.7	2881.53031	2633.82707	153.921087	153.584398	-13.8745174	-8.08173924
12.8	2889.19004	2641.48518	153.229157	153.182399	-13.8385968	-8.0399957
12.8	2896.81527	2649.12331	152.539011	152.78247	-13.8029236	-7.99857156
12.9	2904.40608	2656.74154	151.850636	152.384597	-13.767496	-7.95746359
12.9	2911.96256	2664.33999	151.164021	151.988763	-13.7323124	-7.91666861
13	2919.48481	2671.91875	150.479152	151.594954	-13.6973708	-7.87618347
13	2926.9729	2679.47793	149.796019	151.203154	-13.6626697	-7.83600507
13.1	2934.42693	2687.01762	149.114608	150.813348	-13.6282073	-7.79613035
13.1	2941.84697	2694.53793	148.434909	150.42552	-13.593982	-7.75655627
13.2	2949.23312	2702.03895	147.75691	150.039656	-13.559992	-7.71727985
13.2	2956.58546	2709.52078	147.080598	149.655741	-13.5262357	-7.67829813
13.3	2963.90407	2716.98351	146.405962	149.27376	-13.4927114	-7.6396082
13.3	2971.18904	2724.42724	145.732991	148.8937	-13.4594177	-7.60120716
13.4	2978.44045	2731.85208	145.061674	148.515545	-13.4263527	-7.56309219
13.4	2985.65837	2739.2581	144.391998	148.139282	-13.393515	-7.52526045
13.5	2992.8429	2746.64541	143.723953	147.764897	-13.360903	-7.48770919
13.5	2999.99411	2754.01409	143.057527	147.392375	-13.3285151	-7.45043565
13.6	3007.11208	2761.36425	142.39271	147.021703	-13.2963498	-7.41343711
13.6	3014.1969	2768.69597	141.729489	146.652868	-13.2644055	-7.37671092
13.7	3021.24864	2776.00935	141.067855	146.285855	-13.2326808	-7.34025441

13.7	3028.26738	2783.30447	140.407797	145.920652	-13.2011741	-7.30406498
13.8	3035.2532	2790.58142	139.749302	145.557245	-13.1698839	-7.26814003
13.8	3042.20617	2797.8403	139.092362	145.195621	-13.1388088	-7.23247703
13.9	3049.12638	2805.08119	138.436965	144.835767	-13.1079473	-7.19707345
13.9	3056.0139	2812.30418	137.7831	144.477671	-13.0772981	-7.1619268
14	3062.86881	2819.50935	137.130757	144.121319	-13.0468595	-7.12703462
14	3069.69118	2826.6968	136.479925	143.766699	-13.0166303	-7.09239448
14.1	3076.48109	2833.86661	135.830595	143.413799	-12.9866091	-7.05800396
14.1	3083.2386	2841.01886	135.182755	143.062606	-12.9567944	-7.02386071
14.2	3089.96381	2848.15364	134.536396	142.713108	-12.9271849	-6.98996236
14.2	3096.65677	2855.27104	133.891507	142.365293	-12.8977792	-6.95630661
14.3	3103.31757	2862.37113	133.248078	142.019148	-12.868576	-6.92289116
14.3	3109.94627	2869.454	132.606099	141.674663	-12.839574	-6.88971374
14.4	3116.54294	2876.51974	131.965561	141.331824	-12.8107717	-6.85677212
14.4	3123.10767	2883.56841	131.326452	140.990621	-12.782168	-6.82406408
14.5	3129.64051	2890.60012	130.688764	140.651041	-12.7537615	-6.79158743
14.5	3136.14155	2897.61493	130.052487	140.313074	-12.7255509	-6.75934003
14.6	3142.61084	2904.61292	129.41761	139.976708	-12.697535	-6.72731971
14.6	3149.04846	2911.59418	128.784124	139.641932	-12.6697126	-6.69552439
14.7	3155.45448	2918.55878	128.15202	139.308735	-12.6420823	-6.66395196
14.7	3161.82897	2925.50681	127.521288	138.977105	-12.6146429	-6.63260037
14.8	3168.17199	2932.43834	126.891918	138.647031	-12.5873932	-6.60146758
14.8	3174.48362	2939.35344	126.263902	138.318504	-12.5603321	-6.57055156
14.9	3180.76391	2946.2522	125.637229	137.991511	-12.5334582	-6.53985033
14.9	3187.01294	2953.13469	125.01189	137.666043	-12.5067704	-6.50936191
15	3193.23078	2960.00098	124.387877	137.342089	-12.4802676	-6.47908436
15	3199.41748	2966.85116	123.76518	137.019638	-12.4539486	-6.44901575
15.1	3205.57312	2973.68529	123.143789	136.69868	-12.4278122	-6.41915417
15.1	3211.69775	2980.50345	122.523696	136.379205	-12.4018572	-6.38949775
15.2	3217.79145	2987.30572	121.904892	136.061203	-12.3760827	-6.36004461
15.2	3223.85427	2994.09216	121.287368	135.744664	-12.3504873	-6.33079293
15.3	3229.88629	3000.86285	120.671114	135.429576	-12.3250701	-6.30174088
15.3	3235.88756	3007.61786	120.056123	135.115932	-12.2998298	-6.27288665
15.4	3241.85814	3014.35727	119.442384	134.803721	-12.2747656	-6.24422848
15.4	3247.7981	3021.08114	118.82989	134.492932	-12.2498761	-6.2157646
15.5	3253.70751	3027.78954	118.218632	134.183558	-12.2251605	-6.18749327
15.5	3259.58641	3034.48255	117.608602	133.875587	-12.2006175	-6.15941277
15.6	3265.43488	3041.16023	116.999789	133.569011	-12.1762463	-6.13152139
15.6	3271.25297	3047.82266	116.392187	133.26382	-12.1520457	-6.10381747
15.7	3277.04074	3054.4699	115.785786	132.960005	-12.1280147	-6.07629932
15.7	3282.79826	3061.10202	115.180579	132.657557	-12.1041523	-6.04896531
15.8	3288.52558	3067.71909	114.576556	132.356466	-12.0804575	-6.0218138
15.8	3294.22276	3074.32118	113.973709	132.056724	-12.0569292	-5.99484319
15.9	3299.88985	3080.90835	113.372031	131.758322	-12.0335666	-5.96805189
15.9	3305.52693	3087.48067	112.771513	131.46125	-12.0103686	-5.94143831
16	3311.13404	3094.03821	112.172146	131.1655	-11.9873342	-5.91500091

Appendix A.3.3.5

16	3316.71124	3100.58102	111.573923	130.871063	-11.9644626	-5.88873813
16.1	3322.25859	3107.10919	110.976835	130.57793	-11.9417526	-5.86264846
16.1	3327.77614	3113.62276	110.380875	130.286094	-11.9192035	-5.83673039
16.2	3333.26395	3120.12181	109.786034	129.995545	-11.8968142	-5.81098242
16.2	3338.72208	3126.6064	109.192305	129.706274	-11.8745838	-5.78540308
16.3	3344.15059	3133.0766	108.599679	129.418275	-11.8525115	-5.75999092
16.3	3349.54952	3139.53246	108.00815	129.131538	-11.8305962	-5.73474448
16.4	3354.91893	3145.97405	107.417708	128.846055	-11.8088372	-5.70966234
16.4	3360.25887	3152.40143	106.828346	128.561817	-11.7872335	-5.68474309
16.5	3365.5694	3158.81466	106.240057	128.278818	-11.7657842	-5.65998532
16.5	3370.85057	3165.21381	105.652832	127.997049	-11.7444885	-5.63538766
16.6	3376.10244	3171.59893	105.066665	127.716501	-11.7233454	-5.61094873
16.6	3381.32506	3177.97009	104.481547	127.437168	-11.7023543	-5.58666719
16.7	3386.51847	3184.32735	103.897472	127.159041	-11.6815141	-5.56254168
16.7	3391.68273	3190.67076	103.314431	126.882112	-11.660824	-5.53857089
16.8	3396.8179	3197.00039	102.732416	126.606375	-11.6402833	-5.51475351
16.8	3401.92402	3203.3163	102.151422	126.33182	-11.6198911	-5.49108823
16.9	3407.00114	3209.61854	101.57144	126.058442	-11.5996465	-5.46757378
16.9	3412.04932	3215.90717	100.992462	125.786231	-11.5795488	-5.44420888
17	3417.0686	3222.18225	100.414482	125.515182	-11.5595971	-5.42099227
17	3422.05903	3228.44384	99.8374927	125.245285	-11.5397908	-5.39792271
17.1	3427.02066	3234.69199	99.2614863	124.976535	-11.5201289	-5.37499897
17.1	3431.95355	3240.92677	98.6864557	124.708924	-11.5006107	-5.35221983
17.2	3436.85773	3247.14823	98.1123939	124.442445	-11.4812354	-5.32958409
17.2	3441.73326	3253.35642	97.5392938	124.177091	-11.4620023	-5.30709054
17.3	3446.58019	3259.5514	96.9671483	123.912854	-11.4429107	-5.28473802
17.3	3451.39856	3265.73323	96.3959503	123.649728	-11.4239596	-5.26252535
17.4	3456.18842	3271.90196	95.8256929	123.387705	-11.4051485	-5.24045136
17.4	3460.94981	3278.05764	95.2563691	123.126779	-11.3864766	-5.21851493
17.5	3465.68279	3284.20034	94.6879719	122.866943	-11.3679431	-5.19671491
17.5	3470.3874	3290.3301	94.1204945	122.608191	-11.3495474	-5.17505019
17.6	3475.06368	3296.44699	93.5539301	122.350515	-11.3312887	-5.15351965
17.6	3479.71168	3302.55104	92.9882718	122.093909	-11.3131663	-5.13212219
17.7	3484.33144	3308.64232	92.4235128	121.838366	-11.2951795	-5.11085673
17.7	3488.92301	3314.72088	91.8596464	121.58388	-11.2773276	-5.08972219
17.8	3493.48644	3320.78677	91.2966659	121.330444	-11.2596099	-5.0687175
17.8	3498.02176	3326.84004	90.7345646	121.078052	-11.2420258	-5.04784161
17.9	3502.52903	3332.88074	90.1733359	120.826697	-11.2245746	-5.02709347
17.9	3507.00827	3338.90894	89.6129731	120.576374	-11.2072556	-5.00647205
18	3511.45955	3344.92467	89.0534697	120.327075	-11.1900681	-4.98597633
18	3515.88289	3350.92799	88.4948192	120.078795	-11.1730115	-4.96560529
18.1	3520.27835	3356.91894	87.9370149	119.831527	-11.1560851	-4.94535794
18.1	3524.64596	3362.89759	87.3800505	119.585265	-11.1392884	-4.92523326
18.2	3528.98577	3368.86398	86.8239194	119.340004	-11.1226206	-4.90523029
18.2	3533.29781	3374.81816	86.2686154	119.095736	-11.1060811	-4.88534805
18.3	3537.58213	3380.76017	85.7141319	118.852457	-11.0896694	-4.86558558

Appendix A.3.3.5

18.3	3541.83877	3386.69007	85.1604627	118.61016	-11.0733847	-4.84594192
18.4	3546.06777	3392.60791	84.6076014	118.368839	-11.0572266	-4.82641612
18.4	3550.26916	3398.51373	84.0555416	118.128489	-11.0411943	-4.80700725
18.5	3554.443	3404.40759	83.5042773	117.889103	-11.0252872	-4.78771439
18.5	3558.58931	3410.28953	82.953802	117.650676	-11.0095049	-4.76853662
18.6	3562.70814	3416.1596	82.4041097	117.413202	-10.9938466	-4.74947302
18.6	3566.79953	3422.01784	81.8551941	117.176676	-10.9783119	-4.73052271
18.7	3570.86351	3427.8643	81.3070491	116.941092	-10.9629001	-4.71168478
18.7	3574.90013	3433.69904	80.7596686	116.706444	-10.9476107	-4.69295836
18.8	3578.90941	3439.52209	80.2130464	116.472727	-10.932443	-4.67434258
18.8	3582.89141	3445.33351	79.6671766	116.239935	-10.9173966	-4.65583657
18.9	3586.84615	3451.13333	79.122053	116.008063	-10.9024709	-4.63743946
18.9	3590.77367	3456.92161	78.5776698	115.777106	-10.8876654	-4.61915043
19	3594.67401	3462.69838	78.0340208	115.547057	-10.8729794	-4.60096862
19	3598.54721	3468.46371	77.4911002	115.317913	-10.8584125	-4.5828932
19.1	3602.3933	3474.21762	76.948902	115.089666	-10.8439641	-4.56492335
19.1	3606.21232	3479.96017	76.4074203	114.862313	-10.8296337	-4.54705826
19.2	3610.0043	3485.69139	75.8666493	114.635849	-10.8154208	-4.52929711
19.2	3613.76928	3491.41134	75.326583	114.410267	-10.8013248	-4.51163911
19.3	3617.50729	3497.12006	74.7872158	114.185562	-10.7873453	-4.49408346
19.3	3621.21837	3502.81759	74.2485417	113.961731	-10.7734817	-4.47662937
19.4	3624.90255	3508.50397	73.710555	113.738767	-10.7597336	-4.45927608
19.4	3628.55987	3514.17925	73.17325	113.516666	-10.7461004	-4.44202281
19.5	3632.19036	3519.84346	72.6366209	113.295423	-10.7325817	-4.42486879
19.5	3635.79405	3525.49666	72.100662	113.075032	-10.719177	-4.40781328
19.6	3639.37098	3531.13889	71.5653677	112.855489	-10.7058857	-4.39085552
19.6	3642.92118	3536.77018	71.0307324	112.636789	-10.6927075	-4.37399477
19.7	3646.44469	3542.39058	70.4967503	112.418928	-10.6796418	-4.3572303
19.7	3649.94152	3548.00014	69.9634159	112.2019	-10.6666882	-4.34056137
19.8	3653.41173	3553.59888	69.4307235	111.985701	-10.6538462	-4.32398728
19.8	3656.85533	3559.18686	68.8986678	111.770325	-10.6411154	-4.3075073
19.9	3660.27236	3564.76411	68.367243	111.555769	-10.6284953	-4.29112073
19.9	3663.66286	3570.33068	67.8364437	111.342028	-10.6159854	-4.27482686
20	3667.02685	3575.8866	67.3062645	111.129097	-10.6035854	-4.25862501
20	3670.36436	3581.43192	66.7766997	110.916971	-10.5912948	-4.24251448
20.1	3673.67542	3586.96667	66.2477441	110.705646	-10.5791131	-4.22649459
20.1	3676.96007	3592.4909	65.7193921	110.495118	-10.5670399	-4.21056468
20.2	3680.21834	3598.00465	65.1916383	110.285382	-10.5550749	-4.19472406
20.2	3683.45024	3603.50795	64.6644775	110.076433	-10.5432175	-4.17897208
20.3	3686.65582	3609.00084	64.1379041	109.868268	-10.5314674	-4.16330808
20.3	3689.8351	3614.48336	63.6119129	109.660881	-10.5198241	-4.14773141
20.4	3692.98811	3619.95556	63.0864985	109.454269	-10.5082873	-4.13224142
20.4	3696.11488	3625.41747	62.5616557	109.248427	-10.4968565	-4.11683748
20.5	3699.21544	3630.86912	62.0373791	109.043351	-10.4855314	-4.10151896
20.5	3702.28981	3636.31056	61.5136635	108.839037	-10.4743116	-4.08628522
20.6	3705.33803	3641.74183	60.9905037	108.63548	-10.4631966	-4.07113565

Appendix A.3.3.5

20.6	3708.36012	3647.16296	60.4678944	108.432677	-10.4521862	-4.05606963
20.7	3711.35611	3652.57398	59.9458304	108.230622	-10.4412798	-4.04108654
20.7	3714.32602	3657.97494	59.4243066	108.029313	-10.4304771	-4.0261858
20.8	3717.26988	3663.36588	58.9033177	107.828745	-10.4197779	-4.01136679
20.8	3720.18772	3668.74683	58.3828586	107.628913	-10.4091816	-3.99662892
20.9	3723.07957	3674.11782	57.8629242	107.429815	-10.398688	-3.98197161
20.9	3725.94545	3679.4789	57.3435094	107.231445	-10.3882966	-3.96739427
21	3728.78538	3684.83009	56.824609	107.0338	-10.3780071	-3.95289632
21	3731.59939	3690.17144	56.306218	106.836876	-10.3678193	-3.9384772
21.1	3734.38752	3695.50299	55.7883314	106.640669	-10.3577326	-3.92413633
21.1	3737.14977	3700.82476	55.2709441	106.445176	-10.3477468	-3.90987315
21.2	3739.88618	3706.13679	54.754051	106.250391	-10.3378616	-3.89568711
21.2	3742.59677	3711.43912	54.2376472	106.056313	-10.3280766	-3.88157765
21.3	3745.28157	3716.73178	53.7217276	105.862935	-10.3183914	-3.86754422
21.3	3747.94059	3722.01481	53.2062873	105.670256	-10.3088058	-3.85358629
21.4	3750.57387	3727.28825	52.6913213	105.478271	-10.2993195	-3.83970331
21.4	3753.18143	3732.55212	52.1768247	105.286976	-10.289932	-3.82589475
21.5	3755.76328	3737.80646	51.6627926	105.096368	-10.2806431	-3.81216008
21.5	3758.31946	3743.05131	51.1492199	104.906443	-10.2714525	-3.79849879
21.6	3760.84998	3748.28669	50.6361019	104.717198	-10.2623599	-3.78491034
21.6	3763.35487	3753.51265	50.1234337	104.528628	-10.253365	-3.77139423
21.7	3765.83415	3758.72922	49.6112103	104.34073	-10.2444674	-3.75794995
21.7	3768.28784	3763.93643	49.099427	104.153502	-10.2356669	-3.74457699
21.8	3770.71597	3769.13431	48.5880788	103.966938	-10.2269632	-3.73127485
21.8	3773.11855	3774.3229	48.077161	103.781036	-10.218356	-3.71804303
21.9	3775.49561	3779.50222	47.5666688	103.595792	-10.209845	-3.70488104
21.9	3777.84716	3784.67232	47.0565973	103.411202	-10.2014299	-3.69178839
22	3780.17323	3789.83322	46.5469418	103.227264	-10.1931104	-3.67876461
22	3782.47385	3794.98496	46.0376974	103.043974	-10.1848864	-3.6658092
22.1	3784.74902	3800.12757	45.5288596	102.861327	-10.1767574	-3.65292169
22.1	3786.99877	3805.26109	45.0204234	102.679322	-10.1687233	-3.64010162
22.2	3789.22312	3810.38553	44.5123842	102.497955	-10.1607838	-3.62734852
22.2	3791.42208	3815.50094	44.0047373	102.317222	-10.1529386	-3.61466191
22.3	3793.59569	3820.60734	43.4974779	102.13712	-10.1451874	-3.60204135
22.3	3795.74395	3825.70478	42.9906014	101.957645	-10.13753	-3.58948637
22.4	3797.86689	3830.79327	42.4841031	101.778796	-10.1299662	-3.57699653
22.4	3799.96453	3835.87285	41.9779783	101.600567	-10.1224957	-3.56457138
22.5	3802.03687	3840.94356	41.4722224	101.422957	-10.1151183	-3.55221047
22.5	3804.08395	3846.00541	40.9668307	101.245961	-10.1078337	-3.53991336
22.6	3806.10578	3851.05845	40.4617986	101.069577	-10.1006417	-3.52767962
22.6	3808.10237	3856.1027	39.9571215	100.893801	-10.0935421	-3.51550882
22.7	3810.07375	3861.13819	39.4527948	100.718631	-10.0865345	-3.50340053
22.7	3812.01993	3866.16496	38.9488139	100.544064	-10.0796189	-3.49135431
22.8	3813.94093	3871.18303	38.4451741	100.370095	-10.072795	-3.47936976
22.8	3815.83677	3876.19243	37.941871	100.196723	-10.0660626	-3.46744644
22.9	3817.70745	3881.1932	37.4388999	100.023944	-10.0594214	-3.45558396

22.9	3819.55301	3886.18536	36.9362563	99.8517546	-10.0528712	-3.44378189
23	3821.37345	3891.16894	36.4339358	99.6801526	-10.0464119	-3.43203982
23	3823.16879	3896.14396	35.9319336	99.5091348	-10.0400432	-3.42035737
23.1	3824.93905	3901.11047	35.4302453	99.3386981	-10.0337649	-3.40873411
23.1	3826.68424	3906.06849	34.9288665	99.1688396	-10.0275768	-3.39716966
23.2	3828.40438	3911.01805	34.4277926	98.9995564	-10.0214788	-3.38566362
23.2	3830.09948	3915.95917	33.927019	98.8308456	-10.0154706	-3.37421561
23.3	3831.76955	3920.89188	33.4265414	98.6627044	-10.0095521	-3.36282522
23.3	3833.41462	3925.81622	32.9263553	98.4951297	-10.003723	-3.35149209
23.4	3835.03469	3930.73221	32.4264561	98.328119	-9.99798315	-3.34021582
23.4	3836.62979	3935.63987	31.9268395	98.1616692	-9.99233244	-3.32899604
23.5	3838.19991	3940.53925	31.427501	97.9957775	-9.98677064	-3.31783237
23.5	3839.74509	3945.43036	30.9284361	97.8304413	-9.9812976	-3.30672445
23.6	3841.26532	3950.31323	30.4296404	97.6656577	-9.97591313	-3.2956719
23.6	3842.76063	3955.18789	29.9311096	97.501424	-9.97061707	-3.28467436
23.7	3844.23103	3960.05437	29.4328391	97.3377374	-9.96540926	-3.27373147
23.7	3845.67652	3964.91269	28.9348246	97.1745953	-9.96028953	-3.26284286
23.8	3847.09713	3969.76288	28.4370618	97.0119949	-9.95525773	-3.25200818
23.8	3848.49287	3974.60497	27.9395461	96.8499335	-9.9503137	-3.24122707
23.9	3849.86374	3979.43899	27.4422732	96.6884086	-9.9454573	-3.23049919
23.9	3851.20976	3984.26496	26.9452388	96.5274174	-9.94068836	-3.21982418
24	3852.53094	3989.0829	26.4484385	96.3669573	-9.93600676	-3.2092017
24	3853.82729	3993.89286	25.9518678	96.2070257	-9.93141233	-3.19863141
24.1	3855.09882	3998.69484	25.4555226	96.04762	-9.92690496	-3.18811297
24.1	3856.34555	4003.48888	24.9593984	95.8887377	-9.92248449	-3.17764604
24.2	3857.56749	4008.275	24.4634908	95.7303762	-9.9181508	-3.16723029
24.2	3858.76464	4013.05323	23.9677956	95.572533	-9.91390375	-3.15686538
24.3	3859.93701	4017.8236	23.4723085	95.4152054	-9.90974322	-3.14655099
24.3	3861.08463	4022.58613	22.977025	95.2583911	-9.90566908	-3.13628678
24.4	3862.20749	4027.34084	22.481941	95.1020875	-9.90168122	-3.12607245
24.4	3863.3056	4032.08777	21.987052	94.9462921	-9.89777951	-3.11590766
24.5	3864.37898	4036.82693	21.4923538	94.7910025	-9.89396384	-3.10579209
24.5	3865.42764	4041.55835	20.9978421	94.6362162	-9.89023409	-3.09572544
24.6	3866.45158	4046.28206	20.5035126	94.4819308	-9.88659016	-3.08570738
24.6	3867.45081	4050.99809	20.009361	94.3281439	-9.88303194	-3.07573761
24.7	3868.42535	4055.70645	19.515383	94.1748532	-9.87955932	-3.06581582
24.7	3869.37519	4060.40717	19.0215744	94.0220561	-9.87617221	-3.0559417
24.8	3870.30035	4065.10027	18.5279309	93.8697503	-9.87287051	-3.04611494
24.8	3871.20084	4069.78579	18.0344482	93.7179336	-9.86965412	-3.03633526
24.9	3872.07666	4074.46374	17.541122	93.5666034	-9.86652295	-3.02660234
24.9	3872.92783	4079.13415	17.0479482	93.4157576	-9.86347692	-3.0169159
25	3873.75434	4083.79705	16.5549224	93.2653939	-9.86051593	-3.00727563
25	3874.55621	4088.45245	16.0620404	93.1155098	-9.8576399	-2.99768125
25.1	3875.33344	4093.10038	15.569298	92.9661032	-9.85484876	-2.98813247
25.1	3876.08605	4097.74086	15.0766908	92.8171717	-9.85214242	-2.97862899
25.2	3876.81403	4102.37393	14.5842148	92.6687132	-9.84952081	-2.96917054

25.2	3877.51739	4106.9996	14.0918656	92.5207254	-9.84698386	-2.95975683
25.3	3878.19614	4111.61789	13.599639	92.373206	-9.8445315	-2.95038758
25.3	3878.85029	4116.22883	13.1075308	92.2261529	-9.84216366	-2.94106252
25.4	3879.47983	4120.83244	12.6155368	92.0795638	-9.83988029	-2.93178136
25.4	3880.08479	4125.42875	12.1236528	91.9334366	-9.83768132	-2.92254384
25.5	3880.66515	4130.01777	11.6318744	91.7877691	-9.83556669	-2.91334967
25.5	3881.22093	4134.59953	11.1401976	91.6425592	-9.83353636	-2.9041986
25.6	3881.75213	4139.17406	10.6486181	91.4978047	-9.83159026	-2.89509034
25.6	3882.25876	4143.74138	10.1571317	91.3535034	-9.82972835	-2.88602465
25.7	3882.74082	4148.3015	9.66573415	91.2096534	-9.82795058	-2.87700125
25.7	3883.19831	4152.85445	9.1744213	91.0662524	-9.82625692	-2.86801988
25.8	3883.63124	4157.40026	8.68318894	90.9232984	-9.82464731	-2.85908029
25.8	3884.03962	4161.93895	8.19203285	90.7807893	-9.82312173	-2.85018221
25.9	3884.42344	4166.47053	7.70094884	90.638723	-9.82168014	-2.84132539
25.9	3884.78271	4170.99503	7.20993272	90.4970975	-9.82032251	-2.83250958
26	3885.11743	4175.51247	6.71898028	90.3559108	-9.81904881	-2.82373452
26	3885.42761	4180.02288	6.22808733	90.2151608	-9.81785901	-2.81499996
26.1	3885.71324	4184.52627	5.73724967	90.0748455	-9.81675309	-2.80630566
26.1	3885.97434	4189.02267	5.24646312	89.9349629	-9.81573103	-2.79765138
26.2	3886.2109	4193.51209	4.75572348	89.7955111	-9.81479281	-2.78903686
26.2	3886.42292	4197.99457	4.26502656	89.656488	-9.81393842	-2.78046186
26.3	3886.61041	4202.47012	3.77436817	89.5178917	-9.81316785	-2.77192615
26.3	3886.77337	4206.93876	3.28374411	89.3797202	-9.81248108	-2.76342948
26.4	3886.9118	4211.40051	2.79315021	89.2419716	-9.81187812	-2.75497162
26.4	3887.02571	4215.8554	2.30258226	89.104644	-9.81135896	-2.74655234
26.5	3887.11508	4220.30345	1.81203608	88.9677354	-9.81092359	-2.73817139
26.5	3887.17993	4224.74467	1.32150748	88.831244	-9.81057202	-2.72982856
26.6	3887.22026	4229.17908	0.83099226	88.6951678	-9.81030426	-2.7215236
26.6	3887.23605	4233.60672	0.34048625	88.559505	-9.81012032	-2.71325629
26.7	3887.22733	4238.0276	-0.15001476	88.4242537	-9.8100202	-2.70502641
26.7	3887.19407	4242.44173	-0.64051496	88.289412	-9.81000392	-2.69683373
26.8	3887.1363	4246.84914	-1.13101853	88.1549781	-9.8100715	-2.68867803
26.8	3887.05399	4251.24985	-1.62152968	88.0209502	-9.81022295	-2.68055908
26.9	3886.94717	4255.64389	-2.1120526	87.8873263	-9.8104583	-2.67247667
26.9	3886.81581	4260.03126	-2.60259147	87.7541048	-9.81077758	-2.66443057
27	3886.65993	4264.41199	-3.09315051	87.6212838	-9.81118081	-2.65642058
27	3886.47951	4268.7861	-3.58373392	87.4888614	-9.81166802	-2.64844648
27.1	3886.27457	4273.15361	-4.07434588	87.356836	-9.81223924	-2.64050804
27.1	3886.04509	4277.51455	-4.5649906	87.2252058	-9.81289453	-2.63260508
27.2	3885.79108	4281.86892	-5.0556723	87.0939689	-9.8136339	-2.62473736
27.2	3885.51254	4286.21675	-5.54639517	86.9631237	-9.81445741	-2.61690469
27.3	3885.20945	4290.55805	-6.03716343	86.8326683	-9.81536511	-2.60910685
27.3	3884.88182	4294.89286	-6.52798128	86.7026012	-9.81635703	-2.60134364
27.4	3884.52965	4299.22118	-7.01885294	86.5729204	-9.81743324	-2.59361486
27.4	3884.15294	4303.54304	-7.50978263	86.4436244	-9.81859378	-2.58592031
27.5	3883.75167	4307.85845	-8.00077456	86.3147114	-9.81983871	-2.57825978

Appendix A.3.3.5

27.5	3883.32585	4312.16744	-8.49183297	86.1861798	-9.82116809	-2.57063307
27.6	3882.87548	4316.47002	-8.98296207	86.0580278	-9.82258199	-2.56304
27.6	3882.40054	4320.76621	-9.47416609	85.9302537	-9.82408048	-2.55548035
27.7	3881.90104	4325.05604	-9.96544927	85.802856	-9.82566361	-2.54795393
27.7	3881.37697	4329.33951	-10.4568158	85.675833	-9.82733146	-2.54046055
27.8	3880.82833	4333.61665	-10.9482701	85.549183	-9.82908411	-2.53300003
27.8	3880.25511	4337.88748	-11.4398161	85.4229044	-9.83092163	-2.52557216
27.9	3879.65731	4342.15202	-11.9314583	85.2969956	-9.83284411	-2.51817676
27.9	3879.03492	4346.41028	-12.4232009	85.1714549	-9.83485162	-2.51081364
28	3878.38794	4350.66228	-12.9150481	85.0462808	-9.83694426	-2.50348261
28	3877.71635	4354.90804	-13.4070042	84.9214716	-9.83912211	-2.49618348
28.1	3877.02017	4359.14758	-13.8990735	84.7970258	-9.84138526	-2.48891608
28.1	3876.29938	4363.38092	-14.3912602	84.6729418	-9.84373382	-2.48168023
28.2	3875.55397	4367.60807	-14.8835686	84.549218	-9.84616787	-2.47447572
28.2	3874.78394	4371.82905	-15.376003	84.4258529	-9.84868752	-2.4673024
28.3	3873.98928	4376.04389	-15.8685676	84.3028449	-9.85129288	-2.46016008
28.3	3873.16998	4380.25259	-16.3612668	84.1801924	-9.85398405	-2.45304858
28.4	3872.32604	4384.45518	-16.8541049	84.057894	-9.85676114	-2.44596772
28.4	3871.45746	4388.65167	-17.3470861	83.9359482	-9.85962427	-2.43891734
28.5	3870.56421	4392.84209	-17.8402148	83.8143533	-9.86257355	-2.43189725
28.5	3869.64631	4397.02644	-18.3334952	83.6931079	-9.8656091	-2.42490728
28.6	3868.70373	4401.20475	-18.8269318	83.5722106	-9.86873104	-2.41794727
28.6	3867.73647	4405.37703	-19.3205287	83.4516597	-9.87193951	-2.41101704
28.7	3866.74452	4409.5433	-19.8142905	83.3314539	-9.87523462	-2.40411642
28.7	3865.72787	4413.70358	-20.3082213	83.2115917	-9.87861651	-2.39724524
28.8	3864.68652	4417.85788	-20.8023256	83.0920715	-9.88208531	-2.39040335
28.8	3863.62045	4422.00623	-21.2966076	82.972892	-9.88564117	-2.38359056
28.9	3862.52966	4426.14864	-21.7910718	82.8540516	-9.88928422	-2.37680673
28.9	3861.41414	4430.28512	-22.2857226	82.735549	-9.89301461	-2.37005168
29	3860.27388	4434.41569	-22.7805642	82.6173828	-9.89683249	-2.36332525
29	3859.10886	4438.54037	-23.2756011	82.4995514	-9.900738	-2.35662729
29.1	3857.91908	4442.65918	-23.7708376	82.3820535	-9.9047313	-2.34995763
29.1	3856.70453	4446.77213	-24.2662783	82.2648877	-9.90881255	-2.34331611
29.2	3855.46519	4450.87925	-24.7619274	82.1480526	-9.91298191	-2.33670258
29.2	3854.20106	4454.98053	-25.2577893	82.0315467	-9.91723953	-2.33011688
29.3	3852.91213	4459.07601	-25.7538686	81.9153688	-9.92158559	-2.32355886
29.3	3851.59838	4463.1657	-26.2501696	81.7995174	-9.92602026	-2.31702836
29.4	3850.2598	4467.24961	-26.7466968	81.6839911	-9.93054371	-2.31052522
29.4	3848.89639	4471.32776	-27.2434546	81.5687887	-9.93515611	-2.3040493
29.5	3847.50812	4475.40017	-27.7404475	81.4539086	-9.93985765	-2.29760044
29.5	3846.095	4479.46685	-28.2376799	81.3393497	-9.94464851	-2.29117849
29.6	3844.65699	4483.52782	-28.7351564	81.2251105	-9.94952887	-2.28478331
29.6	3843.19411	4487.58309	-29.2328813	81.1111898	-9.95449893	-2.27841475
29.7	3841.70632	4491.63269	-29.7308593	80.9975862	-9.95955887	-2.27207266
29.7	3840.19362	4495.67662	-30.2290947	80.8842983	-9.9647089	-2.26575689
29.8	3838.65599	4499.7149	-30.7275922	80.771325	-9.96994921	-2.2594673

Appendix A.3.3.5

29.8	3837.09343	4503.74755	-31.2263562	80.6586648	-9.97528001	-2.25320375
29.9	3835.50591	4507.77459	-31.7253913	80.5463165	-9.9807015	-2.24696609
29.9	3833.89343	4511.79602	-32.2247019	80.4342788	-9.98621389	-2.24075418
30	3832.25596	4515.81187	-32.7242928	80.3225504	-9.99181739	-2.23456788
30	3830.5935	4519.82215	-33.2241684	80.21113	-9.99751223	-2.22840704
30.1	3828.90604	4523.82687	-33.7243334	80.1000164	-10.0032986	-2.22227154
30.1	3827.19355	4527.82606	-34.2247922	79.9892084	-10.0091768	-2.21616123
30.2	3825.45602	4531.81971	-34.7255495	79.8787046	-10.015147	-2.21007597
30.2	3823.69343	4535.80786	-35.22661	79.7685038	-10.0212094	-2.20401563
30.3	3821.90578	4539.79052	-35.7279782	79.6586048	-10.0273642	-2.19798008
30.3	3820.09304	4543.7677	-36.2296588	79.5490063	-10.0336118	-2.19196917
30.4	3818.25521	4547.73941	-36.7316564	79.4397072	-10.0399523	-2.18598278
30.4	3816.39225	4551.70567	-37.2339757	79.3307062	-10.0463861	-2.18002077
30.5	3814.50416	4555.6665	-37.7366214	79.222002	-10.0529132	-2.17408301
30.5	3812.59093	4559.62191	-38.2395981	79.1135935	-10.0595341	-2.16816937
30.6	3810.65252	4563.57191	-38.7429106	79.0054796	-10.0662489	-2.16227972
30.6	3808.68894	4567.51652	-39.2465634	78.8976589	-10.0730579	-2.15641393
30.7	3806.70015	4571.45576	-39.7505615	78.7901303	-10.0799614	-2.15057187
30.7	3804.68614	4575.38964	-40.2549095	78.6828926	-10.0869596	-2.14475342
30.8	3802.6469	4579.31817	-40.7596121	78.5759447	-10.0940528	-2.13895845
30.8	3800.5824	4583.24137	-41.2646742	78.4692853	-10.1012414	-2.13318683
30.9	3798.49263	4587.15925	-41.7701005	78.3629134	-10.1085255	-2.12743843
30.9	3796.37758	4591.07182	-42.2758957	78.2568278	-10.1159054	-2.12171314
31	3794.23721	4594.97911	-42.7820648	78.1510272	-10.1233814	-2.11601083
31	3792.07151	4598.88112	-43.2886125	78.0455106	-10.1309539	-2.11033138
31.1	3789.88046	4602.77787	-43.7955437	77.9402769	-10.1386231	-2.10467466
31.1	3787.66405	4606.66938	-44.3028631	77.8353249	-10.1463893	-2.09904057
31.2	3785.42226	4610.55565	-44.8105758	77.7306534	-10.1542529	-2.09342896
31.2	3783.15505	4614.4367	-45.3186865	77.6262614	-10.162214	-2.08783973
31.3	3780.86242	4618.31255	-45.8272001	77.5221478	-10.1702731	-2.08227276
31.3	3778.54434	4622.1832	-46.3361217	77.4183114	-10.1784304	-2.07672794
31.4	3776.2008	4626.04868	-46.845456	77.3147512	-10.1866863	-2.07120513
31.4	3773.83176	4629.909	-47.355208	77.2114659	-10.1950411	-2.06570423
31.5	3771.43722	4633.76416	-47.8653828	77.1084547	-10.2034951	-2.06022513
31.5	3769.01714	4637.61419	-48.3759852	77.0057163	-10.2120486	-2.0547677
31.6	3766.57151	4641.4591	-48.8870203	76.9032497	-10.220702	-2.04933184
31.6	3764.10031	4645.29889	-49.3984931	76.8010538	-10.2294556	-2.04391742
31.7	3761.60351	4649.13359	-49.9104086	76.6991276	-10.2383097	-2.03852435
31.7	3759.08109	4652.96321	-50.4227718	76.59747	-10.2472648	-2.0331525
31.8	3756.53303	4656.78776	-50.9355879	76.4960799	-10.2563211	-2.02780177
31.8	3753.9593	4660.60726	-51.4488618	76.3949563	-10.265479	-2.02247205
31.9	3751.35989	4664.42171	-51.9625988	76.2940981	-10.2747389	-2.01716322
31.9	3748.73476	4668.23114	-52.4768038	76.1935044	-10.2841011	-2.01187518
32	3746.0839	4672.03554	-52.9914821	76.093174	-10.293566	-2.00660781
32	3743.40728	4675.83495	-53.5066388	75.9931059	-10.303134	-2.00136102
32.1	3740.70488	4679.62936	-54.0222791	75.8932992	-10.3128055	-1.9961347

32.1	3737.97667	4683.4188	-54.5384081	75.7937528	-10.3225807	-1.99092874
32.2	3735.22262	4687.20328	-55.0550311	75.6944656	-10.3324602	-1.98574303
32.2	3732.44272	4690.9828	-55.5721534	75.5954367	-10.3424443	-1.98057747
32.3	3729.63694	4694.75739	-56.08978	75.4966651	-10.3525334	-1.97543196
32.3	3726.80525	4698.52705	-56.6079164	75.3981498	-10.3627279	-1.97030638
32.4	3723.94762	4702.2918	-57.1265678	75.2998898	-10.3730282	-1.96520065
32.4	3721.06404	4706.05165	-57.6457396	75.2018841	-10.3834348	-1.96011466
32.5	3718.15447	4709.80661	-58.165437	75.1041316	-10.3939479	-1.95504831
32.5	3715.21888	4713.5567	-58.6856654	75.0066316	-10.4045681	-1.95000149
32.6	3712.25726	4717.30192	-59.2064302	74.9093829	-10.4152958	-1.94497411
32.6	3709.26957	4721.0423	-59.7277367	74.8123846	-10.4261314	-1.93996606
32.7	3706.25579	4724.77784	-60.2495905	74.7156357	-10.4370753	-1.93497725
32.7	3703.21588	4728.50856	-60.7719969	74.6191353	-10.448128	-1.93000759
32.8	3700.14982	4732.23446	-61.2949614	74.5228825	-10.4592899	-1.92505696
32.8	3697.05759	4735.95556	-61.8184895	74.4268762	-10.4705615	-1.92012528
32.9	3693.93915	4739.67188	-62.3425866	74.3311156	-10.4819432	-1.91521246
32.9	3690.79448	4743.38342	-62.8672584	74.2355997	-10.4934354	-1.91031838
33	3687.62354	4747.0902	-63.3925103	74.1403275	-10.5050387	-1.90544297
33	3684.42631	4750.79223	-63.918348	74.0452982	-10.5167536	-1.90058612
33.1	3681.20275	4754.48952	-64.444777	73.9505108	-10.5285804	-1.89574774
33.1	3677.95284	4758.18208	-64.971803	73.8559644	-10.5405196	-1.89092773
33.2	3674.67655	4761.86992	-65.4994316	73.7616581	-10.5525718	-1.88612602
33.2	3671.37385	4765.55307	-66.0276685	73.667591	-10.5647374	-1.88134249
33.3	3668.0447	4769.23152	-66.5565193	73.5737622	-10.577017	-1.87657707
33.3	3664.68908	4772.9053	-67.0859899	73.4801707	-10.589411	-1.87182966
33.4	3661.30695	4776.5744	-67.6160859	73.3868157	-10.6019199	-1.86710016
33.4	3657.89828	4780.23886	-68.1468131	73.2936962	-10.6145443	-1.8623885
33.5	3654.46304	4783.89866	-68.6781773	73.2008115	-10.6272846	-1.85769458
33.5	3651.0012	4787.55384	-69.2101844	73.1081606	-10.6401414	-1.85301831
33.6	3647.51273	4791.2044	-69.7428402	73.0157426	-10.6531152	-1.84835961
33.6	3643.99759	4794.85034	-70.2761505	72.9235567	-10.6662066	-1.84371838
33.7	3640.45575	4798.49169	-70.8101213	72.831602	-10.6794161	-1.83909454
33.7	3636.88717	4802.12846	-71.3447585	72.7398776	-10.6927441	-1.834488
33.8	3633.29183	4805.76065	-71.8800681	72.6483826	-10.7061914	-1.82989869
33.8	3629.66969	4809.38828	-72.416056	72.5571163	-10.7197584	-1.8253265
33.9	3626.02071	4813.01135	-72.9527283	72.4660777	-10.7334457	-1.82077136
33.9	3622.34486	4816.62989	-73.490091	72.3752661	-10.7472538	-1.81623318
34	3618.64211	4820.2439	-74.0281501	72.2846805	-10.7611834	-1.81171189
34	3614.91242	4823.85339	-74.5669119	72.1943201	-10.775235	-1.80720738
34.1	3611.15575	4827.45837	-75.1063823	72.1041841	-10.7894093	-1.80271959
34.1	3607.37207	4831.05886	-75.6465677	72.0142717	-10.8037067	-1.79824843
34.2	3603.56135	4834.65487	-76.1874741	71.924582	-10.8181279	-1.79379382
34.2	3599.72354	4838.2464	-76.7291078	71.8351142	-10.8326736	-1.78935568
34.3	3595.85861	4841.83347	-77.271475	71.7458676	-10.8473442	-1.78493392
34.3	3591.96652	4845.41609	-77.814582	71.6568411	-10.8621405	-1.78052847
34.4	3588.04724	4848.99427	-78.3584351	71.5680342	-10.8770631	-1.77613924

34.4	3584.10073	4852.56802	-78.9030408	71.4794459	-10.8921125	-1.77176616
34.5	3580.12694	4856.13735	-79.4484052	71.3910754	-10.9072895	-1.76740915
34.5	3576.12585	4859.70228	-79.994535	71.302922	-10.9225946	-1.76306813
34.6	3572.09741	4863.26281	-80.5414364	71.2149848	-10.9380286	-1.75874302
34.6	3568.04159	4866.81895	-81.089116	71.1272632	-10.953592	-1.75443375
34.7	3563.95834	4870.37072	-81.6375803	71.0397561	-10.9692856	-1.75014023
34.7	3559.84762	4873.91812	-82.1868358	70.952463	-10.98511	-1.74586239
34.8	3555.7094	4877.46117	-82.7368891	70.865383	-11.001066	-1.74160016
34.8	3551.54364	4880.99988	-83.2877468	70.7785153	-11.0171541	-1.73735345
34.9	3547.35029	4884.53426	-83.8394155	70.6918592	-11.033375	-1.73312221
34.9	3543.12931	4888.06431	-84.391902	70.6054139	-11.0497296	-1.72890634
35	3538.88067	4891.59006	-84.9452129	70.5191786	-11.0662184	-1.72470577
35	3534.60431	4895.1115	-85.4993551	70.4331526	-11.0828423	-1.72052044
35.1	3530.30021	4898.62865	-86.0543351	70.3473351	-11.0996018	-1.71635026
35.1	3525.96831	4902.14152	-86.61016	70.2617253	-11.1164978	-1.71219517
35.2	3521.60858	4905.65013	-87.1668366	70.1763226	-11.133531	-1.7080551
35.2	3517.22097	4909.15447	-87.7243717	70.0911261	-11.1507021	-1.70392996
35.3	3512.80543	4912.65456	-88.2827723	70.0061351	-11.1680119	-1.69981969
35.3	3508.36193	4916.15042	-88.8420453	69.9213489	-11.1854611	-1.69572422
35.4	3503.89042	4919.64205	-89.4021979	69.8367667	-11.2030506	-1.69164348
35.4	3499.39086	4923.12946	-89.9632369	69.7523878	-11.220781	-1.6875774
35.5	3494.86319	4926.61266	-90.5251696	69.6682115	-11.2386532	-1.6835259
35.5	3490.30738	4930.09166	-91.088003	69.5842371	-11.2566679	-1.67948892
35.6	3485.72339	4933.56647	-91.6517443	69.5004638	-11.274826	-1.67546639
35.6	3481.11116	4937.03711	-92.2164007	69.4168909	-11.2931283	-1.67145824
35.7	3476.47064	4940.50357	-92.7819795	69.3335177	-11.3115755	-1.6674644
35.7	3471.8018	4943.96588	-93.3484879	69.2503434	-11.3301686	-1.6634848
35.8	3467.10459	4947.42404	-93.9159333	69.1673674	-11.3489083	-1.65951938
35.8	3462.37895	4950.87807	-94.4843231	69.084589	-11.3677954	-1.65556807
35.9	3457.62484	4954.32796	-95.0536646	69.0020075	-11.3868309	-1.6516308
35.9	3452.84222	4957.77374	-95.6239654	68.9196221	-11.4060156	-1.64770751
36	3448.03103	4961.2154	-96.1952329	68.8374322	-11.4253504	-1.64379813
36	3443.19123	4964.65297	-96.7674747	68.7554371	-11.444836	-1.63990259
36.1	3438.32276	4968.08645	-97.3406984	68.673636	-11.4644735	-1.63602084
36.1	3433.42558	4971.51584	-97.9149116	68.5920284	-11.4842637	-1.63215279
36.2	3428.49963	4974.94117	-98.490122	68.5106135	-11.5042075	-1.6282984
36.2	3423.54488	4978.36244	-99.0663372	68.4293906	-11.5243058	-1.6244576
36.3	3418.56125	4981.77965	-99.6435652	68.3483591	-11.5445596	-1.62063032
36.3	3413.54872	4985.19283	-100.221814	68.2675183	-11.5649697	-1.6168165
36.4	3408.50721	4988.60197	-100.801091	68.1868675	-11.5855372	-1.61301608
36.4	3403.43669	4992.00709	-101.381404	68.106406	-11.6062629	-1.60922899
36.5	3398.3371	4995.40819	-101.962761	68.0261333	-11.6271478	-1.60545517
36.5	3393.20839	4998.8053	-102.545171	67.9460485	-11.648193	-1.60169457
36.6	3388.0505	5002.1984	-103.128641	67.8661512	-11.6693993	-1.59794711
36.6	3382.86338	5005.58753	-103.713179	67.7864405	-11.6907678	-1.59421274
36.7	3377.64697	5008.97267	-104.298794	67.706916	-11.7122995	-1.5904914

36.7	3372.40123	5012.35385	-104.885494	67.6275768	-11.7339953	-1.58678303
36.8	3367.1261	5015.73108	-105.473287	67.5484224	-11.7558564	-1.58308757
36.8	3361.82152	5019.10435	-106.062181	67.4694522	-11.7778836	-1.57940495
36.9	3356.48743	5022.47369	-106.652185	67.3906654	-11.8000782	-1.57573512
36.9	3351.12379	5025.8391	-107.243307	67.3120615	-11.822441	-1.57207802
37	3345.73053	5029.20058	-107.835555	67.2336398	-11.8449733	-1.56843359
37	3340.3076	5032.55816	-108.428939	67.1553998	-11.867676	-1.56480177
37.1	3334.85494	5035.91183	-109.023467	67.0773406	-11.8905502	-1.56118251
37.1	3329.37249	5039.26161	-109.619147	66.9994618	-11.9135971	-1.55757574
37.2	3323.8602	5042.6075	-110.215988	66.9217628	-11.9368178	-1.55398142
37.2	3318.31801	5045.94952	-110.813998	66.8442428	-11.9602133	-1.55039947
37.3	3312.74585	5049.28767	-111.413187	66.7669013	-11.9837848	-1.54682986
37.3	3307.14367	5052.62196	-112.013564	66.6897377	-12.0075334	-1.54327251
37.4	3301.51141	5055.95241	-112.615137	66.6127513	-12.0314604	-1.53972737
37.4	3295.84901	5059.27901	-113.217915	66.5359416	-12.0555668	-1.5361944
37.5	3290.1564	5062.60179	-113.821908	66.4593079	-12.0798538	-1.53267352
37.5	3284.43353	5065.92074	-114.427124	66.3828497	-12.1043227	-1.5291647
37.6	3278.68034	5069.23588	-115.033573	66.3065663	-12.1289746	-1.52566786
37.6	3272.89676	5072.54721	-115.641264	66.2304571	-12.1538107	-1.52218297
37.7	3267.08272	5075.85475	-116.250205	66.1545216	-12.1788323	-1.51870995
37.7	3261.23818	5079.15849	-116.860407	66.0787592	-12.2040406	-1.51524877
37.8	3255.36305	5082.45846	-117.471879	66.0031692	-12.2294369	-1.51179937
37.8	3249.45729	5085.75466	-118.08463	65.9277512	-12.2550224	-1.50836169
37.8	3243.52082	5089.0471	-118.69867	65.8525044	-12.2807985	-1.50493568
37.9	3237.55358	5092.33578	-119.314008	65.7774283	-12.3067663	-1.50152128
37.9	3231.55551	5095.62072	-119.930655	65.7025224	-12.3329272	-1.49811846
38	3225.52653	5098.90192	-120.548619	65.627786	-12.3592826	-1.49472715
38	3219.46659	5102.1794	-121.167911	65.5532187	-12.3858337	-1.49134729
38.1	3213.37561	5105.45315	-121.78854	65.4788197	-12.4125819	-1.48797885
38.1	3207.25353	5108.7232	-122.410516	65.4045886	-12.4395286	-1.48462177
38.2	3201.10028	5111.98954	-123.03385	65.3305248	-12.4666752	-1.481276
38.2	3194.91579	5115.25219	-123.658551	65.2566278	-12.4940229	-1.47794148
38.3	3188.69999	5118.51115	-124.28463	65.1828968	-12.5215734	-1.47461818
38.3	3182.45282	5121.76643	-124.912096	65.1093315	-12.5493278	-1.47130603
38.4	3176.1742	5125.01804	-125.54096	65.0359313	-12.5772878	-1.46800499
38.4	3169.86406	5128.26599	-126.171233	64.9626955	-12.6054547	-1.464715
38.5	3163.52234	5131.51029	-126.802925	64.8896237	-12.63383	-1.46143603
38.5	3157.14895	5134.75095	-127.436045	64.8167153	-12.6624151	-1.45816801
38.6	3150.74384	5137.98796	-128.070606	64.7439698	-12.6912117	-1.45491091
38.6	3144.30691	5141.22135	-128.706617	64.6713866	-12.7202212	-1.45166467
38.7	3137.83812	5144.45112	-129.344089	64.5989651	-12.749445	-1.44842925
38.7	3131.33737	5147.67727	-129.983034	64.5267049	-12.7788848	-1.44520459
38.8	3124.80459	5150.89982	-130.623461	64.4546053	-12.8085422	-1.44199065
38.8	3118.23972	5154.11878	-131.265382	64.382666	-12.8384186	-1.43878738
38.9	3111.64267	5157.33414	-131.908807	64.3108862	-12.8685158	-1.43559474
38.9	3105.01337	5160.54592	-132.553749	64.2392656	-12.8988352	-1.43241268

Appendix A.3.3.5

39	3098.35174	5163.75414	-133.200218	64.1678035	-12.9293786	-1.42924115
39	3091.65771	5166.95878	-133.848225	64.0964995	-12.9601475	-1.42608011
39.1	3084.9312	5170.15987	-134.497783	64.0253531	-12.9911436	-1.4229295
39.1	3078.17213	5173.35741	-135.148901	63.9543636	-13.0223687	-1.41978929
39.2	3071.38042	5176.55141	-135.801592	63.8835306	-13.0538244	-1.41665942
39.2	3064.55599	5179.74188	-136.455868	63.8128536	-13.0855124	-1.41353986
39.3	3057.69876	5182.92882	-137.11174	63.7423321	-13.1174345	-1.41043056
39.3	3050.80865	5186.11224	-137.769219	63.6719655	-13.1495923	-1.40733147
39.4	3043.88559	5189.29215	-138.428319	63.6017534	-13.1819878	-1.40424255
39.4	3036.92949	5192.46856	-139.08905	63.5316952	-13.2146226	-1.40116375
39.5	3029.94026	5195.64148	-139.751425	63.4617905	-13.2474987	-1.39809503
39.5	3022.91783	5198.81091	-140.415456	63.3920386	-13.2806177	-1.39503635
39.6	3015.8621	5201.97685	-141.081155	63.3224393	-13.3139816	-1.39198766
39.6	3008.77301	5205.13933	-141.748534	63.2529918	-13.3475923	-1.38894892
39.7	3001.65046	5208.29834	-142.417607	63.1836958	-13.3814515	-1.38592009
39.7	2994.49436	5211.4539	-143.088385	63.1145508	-13.4155614	-1.38290112
39.8	2987.30464	5214.606	-143.760881	63.0455562	-13.4499236	-1.37989197
39.8	2980.08119	5217.75466	-144.435108	62.9767115	-13.4845403	-1.3768926
39.9	2972.82395	5220.89989	-145.111079	62.9080164	-13.5194134	-1.37390296
39.9	2965.53282	5224.0417	-145.788806	62.8394702	-13.5545449	-1.37092302
40	2958.2077	5227.18008	-146.468303	62.7710726	-13.5899368	-1.36795273
40	2950.84852	5230.31505	-147.149582	62.702823	-13.6255911	-1.36499205
40.1	2943.45518	5233.44661	-147.832658	62.6347209	-13.66151	-1.36204094
40.1	2936.02759	5236.57478	-148.517543	62.566766	-13.6976954	-1.35909936
40.2	2928.56566	5239.69956	-149.20425	62.4989576	-13.7341496	-1.35616727
40.2	2921.0693	5242.82096	-149.892794	62.4312954	-13.7708746	-1.35324462
40.3	2913.53841	5245.93898	-150.583188	62.3637788	-13.8078725	-1.35033138
40.3	2905.97291	5249.05363	-151.275445	62.2964074	-13.8451457	-1.3474275
40.4	2898.3727	5252.16492	-151.96958	62.2291808	-13.8826962	-1.34453295
40.4	2890.73768	5255.27286	-152.665606	62.1620984	-13.9205263	-1.34164769
40.5	2883.06775	5258.37745	-153.363538	62.0951598	-13.9586382	-1.33877168
40.5	2875.36284	5261.4787	-154.06339	62.0283646	-13.9970343	-1.33590487
40.6	2867.62282	5264.57662	-154.765175	61.9617122	-14.0357168	-1.33304723
40.6	2859.84762	5267.67121	-155.46891	61.8952023	-14.0746881	-1.33019872
40.7	2852.03712	5270.76249	-156.174607	61.8288343	-14.1139504	-1.3273593
40.7	2844.19124	5273.85045	-156.882283	61.7626079	-14.1535063	-1.32452893
40.8	2836.30987	5276.93511	-157.591951	61.6965225	-14.1933581	-1.32170757
40.8	2828.39291	5280.01648	-158.303626	61.6305777	-14.2335082	-1.31889519
40.9	2820.44026	5283.09455	-159.017324	61.5647731	-14.2739591	-1.31609175
40.9	2812.45181	5286.16934	-159.73306	61.4991083	-14.3147133	-1.31329721
41	2804.42748	5289.24086	-160.450848	61.4335827	-14.3557733	-1.31051153
41	2796.36714	5292.3091	-161.170705	61.368196	-14.3971417	-1.30773467
41.1	2788.27071	5295.37409	-161.892646	61.3029476	-14.438821	-1.30496661
41.1	2780.13806	5298.43582	-162.616687	61.2378373	-14.4808138	-1.30220729
41.2	2771.9691	5301.4943	-163.342843	61.1728644	-14.5231228	-1.29945669
41.2	2763.76373	5304.54954	-164.071131	61.1080287	-14.5657507	-1.29671477

Appendix A.3.3.5

41.3	2755.52182	5307.60154	-164.801566	61.0433296	-14.6087001	-1.29398148
41.3	2747.24328	5310.65032	-165.534164	60.9787668	-14.6519737	-1.2912568
41.4	2738.928	5313.69588	-166.268943	60.9143398	-14.6955744	-1.2885407
41.4	2730.57586	5316.73822	-167.005918	60.8500481	-14.7395049	-1.28583312
41.5	2722.18676	5319.77735	-167.745107	60.7858914	-14.7837681	-1.28313404
41.5	2713.76058	5322.81328	-168.486525	60.7218692	-14.8283667	-1.28044343
41.6	2705.29721	5325.84602	-169.23019	60.6579812	-14.8733037	-1.27776124
41.6	2696.79654	5328.87558	-169.976119	60.5942268	-14.918582	-1.27508744
41.7	2688.25845	5331.90195	-170.72433	60.5306057	-14.9642046	-1.272422
41.7	2679.68283	5334.92514	-171.474838	60.4671174	-15.0101744	-1.26976488
41.8	2671.06957	5337.94517	-172.227663	60.4037616	-15.0564945	-1.26711605
41.8	2662.41854	5340.96204	-172.982822	60.3405379	-15.103168	-1.26447547
41.9	2653.72963	5343.97576	-173.740331	60.2774457	-15.1501979	-1.26184312
41.9	2645.00272	5346.98632	-174.500211	60.2144848	-15.1975873	-1.25921894
42	2636.23769	5349.99375	-175.262478	60.1516546	-15.2453395	-1.25660292
42	2627.43442	5352.99804	-176.027151	60.0889549	-15.2934577	-1.25399502
42.1	2618.59279	5355.9992	-176.794248	60.0263851	-15.341945	-1.2513952
42.1	2609.71268	5358.99725	-177.563788	59.9639449	-15.3908049	-1.24880343
42.2	2600.79396	5361.99217	-178.33579	59.901634	-15.4400405	-1.24621968
42.2	2591.83651	5364.98399	-179.110273	59.8394518	-15.4896553	-1.24364392
42.3	2582.8402	5367.9727	-179.887256	59.777398	-15.5396527	-1.24107611
42.3	2573.80491	5370.95832	-180.666757	59.7154721	-15.5900361	-1.23851621
42.4	2564.73052	5373.94085	-181.448798	59.6536739	-15.640809	-1.23596421
42.4	2555.61689	5376.9203	-182.233397	59.5920029	-15.691975	-1.23342006
42.5	2546.46389	5379.89667	-183.020573	59.5304587	-15.7435375	-1.23088373
42.5	2537.2714	5382.86996	-183.810348	59.469041	-15.7955003	-1.22835519
42.6	2528.03928	5385.8402	-184.602742	59.4077493	-15.8478669	-1.22583441
42.6	2518.7674	5388.80737	-185.397774	59.3465832	-15.9006412	-1.22332136
42.7	2509.45564	5391.7715	-186.195465	59.2855424	-15.9538267	-1.220816
42.7	2500.10384	5394.73258	-186.995837	59.2246265	-16.0074274	-1.21831831
42.8	2490.71189	5397.69062	-187.798909	59.1638351	-16.061447	-1.21582826
42.8	2481.27964	5400.64563	-188.604703	59.1031678	-16.1158894	-1.2133458
42.9	2471.80696	5403.5976	-189.413241	59.0426242	-16.1707587	-1.21087092
42.9	2462.2937	5406.54656	-190.224544	58.9822041	-16.2260586	-1.20840357
43	2452.73974	5409.49251	-191.038634	58.9219069	-16.2817934	-1.20594374
43	2443.14492	5412.43544	-191.855532	58.8617323	-16.337967	-1.20349139
43.1	2433.5091	5415.37538	-192.675261	58.80168	-16.3945837	-1.20104649
43.1	2423.83216	5418.31232	-193.497844	58.7417495	-16.4516475	-1.198609
43.2	2414.11393	5421.24626	-194.323302	58.6819406	-16.5091627	-1.19617891
43.2	2404.35427	5424.17723	-195.151659	58.6222528	-16.5671336	-1.19375618
43.3	2394.55305	5427.10521	-195.982937	58.5626857	-16.6255646	-1.19134077
43.3	2384.7101	5430.03023	-196.81716	58.5032391	-16.68446	-1.18893267
43.4	2374.82529	5432.95227	-197.654351	58.4439125	-16.7438242	-1.18653184
43.4	2364.89847	5435.87136	-198.494534	58.3847056	-16.8036619	-1.18413825
43.5	2354.92947	5438.78749	-199.337733	58.325618	-16.8639775	-1.18175188
43.5	2344.91816	5441.70068	-200.183972	58.2666494	-16.9247757	-1.17937269

Appendix A.3.3.5

43.6	2334.86437	5444.61092	-201.033275	58.2077993	-16.9860611	-1.17700065
43.6	2324.76796	5447.51823	-201.885667	58.1490675	-17.0478385	-1.17463574
43.7	2314.62876	5450.4226	-202.741172	58.0904536	-17.1101128	-1.17227793
43.7	2304.44662	5453.32406	-203.599817	58.0319573	-17.1728886	-1.1699272
43.8	2294.22139	5456.22259	-204.461625	57.9735781	-17.236171	-1.1675835
43.8	2283.95289	5459.11821	-205.326624	57.9153158	-17.299965	-1.16524682
43.9	2273.64098	5462.01092	-206.194837	57.8571699	-17.3642756	-1.16291712
43.9	2263.28549	5464.90073	-207.066293	57.7991402	-17.4291079	-1.16059438
44	2252.88625	5467.78765	-207.941016	57.7412263	-17.4944671	-1.15827858
44	2242.4431	5470.67168	-208.819034	57.6834278	-17.5603584	-1.15596967
44.1	2231.95588	5473.55282	-209.700374	57.6257444	-17.6267872	-1.15366765
44.1	2221.42442	5476.43109	-210.585061	57.5681758	-17.6937588	-1.15137247
44.2	2210.84854	5479.30648	-211.473125	57.5107216	-17.7612787	-1.14908411
44.2	2200.22808	5482.179	-212.364593	57.4533814	-17.8293525	-1.14680255
44.3	2189.56287	5485.04867	-213.259492	57.3961551	-17.8979856	-1.14452776
44.3	2178.85273	5487.91548	-214.157851	57.3390421	-17.9671839	-1.1422597
44.4	2168.09749	5490.77944	-215.059699	57.2820422	-18.036953	-1.13999837
44.4	2157.29697	5493.64055	-215.965064	57.225155	-18.1072987	-1.13774372
44.5	2146.451	5496.49883	-216.873975	57.1683802	-18.178227	-1.13549573
44.5	2135.5594	5499.35427	-217.786463	57.1117175	-18.2497438	-1.13325438
44.6	2124.62198	5502.20689	-218.702555	57.0551665	-18.3218553	-1.13101964
44.6	2113.63857	5505.05669	-219.622284	56.9987269	-18.3945674	-1.12879148
44.7	2102.60898	5507.90367	-220.545678	56.9423984	-18.4678865	-1.12656988
44.7	2091.53302	5510.74783	-221.472769	56.8861807	-18.5418189	-1.12435482
44.8	2080.41051	5513.5892	-222.403588	56.8300734	-18.6163709	-1.12214626
44.8	2069.24127	5516.42776	-223.338165	56.7740762	-18.691549	-1.11994418
44.9	2058.0251	5519.26353	-224.276533	56.7181887	-18.7673598	-1.11774856
44.9	2046.7618	5522.09651	-225.218723	56.6624108	-18.8438099	-1.11555937
45	2035.4512	5524.92671	-226.164769	56.6067419	-18.9209061	-1.11337658
45	2024.09309	5527.75413	-227.114702	56.5511819	-18.9986551	-1.11120018
45.1	2012.68728	5530.57878	-228.068555	56.4957304	-19.077064	-1.10903013
45.1	2001.23357	5533.40066	-229.026362	56.4403871	-19.1561398	-1.10686642
45.2	1989.73175	5536.21978	-229.988156	56.3851516	-19.2358895	-1.10470901
45.2	1978.18164	5539.03614	-230.953972	56.3300237	-19.3163204	-1.10255789
45.3	1966.58302	5541.84975	-231.923844	56.2750031	-19.3974398	-1.10041302
45.3	1954.9357	5544.66062	-232.897807	56.2200894	-19.479255	-1.09827439
45.4	1943.23946	5547.46875	-233.875896	56.1652823	-19.5617738	-1.09614197
45.4	1931.49409	5550.27414	-234.858146	56.1105815	-19.6450035	-1.09401574
45.5	1919.6994	5553.0768	-235.844593	56.0559867	-19.7289521	-1.09189566
45.5	1907.85516	5555.87674	-236.835275	56.0014976	-19.8136272	-1.08978173
45.6	1895.96116	5558.67396	-237.830227	55.9471139	-19.8990369	-1.08767391
45.6	1884.01719	5561.46847	-238.829486	55.8928353	-19.9851893	-1.08557218

Appendix A.3.3.7.4 Airlock Trade Study

Airlock Options:

Assumptions: 4 spacecraft
airlocks are complex structures for cost estimation

Airlock Designs:

Capacity	Height(m)	Volume(cu m)	Mass(kg)	Cost($M94) NonRec	Recurring
1 person	2.3	1.03	141.5	11.4	3.4
2 person	2.3	1.64	580	27.3	10.3

Procurement # of 1 P	# of 2 P	Airlock mass/mission 1	Mass(kg) mass/mission2	Cost($M94) Nonrec	Rec	Total
4	1	141.5	721.5	38.7	10.2	48.9
4	2	141.5	721.5	38.7	20.5	59.2
0	4	580	580	27.3	30.9	58.2

Appendix A.3.3.7.5 RMS Trade Study

For a circular thin-wall beam, I=PI*InnerRadius^3*thickness

Rinner (m)	thick (m)	I (m^4)	Rinner (m)	thick (m)	I (m^4)	Rinner (m)	thick (m)	I (m^4)
0.02	0.005	1.257E-07	0.05	0.005	1.9635E-06	0.1	0.005	1.5708E-05
0.02	0.01	2.513E-07	0.05	0.01	3.92699E-06	0.1	0.01	3.14159E-05
0.02	0.015	3.770E-07	0.05	0.015	5.89049E-06	0.1	0.015	4.71239E-05
0.02	0.02	5.027E-07	0.05	0.02	7.85398E-06	0.1	0.02	6.28319E-05
0.02	0.025	6.283E-07	0.05	0.025	9.81748E-06	0.1	0.025	7.85398E-05
0.02	0.03	7.540E-07	0.05	0.03	1.1781E-05	0.1	0.03	9.42478E-05
0.02	0.035	8.796E-07	0.05	0.035	1.37445E-05	0.1	0.035	0.000109956
0.02	0.04	1.005E-06	0.05	0.04	1.5708E-05	0.1	0.04	0.000125664
0.02	0.045	1.131E-06	0.05	0.045	1.76715E-05	0.1	0.045	0.000141372
0.02	0.05	1.257E-06	0.05	0.05	1.9635E-05	0.1	0.05	0.00015708
Rinner (m)	thick (m)	I (m^4)	Rinner (m)	thick (m)	I (m^4)	Rinner (m)	thick (m)	I (m^4)
0.2	0.005	0.000125664	0.3	0.005	0.000424115	0.4	0.005	0.00100531
0.2	0.01	0.000251327	0.3	0.01	0.00084823	0.4	0.01	0.002010619
0.2	0.015	0.000376991	0.3	0.015	0.001272345	0.4	0.015	0.003015929
0.2	0.02	0.000502655	0.3	0.02	0.00169646	0.4	0.02	0.004021239
0.2	0.025	0.000628319	0.3	0.025	0.002120575	0.4	0.025	0.005026548
0.2	0.03	0.000753982	0.3	0.03	0.00254469	0.4	0.03	0.006031858
0.2	0.035	0.000879646	0.3	0.035	0.002968805	0.4	0.035	0.007037168
0.2	0.04	0.00100531	0.3	0.04	0.00339292	0.4	0.04	0.008042477
0.2	0.045	0.001130973	0.3	0.045	0.003817035	0.4	0.045	0.009047787
0.2	0.05	0.001256637	0.3	0.05	0.00424115	0.4	0.05	0.010053096
Rinner (m)	thick (m)	I (m^4)	Rinner (m)	thick (m)	I (m^4)	Rinner (m)	thick (m)	I (m^4)
0.5	0.005	0.001963495	0.6	0.005	0.00339292	0.7	0.005	0.005387831
0.5	0.01	0.003926991	0.6	0.01	0.00678584	0.7	0.01	0.010775663
0.5	0.015	0.005890486	0.6	0.015	0.01017876	0.7	0.015	0.016163494
0.5	0.02	0.007853982	0.6	0.02	0.01357168	0.7	0.02	0.021551326
0.5	0.025	0.009817477	0.6	0.025	0.0169646	0.7	0.025	0.026939157
0.5	0.03	0.011780972	0.6	0.03	0.02035752	0.7	0.03	0.032326988
0.5	0.035	0.013744468	0.6	0.035	0.02375044	0.7	0.035	0.03771482
0.5	0.04	0.015707963	0.6	0.04	0.027143361	0.7	0.04	0.043102651
0.5	0.045	0.017671459	0.6	0.045	0.030536281	0.7	0.045	0.048490483
0.5	0.05	0.019634954	0.6	0.05	0.033929201	0.7	0.05	0.053878314
Rinner (m)	thick (m)	I (m^4)	Rinner (m)	thick (m)	I (m^4)	Rinner (m)	thick (m)	I (m^4)
0.8	0.005	0.008042477	0.9	0.005	0.011451105	1	0.005	0.015707963
0.8	0.01	0.016084954	0.9	0.01	0.02290221	1	0.01	0.031415927
0.8	0.015	0.024127432	0.9	0.015	0.034353316	1	0.015	0.04712389
0.8	0.02	0.032169909	0.9	0.02	0.045804421	1	0.02	0.062831853
0.8	0.025	0.040212386	0.9	0.025	0.057255526	1	0.025	0.078539816
0.8	0.03	0.048254863	0.9	0.03	0.068706631	1	0.03	0.09424778
0.8	0.035	0.05629734	0.9	0.035	0.080157737	1	0.035	0.109955743
0.8	0.04	0.064339818	0.9	0.04	0.091608842	1	0.04	0.125663706
0.8	0.045	0.072382295	0.9	0.045	0.103059947	1	0.045	0.141371669
0.8	0.05	0.080424772	0.9	0.05	0.114511052	1	0.05	0.157079633

Mass of arms:	568
Mass of Motors	568
Mass of End Effector:	142
Total Mass	1278
Total Volume	15.8367686

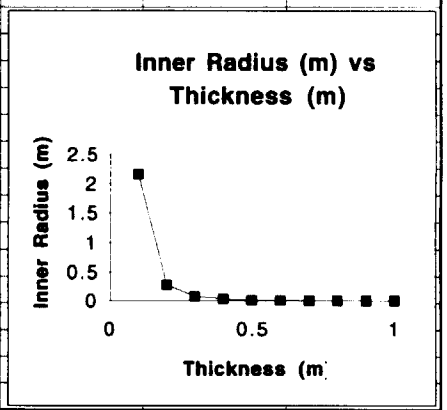

Gr/Ep	dens=1490	I=.0068
Rinner (m)	thick (m)	Mass Gr/Ep(kg)
0.3	0.08016693	2552.389399
0.35	0.05048413	1773.505596
0.4	0.03382043	1320.041961
0.45	0.02375317	1027.102011
0.5	0.01731606	824.5957038
0.55	0.01300981	677.8070864
0.6	0.01002087	567.5894177
0.65	0.00788168	482.5291657
0.7	0.00631052	415.4151066
0.75	0.00513068	361.4811043
0.8	0.00422755	317.4615931

densities in kg/m^3		Inertias in m^4							0.85	0.00352454	281.0520761
Aluminum	dens=2800	I=.0145	Beryllium	dens=1850	I=.0035	Boron/Epoxy	dens=2010	I=.005	Gr/Ep	dens=1490	I=.0068
Rinner (m)	thick (m)	Mass Al (kg)	Rinner (m)	thick (m)	Mass Be (kg)	Rinner (m)	thick (m)	Mass Bo/Ep (k	Rinner (m)	thick (m)	Mass Gr/Ep (kg)
0.02	57.6936669	292998359	0.02	139.260575	1127464031	0.02	198.943679	2499732466	0.02	270.563403	3427192102
0.05	3.69239468	1231769.79	0.05	8.91267681	4668566.59	0.05	12.7323954	10317245.9	0.05	17.3160578	14116759.82
0.1	0.46154933	26858.903	0.1	1.1140846	85086.978	0.1	1.59154943	180050.718	0.1	2.16450723	239571.8721
0.2	0.05769367	2322.79536	0.2	0.13926058	4364.64028	0.2	0.19894368	7524.22997	0.2	0.2705634	8492.685502
0.3	0.01709442	927.927165	0.3	0.04126239	1537.84222	0.3	0.05894628	2452.74447	0.3	0.08016693	2552.389399
0.4	0.00721171	512.074927	0.4	0.01740757	826.986567	0.4	0.02486796	1295.30047	0.4	0.03382043	1320.041961
0.5	0.00369239	325.99929	0.5	0.00891268	522.616767	0.5	0.0127324	814.236846	0.5	0.01731606	824.5957038
0.6	0.0021368	225.957195	0.6	0.0051578	361.268368	0.6	0.00736828	561.761632	0.6	0.01002087	567.5894177
0.7	0.00134562	165.873564	0.7	0.00324806	264.898868	0.7	0.00464009	411.56364	0.7	0.00631052	415.4151066
0.8	0.00090146	126.946483	0.8	0.00217595	202.618931	0.8	0.00310849	314.672664	0.8	0.00422755	317.4615931
0.9	0.00063313	100.282174	0.9	0.00152824	160.012282	0.9	0.0021832	248.449124	0.9	0.00296915	250.585506
1	0.00046155	81.2187389	1	0.00111408	129.572137	1	0.00159155	201.159951	1	0.00216451	202.8593079
Gr/Ep	dens=1490	I=.0068	Magnesium	dens=1770	I=.0231	Steel Ph15-7 M	dens=7600	I=.0052	Titanium	dens=4430	I=.0094
Rinner (m)	thick (m)	Mass Gr/Ep (kg	Rinner (m)	thick (m)	Mass Mg (kg)	Rinner (m)	thick (m)	Mass Steel (kg	Rinner (m)	thick (m)	Mass Ti (kg)
0.02	270.563403	3427192102	0.02	919.119796	4.6977E+10	0.02	206.901426	1.0223E+10	0.02	374.014116	19470451887
0.05	17.3160578	14116759.8	0.05	58.823667	192736958	0.05	13.2416913	42181091.1	0.05	23.9369034	80075578.65
0.1	2.16450723	239571.872	0.1	7.35295837	3088178.09	0.1	1.65521141	733179.549	0.1	2.99211293	1329259.666
0.2	0.2705634	8492.6855	0.2	0.9191198	67418.5639	0.2	0.20690143	29980.9304	0.2	0.37401412	40289.36979
0.3	0.08016693	2552.3894	0.3	0.27233179	13210.0111	0.3	0.06130413	9679.53299	0.3	0.110819	10962.93507
0.4	0.03382043	1320.04196	0.4	0.11488997	5844.86037	0.4	0.02586268	5099.70204	0.4	0.04675176	5509.443278
0.5	0.01731606	824.595704	0.5	0.05882367	3463.36986	0.5	0.01324169	3203.46493	0.5	0.0239369	3411.102443
0.6	0.01002087	567.589418	0.6	0.03404147	2335.93767	0.6	0.00766302	2209.57604	0.6	0.01385237	2340.150027
0.7	0.00631052	415.415107	0.7	0.0214372	1694.41116	0.7	0.00482569	1618.62132	0.7	0.00872336	1710.264088
0.8	0.00422755	317.461593	0.8	0.01436125	1289.18727	0.8	0.00323283	1237.49534	0.8	0.00584397	1306.06552
0.9	0.00296915	250.585506	0.9	0.01008636	1015.21264	0.9	0.00227052	977.033348	0.9	0.00410441	1030.542054
1	0.00216451	202.859308	1	0.00735296	820.746404	1	0.00165521	791.05414	1	0.00299211	834.0859757
Arbitrarily choose values											
corresponding to a 10-m arm catching at Vo <= .05 m/s											

Appendix A-3.2.7.5 continued

Determination of torque req'd to set v=0 over 18°

18° = .457m T=F*Lt

F=M*a=M*dv/dt=M*v*dv/dx

Assume max defl.=.02*Lt=-(Torq*Lt^3/3*EI)

Al=7075-T6,E=71.12E6 Pa

Beryllium,E=293E6 Pa

Boron/Epoxy, E=207E6 Pa

Graphite/Epoxy, E=151.5E6 Pa

Magnesium, E=44.8E6 Pa

Steel=Ph15-7 MO, E=200 E6 Pa

Titanium, E=110E6 Pa

Mmax = Mhubble=11340 kg

Lt=length of arm

assume max length of arm ~2*payload length

i.e. ~20m

assume min length of arm ~ .5*bay ~5m

HUBBLE

V=.3 m/s

	Torque		Minimum Moments of Inertia (m^4)						
Lt	Req.(Nm	EI (Pa*m^4)	Al	Be	Bor/Ep	Gr/Ep	Mg	Steel	Ti
5	11166	4.653E+06	0.0654	0.016	0.022	0.03	0.104	0.023	0.042
6	13400	8.040E+06	0.1131	0.027	0.039	0.05	0.179	0.04	0.073
7	15633	1.277E+07	0.1796	0.044	0.062	0.08	0.285	0.064	0.116
8	17866	1.906E+07	0.268	0.065	0.092	0.13	0.425	0.095	0.173
9	20099	2.713E+07	0.3816	0.093	0.131	0.18	0.606	0.136	0.247
10	22333	3.722E+07	0.5235	0.127	0.18	0.25	0.831	0.186	0.338
11	24566	4.954E+07	0.6968	0.169	0.239	0.33	1.106	0.248	0.45
12	26799	6.432E+07	0.9046	0.22	0.311	0.42	1.436	0.322	0.585
13	29032	8.177E+07	1.1501	0.279	0.395	0.54	1.825	0.409	0.743
14	31266	1.021E+08	1.4365	0.349	0.493	0.67	2.28	0.511	0.928
15	33499	1.256E+08	1.7668	0.429	0.607	0.83	2.804	0.628	1.142
16	35732	1.525E+08	2.1443	0.52	0.737	1.01	3.403	0.762	1.386
17	37965	1.829E+08	2.572	0.624	0.883	1.21	4.082	0.914	1.662
18	40199	2.171E+08	3.0531	0.741	1.049	1.43	4.845	1.085	1.973
19	42432	2.553E+08	3.5907	0.871	1.233	1.69	5.699	1.276	2.321
20	44665	2.978E+08	4.188	1.016	1.438	1.97	6.647	1.489	2.707

V=.2 m/s

	Torque		Minimum Moments of Inertia (m^4)						
Lt	Req.(Nm	EI (Pa*m^4)	Al	Be	Bor/Ep	Gr/Ep	Mg	Steel	Ti
5	4963	2.068E+06	0.0291	0.0071	0.01	0.0136	0.0462	0.0103	0.0188
6	5955	3.573E+06	0.0503	0.0122	0.0173	0.0236	0.0798	0.0179	0.0325
7	6948	5.674E+06	0.0798	0.0194	0.0274	0.0375	0.1267	0.0284	0.0516
8	7940	8.470E+06	0.1191	0.0289	0.0409	0.0559	0.1891	0.0423	0.077
9	8933	1.206E+07	0.1696	0.0412	0.0583	0.0796	0.2692	0.0603	0.1096
10	9926	1.654E+07	0.2327	0.0565	0.0799	0.1092	0.3693	0.0827	0.1504
11	10918	2.202E+07	0.3097	0.0751	0.1064	0.1453	0.4915	0.1101	0.2002
12	11911	2.859E+07	0.402	0.0976	0.1381	0.1887	0.6381	0.1429	0.2599
13	12903	3.634E+07	0.5112	0.124	0.1756	0.2399	0.8113	0.1817	0.3304
14	13896	4.539E+07	0.6384	0.1549	0.2193	0.2996	1.0132	0.227	0.4127
15	14888	5.583E+07	0.7853	0.1906	0.2697	0.3685	1.2462	0.2792	0.5076
16	15881	6.776E+07	0.953	0.2313	0.3273	0.4473	1.5125	0.3388	0.616
17	16874	8.127E+07	1.1431	0.2774	0.3926	0.5365	1.8142	0.4064	0.7389
18	17866	9.648E+07	1.3569	0.3293	0.4661	0.6368	2.1535	0.4824	0.8771
19	18859	1.135E+08	1.5959	0.3873	0.5481	0.749	2.5327	0.5673	1.0315
20	19851	1.323E+08	1.8613	0.4517	0.6393	0.8735	2.954	0.6617	1.2031

V=.1 m/s

	Torque		Minimum Moments of Inertia (m^4)						
Lt	Req.(Nm	EI (Pa*m^4)	Al	Be	Bor/Ep	Gr/Ep	Mg	Steel	Ti
5	1240.7	516958.42	0.0073	0.002	0.002	0	0.012	0.003	0.005
6	1488.8	893304.16	0.0126	0.003	0.004	0.01	0.02	0.004	0.008
7	1737	1418533.9	0.02	0.005	0.007	0.01	0.032	0.007	0.013
8	1985.1	2117461.7	0.0298	0.007	0.01	0.01	0.047	0.011	0.019
9	2233.3	3014901.5	0.0424	0.01	0.015	0.02	0.067	0.015	0.027
10	2481.4	4135667.4	0.0582	0.014	0.02	0.03	0.092	0.021	0.038
11	2729.5	5504573.3	0.0774	0.019	0.027	0.04	0.123	0.028	0.05
12	2977.7	7146433.3	0.1005	0.024	0.035	0.05	0.16	0.036	0.065
13	3225.8	9086061.3	0.1278	0.031	0.044	0.06	0.203	0.045	0.083
14	3474	11348271	0.1596	0.039	0.055	0.07	0.253	0.057	0.103
15	3722.1	13957877	0.1963	0.048	0.067	0.09	0.312	0.07	0.127
16	3970.2	16939694	0.2383	0.058	0.082	0.11	0.378	0.085	0.154
17	4218.4	20318534	0.2858	0.069	0.098	0.13	0.454	0.102	0.185
18	4466.5	24119212	0.3392	0.082	0.117	0.16	0.538	0.121	0.219
19	4714.7	28366543	0.399	0.097	0.137	0.19	0.633	0.142	0.258
20	4962.8	33085339	0.4653	0.113	0.16	0.22	0.739	0.165	0.301

v=.075 m/s

	Torque		Minimum Moments of Inertia (m^4)						
Lt	Req.(Nm	EI (Pa*m^4)	Al	Be	Bor/Ep	Gr/Ep	Mg	Steel	Ti
5	697.89	290789.11	0.0041	0.001	0.0014	0.0019	0.0065	0.0015	0.0026
6	837.47	502483.59	0.0071	0.0017	0.0024	0.0033	0.0112	0.0025	0.0046
7	977.05	797925.33	0.0112	0.0027	0.0039	0.0053	0.0178	0.004	0.0073
8	1116.6	1191072.2	0.0168	0.0041	0.0058	0.0079	0.0266	0.006	0.0108
9	1256.2	1695882.1	0.0239	0.0058	0.0082	0.0112	0.0379	0.0085	0.0154
10	1395.8	2326312.9	0.0327	0.0079	0.0112	0.0154	0.0519	0.0116	0.0211
11	1535.4	3096322.5	0.0435	0.0106	0.015	0.0204	0.0691	0.0155	0.0281
12	1674.9	4019868.7	0.0565	0.0137	0.0194	0.0265	0.0897	0.0201	0.0365
13	1814.5	5110909.5	0.0719	0.0174	0.0247	0.0337	0.1141	0.0256	0.0465
14	1954.1	6383402.6	0.0898	0.0218	0.0308	0.0421	0.1425	0.0319	0.058
15	2093.7	7851306.1	0.1104	0.0268	0.0379	0.0518	0.1753	0.0393	0.0714
16	2233.3	9528577.7	0.134	0.0325	0.046	0.0629	0.2127	0.0476	0.0866
17	2372.8	11429175	0.1607	0.039	0.0552	0.0754	0.2551	0.0571	0.1039
18	2512.4	13567057	0.1908	0.0463	0.0655	0.0896	0.3028	0.0678	0.1233
19	2652	15956180	0.2244	0.0545	0.0771	0.1053	0.3562	0.0798	0.1451
20	2791.6	18610503	0.2618	0.0635	0.0899	0.1228	0.4154	0.0931	0.1692

ORIGINAL PAGE IS OF POOR QUALITY

Appendix A.3.3.7.5, continued

V=.05 m/s

	Torque		Minimum Moments of Inertia (m^4)						
Lt	Req.(Nm	EI (Pa*m^4)	Al	Be	Bor/Ep	Gr/Ep	Mg	Steel	Ti
5	310	1.292E+05	0.0018	0.0004	0.0006	0.0009	0.0029	0.0006	0.0012
6	372	2.233E+05	0.0031	0.0008	0.0011	0.0015	0.005	0.0011	0.002
7	434	3.546E+05	0.005	0.0012	0.0017	0.0023	0.0079	0.0018	0.0032
8	496	5.294E+05	0.0074	0.0018	0.0026	0.0035	0.0118	0.0026	0.0048
9	558	7.537E+05	0.0106	0.0026	0.0036	0.005	0.0168	0.0038	0.0069
10	620	1.034E+06	0.0145	0.0035	0.005	0.0068	0.0231	0.0052	0.0094
11	682	1.376E+06	0.0194	0.0047	0.0066	0.0091	0.0307	0.0069	0.0125
12	744	1.787E+06	0.0251	0.0061	0.0086	0.0118	0.0399	0.0089	0.0162
13	806	2.272E+06	0.0319	0.0078	0.011	0.015	0.0507	0.0114	0.0207
14	868	2.837E+06	0.0399	0.0097	0.0137	0.0187	0.0633	0.0142	0.0258
15	931	3.489E+06	0.0491	0.0119	0.0169	0.023	0.0779	0.0174	0.0317
16	993	4.235E+06	0.0596	0.0145	0.0205	0.028	0.0945	0.0212	0.0385
17	1055	5.080E+06	0.0714	0.0173	0.0245	0.0335	0.1134	0.0254	0.0462
18	1117	6.030E+06	0.0848	0.0206	0.0291	0.0398	0.1346	0.0301	0.0548
19	1179	7.092E+06	0.0997	0.0242	0.0343	0.0468	0.1583	0.0355	0.0645
20	1241	8.271E+06	0.1163	0.0282	0.04	0.0546	0.1846	0.0414	0.0752

V=.025 m/s

	Torque		Minimum Moments of Inertia (m^4)						
Lt	Req.(Nm	EI (Pa*m^4)	Al	Be	Bor/Ep	Gr/Ep	Mg	Steel	Ti
5	78	3.231E+04	0.0005	0.0001	0.0002	0.0002	0.0007	0.0002	0.0003
6	93	5.583E+04	0.0008	0.0002	0.0003	0.0004	0.0012	0.0003	0.0005
7	109	8.866E+04	0.0012	0.0003	0.0004	0.0006	0.002	0.0004	0.0008
8	124	1.323E+05	0.0019	0.0005	0.0006	0.0009	0.003	0.0007	0.0012
9	140	1.884E+05	0.0027	0.0006	0.0009	0.0012	0.0042	0.0009	0.0017
10	155	2.585E+05	0.0036	0.0009	0.0012	0.0017	0.0058	0.0013	0.0023
11	171	3.440E+05	0.0048	0.0012	0.0017	0.0023	0.0077	0.0017	0.0031
12	186	4.467E+05	0.0063	0.0015	0.0022	0.0029	0.01	0.0022	0.0041
13	202	5.679E+05	0.008	0.0019	0.0027	0.0037	0.0127	0.0028	0.0052
14	217	7.093E+05	0.01	0.0024	0.0034	0.0047	0.0158	0.0035	0.0064
15	233	8.724E+05	0.0123	0.003	0.0042	0.0058	0.0195	0.0044	0.0079
16	248	1.059E+06	0.0149	0.0036	0.0051	0.007	0.0236	0.0053	0.0096
17	264	1.270E+06	0.0179	0.0043	0.0061	0.0084	0.0283	0.0063	0.0115
18	279	1.507E+06	0.0212	0.0051	0.0073	0.01	0.0336	0.0075	0.0137
19	295	1.773E+06	0.0249	0.0061	0.0086	0.0117	0.0396	0.0089	0.0161
20	310	2.068E+06	0.0291	0.0071	0.01	0.0136	0.0462	0.0103	0.0188

Assume one astronaut can
produce a holding
force =100lb=445N

ASTRONAUT

	Torque		Minimum Moments of Inertia (m^4)						
Lt	(Nm)	EI (Pa*m^4)	Al	Be	Bor/Ep	Gr/Ep	Mg	Steel	Ti
5	2225	9.271E+05	0.013	0.0032	0.0045	0.0061	0.0207	0.0046	0.0084
6	2670	1.602E+06	0.0225	0.0055	0.0077	0.0106	0.0358	0.008	0.0146
7	3115	2.544E+06	0.0358	0.0087	0.0123	0.0168	0.0568	0.0127	0.0231
8	3560	3.797E+06	0.0534	0.013	0.0183	0.0251	0.0848	0.019	0.0345
9	4005	5.407E+06	0.076	0.0185	0.0261	0.0357	0.1207	0.027	0.0492
10	4450	7.417E+06	0.1043	0.0253	0.0358	0.049	0.1656	0.0371	0.0674
11	4895	9.872E+06	0.1388	0.0337	0.0477	0.0652	0.2203	0.0494	0.0897
12	5340	1.282E+07	0.1803	0.0437	0.0619	0.0846	0.2861	0.0641	0.1165
13	5785	1.629E+07	0.2292	0.0556	0.0787	0.1076	0.3637	0.0815	0.1481
14	6230	2.035E+07	0.2862	0.0695	0.0983	0.1343	0.4543	0.1018	0.185
15	6675	2.503E+07	0.3521	0.0854	0.1209	0.1652	0.5587	0.1252	0.2276
16	7120	3.038E+07	0.4273	0.1037	0.1468	0.2005	0.6781	0.1519	0.2762
17	7565	3.644E+07	0.5125	0.1244	0.176	0.2405	0.8134	0.1822	0.3313
18	8010	4.325E+07	0.6084	0.1476	0.209	0.2855	0.9655	0.2163	0.3932
19	8455	5.087E+07	0.7155	0.1736	0.2458	0.3358	1.1355	0.2544	0.4625
20	8900	5.933E+07	0.8345	0.2025	0.2866	0.3916	1.3244	0.2967	0.5394

Appendix A.3.4.0.1 Mission Sub-functions

Function	IPS	Frame Rate	Insrtc. / Exec.	Lag Time [ms]	COST [$M92]	COST [$M94]
Navigation						
General						
IMU Processing	948,261	100	9,483	10.00	3.56	$3.81
GPS Processing	948,261	100	9,483	10.00	3.56	$3.81
Error Compensation	80,978	300	270	1.00	0.78	$0.84
Kalman Filtering	1,264,810	25	50,592	36.00	8.70	$9.32
Nav. Exec.	25,239	100	252	6.00	0.14	$0.15
Bending Process	30,367	100	304	0.10	8.57	$9.19
FDI	66,098	50	1,322	0.50	7.56	$8.10
Ascent						
On-Orbit						
Docking	*100,000*	*10*	*10,000*	*15.00*	2.81	$3.02
Return						
Landing	*2,500,000*	*50*	*50,000*	*15.00*	14.06	$15.08
Guidance						
Ascent						
Two-Body Linear Guidance	25,761	50	515	15.00	0.14	$0.16
Non-Linear Traj. Shaping	947,257	1	947,257	960.00	91.58	$98.17
Contingency Control	978	1	978	15.00	0.28	$0.29
Determine G&C Wind Deltas						
Load Relief	25,000	100	250	10.00	0.09	$0.10
Estimate Fluctuation Stats	25,000	100	250	10.00	0.09	$0.10
On-Orbit						
Return						
Control						
Ascent						
Model Reference Adp. Con.	166,606	50	3,332	10.00	1.25	$1.34
Classical AutoPilot	213,289	50	4,266	10.00	1.60	$1.71
System Identification	648,839	25	25,954	10.00	9.73	$10.43
On-Orbit						
RCS Control	73,075	50	1,462	15.00	0.41	$0.44
Payload Pointing	*500*	*1*	*500*	*40.00*	0.08	$0.09
Return						
Avionics System Management						
System Redundancy Mangement.						
Fault Response	20,630	25	825	10.00	0.31	$0.33
Fault Isolation	20,630	25	825	10.00	0.31	$0.33
Configuration Manager	20,630	25	825	10.00	0.31	$0.33
Miscellaneous	*10,000*	*1*	*10,000*	*11.00*	*3.49*	$3.75
Winds Ahead Determination						
Other	124,598	1	124,598	500.00	12.38	$13.27
Mang. Measurement Resources						
Lidar Cal. & Checkout	500	1	500	15.00	0.14	$0.15
Lidar BIT	11,527	25	461	15.00	0.13	$0.14
Lidar Fault Handing	6,250	25	250	15.00	0.07	$0.08
Lidar Health Monitoring	19,826	50	397	15.00	0.11	$0.12
Other	274	1	274	15.00	0.08	$0.08
Compute Wind Profile						
Lidar Mode Control	500	1	500	15.00	0.14	$0.15
Winds Measurement Fitting	149,517	1	149,517	950.00	14.46	$15.50
Vibration Compensation	20,543	50	411	15.00	0.12	$0.12
Bending Compensation	29,783	50	596	5.00	0.39	$0.42
Control Velocimeter						
Other	50,957	100	510	15.00	0.14	$0.15
Redundant Lidar Config. Con.	25,000	100	250	10.00	0.09	$0.10
Lidar Power Control	6,250	25	250	40.00	0.04	$0.04
Receive & Process Wind Info.						
Detection	500	1	500	15.00	0.14	$0.15
Pulse Deconvolution	500	1	500	15.00	0.14	$0.15
Range Determination	500	1	500	15.00	0.14	$0.15
Doppler Freq. Estimation	500	1	500	15.00	0.14	$0.15
Data Collection & Formatting	787	1	787	10.00	0.30	$0.32

Appendix A.3.4.0.1 Mission Sub-functions

Other	25,383	50	508	15.00	0.14	$0.15
Propulsion Control	**4,807,609**	**50**	**96,152**	**15.00**	**27.04**	**$28.99**
Engine System Start Control						
Engine System Shut-Off Control						
Duration Control						
Engine System Safety Control						
Engine System Control Calibration						
Engine System Checkout & Test Control						
Engine Thrust Control						
Propellant-Mixture Ratio Control						
Thrust-Vector Control						
Fluids Management	**18,025**	**25**	**721**	**15.00**	**0.20**	$0.22
Tank Pressurization Control						
Miscellaneous						
Power Management	**18,025**	**25**	**721**	**15.00**	**0.20**	$0.22
Fire Control Management						
Detection	*27,009*	*50*	*540*	*1.00*	*1.57*	$1.68
Suppression	*500*	*1*	*500*	*1.00*	*1.45*	$1.56
Life Support Management	***50,957***	***100***	***510***	***15.00***	**0.14**	$0.15
RMS Control	***7500***	***10***	***750***	***40.00***	**0.12**	$0.13
Thermal Control	***500,000***	***50***	***10,000***	***100.00***	***1.22***	$1.31
Stage Separation	***25,000***	***50***	***500***	***100.00***	***0.06***	$0.07
Communications						
Command & Tlm. Processing	134,918	25	5,397	40.00	0.89	$0.95
Voice Communications	*50,000*	*50*	*1,000*	*50.00*	*0.15*	$0.16
Sensor Processing						
Other	237,505	25	9,500	34.00	1.68	$1.80
Categorize Sensor Data						
Other	9,239	25	370	34.00	0.07	$0.07
Identitify Format	65,360	50	1,307	40.00	0.21	$0.23
Filter & Store	413,348	50	8,267	16.00	2.23	$2.39
Format-B Convert & Store	14,891	25	596	40.00	0.10	$0.10
Format-A Convert & Store	250	1	250	15.00	0.07	$0.08
Type Processing	68,043	50	1,361	5.00	0.89	$0.96
Calibration & Validation	49,728	25	1,989	15.00	0.56	$0.60
Sensor Fault Tolerance	138,783	75	1,850	15.00	0.52	$0.56
Error & Failing Reporting	411	1	411	15.00	0.12	$0.12
Abort Controls	***134,918***	***25***	***5,397***	***1.00***	**15.68**	$16.81
Adaptive Abort Determination						
Flight Termination						
Capsule Ejection						

Appendix A.3.4.0.2 Function Performance Levels

Functions	Detection of certain forms of very low energy levels	Sensitivity to an extremely wide range of stimuli	Perceiving patterns and making generalizations about them	Ability to exercise judgment where events cannot be completely defined	Improvising & adopting flexible procedures	Ability to react to unexpected, low-probability events	Applying originality in solving problem	Ability to profit form experience and alter course of action	Ability to preform fine manipulation	Ability to preform when overloaded	Ability to reason inductively	Monitoring (people and machines)	Performing routine, repetitive, or precise operations	Responding very quickly to control signals	Storing and recalling large amounts of info. in short time periods	Preforming complex & rapid computations w/ high accuracy	Sensitivity to stimuli beyond the range of humans (infrared,radio,etc.)	Doing many different things at one time	Exerting large amounts of force smoothly & precisely	Insensitivity to extraneous factors	Deductive processes	Operating in environments which are hostile to humans	Can repeat operations rapidly,continuosly, & precisely oever long times	Human Score	Machine Score	Human	Both	Machine - Hardware	Machine - Software
	People excel in . . .													Machines excel in . . .										Scores		Allocation			
Navigation	0	0	0	2	3	2	1	5	0	2	0	5	3	5	0	5	0	4	0	3	0	0	3	15	28			xxxx	xxxx
Guidance	0	0	2	3	4	3	1	3	0	2	0	4	5	5	5	5	0	4	0	3	0	0	3	18	34				xxxx
Control	4	3	1	5	4	4	5	4	5	1	2	4	5	5	2	5	2	4	5	2	0	5	4	38	43		xxxx		
Avionics System Management	2	1	2	3	0	3	0	0	0	4	0	5	5	3	3	5	5	4	0	0	0	0	5	15	35				xxxx
Winds Ahead Determination	0	0	0	3	3	0	0	0	0	0	0	5	0	4	2	5	5	0	0	0	0	0	0	6	21			xxxx	xxxx
Propulsion Control	0	2	3	2	4	0	5	0	0	4	0	5	4	5	0	3	5	5	3	2	2	0	2	20	36			xxxx	xxxx
Fluids Management	1	0	1	3	0	3	0	0	0	3	0	5	5	2	0	0	5	3	0	0	0	0	4	11	24			xxxx	xxxx
Power Management	1	0	1	3	0	3	0	0	0	3	0	5	5	2	0	0	5	3	0	0	0	0	4	11	24			xxxx	xxxx
Fire Control Management	1	0	2	0	5	4	4	3	0	0	1	5	3	5	0	0	5	0	0	5	0	5	1	20	29			xxxx	xxxx
Life Support Management	1	0	1	3	0	3	0	0	0	3	0	5	5	2	0	0	5	3	0	0	0	0	4	11	24			xxxx	xxxx
RMS Control	2	1	5	5	4	5	5	5	5	0	0	2	5	3	0	0	4	2	3	3	2	5	3	37	32		xxxx		
Thermal Control	1	0	1	3	0	3	0	0	0	3	0	5	5	2	0	0	5	3	0	0	0	0	4	11	24			xxxx	xxxx
Stage Seperation	0	0	0	0	3	2	0	0	0	3	0	3	0	5	0	0	3	4	0	1	0	0	0	8	16			xxxx	xxxx
Communications	0	2	2	2	4	4	4	3	0	0	0	5	5	5	4	3	5	5	0	0	0	0	5	21	37			xxxx	xxxx
Sensor Processing	5	4	0	0	3	3	4	0	0	3	0	5	5	5	3	5	5	5	0	4	2	4	5	22	48			xxxx	xxxx
Abort Control	2	2	4	5	5	5	5	5	1	5	5	5	3	5	3	5	5	5	5	4	1	3	1	44	45		xxxx		

Appendix 3.4.1.4.1.1 Sensor Data Rates

LH2 Tank Pressure	Pressure Transducer	2	50	16	1600
LH2 Tank Temperature	Thermocouple	2	50	16	1600
General Fluid Management Actuator	ON/OFF Servoswitches	16	100	1	1600
Power Management		**33**			**5520**
Fuel Cell Sensors					
LOX Tank Pressure	Pressure Transducer	4	10	16	640
LH2 Tank Pressure	Pressure Transducer	4	10	16	640
Position Senors	RVDT - LVDT	8	10	16	1280
Control Value	Proportional Servovalves	8	10	16	1280
Over Pressure Relief Value	ON/OFF Pneumatic Values	8	10	1	80
Battery Charge	Voltmeter	1	100	16	1600
Fire Control		**6**			**336**
Fire Detection	Smoke Detector	4	10	8	320
Fire Suppression	Extinguisher	2	1	8	16
Life Support Management		**35**			**4872**
Life Support Sensors					
O2 Partial Pressure	Polargraphic Electrode	1	1	8	8
N2 Partial Pressure	Polargraphic Electrode	1	1	8	8
CO2 Partial Pressure . . .	Mass Spectromiter	1	100	16	1600
& Foriegn Contaminates in Cabin					
Total Cabin Pressure Sensor	Pressrue Transducer	4	10	16	640
Airlock Pressure	Pressrue Transducer	1	100	16	1600
Cabin Humidity	Thermo-electric/photocell	1	10	16	160
Cabin Temperature	Thermocouple	4	10	16	640
LiOH Content	Electrode Sensor	2	1	8	16
Liquid Oxygen Converter	ON/OFF Servoswitches	6	10	1	60
Liquid Nitorgen Converter	ON/OFF Servoswitches	6	10	1	60
CO2 Removal System	ON/OFF Servoswitches	8	10	1	80
RMS Control		**8**			**3200**
Posistion Sensors	Differ. GPS	2	50	8	800
Velocity Sensors	Rate Sensors	3	50	8	1200
Arm Actuators		2	50	8	800
End Effector		1	50	8	400
Thermal Control		**48**			**2036**
Avionics Thermal Control					
Processor Unit Temp. Sensors	Thermocouple	12	1	8	96
Cooling Fluid Pump RPM Sensor		2	50	8	800
Cooling Fluid Pump Temp Sensor	Thermocouple	2	10	8	160
Cooling Fluid Pump Control		2	10	8	160
Cooling Fluid Sensors	Pressure Transducers	10	10	8	800
Cooling Fluid Control	On/Off Servovaulves	20	1	1	20
Stage Seperation		**18**			**1800**
Explosive Bolts Trigger	Ignitor	12	100	1	1200

Appendix 3.4.1.4.1.1 Sensor Data Rates

Function	Hardware	Quantity	Sampling Rate [Hz]	Bits / Signal	Bandwith [b/sec]
Navigation					352
General	GPS reciever	2	2	80	320
General	IMU				
On-Orbit	Star Tracker	2	1	16	32
Landing	MLS				
Landing					
Control		**110**			**61040**
RCS/OMS Sensors					
He Tank Pressure Sensor	Pressure Transducer	4	10	8	320
He Tank Temperature Sensor	Thermocouple	4	10	8	320
Oxidizer Tank Pressure Sensor	Pressure Transducer	4	10	8	320
Oxidizer Tank Temperature Sensor	Thermocouple	4	10	8	320
Fuel Tank Pressure Sensor	Pressure Transducer	4	10	8	320
Fuel Tank Temperature Sensor	Thermocouple	4	10	8	320
Nitrogen Tank Pressure Sensor	Pressure Transducer	4	10	8	320
Nitrogen Tank Temp. Sensor	Thermocouple	4	10	8	320
Propellant Feed Sensors	LVDT	8	10	8	640
Speed/Flow Sensors		8	10	8	640
RCS Over-Heat Sensors		12	100	8	9600
RCS/OMS Actuators					0
Propellant Feed Control	Pressure Regulator	8	100	16	12800
OMS Actuators	Proportional Servovalues	8	10	8	640
Vernier Actuators	On/Off Servovalues	8	10	1	80
RCS Actuators	Proportional Servovalues	24	10	8	1920
OMS Actuators	Gibals	2	10	8	160
Aerodynamic Control Surfaces	EMA	20	100	16	32000
Propulsion Control per Engine		**163**			**503500**
General Engine Sensors					
Pressure	Pressure Transducer	30	50	16	24000
Temperature Sensor	Thermocouple	14	50	16	11200
Acoustic Vibrations		6	4000	16	384000
Speed/Flow Sensors		45	50	16	36000
Position Sensors	RVDT - LVDT	25	50	16	20000
Igniter	Spark Igniter	6	100	16	9600
General Engine Actuator	ON/OFF Pneumatic Values	12	100	1	1200
General Engine Actuator	ON/OFF Servoswitches	15	100	1	1500
General Engine Actuator	Proportional Servovalves	10	100	16	16000
Fluid Management (per Module)		**41**			**21600**
Fluid Management Sensors					
Valve Position Sensors	RVDT - LVDT	16	50	16	12800
Intertank Pressure	Pressure Transducer	1	50	16	800
Leak Sensors ?					
LOX Tank Pressure	Pressure Transducer	2	50	16	1600
LOX Tank Temperature	Thermocouple	2	50	16	1600

Appendix 3.4.1.4.1.1 Sensor Data Rates

Speration Sensors	Proximtiy Detector	6	100	1	600
Communications					
Command & Tlm. Processing					
Voice Communications	Mic/Speaker	2			128000
Sensor Processing					
Remote Data Unit BIT	BIT chip				16
Remote Data Unit Configuration	Processor Chip				100
Abort Control					
Flight Termination	Explosive Device	6	100	1	600
Capsule Ejection	Solid Rocket Ignitors	6	100	16	9600

Appendix A.3.4.2.2 GPS/INS Comparison

		GPS/INS ($)	Pure INS ($)
Production Cost			
Inertial Sensing		6K (X3)	90K (X2)
Inertial Sensing Elect.		6K (X3)	12K (X2)
GPS Antenna		3K (X4)	
GPS Ant. Elect		5.5K (X4)	
GPS IF to Dig. convert.		7K (X2)	
Gps Process.		10K (X2)	
Inertial Process.		10K (X3)	17K (X2)
Guid. Process.		15K (X3)	15K (X3)
Housing Assem. & Ck.out		50K tot	210k tot
Total Prod. cost		**229K**	**493K**
Operations Cost			
Sparing		1.15M	2.465M
Sys. perf. test		7.2K (X150)	36K (X150)
Calib.		1.8K (X150)	31K (X150)
Sys. fn. test		2K (X150)	13K (x150)
Vendor rework		320K	740K
Alignment Install		0.2K (X150)	1.6K (X150)
Launch Recycle		1.2K (X150)	2.4K (X150)
Totals (150 Missions)		3.5M	15.9M

Table A.3.4.2.2.a Itemized cost comparison of GPS/INS with pure INS, Gen. Dyn. Space Sys. Div

	GPS/INS	**Pure INS**
Inertial Perf.	IFOG/Pend.	RLG/Pend.
	1 deg/hr	.0088 deg/hr
	1 milli-g	42 micro-g
position	35 m sep	1000m rms
Velocity	.1m/s	1m/s
Attitude	.1 deg	.1 deg

Table A.3.4.2.2.b Performance of sensors used in the study, Gen. Dyn. Space Sys. Div

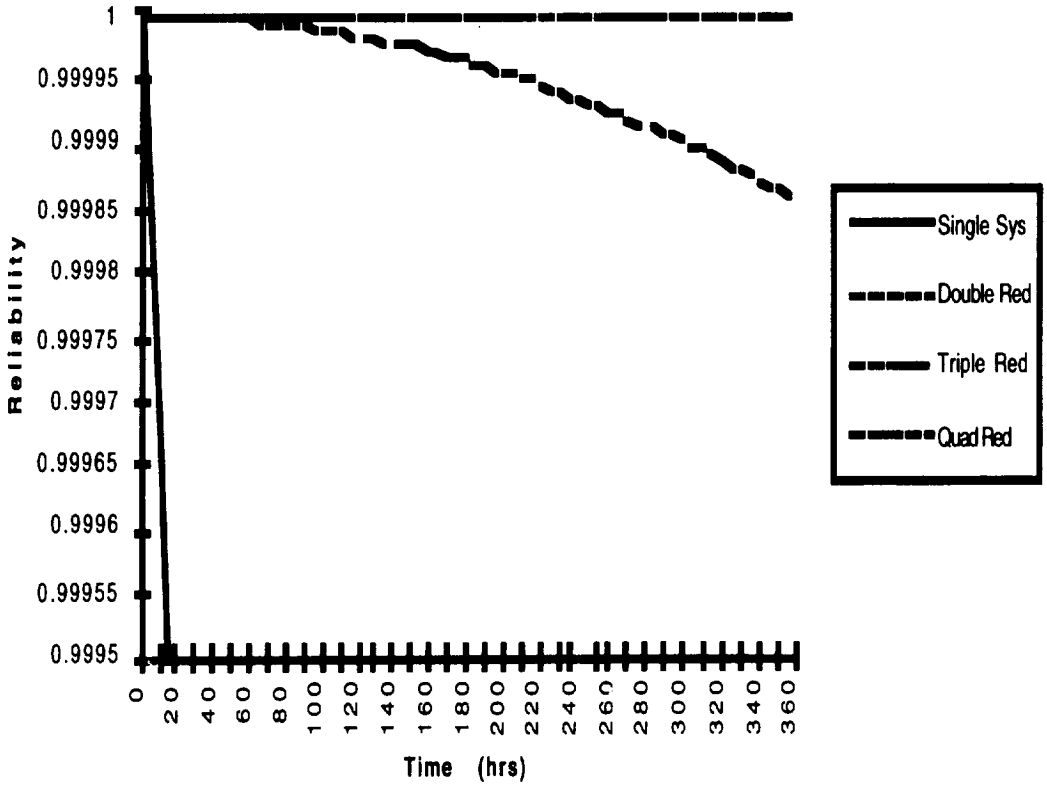

Figure A.3.4.2.2.a Reliability curve for GPS/INS.

Appendix A.3.4.3.2 General Information on TDRSS and STDN

TDRSS

The TDRSS consists of two operating satellites (TDRS-3 and TDRS-4) located 130° apart, and a spare (TDRS-1) located between the other two (TDRS-2 was lost in the Challenger accident). The following picture shows the general configuration of the TDRSS.

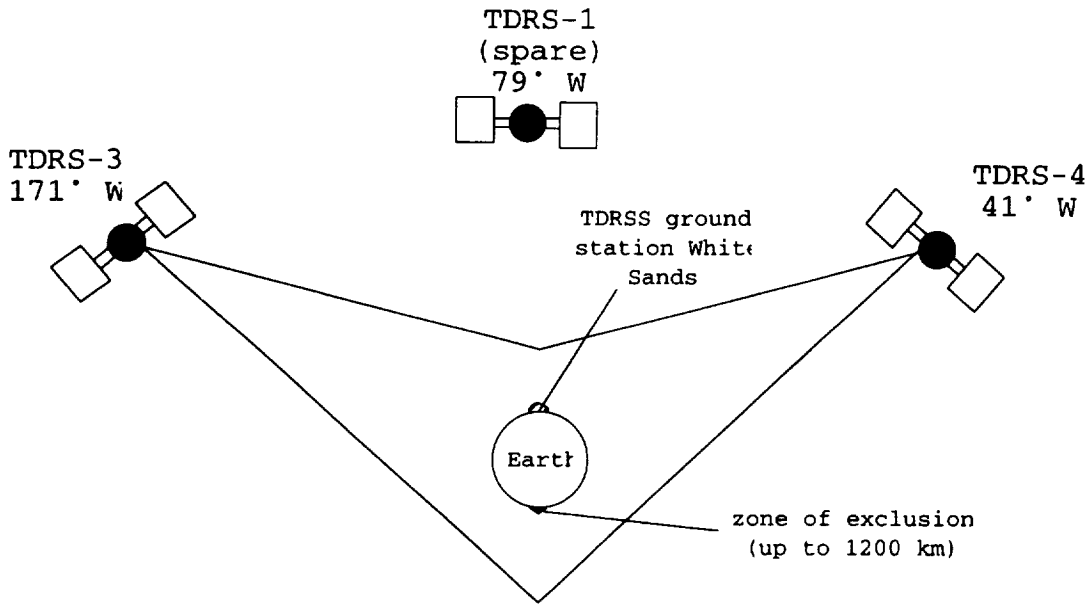

The link budgets were based on links through the single access S & K Band antenna. It is 4.9 meters in diameter and operates on a 26 W solid state power amplifier (SSPA). The method of modulation used by the TDRSS is Quadrature Phase Shift Keying (QPSK).

Downlink (From MARS to the TDRSS)

	frequency (GHz)	Max. Data Rates
S-Band	2.2-2.3	12 kbps
K-Band	15.0034	300 Mbps

Uplink (From the TDRSS to MARS)

	frequency (GHz)	Max. Data Rates
S-Band	2.025-2.120	300 kbps
K-Band	13.775	25 Mbps

STDN

The information on the ground stations was based on the tracking station in Chilton U.K.. The relevant parameters are listed below.

Attribute	Value	Notes
Diameter	9 m	*
Antenna Gain	46 dB	at 2.253 GHz
Beamwidth	0.7 deg	
System Noise Temp.	115 K	at zenith
Pointing Error	0.05 deg	max.

*- Diameter for Chilton is actually 12 m, however the average station in the STDN has a diameter of 9m.

The power used in the link budget for the ground stations was a conservative estimate of one Watt. The Mars station at Goldstone California is capable of achieving 500 W power.

Appendix A.3.4.3.3 Power Vs. Data Rate

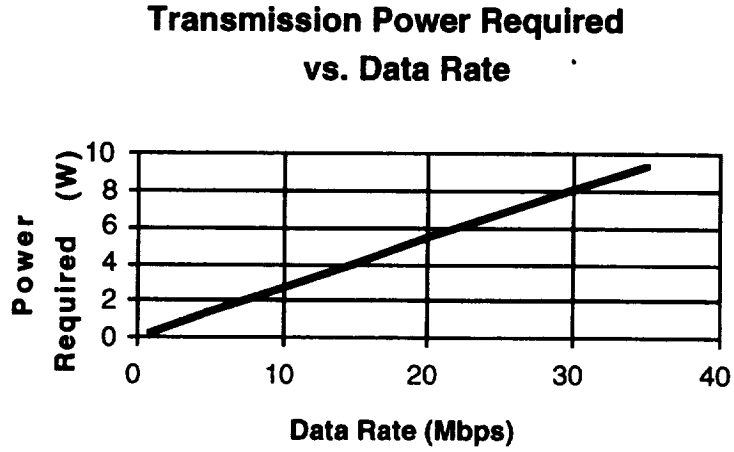

This graph was based on a parabolic reflector 1m in diameter with a constant margin of 10 dB and a transmitting frequency of 15.003.

Appendix A.3.4.3.4.1 Power Vs. Data Rate

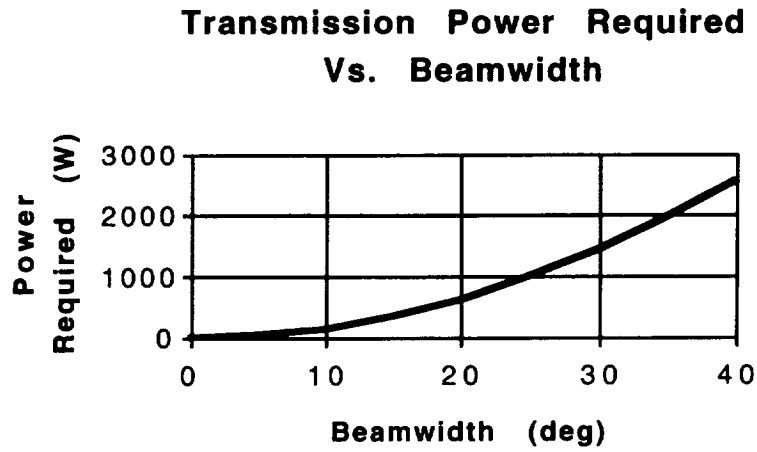

This graph is based on parabolic reflector with transmitting frequency of 15.0034 and a consttant margin of 10 dB

Appendix A.3.4.3.5.2 Earth Coverage Beamwidth

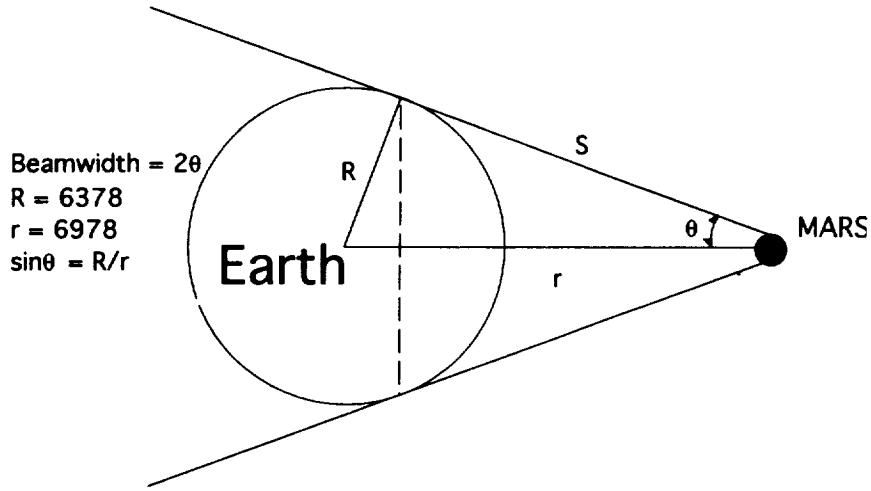

Beamwidth is 132°.

Appendix A.3.4.3.7 - Link Budgets

The method of determining the downlinking budget is listed below. For the uplink, the method is the same except the signal travels in the opposite direction. Although most of the following is not in dB's, most of the units are eventually converted into dB's.

D=diameter, L=length, W=width, $C=\pi D$, λ=wavelength (c/f) and η=efficiency

1. Frequency (f) See section 3.3.3.2

2. Transmitter Power (P)-Values of power and beamwidth were varied until a decent margin was obtained.

3. Transmitter Line Loss (L_l)-Generally this is estimated to be between -1dB and -3dB, for this analysis, the worst case was used.

4. Transmit Antenna Beamwidth(θ_t) - See section 3.3.3.5

5. Peak Transmit Antenna Gain - $G_{pt} = 27000/\theta_t^2$ for a parabolic reflector
$G_{pt} = 10.3(C^2L/\lambda^3)$ for a helix antenna
$G_{pt} = -[10\log(4\pi LW/\lambda)-\alpha(L+W)/2$ (in dB's)$]/2$
for a micro-strip antenna where $\alpha \approx 0.4$
for a 50 Ω line on 0.79 mm teflon fiberglass @ 2.2 GHz.

6. Transmit Antenna Diameter- $D_t = 21/(f_{GHz}\theta_t)$ for a parabolic reflector.
$D_t = 52/[\theta_t\sqrt{(L/\lambda^3)}]$

7. Transmit Antenna Diameter Pointing Offset (e_t)-This was estimated to be 10% of the beamwidth for a steerable antenna and 0 for fixed antennae.

8. Transmit Antenna Pointing Loss - $L_{pt} = -12(e_t/\theta_t)^2$

9. Transmit Antenna Gain - $G_t = G_{pt} + L_{pt}$ (all units in dB's).

10. Effective Isotropic Radiated Power - EIRP = $P_t+L_l+G_t$ (all units in dB's).

11. Propagation Path Length(S) - See section 3.3.3.6

12. Space Loss - $L_S = (\lambda/4\pi S)^2$.

13. Propagation and Polarization Losses were not a concern for satellite to satellite communications because they do not penetrate the atmosphere. For the direct STDN link, they were estimated at -0.5 dB (Firesat).

14. Receive Antenna Diameter(D_r) - See Appendix 3.3.3.2 for TDRSS and STDN applications. For EVA, it was estimated as 1cm (Helix).

15. Receive Antenna Peak Gain - $G_{pr} = (\pi D_r/\lambda)^2\eta$ (η=0.55) for links through the TDRSS. For STDN it is given in Appendix 3.3.3.2. $G_{pr} = 10.3(C^2L/\lambda^3)$ for EVA suits.

16. Receive Antenna Beamwidth - $\theta_r = 21/(f_{GHz}D_r)$ for TDRSS, see Appendix 3.3.3.2 for STDN, and estimated at 180° for EVA.

17. The Receive Antenna Pointing Error(e_r) - estimated to be about 10% of θ_r. for TDRSS, gotten from appendix 3.3.3.2 for STDN and assumed as 0 for EVA.

18. Receive Antenna Pointing Loss - $L_{pr} = -12(e_r/\theta_r)^2$

19. Receive Antenna Gain - $G_r = G_{pr} + L_{pr}$ (in dB's)

20. System Noise Temperature (T_s) - estimated using table 13-10 from L&W pg 527 based on frequency.

21 Data Rate (R) - See section 3.3.3.3

22. E_b/N_o - $E_b/N_o = (EIRP)L_sG_r/kT_sR$.

23. Carrier-to-noise ratio - $C/N_o = (E_b/N_o)R$.

24. Bit Error Rate (BER) - was estimated at $1x10^{-5}$

25. Required E_b/N_o - obtained from Figure 13-9 L&W based on BER.

26. Implementation Loss - not a concern for links through the TDRSS and to EVA astronauts because it does not rain in space. For STDN link it was estimated at -2 dB (Firesat)

27. Margin - The margin is the difference between the required E_b/N_o and the actual E_b/N_o with the implementation loss taken into account. According to L&W, it is good to have a margin between 4 and 5 dB for C-Band communications and a margin between 6 and 20 dB for frequencies above 10 GHz.

3.3.3.7.1 S-Band Link Budget Through the TDRSS

Parameter	Downlink	Uplink	Units
f	2.25	2.1	GHz
P_t	50	26	W
L_l	-3	-3	dB
θ_t	91	2.04	deg
G_{pt}	5.3	38.1	dB
L	0.06	N/A	m
D_t	0.036	4.9	deg
e_t	0	0.204	dB
L_{pt}	0	-0.12	dB
G_t	5.3	38.0	dBW
EIRP	19.3	49.1	km
S	45631	45631	dB
L_s	-192.7	-192.1	dB
D_r	4.9	0.036	m
G_{rp}	38.66	4.45	dB
θ_r	1.9	22.5	deg
e_r	0.19	0	deg
L_{pr}	-0.1	0	dB
G_r	38.5	4.4	dB
T_s	552	552	K
R	137	40	kbps
Eb/No	15.0	16.7	dB
C/No	66.4	62.7	dB
BER	10^{-5}	10^{-5}	-
Req. Eb/No	9.6	9.6	dB-Hz
Margin	5.4	7.1	dB

3.3.3.7.2 K-Band Link Budget Through the TDRSS

Parameter	Downlink	Uplink	Units
f	15.0034	13.775	GHz
P_t	5	26	W
L_l	-3	-3	dB
θ_t	1.4	0.31	deg
G_{pt}	41.4	54.5	dB
D_t	1.0	4.9	deg
e_t	0.14	0.031	dB
L_{pt}	-0.12	-0.12	dB

G_t	41.3	54.3	dBW
EIRP	45.3	65.5	km
S	45,631	45,631	dB
L_s	-209.2	-208.4	dB
D_r	4.9	1.0	m
G_{rp}	55.14	40.59	dB
θ_r	0.3	1.5	deg
e_r	0.029	0.15	deg
L_{pr}	-0.1	-0.12	dB
G_r	55.0	40.5	dB
T_s	552	1,295	K
R	11,680	184	kbps
Eb/No	21.6	42.4	dB
C/No	92.3	95.0	dB
BER	10^{-5}	10^{-5}	-
Req. Eb/No	9.6	9.6	dB-Hz
Margin	12.0	32.8	dB

3.3.3.7.3 S-Band Link Budget Through the STDN

Parameter	Downlink	Uplink	Units
f	2.25	2.1	GHz
P_t	0.5	1	W
L_l	-3	-3	dB
θ_t	91	0.7	deg
G_{pt}	5.3	47.4	dB
L	6.0	N/A	cm
D_t	0.036	9	deg
e_t	0	0.05	dB
L_{pt}	0	-0.061	dB
G_t	5.3	46.0	dBW
EIRP	-0.7	43.0	km
S	2831	2831	dB
L_s	-168.5	-167.9	dB
L_a	-0.5	-0.5	dB
D_r	9	0.036	m
G_{rp}	43.94	4.45	dB
θ_r	1.0	102.0	deg
e_r	0.05	0	deg
L_{pr}	-0.028	0	dB
G_r	43.9	4.4	dB
T_s	115	1295	K

R	137	40	kbps
E_b/N_o	30.8	31.5	dB
C/N_o	82.2	77.5	dB
BER	10^{-5}	10^{-5}	-
Req. E_b/N_o	9.6	9.6	dB-Hz
Implementation	-2.0	-2.0	dB
Margin	19.2	19.9	dB

3.3.3.7.4 Launch Link Budget

Parameter	Downlink	Uplink	Units
f	2.25	2.1	GHz
P_t	1	1	W
L_l	-3	-3	dB
θ_t	360	0.7	deg
L	4.2	N/A	cm
W	12.57	N/A	m
G_{pt}	-8.7	47.4	dB
D_t	N/A	9	deg
e_t	0	0.05	dB
L_{pt}	0	-0.061	dB
G_t	-8.7	46.0	dBW
EIRP	-11.7	43.0	km
S	2831	2831	dB
L_s	-168.5	-167.9	dB
L_a	-0.5	-0.5	dB
D_r	9	N/A	m
G_{rp}	43.94	-8.71	dB
θ_r	1.0	360.0	deg
e_r	0.05	36	deg
L_{pr}	-0.028	-0.12	dB
G_r	43.9	-8.8	dB
T_s	115	1295	K
R	137	40	kbps
E_b/N_o	19.8	18.2	dB
C/N_o	71.2	64.2	dB
BER	10^{-5}	10^{-5}	-
Req. E_b/N_o	9.6	9.6	dB-Hz
Implementation	-2.0	-2.0	dB
Margin	8.2	6.6	dB

3.3.3.7.5 EVA link Budget

This particular link is different in that it uses an analog signal. Much of the link budget is the same, except the final margin depends on the carrier to noise ratio (C/N_o). The required C/N_o was obtained from Fortescue (pg 331). The antennae on the EVA suits were assumed to be helix antennae with a length of 20 cm and a diameter of 1 cm (Note: Johnson space flight center was contacted for this information, but sent irrelevant information).

Parameter	Downlink	Uplink	Units
f	259.7	243	MHz
P_t	0.5	0.5	W
L_l	-3	-3	dB
θ_t	180	360	deg
G_{pt}	0.5	-30.3	dB
L	0.3	0.2	m
D_t	0.21	0.01	deg
e_t	180	180	dB
L_{pt}	-12	-0.013	dB
G_t	-12.5	-30.3	dBW
EIRP	-18.5	-36.3	km
S	2	2	dB
L_s	-86.8	-86.2	dB
L	0.2	0.3	m
D_r	0.01	0.21	dB
G_{rp}	-29.41	-1.35	deg
θ_r	360	198.87	deg
e_r	180	180	dB
L_{pr}	-0.02	-9.83	dB
G_r	-29.4	-1.4	K
T_s	375	375	kbps
C/N_o	68.2	79.0	dB
Req. E_b/N_o	53.3	53.3	dB
Margin	14.9	25.7	dB-Hz

Appendix A.3.5.1 Mass Estimation Relations from NASA CR 2420

density(LH2) = 112 kg/m^3
density(LOX) = 1140 kg/m^3
density(storable) ~= 1000 kg/m^3

TANKS
W(LH2tank)(lb) = 0.4856*V(ft^3) + 800
M(LH2tank)(kg) = 0.0694*M(LH2)(kg) + 363
M(LOXtank)(kg) = 0.0152*M(LOX)(kg) + 318
M(storables tank)(kg) = 0.316*[M(contents)(kg)]^0.6
M(smalltank)(kg) = 0.1*M(contents)(kg) {Small tank -> M(content < 500 kg)}

INSULATION
M(LH2ins)(kg) = 2.88*A(tank)(m^2)
M(LOXins)(kg) = 1.123*A(tank)(m^2)

FAIRINGS AND SHROUDS
M(kg) = 32.2*A(m^2)

LIQUID ROCKET ENGINES
M(eng)(kg) = (7.81E-4)*T(N) + 3.37E-5*T(N)*[Ae(m^2)/At(m^2)]^0.5 + 59

SOLID MOTOR CASING
M(kg) = (0.007)*M(prop)(kg)

THRUST STRUCTURES
M(kg) = (2.55E-4)*T(N)

GIMBAL TORQUE
T(gimbal)(Nm) = 9.896E6*[T(perengine)(N)/Po(N/m^2)]^1.25

GIMBAL MASS
M(gimbal)(kg) = (7.58E-3)*[T(gimbal)(Nm)]^0.75

AVIONICS
M(avionics)(kg) = 40.06*[M(total gross mass of vehicle)(kg)]^0.361

ELECTRICAL WIRING
M(elec)(kg) = 1.058*{[M(total gross mass of vehicle)]^0.5}*[(max vehicle length)(m)]^0.25

Appendix A.3.5.3.1 Wing Size Selection Spreadsheet

Variable	Description
c	Effective chord length
S	Total area
Sl	Area of lower surface
Sw	Wing area
Sf	Areo of fins
b	Wing span
mc	Tip chord
hf	Height of fins
Lle	Length of leading edge of wings
lf	Length of leading edge of fins
rn	Radius of nose
rle	Radius of leading edge
rf	Radius of fins
Kn	K factor of nose
Ka	K factor of lower surface
Kf	K factor of fins
Kle	K factor of leading edge

Appendix A.3.5.3.1

V∞	alpha	Mass(kg)	g(sl,m/s^2)		L/D(max)	Pi	ULF				n(lam)	n(turb)	
8000	0.524	44000	9.81		0.000	3.14159	12				0.5	0.8	
aoa	side slip			nu	ball(min)	d2r	m2f						
30	0			551	0.00	0.01745	3.28084					leading	
	0	Dimension	(m)				length	hull	taper			edges	
S	Sl	Sw	Sf	c	b	mc	flap	dia.	ratio	hf	Lle	lf	rn
148.77	143.77	59.38	5.00	21.50	8.50	4.00	0.50	4.00	0.19	2.50	21.92	4.72	0.50
155.14	150.14	65.75	5.00	21.50	9.00	4.00	0.50	4.00	0.19	2.50	21.97	4.72	0.50
158.33	153.33	68.94	5.00	21.50	9.25	4.00	0.50	4.00	0.19	2.50	21.99	4.72	0.50
161.52	156.52	72.13	5.00	21.50	9.50	4.00	0.50	4.00	0.19	2.50	22.02	4.72	0.50
164.71	159.71	75.31	5.00	21.50	9.75	4.00	0.50	4.00	0.19	2.50	22.05	4.72	0.50
167.89	162.89	78.50	5.00	21.50	10.00	4.00	0.50	4.00	0.19	2.50	22.07	4.72	0.50
171.08	166.08	81.69	5.00	21.50	10.25	4.00	0.50	4.00	0.19	2.50	22.10	4.72	0.50
174.27	169.27	84.88	5.00	21.50	10.50	4.00	0.50	4.00	0.19	2.50	22.13	4.72	0.50
177.46	172.46	88.06	5.00	21.50	10.75	4.00	0.50	4.00	0.19	2.50	22.16	4.72	0.50
180.64	175.64	91.25	5.00	21.50	11.00	4.00	0.50	4.00	0.19	2.50	22.19	4.72	0.50
183.83	178.83	94.44	5.00	21.50	11.25	4.00	0.50	4.00	0.19	2.50	22.22	4.72	0.50
187.02	182.02	97.63	5.00	21.50	11.50	4.00	0.50	4.00	0.19	2.50	22.26	4.72	0.50
190.21	185.21	100.81	5.00	21.50	11.75	4.00	0.50	4.00	0.19	2.50	22.29	4.72	0.50
193.39	188.39	104.00	5.00	21.50	12.00	4.00	0.50	4.00	0.19	2.50	22.32	4.72	0.50
196.58	191.58	107.19	5.00	21.50	12.25	4.00	0.50	4.00	0.19	2.50	22.36	4.72	0.50
199.77	194.77	110.38	5.00	21.50	12.50	4.00	0.50	4.00	0.19	2.50	22.39	4.72	0.50
202.96	197.96	113.56	5.00	21.50	12.75	4.00	0.50	4.00	0.19	2.50	22.43	4.72	0.50
206.14	201.14	116.75	5.00	21.50	13.00	4.00	0.50	4.00	0.19	2.50	22.46	4.72	0.50
209.33	204.33	119.94	5.00	21.50	13.25	4.00	0.50	4.00	0.19	2.50	22.50	4.72	0.50
212.52	207.52	123.13	5.00	21.50	13.50	4.00	0.50	4.00	0.19	2.50	22.53	4.72	0.50
215.71	210.71	126.31	5.00	21.50	13.75	4.00	0.50	4.00	0.19	2.50	22.57	4.72	0.50
218.89	213.89	129.50	5.00	21.50	14.00	4.00	0.50	4.00	0.19	2.50	22.61	4.72	0.50

Appendix A.3.5.3.1 Wing Size Selection Spreadsheet

	Variable Description
c	Effective chord length
S	Total area
Sl	Area of lower surface
Sw	Wing area
Sf	Area of fins
b	Wing span
mc	Tip chord
hf	Height of fins
Lle	Length of leading edge of wings
lf	Length of leading edge of fins
rn	Radius of nose
rle	Radius of leading edge
rf	Radius of fins
Kn	K factor of nose
Ka	K factor of lower surface
Kf	K factor of fins
Kle	K factor of leading edge

curved surfaces

		wing	fin sweep					shape factors					
rle	rf	sweep	z	y	kn	ka	kf	kle	lam e	alpha e	lm	a1	a2
0.75	0.13	76.35	0.00	57.99	23.88	6.30	11.94	1.99	0.8416	0.4088	8.50	74.38	34.00
0.75	0.13	75.58	0.00	57.99	23.88	6.30	11.94	1.99	0.8387	0.4314	9.00	78.75	36.00
0.75	0.13	75.20	0.00	57.99	23.88	6.30	11.94	1.99	0.8373	0.4426	9.25	80.94	37.00
0.75	0.13	74.81	0.00	57.99	23.88	6.30	11.94	1.99	0.8358	0.4537	9.50	83.13	38.00
0.75	0.13	74.43	0.00	57.99	23.88	6.30	11.94	1.99	0.8343	0.4648	9.75	85.31	39.00
0.75	0.13	74.05	0.00	57.99	23.88	6.30	11.94	1.99	0.8327	0.4758	10.00	87.50	40.00
0.75	0.13	73.68	0.00	57.99	23.88	6.30	11.94	1.99	0.8311	0.4868	10.25	89.69	41.00
0.75	0.13	73.30	0.00	57.99	23.88	6.30	11.94	1.99	0.8295	0.4977	10.50	91.88	42.00
0.75	0.13	72.93	0.00	57.99	23.88	6.30	11.94	1.99	0.8279	0.5085	10.75	94.06	43.00
0.75	0.13	72.55	0.00	57.99	23.88	6.30	11.94	1.99	0.8262	0.5193	11.00	96.25	44.00
0.75	0.13	72.18	0.00	57.99	23.88	6.30	11.94	1.99	0.8245	0.5300	11.25	98.44	45.00
0.75	0.13	71.81	0.00	57.99	23.88	6.30	11.94	1.99	0.8228	0.5407	11.50	100.63	46.00
0.75	0.13	71.44	0.00	57.99	23.88	6.30	11.94	1.99	0.8210	0.5512	11.75	102.81	47.00
0.75	0.13	71.08	0.00	57.99	23.88	6.30	11.94	1.99	0.8192	0.5617	12.00	105.00	48.00
0.75	0.13	70.71	0.00	57.99	23.88	6.30	11.94	1.99	0.8174	0.5722	12.25	107.19	49.00
0.75	0.13	70.35	0.00	57.99	23.88	6.30	11.94	1.99	0.8156	0.5826	12.50	109.38	50.00
0.75	0.13	69.98	0.00	57.99	23.88	6.30	11.94	1.99	0.8137	0.5928	12.75	111.56	51.00
0.75	0.13	69.62	0.00	57.99	23.88	6.30	11.94	1.99	0.8118	0.6031	13.00	113.75	52.00
0.75	0.13	69.26	0.00	57.99	23.88	6.30	11.94	1.99	0.8099	0.6132	13.25	115.94	53.00
0.75	0.13	68.91	0.00	57.99	23.88	6.30	11.94	1.99	0.8080	0.6233	13.50	118.13	54.00
0.75	0.13	68.55	0.00	57.99	23.88	6.30	11.94	1.99	0.8061	0.6333	13.75	120.31	55.00
0.75	0.13	68.20	0.00	57.99	23.88	6.30	11.94	1.99	0.8041	0.6433	14.00	122.50	56.00

Appendix A.3.5.3.1

	Vehicle parameters					Nose equations		Wing le		Lower surface						
L/D	Cl	Cd	Cn	Ca	Cn	Ca	Cn	Ca	Cn	Ca	Ca (lam)	Ca(turb)	G (lam)	G (turb)	Re	Cn
1.4460	1.3856	0.9582	1.6790	0.1370	0.0294	0.0549	0.1276	0.0262	1.5221	0.0559	0.0941	0.0178	2.3864	1.2429	0.00	-2.18E-05
1.4414	1.3826	0.9592	1.6769	0.1394	0.0282	0.0526	0.1245	0.0274	1.5242	0.0594	0.0999	0.0189	2.3864	1.2429	0.00	-2.09E-05
1.4391	1.3811	0.9597	1.6760	0.1406	0.0276	0.0516	0.1231	0.0280	1.5253	0.0610	0.1026	0.0194	2.3864	1.2429	0.00	-2.05E-05
1.4369	1.3797	0.9602	1.6750	0.1417	0.0271	0.0505	0.1217	0.0286	1.5262	0.0626	0.1053	0.0198	2.3864	1.2429	0.00	-2.01E-05
1.4347	1.3784	0.9607	1.6741	0.1428	0.0266	0.0496	0.1204	0.0292	1.5272	0.0640	0.1078	0.0203	2.3864	1.2429	0.00	-1.97E-05
1.4326	1.3771	0.9613	1.6733	0.1439	0.0261	0.0486	0.1191	0.0298	1.5281	0.0655	0.1102	0.0208	2.3864	1.2429	0.00	-1.93E-05
1.4305	1.3759	0.9618	1.6724	0.1450	0.0256	0.0477	0.1179	0.0304	1.5290	0.0669	0.1126	0.0212	2.3864	1.2429	0.00	-1.90E-05
1.4285	1.3747	0.9623	1.6716	0.1461	0.0251	0.0468	0.1168	0.0310	1.5298	0.0682	0.1148	0.0216	2.3864	1.2429	0.00	-1.86E-05
1.4265	1.3735	0.9628	1.6709	0.1471	0.0246	0.0460	0.1156	0.0316	1.5306	0.0695	0.1170	0.0220	2.3864	1.2429	0.00	-1.83E-05
1.4246	1.3723	0.9634	1.6702	0.1481	0.0242	0.0452	0.1146	0.0322	1.5314	0.0707	0.1191	0.0224	2.3864	1.2429	0.00	-1.80E-05
1.4226	1.3712	0.9639	1.6695	0.1491	0.0238	0.0444	0.1135	0.0328	1.5322	0.0719	0.1211	0.0227	2.3864	1.2429	0.00	-1.77E-05
1.4207	1.3702	0.9644	1.6688	0.1501	0.0234	0.0436	0.1125	0.0334	1.5329	0.0731	0.1230	0.0231	2.3864	1.2429	0.00	-1.74E-05
1.4189	1.3691	0.9649	1.6682	0.1511	0.0230	0.0429	0.1116	0.0340	1.5336	0.0742	0.1249	0.0234	2.3864	1.2429	0.00	-1.71E-05
1.4170	1.3681	0.9655	1.6675	0.1521	0.0226	0.0422	0.1107	0.0346	1.5343	0.0753	0.1268	0.0238	2.3864	1.2429	0.00	-1.68E-05
1.4152	1.3671	0.9660	1.6669	0.1530	0.0223	0.0415	0.1098	0.0352	1.5349	0.0763	0.1285	0.0241	2.3864	1.2429	0.00	-1.65E-05
1.4134	1.3661	0.9665	1.6664	0.1540	0.0219	0.0409	0.1089	0.0358	1.5356	0.0773	0.1302	0.0244	2.3864	1.2429	0.00	-1.63E-05
1.4117	1.3652	0.9671	1.6658	0.1549	0.0216	0.0402	0.1081	0.0364	1.5362	0.0783	0.1319	0.0247	2.3864	1.2429	0.00	-1.60E-05
1.4100	1.3643	0.9676	1.6653	0.1558	0.0212	0.0396	0.1073	0.0370	1.5368	0.0793	0.1335	0.0250	2.3864	1.2429	0.00	-1.58E-05
1.4083	1.3634	0.9681	1.6648	0.1567	0.0209	0.0390	0.1065	0.0376	1.5374	0.0802	0.1351	0.0253	2.3864	1.2429	0.00	-1.55E-05
1.4066	1.3625	0.9687	1.6643	0.1576	0.0206	0.0384	0.1058	0.0382	1.5379	0.0811	0.1366	0.0256	2.3864	1.2429	0.00	-1.53E-05
1.4049	1.3616	0.9692	1.6638	0.1585	0.0203	0.0378	0.1050	0.0388	1.5385	0.0819	0.1380	0.0258	2.3864	1.2429	0.00	-1.51E-05
1.4033	1.3608	0.9697	1.6633	0.1594	0.0200	0.0373	0.1043	0.0394	1.5390	0.0828	0.1395	0.0261	2.3864	1.2429	0.00	-1.48E-05

Appendix A.3.5.3.1

vertical fin			wing mass				
Ca	gvw(lb)	span(ft)	alpha	weight(lb)	mass(kg)	ball param	b
1.36E-05	97004	27.89	4.22E+09	2065.70	937.40	319.40	8.50
1.31E-05	97004	29.53	4.94E+09	2275.57	1032.63	305.52	9.00
1.28E-05	97004	30.35	5.33E+09	2381.36	1080.64	299.01	9.25
1.26E-05	97004	31.17	5.72E+09	2487.73	1128.91	292.76	9.50
1.23E-05	97004	31.99	6.13E+09	2594.66	1177.43	286.76	9.75
1.21E-05	97004	32.81	6.56E+09	2702.16	1226.21	281.00	10.00
1.19E-05	97004	33.63	6.99E+09	2810.23	1275.25	275.46	10.25
1.17E-05	97004	34.45	7.44E+09	2918.85	1324.55	270.13	10.50
1.14E-05	97004	35.27	7.91E+09	3028.03	1374.09	264.99	10.75
1.12E-05	97004	36.09	8.38E+09	3137.75	1423.88	260.04	11.00
1.10E-05	97004	36.91	8.87E+09	3248.02	1473.92	255.26	11.25
1.09E-05	97004	37.73	9.38E+09	3358.83	1524.20	250.66	11.50
1.07E-05	97004	38.55	9.89E+09	3470.17	1574.73	246.21	11.75
1.05E-05	97004	39.37	1.04E+10	3582.03	1625.49	241.91	12.00
1.03E-05	97004	40.19	1.10E+10	3694.41	1676.49	237.75	12.25
1.02E-05	97004	41.01	1.15E+10	3807.30	1727.72	233.73	12.50
1.00E-05	97004	41.83	1.21E+10	3920.70	1779.18	229.84	12.75
9.85E-06	97004	42.65	1.27E+10	4034.60	1830.86	226.08	13.00
9.70E-06	97004	43.47	1.33E+10	4148.99	1882.77	222.43	13.25
9.55E-06	97004	44.29	1.39E+10	4263.87	1934.90	218.89	13.50
9.41E-06	97004	45.11	1.45E+10	4379.23	1987.25	215.46	13.75
9.28E-06	97004	45.93	1.51E+10	4495.07	2039.82	212.13	14.00

Appendix 3.6.3.2 Mass and Cost Analysis on Various Power Sources

	Solar Energy	Nuclear Energy	Fuel Cells	Batteries	
Specific Power (W/kg)	50	100	75	350	Wh/kg
Specific Cost ($FY92/W)	2500	500	120	40	$/Wh
Cost per kg	125000	50000	9000	14000	$/kg
		13500 for shielding			
Mass (kg)					
Days	Solar Arrays	Nuclear Reactors	Fuel Cells	Batteries	
1	760	14200	176	480	
2	776	14200	260	960	
3	800	14200	343	1440	
5	848	14200	509	2400	
10	905	14200	925	4800	
15	992	14200	1341	7200	
Cost ($FY94)					
Days	Solar Arrays	Nuclear Reactors	Fuel Cells	Batteries	
1	102	761	2	7	
2	104	761	3	14	
3	107	761	3	22	
5	114	761	5	36	
10	121	761	9	72	
15	133	761	13	108	

Appendix A.4.5.4 Third Stage Mass Spreadsheet

Load (kg.)	Drag from glider		**R (m)**	**Drag (N)**
51000.00	34738.10			
			1.88	0.00
Rigidity requirements Hz.			1.90	0.00
axial	bending		1.92	0.00
20.00	20.00		1.94	0.00
			1.96	0.00
Load Factors			1.98	0.00
axial	lateral	**Ellipse**	2.00	0.00
7.00	6.00	**Info**	2.02	698.24
			2.04	1403.42
Vreq. LH2 (m^3)	**Mass LH2 (kg.)**	**k = r/b**	2.06	2115.55
131.48	8366.67	2.00	2.08	2834.63
Vreq. LOx (m^3)	**Mass LOx (kg.)**		2.10	3560.66
40.37	41833.33	**E'**	2.12	4293.63
		5.52	2.14	5033.55
Initial LH2 Tank mass assumption (kg)			2.16	5780.42
943.65		**e**	2.18	6534.24
Initial LOx Tank mass assumption (kg)		0.87	2.20	7295.00
445.17			**2.22**	**8062.71**
		K	2.24	8837.37
Al 2024 properties		1.50	2.26	9618.98
E (N/m^2)	72000000000.00		2.28	10407.53
Ftu (N/m^2)	482000000.00		2.30	11203.04
Fyu (N/m^2)	413000000.00		2.32	12005.49
density (kg/m^3)	2770.00		2.34	12814.88
			2.36	13631.23
Pressure LOx (N/m^2)	Pressure LH2 (N/m^2)		2.38	14454.52
450000.00	520000.00		2.40	15284.76
			2.42	16121.95
Stage Inert Weight(kg.)			2.44	16966.09
8860.00			2.46	17817.17
			2.48	18675.20
			2.50	19540.18
			2.52	20412.11
			2.54	21290.98

Appendix A.4.5.4 Third Stage Mass Spreadsheet

			Top Fairing					
L (M)	t axial rigidity (mm)	t bending rigidity (mm)	Equivalent Load (MN)	t: ult. strength LH2 (mm.)	Max. t (mm)	R/t	Ncr. (MN)	Mass
2.84	0.0065	0.0059	8.39	2.72	2.72	692.45	16.35	262.31
2.85	0.0065	0.0058	8.35	2.68	2.68	710.15	15.95	262.16
2.86	0.0064	0.0057	8.32	2.64	2.64	728.10	15.56	262.03
2.87	0.0064	0.0056	8.29	2.60	2.60	746.28	15.19	261.91
2.88	0.0063	0.0054	8.25	2.56	2.56	764.71	14.83	261.81
2.89	0.0063	0.0053	8.22	2.53	2.53	783.38	14.48	261.72
2.90	0.0062	0.0052	8.19	2.49	2.49	802.29	14.15	261.64
2.91	0.0062	0.0051	8.16	2.46	2.46	821.44	13.83	261.57
2.92	0.0062	0.0050	8.13	2.43	2.43	840.84	13.52	261.52
2.93	0.0061	0.0049	8.10	2.39	2.39	860.48	13.22	261.48
2.94	0.0061	0.0048	8.07	2.36	2.36	880.36	12.93	261.45
2.95	0.0060	0.0048	8.05	2.33	2.33	900.49	12.65	261.43
2.96	0.0060	0.0047	8.02	2.30	2.30	920.86	12.39	261.42
2.97	0.0060	0.0046	7.99	2.27	2.27	941.47	12.13	261.43
2.98	0.0059	0.0045	7.97	2.24	2.24	962.33	11.88	261.44
2.99	0.0059	0.0044	7.94	2.22	2.22	983.43	11.64	261.46
3.00	0.0059	0.0044	7.91	2.19	2.19	1004.78	11.40	261.50
3.01	**0.0058**	**0.0043**	**7.89**	**2.16**	**2.16**	**1026.37**	**11.18**	**261.54**
3.02	0.0058	0.0042	7.87	2.14	2.14	1048.20	10.96	261.60
3.03	0.0058	0.0041	7.84	2.11	2.11	1070.28	10.75	261.66
3.04	0.0057	0.0041	7.82	2.09	2.09	1092.61	10.54	261.73
3.05	0.0057	0.0040	7.79	2.06	2.06	1115.18	10.34	261.81
3.06	0.0057	0.0039	7.77	2.04	2.04	1138.00	10.15	261.90
3.07	0.0056	0.0039	7.75	2.02	2.02	1161.06	9.96	261.99
3.08	0.0056	0.0038	7.73	1.99	1.99	1184.37	9.78	262.10
3.09	0.0056	0.0038	7.70	1.97	1.97	1207.92	9.61	262.21
3.10	0.0056	0.0037	7.68	1.95	1.95	1231.72	9.44	262.33
3.11	0.0055	0.0036	7.66	1.93	1.93	1255.77	9.27	262.45
3.12	0.0055	0.0036	7.64	1.91	1.91	1280.06	9.11	262.59
3.13	0.0055	0.0035	7.62	1.89	1.89	1304.60	8.95	262.73
3.14	0.0054	0.0035	7.60	1.87	1.87	1329.39	8.80	262.88
3.15	0.0054	0.0034	7.58	1.85	1.85	1354.43	8.65	263.03
3.16	0.0054	0.0034	7.56	1.83	1.83	1379.71	8.51	263.19
3.17	0.0054	0.0033	7.54	1.81	1.81	1405.24	8.37	263.36

Appendix A.4.5.4 Third Stage Mass Spreadsheet

INTER-TANK FAIRING									
L (M)	t axial rigidity (mm)	t bending rigidity (mm)	Equivalent Load (MN)	t: ult. strength LH2 (mm.)	Max. t (mm)	R/t	Ncr. (MN)	Mass	L (M)
2.38	0.0054	0.0035	9.99	3.23	3.23	581.24	24.53	261.88	3.15
2.40	0.0054	0.0035	9.94	3.18	3.18	596.84	23.84	262.68	3.16
2.42	0.0054	0.0034	9.89	3.13	3.13	612.56	23.19	263.54	3.17
2.44	0.0054	0.0034	9.84	3.09	3.09	628.41	22.58	264.44	3.18
2.46	0.0054	0.0034	9.80	3.04	3.04	644.40	22.00	265.38	3.19
2.48	0.0054	0.0034	9.75	3.00	3.00	660.51	21.44	266.36	3.20
2.50	0.0054	0.0034	9.71	2.96	2.96	676.76	20.92	267.39	3.21
2.52	0.0054	0.0033	9.68	2.92	2.92	692.38	20.47	268.74	3.22
2.54	0.0054	0.0033	9.66	2.88	2.88	708.10	20.04	270.13	3.23
2.56	0.0053	0.0033	9.63	2.85	2.85	723.90	19.63	271.56	3.24
2.58	0.0053	0.0033	9.61	2.81	2.81	739.80	19.25	273.03	3.25
2.60	0.0053	0.0033	9.59	2.78	2.78	755.78	18.87	274.53	3.26
2.62	0.0053	0.0032	9.57	2.75	2.75	771.85	18.52	276.06	3.27
2.64	0.0053	0.0032	9.55	2.72	2.72	788.02	18.18	277.63	3.28
2.66	0.0053	0.0032	9.53	2.69	2.69	804.27	17.86	279.23	3.29
2.68	0.0053	0.0032	9.52	2.66	2.66	820.61	17.55	280.86	3.30
2.70	0.0053	0.0032	9.50	2.63	2.63	837.04	17.25	282.51	3.31
2.72	**0.0053**	**0.0032**	**9.49**	**2.60**	**2.60**	**853.56**	**16.97**	**284.19**	**3.32**
2.74	0.0053	0.0031	9.47	2.57	2.57	870.17	16.69	285.90	3.33
2.76	0.0053	0.0031	9.46	2.55	2.55	886.87	16.43	287.63	3.34
2.78	0.0052	0.0031	9.45	2.52	2.52	903.66	16.18	289.39	3.35
2.80	0.0052	0.0031	9.44	2.50	2.50	920.54	15.93	291.17	3.36
2.82	0.0052	0.0031	9.43	2.47	2.47	937.50	15.70	292.97	3.37
2.84	0.0052	0.0031	9.43	2.45	2.45	954.55	15.47	294.80	3.38
2.86	0.0052	0.0031	9.42	2.43	2.43	971.69	15.26	296.64	3.39
2.88	0.0052	0.0030	9.41	2.41	2.41	988.91	15.05	298.51	3.40
2.90	0.0052	0.0030	9.41	2.39	2.39	1006.23	14.84	300.40	3.41
2.92	0.0052	0.0030	9.40	2.36	2.36	1023.63	14.65	302.30	3.42
2.94	0.0052	0.0030	9.40	2.34	2.34	1041.11	14.46	304.23	3.43
2.96	0.0052	0.0030	9.39	2.32	2.32	1058.68	14.27	306.17	3.44
2.98	0.0052	0.0030	9.39	2.30	2.30	1076.34	14.10	308.14	3.45
3.00	0.0052	0.0030	9.39	2.29	2.29	1093.79	13.93	310.20	3.46
3.02	0.0052	0.0030	9.40	2.27	2.27	1110.53	13.80	312.50	3.47
3.04	0.0052	0.0029	9.40	2.25	2.25	1127.35	13.67	314.81	3.48

Appendix A.4.5.4 Third Stage Mass Spreadsheet

		Nozzle Shroud							
t axial rigidity (mm)	t bending rigidity (mm)	Equivalent Load (MN)	t: ult. strength LH2 (mm.)	Max. t (mm)	R/t	Ncr. (MN)	Mass	L LH2(m)	L LOx(m)
0.0072	0.0081	18.86	6.10	6.10	307.98	59.66	653.74	10.59	2.38
0.0072	0.0079	18.72	6.00	6.00	316.83	57.26	651.12	10.33	2.29
0.0071	0.0077	18.59	5.89	5.89	325.80	55.00	648.65	10.07	2.21
0.0071	0.0075	18.47	5.79	5.79	334.87	52.87	646.32	9.83	2.12
0.0070	0.0074	18.35	5.70	5.70	344.05	50.87	644.13	9.59	2.04
0.0070	0.0072	18.23	5.60	5.60	353.34	48.97	642.07	9.35	1.96
0.0069	0.0071	18.12	5.51	5.51	362.74	47.19	640.13	9.13	1.88
0.0069	0.0069	18.02	5.43	5.43	372.00	45.57	638.73	8.91	1.80
0.0068	0.0068	17.93	5.35	5.35	381.29	44.06	637.55	8.70	1.73
0.0068	0.0067	17.85	5.27	5.27	390.65	42.64	636.50	8.49	1.65
0.0067	0.0065	17.77	5.20	5.20	400.11	41.28	635.54	8.29	1.58
0.0067	0.0064	17.69	5.13	5.13	409.65	39.99	634.66	8.09	1.51
0.0066	0.0063	17.61	5.06	5.06	419.30	38.76	633.88	7.90	1.45
0.0066	0.0062	17.54	4.99	4.99	429.03	37.60	633.17	7.71	1.38
0.0066	0.0061	17.47	4.92	4.92	438.86	70.21	632.53	7.53	1.31
0.0065	0.0059	17.40	4.86	4.86	448.78	68.58	631.97	7.35	1.25
0.0065	0.0058	17.33	4.80	4.80	458.80	67.01	631.48	7.18	1.19
0.0064	**0.0057**	**17.27**	**4.73**	**4.73**	**468.91**	**65.51**	**631.06**	**7.01**	**1.13**
0.0064	0.0056	17.21	4.68	4.68	479.11	64.07	630.70	6.85	1.07
0.0064	0.0055	17.15	4.62	4.62	489.40	62.69	630.40	6.69	1.01
0.0063	0.0054	17.09	4.56	4.56	499.78	61.36	630.16	6.53	0.95
0.0063	0.0053	17.03	4.51	4.51	510.26	60.08	629.97	6.38	0.90
0.0062	0.0052	16.98	4.45	4.45	520.83	58.85	629.84	6.23	0.84
0.0062	0.0052	16.93	4.40	4.40	531.49	57.66	629.76	6.08	0.79
0.0062	0.0051	16.88	4.35	4.35	542.24	56.52	629.73	5.94	0.73
0.0061	0.0050	16.83	4.30	4.30	553.08	55.42	629.74	5.80	0.68
0.0061	0.0049	16.78	4.26	4.26	564.01	54.36	629.81	5.67	0.63
0.0061	0.0048	16.73	4.21	4.21	575.03	53.34	629.91	5.53	0.58
0.0060	0.0048	16.69	4.16	4.16	586.15	52.35	630.06	5.40	0.53
0.0060	0.0047	16.65	4.12	4.12	597.35	51.40	630.26	5.28	0.48
0.0060	0.0046	16.60	4.07	4.07	608.65	50.48	630.49	5.15	0.44
0.0060	0.0045	16.56	4.03	4.03	619.93	49.61	630.86	5.03	0.39
0.0059	0.0045	16.54	3.99	3.99	631.02	48.81	631.55	4.91	0.34
0.0059	0.0044	16.51	3.96	3.96	642.20	48.04	632.26	4.79	0.30

Appendix A.4.5.4 Third Stage Mass Spreadsheet

		TANKS						
T ellipse LH2	t LH2 : axial rigidity (mm.)	T ellipse LOx	t LOx: axial rigidity (mm.)	t LH2: bending rigidity (mm.)	t LOx: bending rigidity (mm.)	Equivalent Load LH2 (MN)	Equivalent Load LOx (MN)	t: ult. strength LH2 (mm.)
2.80	0.08	2.96	0.04	0.96	0.01	42.48	13.85	13.75
2.83	0.07	2.99	0.03	0.87	0.00	41.25	13.50	13.21
2.86	0.07	3.03	0.03	0.78	0.00	40.07	13.17	12.70
2.89	0.07	3.06	0.03	0.70	0.00	38.94	12.86	12.22
2.92	0.07	3.09	0.03	0.63	0.00	37.85	12.56	11.75
2.95	0.06	3.12	0.03	0.57	0.00	36.81	12.26	11.32
2.98	0.06	3.15	0.03	0.51	0.00	35.81	11.98	10.90
3.00	0.06	3.18	0.03	0.46	0.00	34.87	11.72	10.51
3.03	0.06	3.21	0.03	0.42	0.00	33.97	11.47	10.14
3.06	0.06	3.25	0.03	0.38	0.00	33.10	11.23	9.78
3.09	0.05	3.28	0.03	0.34	0.00	32.27	11.00	9.44
3.12	0.05	3.31	0.02	0.31	0.00	31.47	10.78	9.12
3.15	0.05	3.34	0.02	0.28	0.00	30.70	10.57	8.81
3.18	0.05	3.37	0.02	0.25	0.00	29.95	10.36	8.52
3.21	0.05	3.40	0.02	0.23	0.00	29.24	10.16	8.24
3.24	0.05	3.43	0.02	0.21	0.00	28.54	9.97	7.97
3.27	0.04	3.47	0.02	0.19	0.00	27.88	9.79	7.71
3.30	**0.04**	**3.50**	**0.02**	**0.17**	**0.00**	**27.24**	**9.61**	**7.47**
3.33	0.04	3.53	0.02	0.15	0.00	26.62	9.44	7.23
3.36	0.04	3.56	0.02	0.14	0.00	26.02	9.27	7.01
3.39	0.04	3.59	0.02	0.13	0.00	25.44	9.11	6.79
3.42	0.04	3.62	0.02	0.12	0.00	24.89	8.96	6.59
3.45	0.04	3.66	0.02	0.10	0.00	24.35	8.81	6.39
3.48	0.04	3.69	0.02	0.09	0.00	23.83	8.67	6.20
3.51	0.03	3.72	0.02	0.09	0.00	23.33	8.53	6.02
3.54	0.03	3.75	0.02	0.08	0.00	22.84	8.39	5.84
3.57	0.03	3.78	0.02	0.07	0.00	22.37	8.26	5.67
3.60	0.03	3.81	0.01	0.06	0.00	21.92	8.14	5.51
3.63	0.03	3.84	0.01	0.06	0.00	21.48	8.02	5.36
3.66	0.03	3.88	0.01	0.05	0.00	21.05	7.90	5.21
3.69	0.03	3.91	0.01	0.05	0.00	20.64	7.79	5.07
3.72	0.03	3.94	0.01	0.04	0.00	20.25	7.68	4.93
3.75	0.03	3.97	0.01	0.04	0.00	19.86	7.57	4.80
3.78	0.03	4.00	0.01	0.04	0.00	19.49	7.47	4.67

Appendix A.4.5.4 Third Stage Mass Spreadsheet

t: ult. strength LOx (mm.)	t: yeild strength LH2 (mm.)	t: yeild strength LOx (mm.)	t: ult. hoop stress LH2 (mm.)	t: ult. hoop stress LOx (mm.)	t: yeild hoop stress LH2 (mm.)	t: yeild hoop stress LOx (mm.)	Max t so far LH2 (mm.)	Max t so far LOx (mm.)
4.48	12.84	4.19	3.74	3.26	3.03	3.05	13.75	4.48
4.33	12.34	4.04	3.78	3.30	3.06	3.08	13.21	4.33
4.18	11.86	3.90	3.82	3.33	3.09	3.11	12.70	4.18
4.03	11.41	3.77	3.86	3.36	3.12	3.14	12.22	4.03
3.90	10.98	3.64	3.90	3.40	3.15	3.17	11.75	3.90
3.77	10.57	3.52	3.94	3.43	3.19	3.21	11.32	3.77
3.65	10.18	3.41	3.98	3.47	3.22	3.24	10.90	3.65
3.53	9.81	3.30	4.02	3.50	3.25	3.27	10.51	3.53
3.42	9.47	3.20	4.06	3.54	3.28	3.30	10.14	3.54
3.32	9.13	3.10	4.10	3.57	3.32	3.33	9.78	3.57
3.22	8.82	3.01	4.14	3.60	3.35	3.37	9.44	3.60
3.12	8.52	2.92	4.18	3.64	3.38	3.40	9.12	3.64
3.03	8.23	2.83	4.22	3.67	3.41	3.43	8.81	3.67
2.95	7.96	2.75	4.26	3.71	3.44	3.46	8.52	3.71
2.86	7.69	2.67	4.30	3.74	3.48	3.49	8.24	3.74
2.78	7.44	2.60	4.34	3.77	3.51	3.53	7.97	3.77
2.71	7.20	2.53	4.38	3.81	3.54	3.56	7.71	3.81
2.63	**6.97**	**2.46**	**4.42**	**3.84**	**3.57**	**3.59**	**7.47**	**3.84**
2.56	6.75	2.39	4.46	3.88	3.60	3.62	7.23	3.88
2.50	6.54	2.33	4.50	3.91	3.64	3.65	7.01	3.91
2.43	6.34	2.27	4.54	3.95	3.67	3.69	6.79	3.95
2.37	6.15	2.21	4.58	3.98	3.70	3.72	6.59	3.98
2.31	5.97	2.16	4.62	4.01	3.73	3.75	6.39	4.01
2.25	5.79	2.11	4.66	4.05	3.76	3.78	6.20	4.05
2.20	5.62	2.05	4.70	4.08	3.80	3.81	6.02	4.08
2.15	5.46	2.00	4.74	4.12	3.83	3.84	5.84	4.12
2.10	5.30	1.96	4.78	4.15	3.86	3.88	5.67	4.15
2.05	5.15	1.91	4.82	4.19	3.89	3.91	5.51	4.19
2.00	5.00	1.87	4.86	4.22	3.93	3.94	5.36	4.22
1.96	4.86	1.83	4.90	4.25	3.96	3.97	5.21	4.25
1.91	4.73	1.79	4.94	4.29	3.99	4.00	5.07	4.29
1.87	4.60	1.75	4.98	4.32	4.02	4.04	4.98	4.32
1.83	4.48	1.71	5.02	4.36	4.05	4.07	5.02	4.36
1.79	4.36	1.67	5.05	4.39	4.09	4.10	5.05	4.39

Appendix A.4.5.4 Third Stage Mass Spreadsheet

R/t LH2	R/t LOx	Ncr. with pressure LH2(MN)	Ncr. with pressure LO2(MN)	L/D LH2	L/D LOx	Mass LH2 Tank(kg)	Mass LH2 insulation estimate	Mass LOx Tank(kg)
136.70	419.35	495.46	49.91	3.82	1.63	6167.47	402.75	759.03
143.79	439.22	451.51	48.22	3.72	1.60	5882.65	398.12	730.98
151.16	459.74	412.29	44.92	3.62	1.57	5614.67	393.57	704.51
158.81	480.91	377.24	41.91	3.53	1.55	5362.37	389.10	679.49
166.75	502.74	345.90	39.16	3.45	1.52	5124.66	384.71	655.85
174.99	525.24	317.85	36.65	3.36	1.49	4900.55	380.40	633.48
183.53	548.41	292.71	34.35	3.28	1.47	4689.13	376.16	612.30
192.25	571.85	270.62	32.29	3.21	1.45	4492.64	372.00	592.68
201.28	577.01	250.77	32.73	3.13	1.42	4306.98	367.90	592.92
210.62	577.09	232.93	33.84	3.06	1.40	4131.44	363.87	598.48
220.28	577.16	216.90	35.00	2.99	1.38	3965.37	359.91	604.15
230.26	577.24	202.47	36.20	2.93	1.36	3808.17	356.01	609.93
240.57	577.31	189.49	37.45	2.86	1.34	3659.27	352.17	615.83
251.22	577.38	177.80	38.76	2.80	1.32	3518.15	348.39	621.84
262.21	577.45	167.29	40.12	2.74	1.30	3384.34	344.67	627.97
273.55	577.52	157.83	41.55	2.69	1.29	3257.38	341.00	634.22
285.25	577.58	149.31	43.05	2.63	1.27	3136.86	337.39	640.58
297.30	**577.64**	**141.66**	**44.63**	**2.58**	**1.25**	**3022.39**	**333.83**	**647.06**
309.73	577.70	134.78	46.30	2.53	1.24	2913.61	330.32	653.66
322.52	577.76	128.60	48.07	2.48	1.22	2810.18	326.86	660.38
335.69	577.82	123.05	49.97	2.43	1.21	2711.79	323.45	667.22
349.25	577.88	118.09	52.00	2.39	1.19	2618.14	320.09	674.19
363.20	577.93	113.65	54.19	2.34	1.18	2528.97	316.77	681.27
377.55	577.99	109.69	56.57	2.30	1.17	2444.02	313.50	688.49
392.29	578.04	106.16	59.17	2.26	1.16	2363.05	310.27	695.83
407.45	578.09	103.03	62.05	2.22	1.14	2285.84	307.08	703.29
423.02	578.14	100.27	65.27	2.18	1.13	2212.18	303.93	710.88
439.00	578.19	97.41	68.92	2.14	1.12	2141.87	300.82	718.61
455.41	578.24	91.83	73.11	2.11	1.11	2074.74	297.75	726.46
472.25	578.28	86.65	78.00	2.07	1.10	2010.61	294.72	734.44
489.52	578.33	81.82	83.82	2.04	1.09	1949.33	291.73	742.56
502.47	578.37	79.02	90.94	2.01	1.08	1908.64	288.77	750.80
502.48	578.42	81.01	99.88	1.97	1.07	1918.33	285.84	759.19
502.49	578.46	83.03	111.54	1.94	1.06	1928.18	282.95	767.70

Appendix A.4.5.4 Third Stage Mass Spreadsheet

Mass LOx insulation estimate	M total	R (m)	L total			
123.60	8630.78	1.88	26.35			
121.91	8309.62	1.90	25.97			
120.24	8007.20	1.92	25.60			
118.59	7722.22	1.94	25.25			
116.96	7453.50	1.96	24.90			
115.35	7199.94	1.98	24.57			
113.77	6960.51	2.00	24.24			
112.20	6738.56	2.02	23.93			
110.65	6547.64	2.04	23.63			
109.12	6372.44	2.06	23.34			
107.60	6207.04	2.08	23.05			
106.10	6050.83	2.10	22.77			
104.62	5903.25	2.12	22.51			
103.16	5763.76	2.14	22.25			
101.70	5631.88	2.16	22.00			
100.27	5507.16	2.18	21.75			
98.84	5389.16	2.20	21.51			
97.43	**5277.50**	**2.22**	**21.28**			
96.03	5171.81	2.24	21.06			
94.65	5071.75	2.26	20.84			
93.28	4977.01	2.28	20.63			
91.91	4887.28	2.30	20.43			
90.56	4802.28	2.32	20.23			
89.22	4721.77	2.34	20.03			
87.89	4645.50	2.36	19.85			
86.58	4573.25	2.38	19.66			
85.27	4504.79	2.40	19.49			
83.97	4439.94	2.42	19.31			
82.67	4378.51	2.44	19.14			
81.39	4320.33	2.46	18.98			
80.12	4265.23	2.48	18.82			
78.85	4231.16	2.50	18.67			
77.59	4248.20	2.52	18.51			
76.34	4265.61	2.54	18.37			

Appendix A.4.5.4 Third Stage Mass Spreadsheet

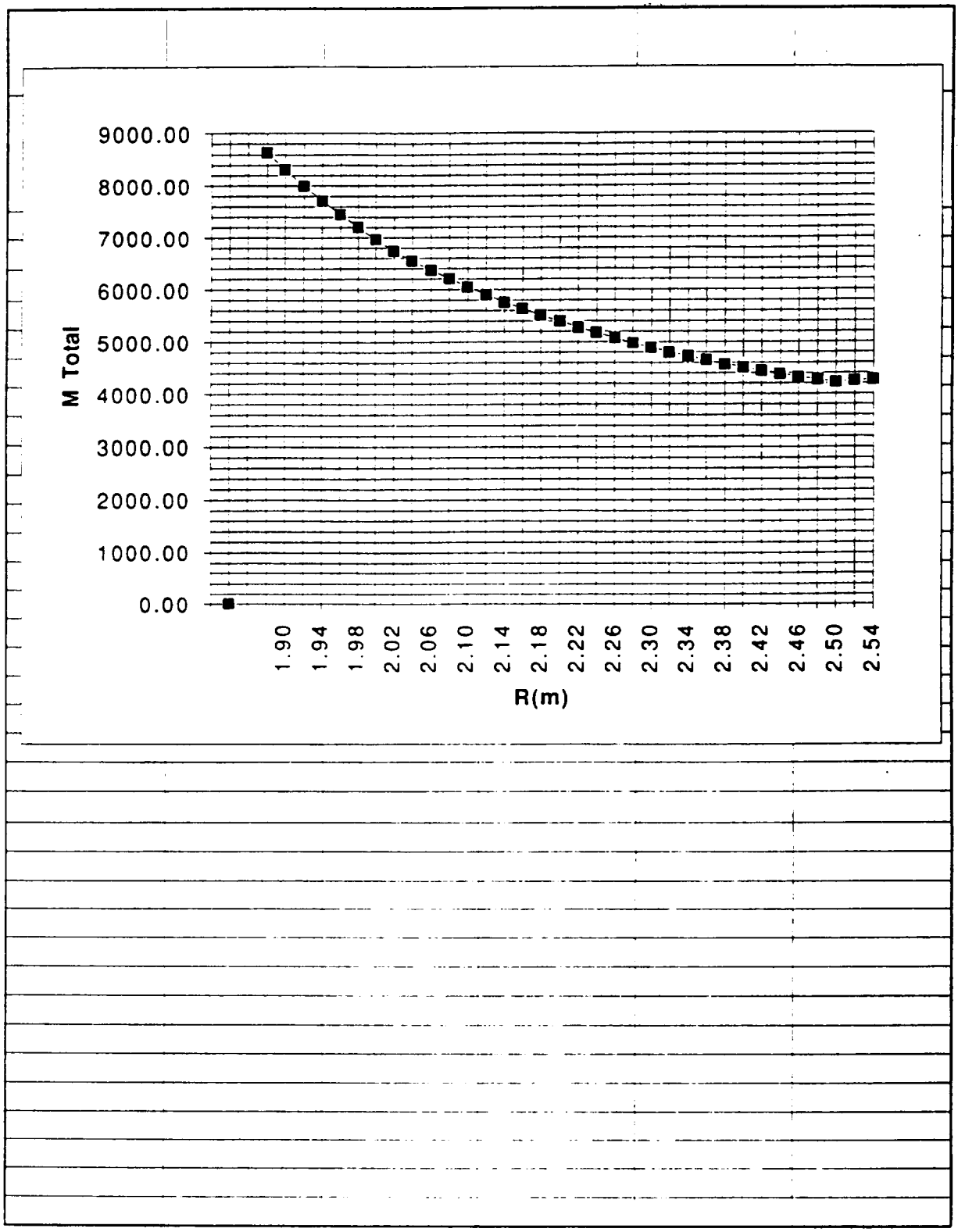

Appendix A.4.5.5 Module Mass Spreadsheet

			R (m)	Drag (N)
Load (kg.)	3.37			
220260.00				
			3.82	91989.96
Rigidity requirements Hz.			3.84	93320.43
axial	bending		3.86	94657.84
20.00	20.00	V LOx Sphere	3.88	96002.21
		3.37	3.90	97353.52
Load Factors			3.92	98711.78
axial	lateral	**Ellipse**	3.94	100076.99
7.00	6.00	**Info**	3.96	101449.14
			3.98	102828.24
Vreq. LH2 (m^3)	**Mass LH2 (kg.)**	**k = r/b**	4.00	104214.29
520.19	36413.33	2.00	**4.02**	**105607.29**
Vreq. LOx (m^3)	**Mass LOx (kg.)**		4.04	107007.24
159.71	182066.67	**E'**	4.06	108414.13
		5.52	4.08	109827.97
LH2 Tank mass assumption (kg)			4.10	111248.76
2890.09		**e**	4.12	112676.49
LOx Tank mass assumption (kg)		0.87	4.14	114111.18
871.48			4.16	115552.81
		K	4.18	117001.39
Al 2024 properties		1.20	4.20	118456.91
E (N/m^2)	72000000000.00		4.22	119919.39
Ftu (N/m^2)	482000000.00		4.24	121388.81
Fyu (N/m^2)	413000000.00		4.26	122865.18
density (kg/m^3)	2770.00		4.28	124348.50
			4.30	125838.76
Pressure LOx (N/m^2)	Pressure LH2 (N/m^2)		4.32	127335.97
390000.00	520000.00		4.34	128840.13
			4.36	130351.24
Stage Inert Mass (kg.)			4.38	131869.29
38560.00			4.40	133394.30
			4.42	134926.25
			4.44	136465.14
			4.46	138010.99
			4.48	139563.78
			4.50	175861.62

Appendix A.4.5.5 Module Mass Spreadsheet

			Top Fairing						
L (M)	t axial rigidity (mm)	t bending rigidity (mm)	Equivalent Load (MN)	t: ult. strength LH2 (mm.)	Max. t (mm)	R/t	Ncr. (MN)	Mass	L (M)
3.85	0.0043	0.0018	28.19	4.49	4.49	850.47	88.16	1195.37	4.32
3.86	0.0043	0.0017	28.16	4.46	4.46	860.45	87.26	1197.01	4.34
3.87	0.0043	0.0017	28.12	4.43	4.43	870.48	86.36	1198.67	4.36
3.88	0.0043	0.0017	28.09	4.41	4.41	880.58	85.49	1200.33	4.38
3.89	0.0043	0.0017	28.06	4.38	4.38	890.73	84.63	1202.00	4.40
3.90	0.0043	0.0017	28.02	4.35	4.35	900.95	83.78	1203.68	4.42
3.91	0.0043	0.0017	27.99	4.32	4.32	911.22	82.95	1205.36	4.44
3.92	0.0043	0.0017	27.96	4.30	4.30	921.56	82.13	1207.05	4.46
3.93	0.0042	0.0017	27.93	4.27	4.27	931.96	81.33	1208.75	4.48
3.94	0.0042	0.0016	27.90	4.24	4.24	942.41	80.53	1210.45	4.50
3.95	**0.0042**	**0.0016**	**27.86**	**4.22**	**4.22**	**952.93**	**79.76**	**1212.16**	**4.52**
3.96	0.0042	0.0016	27.83	4.19	4.19	963.50	78.99	1213.88	4.54
3.97	0.0042	0.0016	27.80	4.17	4.17	974.14	78.24	1215.61	4.56
3.98	0.0042	0.0016	27.77	4.14	4.14	984.84	77.50	1217.34	4.58
3.99	0.0042	0.0016	27.74	4.12	4.12	995.59	76.77	1219.07	4.60
4.00	0.0042	0.0016	27.71	4.09	4.09	1006.41	76.06	1220.82	4.62
4.01	0.0042	0.0016	27.68	4.07	4.07	1017.29	75.35	1222.57	4.64
4.02	0.0042	0.0015	27.65	4.05	4.05	1028.23	74.66	1224.32	4.66
4.03	0.0041	0.0015	27.62	4.02	4.02	1039.22	73.98	1226.09	4.68
4.04	0.0041	0.0015	27.60	4.00	4.00	1050.28	73.30	1227.85	4.70
4.05	0.0041	0.0015	27.57	3.98	3.98	1061.40	72.64	1229.63	4.72
4.06	0.0041	0.0015	27.54	3.95	3.95	1072.58	71.99	1231.41	4.74
4.07	0.0041	0.0015	27.51	3.93	3.93	1083.82	71.35	1233.19	4.76
4.08	0.0041	0.0015	27.48	3.91	3.91	1095.12	70.72	1234.98	4.78
4.09	0.0041	0.0015	27.46	3.89	3.89	1106.47	70.10	1236.78	4.80
4.10	0.0041	0.0015	27.43	3.86	3.86	1117.89	69.49	1238.58	4.82
4.11	0.0041	0.0015	27.40	3.84	3.84	1129.37	68.88	1240.38	4.84
4.12	0.0041	0.0014	27.38	3.82	3.82	1140.91	68.29	1242.20	4.86
4.13	0.0041	0.0014	27.35	3.80	3.80	1152.51	67.70	1244.01	4.88
4.14	0.0040	0.0014	27.32	3.78	3.78	1164.17	67.13	1245.83	4.90
4.15	0.0040	0.0014	27.30	3.76	3.76	1175.89	66.56	1247.66	4.92
4.16	0.0040	0.0014	27.27	3.74	3.74	1187.68	66.00	1249.49	4.94
4.17	0.0040	0.0014	27.25	3.72	3.72	1199.52	65.45	1251.33	4.96
4.18	0.0040	0.0014	27.22	3.70	3.70	1211.42	64.91	1253.17	4.98
4.19	0.0040	0.0014	27.20	3.68	3.68	1223.38	64.37	1255.02	5.00

Appendix A.4.5.5 Module Mass Spreadsheet

INTER-TANK FAIRING								
t axial rigidity (mm)	t bending rigidity (mm)	Equivalent Load (MN)	t: ult. strength LH2 (mm.)	Max. t (mm)	R/t	Ncr. (MN)	Mass	L (M)
0.0049	0.0025	57.89	9.22	9.22	414.17	240.86	2754.29	4.12
0.0049	0.0025	57.85	9.17	9.17	418.79	237.79	2765.21	4.13
0.0049	0.0025	57.82	9.12	9.12	423.43	234.78	2776.18	4.14
0.0049	0.0025	57.78	9.06	9.06	428.10	231.83	2787.21	4.15
0.0049	0.0025	57.75	9.01	9.01	432.78	228.95	2798.28	4.16
0.0049	0.0025	57.71	8.96	8.96	437.47	226.13	2809.40	4.17
0.0049	0.0025	57.68	8.91	8.91	442.19	223.37	2820.57	4.18
0.0048	0.0025	57.65	8.86	8.86	446.93	220.67	2831.78	4.19
0.0048	0.0024	57.62	8.81	8.81	451.68	218.03	2843.04	4.20
0.0048	0.0024	57.59	8.76	8.76	456.46	215.44	2854.34	4.21
0.0048	**0.0024**	**57.57**	**8.72**	**8.72**	**461.25**	**212.90**	**2865.69**	**4.22**
0.0048	0.0024	57.54	8.67	8.67	466.06	210.41	2877.08	4.23
0.0048	0.0024	57.52	8.62	8.62	470.89	402.55	2888.51	4.24
0.0048	0.0024	57.49	8.58	8.58	475.73	399.05	2899.98	4.25
0.0048	0.0024	57.47	8.53	8.53	480.60	395.61	2911.49	4.26
0.0048	0.0024	57.45	8.49	8.49	485.48	392.24	2923.04	4.27
0.0048	0.0024	57.43	8.44	8.44	490.39	388.92	2934.63	4.28
0.0048	0.0024	57.41	8.40	8.40	495.31	385.67	2946.25	4.29
0.0048	0.0024	57.39	8.36	8.36	500.25	382.47	2957.92	4.30
0.0048	0.0024	57.37	8.31	8.31	505.21	379.33	2969.62	4.31
0.0048	0.0024	57.35	8.27	8.27	510.18	376.25	2981.35	4.32
0.0048	0.0024	57.34	8.23	8.23	515.18	373.22	2993.13	4.33
0.0048	0.0024	57.32	8.19	8.19	520.19	370.24	3004.94	4.34
0.0048	0.0024	57.31	8.15	8.15	525.22	367.31	3016.78	4.35
0.0048	0.0024	57.29	8.11	8.11	530.27	364.43	3028.66	4.36
0.0048	0.0024	57.28	8.07	8.07	535.34	361.60	3040.57	4.37
0.0048	0.0024	57.27	8.03	8.03	540.43	358.82	3052.51	4.38
0.0048	0.0024	57.25	7.99	7.99	545.54	356.08	3064.48	4.39
0.0048	0.0024	57.24	7.95	7.95	550.66	353.39	3076.49	4.40
0.0048	0.0024	57.23	7.92	7.92	555.80	350.74	3088.53	4.41
0.0048	0.0024	57.22	7.88	7.88	560.96	348.14	3100.60	4.42
0.0048	0.0024	57.22	7.84	7.84	566.10	345.63	3112.94	4.43
0.0048	0.0024	57.23	7.81	7.81	571.09	343.40	3126.22	4.44
0.0048	0.0024	57.24	7.78	7.78	576.10	341.19	3139.52	4.45
0.0048	0.0024	57.73	7.81	7.81	576.34	345.45	3178.98	5.25

Appendix A.4.5.5 Module Mass Spreadsheet

		Nozzle Shroud						
t axial rigidity (mm)	t bending rigidity (mm)	Equivalent Load (MN)	t: ult. strength LH2 (mm.)	Max. t (mm)	R/t	Ncr. (MN)	Mass	L LH2(m)
0.0046	0.0021	62.08	9.89	9.89	386.19	289.93	2815.70	8.80
0.0046	0.0021	61.98	9.82	9.82	390.87	285.60	2817.98	8.67
0.0046	0.0021	61.89	9.76	9.76	395.58	281.37	2820.33	8.54
0.0046	0.0021	61.79	9.69	9.69	400.31	277.24	2822.75	8.41
0.0046	0.0021	61.70	9.63	9.63	405.07	273.22	2825.25	8.29
0.0046	0.0021	61.60	9.56	9.56	409.85	269.28	2827.82	8.16
0.0046	0.0020	61.51	9.50	9.50	414.65	265.44	2830.45	8.04
0.0046	0.0020	61.42	9.44	9.44	419.47	261.69	2833.15	7.92
0.0045	0.0020	61.34	9.38	9.38	424.31	258.02	2835.92	7.80
0.0045	0.0020	61.25	9.32	9.32	429.18	254.44	2838.75	7.68
0.0045	**0.0020**	**61.17**	**9.26**	**9.26**	**434.07**	**250.93**	**2841.64**	**7.57**
0.0045	0.0020	61.09	9.20	9.20	438.99	247.51	2844.59	7.45
0.0045	0.0020	61.01	9.15	9.15	443.92	244.16	2847.60	7.34
0.0045	0.0019	60.93	9.09	9.09	448.88	240.89	2850.67	7.23
0.0045	0.0019	60.85	9.03	9.03	453.86	237.68	2853.79	7.12
0.0045	0.0019	60.78	8.98	8.98	458.87	234.55	2856.97	7.01
0.0044	0.0019	60.71	8.92	8.92	463.89	231.48	2860.21	6.90
0.0044	0.0019	60.63	8.87	8.87	468.94	439.53	2863.50	6.79
0.0044	0.0019	60.56	8.82	8.82	474.01	435.09	2866.84	6.69
0.0044	0.0019	60.50	8.77	8.77	479.10	430.74	2870.23	6.59
0.0044	0.0018	60.43	8.72	8.72	484.22	426.47	2873.67	6.48
0.0044	0.0018	60.36	8.66	8.66	489.36	422.29	2877.16	6.38
0.0044	0.0018	60.31	8.62	8.62	494.44	418.34	2881.18	6.28
0.0044	0.0018	60.25	8.57	8.57	499.59	414.36	2884.91	6.19
0.0044	0.0018	60.19	8.52	8.52	504.77	410.45	2888.69	6.09
0.0044	0.0018	60.13	8.47	8.47	509.97	406.61	2892.52	5.99
0.0043	0.0018	60.07	8.42	8.42	515.19	402.85	2896.39	5.90
0.0043	0.0017	60.01	8.38	8.38	520.44	399.15	2900.30	5.80
0.0043	0.0017	59.96	8.33	8.33	525.70	395.52	2904.27	5.71
0.0043	0.0017	59.91	8.29	8.29	530.99	391.96	2908.27	5.62
0.0043	0.0017	59.85	8.24	8.24	536.30	388.45	2912.32	5.53
0.0043	0.0017	59.81	8.20	8.20	541.59	385.08	2916.60	5.44
0.0043	0.0017	59.78	8.16	8.16	546.75	381.99	2921.72	5.35
0.0043	0.0017	59.75	8.12	8.12	551.94	378.95	2926.86	5.26
0.0050	0.0027	65.06	8.80	8.80	511.44	452.57	3758.64	5.18

Appendix A.4.5.5 Module Mass Spreadsheet

			TANKS						
L LOx(m)	T ellipse LH2	t LH2 : axial rigidity (mm.)	T ellipse LOx	t LOx: axial rigidity (mm.)	t LH2: bending rigidity (mm.)	t LOx: bending rigidity (mm.)	Equivalent Load LH2 (MN)	Equivalent Load LOx (MN)	t: ult. strength LH2 (mm.)
0.94	1.00	0.10	1.06	0.03	0.20	0.00	92.16	34.33	14.68
0.89	1.01	0.09	1.07	0.03	0.19	0.00	90.96	34.00	14.42
0.84	1.01	0.09	1.07	0.03	0.18	0.00	89.79	33.67	14.16
0.79	1.02	0.09	1.08	0.03	0.17	0.00	88.65	33.35	13.91
0.74	1.02	0.09	1.09	0.03	0.16	0.00	87.52	33.04	13.66
0.69	1.03	0.09	1.09	0.03	0.15	0.00	86.42	32.73	13.42
0.65	1.03	0.08	1.10	0.03	0.14	0.00	85.34	32.43	13.18
0.60	1.04	0.08	1.10	0.03	0.13	0.00	84.28	32.13	12.95
0.56	1.05	0.08	1.11	0.02	0.12	0.00	83.25	31.85	12.73
0.51	1.05	0.08	1.11	0.02	0.12	0.00	82.23	31.56	12.51
0.47	**1.06**	**0.08**	**1.12**	**0.02**	**0.11**	**0.00**	**81.24**	**31.29**	**12.30**
0.42	1.06	0.08	1.12	0.02	0.10	0.00	80.26	31.02	12.09
0.38	1.07	0.07	1.13	0.02	0.10	0.00	79.31	30.75	11.89
0.33	1.07	0.07	1.14	0.02	0.09	0.00	78.37	30.49	11.69
0.29	1.08	0.07	1.14	0.02	0.09	0.00	77.45	30.23	11.50
0.25	1.08	0.07	1.15	0.02	0.08	0.00	76.55	29.98	11.31
0.21	1.09	0.07	1.15	0.02	0.08	0.00	75.66	29.74	11.12
0.16	1.09	0.07	1.16	0.02	0.07	0.00	74.80	29.50	10.94
0.12	1.10	0.07	1.16	0.02	0.07	0.00	73.95	29.26	10.77
0.08	1.10	0.07	1.17	0.02	0.06	0.00	73.11	29.03	10.59
0.04	1.11	0.06	1.17	0.02	0.06	0.00	72.29	28.80	10.43
0.00	1.11	0.06	1.18	0.02	0.06	0.00	71.49	28.58	10.26
0.10	1.12	0.06	1.19	0.02	0.05	0.00	70.70	29.16	10.10
0.10	1.12	0.06	1.19	0.02	0.05	0.00	69.93	29.17	9.94
0.10	1.13	0.06	1.20	0.02	0.05	0.00	69.17	29.17	9.79
0.10	1.13	0.06	1.20	0.02	0.04	0.00	68.43	29.18	9.64
0.10	1.14	0.06	1.21	0.02	0.04	0.00	67.69	29.19	9.49
0.10	1.15	0.06	1.21	0.02	0.04	0.00	66.98	29.20	9.35
0.10	1.15	0.05	1.22	0.02	0.04	0.00	66.27	29.21	9.21
0.10	1.16	0.05	1.22	0.02	0.03	0.00	65.58	29.22	9.07
0.10	1.16	0.05	1.23	0.02	0.03	0.00	64.90	29.22	8.94
0.10	1.17	0.05	1.24	0.02	0.03	0.00	64.23	29.23	8.81
0.10	1.17	0.05	1.24	0.01	0.03	0.00	63.58	29.24	8.68
0.10	1.18	0.05	1.25	0.01	0.03	0.00	62.94	29.25	8.55
0.10	1.18	0.05	1.25	0.01	0.03	0.00	62.82	29.51	8.50

Appendix A.4.5.5 Module Mass Spreadsheet

t: ult. strength LOx (mm.)	t: yeild strength LH2 (mm.)	t: yeild strength LOx (mm.)	t: ult. hoop stress LH2 (mm.)	t: ult. hoop stress LOx (mm.)	t: yeild hoop stress LH2 (mm.)	t: yeild hoop stress LOx (mm.)	Max t so far LH2 (mm.)	Max t so far LOx (mm.)
5.47	13.71	5.11	7.61	5.76	5.33	5.37	14.68	5.76
5.39	13.46	5.03	7.65	5.78	5.36	5.40	14.42	5.78
5.31	13.22	4.96	7.69	5.81	5.39	5.43	14.16	5.81
5.23	12.99	4.89	7.73	5.84	5.41	5.46	13.91	5.84
5.16	12.76	4.81	7.77	5.87	5.44	5.49	13.66	5.87
5.08	12.53	4.75	7.81	5.90	5.47	5.51	13.42	5.90
5.01	12.31	4.68	7.85	5.93	5.50	5.54	13.18	5.93
4.94	12.10	4.61	7.89	5.96	5.53	5.57	12.95	5.96
4.87	11.89	4.55	7.93	5.99	5.55	5.60	12.73	5.99
4.80	11.69	4.49	7.97	6.02	5.58	5.62	12.51	6.02
4.74	**11.49**	**4.42**	**8.00**	**6.05**	**5.61**	**5.65**	**12.30**	**6.05**
4.67	11.29	4.36	8.04	6.08	5.64	5.68	12.09	6.08
4.61	11.10	4.31	8.08	6.11	5.67	5.71	11.89	6.11
4.55	10.92	4.25	8.12	6.14	5.69	5.73	11.69	6.14
4.49	10.74	4.19	8.16	6.17	5.72	5.76	11.50	6.17
4.43	10.56	4.14	8.20	6.20	5.75	5.79	11.31	6.20
4.37	10.39	4.08	8.24	6.23	5.78	5.82	11.12	6.23
4.32	10.22	4.03	8.28	6.26	5.80	5.84	10.94	6.26
4.26	10.06	3.98	8.32	6.29	5.83	5.87	10.77	6.29
4.21	9.89	3.93	8.36	6.32	5.86	5.90	10.59	6.32
4.15	9.74	3.88	8.40	6.35	5.89	5.93	10.43	6.35
4.10	9.58	3.83	8.44	6.38	5.92	5.95	10.26	6.38
4.17	9.43	3.89	8.48	6.41	5.94	5.98	10.10	6.41
4.15	9.29	3.87	8.52	6.43	5.97	6.01	9.94	6.43
4.13	9.14	3.86	8.56	6.46	6.00	6.04	9.79	6.46
4.11	9.00	3.84	8.60	6.49	6.03	6.07	9.64	6.49
4.09	8.87	3.82	8.64	6.52	6.05	6.09	9.49	6.52
4.08	8.73	3.81	8.68	6.55	6.08	6.12	9.35	6.55
4.06	8.60	3.79	8.72	6.58	6.11	6.15	9.21	6.58
4.04	8.47	3.77	8.76	6.61	6.14	6.18	9.07	6.61
4.02	8.35	3.76	8.80	6.64	6.17	6.20	8.94	6.64
4.01	8.22	3.74	8.84	6.67	6.19	6.23	8.84	6.67
3.99	8.10	3.73	8.88	6.70	6.22	6.26	8.88	6.70
3.97	7.99	3.71	8.92	6.73	6.25	6.29	8.92	6.73
3.99	7.94	3.73	8.96	6.76	6.28	6.31	8.96	6.76

Appendix A.4.5.5 Module Mass Spreadsheet

R/t LH2	R/t LOx	Ncr. with pressure LH2(MN)	Ncr. with pressure LO2(MN)	L/D LH2	L/D LOx	Mass LH2 Tank(kg)	Mass LH2 insulation estimate
260.16	663.75	925.26	196.45	2.15	1.12	14283.79	792.77
266.34	663.82	894.73	203.61	2.13	1.12	13994.59	788.78
272.64	663.89	865.91	211.45	2.11	1.11	13713.70	784.82
279.03	663.96	838.71	220.10	2.08	1.10	13440.83	780.91
285.54	664.03	813.04	229.72	2.06	1.10	13175.70	777.04
292.15	664.09	788.82	240.51	2.04	1.09	12918.06	773.21
298.87	664.16	765.95	252.73	2.02	1.08	12667.64	769.42
305.70	664.22	744.39	266.72	2.00	1.08	12424.21	765.67
312.64	664.28	724.04	282.95	1.98	1.07	12187.54	761.96
319.69	664.34	704.85	302.04	1.96	1.06	11957.38	758.29
326.85	**664.40**	**686.75**	**324.86**	**1.94**	**1.06**	**11733.54**	**754.65**
334.12	664.46	669.69	352.67	1.92	1.05	11515.80	751.05
341.51	664.52	653.61	387.35	1.90	1.05	11303.97	747.49
349.00	664.58	638.47	431.80	1.89	1.04	11097.84	743.97
356.62	664.64	624.21	490.74	1.87	1.04	10897.23	740.48
364.35	664.69	610.79	572.37	1.85	1.03	10701.98	737.03
372.19	664.75	598.16	692.10	1.83	1.02	10511.90	733.61
380.16	664.80	586.29	882.46	1.82	1.02	10326.82	730.23
388.24	664.86	575.14	1224.29	1.80	1.01	10146.60	726.88
396.43	664.91	564.68	1980.79	1.78	1.01	9971.08	723.56
404.75	664.96	554.86	4636.21	1.77	1.00	9800.11	720.28
413.19	665.02	545.66	503284.30	1.75	1.00	9633.54	717.02
421.74	665.07	537.07	1666.16	1.74	1.01	9471.47	713.80
430.41	665.12	529.02	1698.52	1.72	1.01	9313.38	710.62
439.21	665.17	521.51	1731.35	1.71	1.01	9159.30	707.46
448.13	665.22	514.51	1764.67	1.69	1.01	9009.10	704.33
457.17	665.26	507.99	1798.49	1.68	1.01	8862.67	701.24
466.34	665.31	501.93	1832.80	1.67	1.01	8719.90	698.17
475.63	665.36	489.97	1867.61	1.65	1.01	8580.68	695.13
485.04	665.41	475.36	1902.93	1.64	1.01	8444.89	692.12
494.58	665.45	461.31	1938.77	1.63	1.01	8312.44	689.14
502.32	665.50	451.77	1975.12	1.61	1.01	8214.74	686.19
502.32	665.54	458.40	2012.00	1.60	1.01	8245.20	683.27
502.33	665.58	465.13	2049.40	1.59	1.01	8275.93	680.37
502.33	665.63	471.94	2087.34	1.58	1.01	8306.94	677.50

Appendix A.4.5.5 Module Mass Spreadsheet

Mass LOx Tank(kg)	Mass LOx insulation estimate	M total	R (m)	L total	Frontal Area	
2470.24	249.22	24561.37	3.82	27.53	45.84	
2487.10	248.05	24298.72	3.84	27.36	46.32	
2504.14	246.90	24044.74	3.86	27.20	46.81	
2521.36	245.76	23799.14	3.88	27.03	47.29	
2538.76	244.63	23561.66	3.90	26.87	47.78	
2556.34	243.52	23332.02	3.92	26.71	48.27	
2574.11	242.42	23109.97	3.94	26.55	48.77	
2592.06	241.33	22895.26	3.96	26.40	49.27	
2610.20	240.25	22687.65	3.98	26.25	49.76	
2628.52	239.19	22486.92	4.00	26.10	50.27	
2647.03	**238.14**	**22292.85**	**4.02**	**25.96**	**50.77**	
2665.73	237.10	22105.23	4.04	25.81	51.28	
2684.61	236.07	21923.85	4.06	25.67	51.78	
2703.69	235.05	21748.53	4.08	25.53	52.30	
2722.95	234.05	21579.07	4.10	25.40	52.81	
2742.41	233.05	21415.30	4.12	25.26	53.33	
2762.06	232.07	21257.04	4.14	25.13	53.85	
2781.90	231.10	21104.12	4.16	25.00	54.37	
2801.93	230.13	20956.39	4.18	24.87	54.89	
2822.16	229.18	20813.68	4.20	24.75	55.42	
2842.59	228.24	20675.86	4.22	24.63	55.95	
2863.21	227.31	20542.78	4.24	24.50	56.48	
2952.53	237.08	20494.20	4.26	24.66	57.01	
2993.85	239.28	20393.80	4.28	24.62	57.55	
3035.55	241.48	20297.91	4.30	24.59	58.09	
3077.64	243.70	20206.43	4.32	24.55	58.63	
3120.12	245.93	20119.24	4.34	24.52	59.17	
3162.99	248.16	20036.21	4.36	24.48	59.72	
3206.25	250.41	19957.23	4.38	24.45	60.27	
3249.91	252.66	19882.21	4.40	24.42	60.82	
3293.96	254.93	19811.05	4.42	24.39	61.38	
3338.40	257.20	19775.58	4.44	24.36	61.93	
3383.25	259.49	19870.47	4.46	24.33	62.49	
3428.50	261.79	19966.13	4.48	24.30	63.05	
3474.15	264.09	20915.32	4.50	25.06	63.62	

Appendix A.4.5.5 Module Mass Spreadsheet

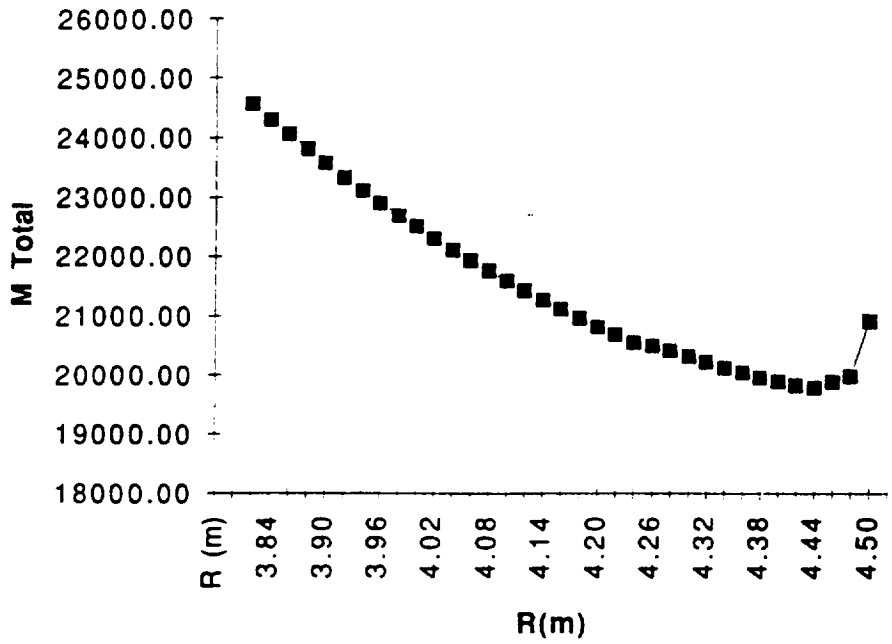

Appendix A.4.6.2.1 Mass Analysis of the Combustion Chamber and Nozzle

Chamber Pressure (MPa)	Wall Thickness (m)	Nozzle Thickness (m)*	Volume of comb chamber (m^3)	Volume of conv/ div duct (m^3)	Volume of nozzle (m^3)	Mass of Combustion Chamber and Nozzle (kg)
5.516	0.0099	0.0025	0.0117	0.0327	0.0342	618.0
8.274	0.0127	0.0025	0.0124	0.0269	0.0337	573.9
11.032	0.0145	0.0025	0.0124	0.0226	0.0331	534.9
13.79	0.0161	0.0025	0.0123	0.0198	0.0325	507.7
16.548	0.0175	0.0025	0.0123	0.0178	0.0319	487.1
19.306	0.0188	0.0025	0.0123	0.0162	0.0314	470.7
22.064	0.0200	0.0025	0.0122	0.0150	0.0309	457.2
*Nozzle thickness based on heat transfer			Ultimate Yield of Alloy Steel= 345 MPa			Density = 7860 kg/m^3

Appendix A.4.6.2.3.a Equations Used for Combustion Chamber and Nozzle Design

Isp	=	Specific Impulse (s)
T	=	Thrust (N)
$\dot{m}$	=	Propellant Mass Flow (kg/s)
g	=	Gravity Constant (kg·m/s^2)
C*	=	Characteristic Velocity (m/s)
Pc	=	Combustion Chamber Pressure (N/m^2)
At	=	Throat Area (m^2)
γ	=	Ratio of Specific Heats
R	=	Universal Gas Constant (N·m)/(kg·K)
Tc	=	Combustion Chamber Temperature (K)
Cf	=	Thrust Coefficient
Pe	=	Nozzle Exit Pressure (N/m^2)
ε	=	Expansion Ratio
Pa	=	Ambient Pressure (N/m^2)
L*	=	Characteristic Length (m)
Vc	=	Total Volume of Combustion Chamber (m^3)
Lcone	=	Length of Convergent Conical Section (m)
Dt	=	Throat Diameter (m)
ε_c	=	Combustion Chamber Expansion Ratio
$\Re$	=	Circular Arc Radius (m)
α	=	Half-angle of Convergent Conical Section (deg)
a	=	Half-angle of Divergent Conical Section (deg)
Vcone	=	Volume of Convergent Conical Section (m^3)
Dc	=	Combustion Diameter (m)
Vchamber	=	Volume of Cylindrical Chamber Section (m^3)
Lchamber	=	Length of Cylindrical Chamber Section (m)
Ltotal	=	Total Length of Combustion Chamber (m)
Lf	=	"Bell Nozzle" Equivalence Factor
ε_n	=	Nozzle Expansion Ratio
$\Re_n$	=	**Circular Arc of Nozzle Radius (m)**

Engine Performance Calculations

Specific Impulse Isp:

$$Isp = \frac{T}{\dot{m} \cdot g}$$

Characteristic Velocity C*:

$$C^* = \frac{Pc \cdot At}{\dot{m}}$$

$$C^* = \frac{\sqrt{g \cdot \gamma \cdot R \cdot Tc}}{\gamma \cdot \sqrt{\left[\frac{2}{\gamma+1}\right]^{\frac{\gamma+1}{\gamma-1}}}}$$

Thrust Coefficient Cf:

$$Cf = \frac{T}{Pc \cdot At}$$

$$Cf = \sqrt{\frac{2 \cdot \gamma^2}{\gamma-1} \cdot \left[\frac{2}{\gamma+1}\right]^{\frac{\gamma+1}{\gamma-1}} \cdot \left[1 - \left(\frac{Pe}{Pc}\right)^{\frac{\gamma-1}{\gamma}}\right]} + \varepsilon \cdot \left[\frac{Pe - Pa}{Pc}\right]$$

Nozzle Area Ratio ε:

$$\varepsilon = \frac{1}{\left(\frac{\gamma+1}{2}\right)^{\frac{1}{\gamma-1}} \cdot \left(\frac{Pe}{Pc}\right)^{\frac{1}{\gamma}} \cdot \sqrt{\frac{\gamma+1}{\gamma-1} \cdot \left(1 - \left(\frac{Pe}{Pc}\right)^{\frac{\gamma-1}{\gamma}}\right)}}$$

Characteristic Length L*:

$$L^* = \frac{Vc}{At}$$

Approximate Length of Convergent Conical Section Lcone:

$$L_{cone} = \frac{\frac{Dt}{2}\cdot\left(\sqrt{\varepsilon_c}-1\right)+\Re\cdot\left(\sec(\alpha)-1\right)}{\tan(a)}$$

Approximate Volume of Convergent Conical Section Vcone:

$$V_{cone} = \frac{\pi}{3}\cdot L_{cone}\cdot\left[\left(\frac{Dt}{2}\right)^2+\left(\frac{Dc}{2}\right)^2+\left(\frac{Dt}{2}\right)\cdot\left(\frac{Dc}{2}\right)\right]$$

Volume of Cylindrical Chamber Section Vchamber:

$$V_{chamber} = V_c - V_{cone}$$

Length of Cylindrical Chamber Section Lchamber:

$$L_{chamber} = \frac{V_{chamber}}{\varepsilon_c\cdot At}$$

Total Length of Combustion Chamber (cylinder+cone) Ltotal:

$$L_{total} = L_{chamber} + L_{cone}$$

Approximate Length of 80% Bell Nozzle using 15-deg-half-angle Conical Nozzle Ln:

$$Ln = Lf\cdot\left(\frac{\frac{Dt}{2}\cdot\left(\sqrt{\varepsilon_n}-1\right)+\Re_n\cdot\left(\sec(15)-1\right)}{\tan(15)}\right)$$

Appendix A.4.6.2.3.b Specifications of Modular Engine and Top-Stage Engine

	Pe (3 km)	7.01E+04	Pe2 (10 km)	2.65E+04
	Eta	21.80728674	Eta2	46.2397715
	O/F	5	M	12
G-1 Engine Characteristics		G-2c Engine Characteristics		
	Total mdot	1373.567468		
Ga - ratio of specific heats	Ga	1.22	Ga	1.22
Isp (s)	Isp	432.8	Isp	432.8
mdot - propellant mass flow (kg/s)	mdot	457.8558226	mdotc	457.855823
Thrust (N)	Thrust	1.94E+06	Thrustc	1.94E+06
Cstar - characteristic velocity (m/s)	Cstar	2528.421638	Cstar	2528.42164
Cf - thrust coefficient	Cf	1.679216764	Cf	1.59230162
Pc - chamber pressure (N/m^2)	Pc	1.65E+07	Pc	1.65E+07
Tc - chamber temperature (K)	Tc	3000	Tc	3000
Dc - chamber diameter (m)	Dc	0.365524972	Dcc	0.36552497
Lcham - chamber length (m)	Lcham	0.61283348	Lchamc	0.61283348
Vcham - chamber volume (m^3)	Vcham	0.064308217	Vchamc	0.06430822
Dt - throat diameter (m)	Dt	0.29844989	Dtc	0.29844989
At - throat area (m^2)	At	0.06995725	Atc	0.06995725
ArcR - circular arc of cone radius (m)	ArcR	0.223837417	ArcRc	0.22383742
Lconv - convergent cone length (m)	Lconv	0.065037835	Lconvc	0.06503783
Vconv - convergent cone volume (m^3)	Vconv	0.005649033	Vconvc	0.00564903
Ltotal - total length of chamber+cone (m)	Ltotal	0.677871314	Ltotalc	0.67787131
Vtotal - total chamber volume (m^3)	Vtotal	0.06995725	Vtotalc	0.06995725
De - exit diameter (m)	De	1.393709435	Dec	2.02945424
Ae - exit area (m^2)	Ae	1.525577805	Aec	3.23480724
ArcRn - circular arc of nozzle radius (m)	ArcRn	0.057003929	ArcRnc	0.05700393
Nt - length of diverging arc fr throat (m)	Nt	0.033506069	Ntc	0.03350607
Na - dist of diver arc fr centerline (m)	Na	0.160111727	Nac	0.16011173
Ln - nozzle length (m)	Ln	1.435900791	Lnc	2.26632196

Appendix A.4.6.3.1 Turbopump Cycles

Open Cycles

Gas Generator Cycle: The gas generator cycle is similar to the staged combustion cycle used for the main engines of the launch vehicle. After the fuel has been pumped through the cooling cycle and the oxidizer has been pumped, the propellants are burned in a precombustor (in this case called a gas generator) with a different O/F ratio than the main thrust chamber. The gases are then run through the turbine and exhausted in the nozzle downstream of the throat. This cycle is less efficient than the staged combustion cycle and expander bleed cycle, which are closed cycles, since the turbine exhaust gases are not expanded through the full pressure ratio in the nozzle.

Combustion Tap-Off Cycle: This cycle bleeds off hot gases from the nozzle to use as the working fluid in the turbines. The fuel is once again used in the regenerative cooling cycle to cool the nozzle. The hot gases used in to run the turbines are exhausted in the nozzle downstream of the throat.

Closed Cycles

Expander Cycle: In this cycle once the fuel is pumped it is once again used to cool the nozzle. The thermal energy gained by the fuel in the cooling cycle is used to run the turbines. Once the fuel has been run through the turbines it is injected into the nozzle along with the propellant and combusted. The expander cycle is most efficient with low chamber pressure and low pump pressure rise engines.

Appendix A.4.6.3.3 Turbopump Analysis

Assumptions:

Turbine Efficiency: 70%
Pump Efficiency: 65%
Cooling Jacket Losses: 25%
Injector Loss: 20%
Line and Valve Losses: 5%

Losses estimated or derived from analogy with existing or proposed systems. Losses are estimated as a percentage of chamber pressure. Efficiencies based on space shuttle SSME's or other similar systems.

<u>Determination of pump parameters</u>

The LOX pumps were characterized first as follows:

1.) The available suction head above vapor pressure was calculated assuming a tank head (tank pressure) and subtracting line and vapor pressure head losses.

2.) Using the chamber pressure and adding on the line losses the pump discharge pressure was calculated.

3.) Factoring in a margin of safety the suction head required is obtained from the suction head available.

4.) The following steps are then followed to calculate the diameter of the impellers.

Calculate Thorma parameter from $\sigma = (H_s)_R / \Delta H$.

Calculate Suction specific speed $N_s = S(\sigma)^{3/4}$.

Calculate the pump shaft speed $N = N_s(\Delta H)^{3/4} / (21.2 * \sqrt{N})$

Calculate the impeller tip speed $U = \psi(\sqrt{2 g_o \Delta H}$

Calculate impeller diameter $D = U * 2 / N$

The tank storage pressure was varied so as to provide a range of inlet pressures to the pump and to find an optimum range of tank storage pressures based on the mass of the pump and tank. The pump was modeled as a cylinder with a thickness calculated from the maximum internal pressure in the pump. The impellers were modeled as flat discs.

After the LOX pumps were characterized the following strategy was used to calculate the turbine requirements and the LH2 pump characteristics.

Calculate fluid horsepower output in LOX pump $fhp = \dot{m} * \Delta H / 550$

Calculate turbine brake horsepower requirements from $bhp = fhp / \eta_p$

Calculate pressure ratio across turbine $P_T = \eta_T * \dot{m}_T * C_p * T_1 * (1 - (p_2 / p_1)^{\gamma-1/\gamma})$

From thrust chamber pressure and assumed losses in lines turbine discharge pressure was calculated. From the pressure ratio obtained for the turbine the turbine inlet pressure was calculated which was assumed to equal the precombustor chamber pressure. From the precombustor chamber pressure and assumed losses in the cooling jacket, lines, and valves, the LH2 pump discharge pressure was readily calculated. An analysis similar to the LOX pump analysis was then performed on the LH2 pumps to characterize the pumps and the LH2 turbines.

Appendix A.5.2 Center of Gravity Analysis Spreadsheet

Component Level Mass Breakdown						
Inital Gross Mass Guess [lbs]	112407.41					
System/component	**Mass [kg]**	**M Spacecraft**	**M Module**	**M Stage 3**	**M Config 1-2**	**M Config 3**
Structures						
Module						
Module LOX Tank	2647		2,647		7,941	2,647
Module LH2 Tank	11734		11,734		35,202	11,734
Module LOX Insulation	238		238		714	238
Module LH2 Insulation	755		755		2,265	755
Module Thrust Structure	494.7		495		1,484	495
Module Helium Tank	55		55		165	55
Inter-Stage Faring/Nose Cone	1212		1,212		3,636	1,212
Module Inter Tank Faring	285		285		855	285
Nozzle Shroud	2816		2,816		8,448	2,816
Secondary Inert Mass	646		646		1,938	646
Upper Stage						
LOX Tank	647			647	647	647
LH2 Tank	3022			3,022	3,022	3,022
LOX Insulation	98			98	98	98
LH2 Insulation	334			334	334	334
Thrust Structure	494.7			495	495	495
Helium Tank	14			14	14	14
Inter-Stage Faring	262			262	262	262
Inter Tank Faring	285			285	285	285
Nozzle Shroud	631			631	631	631
Secondary Inert Mass	646			646	646	646
Wings	986	986			986	
Vertical Stabilizers	398	398			398	
Landing Gear						
Nose	394	394			394	
Main	1,446	2,893			2,893	
Fuselage	11,851	11,851			11,851	
Escape System	2400	2,400			2,400	
Secondary Structure	1,614	1,614			1,614	
Thermal Protection						
REI Mullite	300	300			300	
Titanium Sub-structure	600	600			600	
Nose	30	30			30	
Leading Edges	1670	1,670			1,670	
Fasteners and Adhesives	520	520			520	
Propulsion						
Main Engine						
Chamber & Nozzle	658		1,974	658	6,580	2,632
Turbopump LOX	301		903	301	3,010	1,204
Turbopump LH2	301		903	301	3,010	1,204
Piping	340		1,020	340	3,400	1,360
Injector	70		210	70	700	280
Gimbal Structure	60		180	60	600	240
Gimbal EMA	20.5		615	205	2,050	820
Valve EMA	1.6		480	160	1,600	640
Instruments, sensors, etc.	75		225	75	750	300
Secondary Inert Mass	75		225	75	750	300
Power Supply- Baterries	376		1,128	376	3,760	1,504
(350 W/kg;14000$/kg; 131KW)						
OMS Engine						
Chamber & Nozzle	100	200			200	
Gimbal Structure	25	50			50	
OMS Gimbal EMA	4.5	36			36	
OMS Valve EMA	0.3	12			12	
RCS Thruster						
Chamber & Nozzle	4	124			124	
RCS Valve EMA	0.1	124			124	

Appendix A.5.2 Center of Gravity Analysis Spreadsheet

RCS & OMS Feed System							
Forward Propellant Tank	24	48			48		
Forward Pessurant Tank	33	33			33		
Aft Propellent Tank	156	312			312		
Aft Pressurant Tank	187	187			187		
Power							
Fuel Cell	73	219			219		
24 Hour Back up Battery	374	374			374		
Electrical Bus Wiring	200	200			200		
LOX Tank	35	105			105		
LH2 Tank	3	9			9		
LOX Insulation	2	6			6		
LH2 Insulation	1	2			2		
Spacecraft APU	40	80			80		
Avionics							
Guidance sensors							
GPSR	4.5	9			9	9	
INS	57.0	171			171	114	
Star tracker	26.0	52			52		
Microwave landing system	32.1	96			96		
Radar Altimiter	6.1	18			18		
Proximity	6.1	12			12		
Rendezous Sensors	6.1	12			12		
Communications							
Helix S-Band Antenna	3.0	21			21		
Parabolic Antenna	135.0	135			135		
Omni. Micro. Ant. x12.57	2.0	2			2	2	
Omni. Micro. Ant. x25.13	4.0	8			8		
Helix EVA Antenna	3.0	21			21		
VTR (Digital)	22.7	45			45		
Tape Recorder	33.3	67			67		
K Band Transceiver	4.5	9			9		
S Band Transceiver	6.9	27			27		
L Band Transceiver	4.8	10			10		
Stanard Modules							
Inter Comp. Interface Seq. Mod.	1.4	7			7	7	
Shared Memory Module	1.4	7			7	7	
Memory Module	1.4	14			14	14	
Comp. Processor Module	1.4	7			7	7	
I/O Processor Module	1.4	14			14	7	
Power Module	1.4	7			7	7	
I/O Sequencer Module	1.4	14			14	14	
Remote Data Unit	4.5	108	81	32	383	113	
Envirmental Housing (computer unit)	7	35			35	35	
Envirmental Housing (RDU)	2	48	36	14	170	50	
Fiber Optic Bus (module)	20		20		60	20	
Fiber Optic Bus (upper stage)	20			20	20	20	
Fiber Optic Bus (spacecraft)	20	20			20		
Flight Control EMA	4	80			80		
Human Factors							
EVA							
2 p Airlock	550.0	550			550		
4 Shuttle EMU	61.4	245			245		
RMS	1240.0	1,240			1,240		
Atmosphere							
E Ox Tanks	120.0	120.0			120		
Nit Tanks	249.0	249.0			249		
Filtering System	120.0	249.0			249		
Activated Charcoal	50.9	50.9			51		
Air System	20.0	20.0			20		
Thermal System	100.0	100.0			100		
Water supply							
Water tanks	20.0	40			40		
Food							
Storage	5.0	5.0			5		

Appendix A.5.2 Center of Gravity Analysis Spreadsheet

Preparation Unit	5.0	5.0			5	
Refrigerator	5.0	5.0			5	
Sanitation						
Trash Storage	75.0	75.0			75	
Toilet	20.0	20.0			20	
Waste holding tanks	10.0	10.0			10	
Safety Equipment						
Medical Equipment	4.0	4.0			4	
Fire Dectection/Suppression	2.0	12.0			12	
Emergency Breathing	1.0	6.0			6	
Crew Cabin						
Lighting	2.0	20			20	
Sleeping Berths	20.0	20			20	
Individual Lockers	5.0	30			30	
Dry Masses		29,929	28,883	9,120	125,697	38,225
Returning mass						
Res. Propellant			4,370	1,004	14,114	5,374
Retrun Payload	5500	5500			5,500	
Crew	510	510			510	
Emergency O2	135	135			135	
SUB TOTALS		36,074	33,253	10,124	145,956	43,599
Sub Total w/ 10% margin		39,681	36,578	11,137	160,552	47,715
Wet mass						
LOX		725.00	177697	40829	574645	218526.00
Spacecraft		725.00				
Module			177697			
Upper Stage				40829		
LH2		90.00	36413.00	8367.00	117696	44780.00
Spacecraft		90.00				
Module			36413.00			
Upper Stage				8367.00		
He			100.00	100.00	400.00	200.00
Module			100.00			
Upper Stage				100.00		
Hydrazine		4,600			4,600	
N2O4		4,600			4,600	
Nitrogen		50			50	
Water		810			810	
Food		380			380	
Payload		0			0	7,000
WET Totals		50,936	250,788	60,433	863,733	318,221
				Check	863,733	318,221

Appendix A.5.2 Center of Gravity Analysis Spreadsheet

Y-Axis Rel. to bottom(m)	Individual Module		Upper Stage		Spacecraft	
6.38	2647.00	16887.86				
15.24	11734.00	178826.16				
6.35	238.00	1511.30				
15.24	755.00	11506.20				
2.55	494.70	1261.49				
22.47	55.00	1235.85				
23.92	1212.00	28991.04				
9.25	285.00	2636.25				
0.72	2816.00	2027.52				
13.45	646.00	8688.70				
30.8			647.00	19927.60		
37.6			3022.00	113627.20		
30.8			98.00	3018.40		
37.6			334.00	12558.40		
27.98			494.70	13841.71		
43.27			14.00	605.78		
45.3			262.00	11868.60		
32.745			285.00	9332.33		
25.76			631.00	16254.56		
34.5			646.00	22287.00		
55.46					986	54673.60
48.41					398	19286.34
					0	0.00
65.64					394	25893.18
48.41					2,893	140040.37
56.64					11,851	671261.98
62.84					2,400	150816.00
56.64					1,614	91426.52
					0	0.00
56.64					300	16992.00
56.64					600	33984.00
66.14					30	1984.20
55.46					1,670	92618.20
56.64					520	29452.80
0.72	1974.00	1421.28	658.00	473.76		
2.29	903.00	2067.87	301.00	689.29		
2.29	903.00	2067.87	301.00	689.29		
2.17	1020.00	2213.40	340.00	737.80		
2.08	210.00	436.80	70.00	145.60		
1.69	180.00	304.20	60.00	101.40		
1.69	615.00	1039.35	205.00	346.45		
1.69	480.00	811.20	160.00	270.40		
2.17	225.00	488.25	75.00	162.75		
2.29	225.00	515.25	75.00	171.75		
2.29	1128.00	2583.12	376.00	861.04		
46.4					200.00	9280.00
47					50.00	2350.00
47.31					36.00	1703.16
47.31					12.00	567.72
58.44					124.00	7246.56
58.44					124.00	7246.56

Appendix A.5.2 Center of Gravity Analysis Spreadsheet

						0.00
65.4					48.00	3139.20
65.84					33.00	2172.72
48.16					312.00	15025.92
49.02					187.00	9166.74
49.61					219.00	10864.59
61.8					374.00	23113.20
56.64					200.00	11328.00
64.9					105.00	6814.50
65.03					9.00	585.27
64.9					6.00	389.40
65.03					1.50	97.55
46.99					80.00	3759.20
61.36					9.08	557.15
62.67					171.00	10716.57
64.97					52.00	3378.44
66.93					96.30	6445.36
66.93					18.36	1228.83
67.13					12.24	821.67
67.13					12.24	821.67
60.64					21.00	1273.44
58.65					135.00	7917.75
63.14					2.00	126.28
63.14					8.00	505.12
57.74					21.00	1212.54
56.64					45.46	2574.85
63.64					66.60	4238.42
62.64					8.90	557.50
62.64					27.48	1721.35
62.64					9.50	595.08
63.64					6.80	433.01
63.64					6.80	433.01
62.64					13.61	852.41
61.64					6.80	419.40
63.64					13.61	866.01
63.64					6.80	433.01
57.64					13.61	784.37
60.64	81.00	4911.84	31.50	1910.16	108.00	6549.12
63.59					35.00	2225.65
63.59	36.00	2289.24	14.00	890.26	48.00	3052.32
2.30	20.00	46.00				
27.90			20.00	558.00		
56.64					20.00	1132.80
63.64					80.00	5091.20
61.97					550.00	34083.50
62.30					245.40	15288.42
55.40					1240.00	68696.00
64.08					120.00	7689.60
63.46					249.00	15801.54
64.39					249.00	16033.11
64.39					50.85	3274.23
64.39					20.00	1287.80
60.64					100.00	6064.00
61.04					40.00	2441.60
62.30					5.00	311.50

Appendix A.5.2 Center of Gravity Analysis Spreadsheet

62.30					5.00	311.50	
62.30					5.00	311.50	
61.80					75.00	4635.00	
61.80					20.00	1236.00	
61.80					10.00	618.00	
63.82					4.00	255.28	
63.82					12.00	765.84	
63.82					6.00	382.92	
61.97					20.00	1239.40	
61.97					20.00	1239.40	
61.97					30.00	1859.10	
	28882.70		9120.20		29928.98		
65.40	4370.00	285798.00	1004.00	65661.60			
55.40					5500.00	304700.00	
61.97					510.00	31604.70	
64.08					135.00	8650.80	
	33252.70	560566.04	10124.20	296991.12	36073.98	2039024.53	
	36577.97	16.86	11136.62	29.33	39681.38	56.52	10.88
		-^^dry cg		-^^dry cg		-^^dry cg	
64.9					725.00	47052.50	
6.38	177697.00	1133706.86					
30.8			40829.00	1257533.20			
65.03					90.00	5852.70	
15.24	36413.00	554934.12					
37.6			8367.00	314599.20			
22.47	100.00	2247.00					
43.27			100.00	4327.00			
48.16					4600.00	221536.00	
65.40					4600.00	300840.00	
63.46					50.00	3173.00	
61.04					810.00	49442.40	
62.30					380.00	23674.00	
55.40					0.00		
		2251454.02		1873450.52		2690595.13	
	Corrected?>>	9.10		31.53		56.85	11.21
	250787.97	20.19	60432.62	66.92	50936.38	145.68	
		-^^ this is the		-^^ this is the		-^^This is the	
		module wet cg		upper stage wet cg		s/c wet cg	
		Dry Mass	Dry CG	Wet Mass	Wet CG		
	Module	560566.04	16.86	2251454.02	9.10		
	Upper Stage	296991.12	29.33	1873450.52	31.53		
	Spacecraft	2039024.53	56.52	2690595.13	56.85		
	Unmanned Pay	9360	70.14	9360	48.19		
	Config 1-2	4017713.75	37.91	11318407.69	24.16		
	Config 3	866917.16	21.7072683	4134264.54	19.35		
			Config 1-2	Config 3			
	Launch		24.16	19.29			
	Stage 1 Burnout/Separation						
	Stage 2 Ignition						
	Stage 2 Burnout/Separation						
	Stage 3 Burnout/Separation						
	After Deorbit Burn						

Appendix A.5.3.1 Cost Estimating Relations

Systems Level CERs	Nonrecurring				Recurring			
	English Units		MKS Units		English Units		MKS Units	
Quantity	A	B	A	B	A	B	A	B
Structure (complex)	0.278	0.623	0.501	0.623	0.032	0.789	0.066	0.789
Structure (simple)	0.267	0.454	0.421	0.454	0.041	0.536	0.069	0.536
Thermal Control	0.168	0.572	0.291	0.572	0.063	0.584	0.110	0.584
Power source, storage, & dist.	0.040	0.893	0.089	0.893	0.020	0.894	0.045	0.894
Comm. & data handling	0.586	0.762	1.178	0.762	0.073	0.971	0.173	0.971
Att. control	0.337	0.768	0.681	0.768	0.068	0.888	0.151	0.888
Reaction cntl	0.255	0.667	0.476	0.667	0.171	0.536	0.288	0.536

Component Level CERs				MKS Units			
	English Units			Nonrecurring		Recurring	
Quantity	A	B	%NR	A	B	A	B
Module Structure	0.034	0.663	0.60	0.038	0.663	0.025	0.663
Solar array structure	0.010	1.000	0.50	0.012	1.000	0.012	1.000
Sail Structure	0.011	1.000	0.45	0.012	1.000	0.015	1.000
Wheel Assy	0.005	1.000	0.55	0.007	1.000	0.005	1.000
Pointing system	0.720	0.200	0.60	0.557	0.200	0.371	0.200
Support boom	0.023	0.900	0.45	0.023	0.900	0.028	0.900
Drive Mechanism	0.012	1.160	0.50	0.017	1.160	0.017	1.160
Other support structure	0.021	0.789	0.50	0.022	0.789	0.022	0.789
Active thermal control	0.014	0.960	0.75	0.025	0.960	0.008	0.960
Passive thermal control	0.047	0.482	0.55	0.042	0.482	0.034	0.482
Solar array	0.029	0.946	0.35	0.024	0.946	0.044	0.946
Battery	0.005	1.145	0.55	0.007	1.145	0.006	1.145
Power supply electronics	0.489	0.500	0.65	0.520	0.500	0.280	0.500
Power supply components	0.116	0.638	0.60	0.127	0.638	0.085	0.638
Wiring harness	0.073	0.593	0.50	0.064	0.593	0.064	0.593
Fixed antenna	0.144	0.793	0.60	0.178	0.793	0.119	0.793
Deployable antenna	0.098	0.913	0.60	0.133	0.913	0.089	0.913
Transponder	0.161	0.898	0.60	0.216	0.898	0.144	0.898
Receiver	0.250	0.697	0.55	0.263	0.697	0.215	0.697
Transmitter	0.155	0.793	0.50	0.160	0.793	0.160	0.793
Tape Recorder	0.006	1.610	0.45	0.011	1.610	0.013	1.610
Signal conditioning	0.071	0.938	0.55	0.090	0.938	0.074	0.938
Processor	0.158	0.690	0.55	0.165	0.690	0.135	0.690
Horizon sensor	0.126	1.000	0.50	0.153	1.000	0.153	1.000
Sun sensor	0.112	1.321	0.40	0.140	1.321	0.210	1.321
Star tracker	0.197	1.000	0.60	0.287	1.000	0.191	1.000
Gyro	0.081	1.000	0.50	0.098	1.000	0.098	1.000
Mom/reaction wheel	0.006	1.217	0.50	0.009	1.217	0.009	1.217
Magnetic torquer	0.018	1.000	0.55	0.024	1.000	0.020	1.000
Nutation damper	0.061	1.000	0.45	0.067	1.000	0.081	1.000
Att. cntl. electronics	0.217	0.888	0.60	0.289	0.888	0.193	0.888
Hydrazine thruster (small)	0.033	1.129	0.60	0.053	1.129	0.035	1.129
Hydrazine tank	0.007	1.000	0.45	0.008	1.000	0.009	1.000
Solid prop. motor	0.070	1.000	0.25	0.042	1.000	0.127	1.000

All MKS relation are of the form: Cost($M93)=A * [Mass(kg)]^B

Appendix A.5.3.4 Raw Component Level Costs

System/component	Mass [kg]	R&D [$M94]	First Unit [$M94]	Type
Structures				
Module				
Module LOX Tank	2,647	$15.59	$4.87	simple
Module LH2 Tank	11,734	$30.64	$10.83	simple
Module LOX Insulation	238	$5.22	$1.34	simple
Module LH2 Insulation	755	$8.82	$2.49	simple
Module Thrust Structure	495	$3.04	$1.98	thrust structure 488
Module Helium Tank	55	$2.68	$0.61	simple
Inter-Stage Faring/Nose Cone	1,212	$10.93	$3.21	simple
Module Inter Tank Faring	285	$5.67	$1.48	simple
Nozzle Shroud	2,816	$16.03	$5.04	simple
Secondary Inert Mass	646	$8.22	$2.29	simple
Upper Stage				
LOX Tank	647	$8.22	$2.29	Tank 488
LH2 Tank	3,022	$16.55	$5.23	Tank 488
LOX Insulation	98	$3.49	$0.83	Insulation 488
LH2 Insulation	334	$6.09	$1.61	Insulation 488
Thrust Structure	495	$3.04	$1.98	thrust structure 488
Helium Tank	14	$1.44	$0.29	simple
Inter-Stage Faring	262	$5.45	$1.41	simple
Inter Tank Faring	285	$5.67	$1.48	simple
Nozzle Shroud	631	$8.13	$2.26	simple
Secondary Inert Mass	646	$8.22	$2.29	simple
Wings	986	$9.95	$2.87	simple
Vertical Stabilizers	398	$6.60	$1.77	simple
Landing Gear	0			
Nose	394	$21.46	$7.63	complex
Main	1,446	$48.22	$21.26	complex
Fuselage	11,851	$30.78	$10.89	simple
Escape System	2,400	$66.10	$31.70	complex
Secondary Structure	1,614	$51.63	$23.18	complex
Thermal Protection				
REI Mullite	300	$18.10	$6.14	complex
Titanium Sub-structure	600	$27.87	$10.62	complex
Nose	30	$4.31	$1.00	complex
Leading Edges	1,670	$52.74	$23.81	complex
Fasteners and Adhesives	520	$25.49	$9.48	complex
Propulsion				
Main Engine				
Chamber & Nozzle	658	$27.96	$9.58	simple & complex
Turbopump LOX	301	$18.13	$6.16	complex
Turbopump LH2	301	$18.13	$6.16	complex
Piping	340	$6.14	$1.62	simple
Injector	70	$7.31	$1.95	complex
Gimbal Structure	60	$6.64	$1.73	complex
Gimbal EMA	21	$0.58	$0.58	drive mechanism
Valve EMA	2	$0.03	$0.03	drive mechanism
Instruments, sensors, etc.	75	$7.63	$2.06	complex
Secondary Inert Mass	75	$3.09	$0.72	simple
Power Supply- Baterries	376	$6.43	$6.43	Battery
(350 W/kg;14000$/kg; 131KW)				
OMS Engine				
Chamber & Nozzle	100	$9.23	$2.34	simple & complex

Gimbal Structure	25	$3.85	$0.87	complex
OMS Gimbal EMA	5	$0.10	$0.10	drive mechanism
OMS Valve EMA	0	$0.00	$0.00	drive mechanism
RCS Thruster				
Chamber & Nozzle	4	$1.45	$0.23	simple & complex
RCS Valve EMA	0	$0.00	$0.00	drive mechanism
RCS & OMS Feed System				
Forward Propellant Tank	24	$0.20	$0.22	Hydrazine Tank
Forward Pessurant Tank	33	$2.13	$0.46	simple
Aft Propellent Tank	156	$1.29	$1.45	Hydrazine Tank
Aft Pressurant Tank	187	$4.68	$1.18	simple
Power				
Fuel Cell	73	$4.24	$2.16	Power
24 Hour Back up Battery	374	$6.39	$6.39	Battery
Electrical Bus Wiring	200	$1.53	$1.53	Wiring
LOX Tank	35	$2.19	$0.48	Simple
LH2 Tank	3	$0.72	$0.13	Simple
LOX Insulation	2	$0.60	$0.10	Simple
LH2 Insulation	1	$0.32	$0.05	Simple
Spacecraft APU	40	$2.48	$1.26	Power
Avionics				
Guidance sensors				
GPSR	5	$1.35	$0.90	Star Tracker
INS	57	$16.92	$11.26	Star Tracker
Star tracker	26	$7.72	$5.13	Star Tracker
Microwave landing system	32	$9.53	$6.34	Star Tracker
Radar Altimiter	6	$1.82	$1.21	Star Tracker
Proximity	6	$1.82	$1.21	Star Tracker
Rendezous Sensors	6	$1.82	$1.21	Star Tracker
Communications				
Helix S-Band Antenna	3	$0.44	$0.29	Fixed Antenna
Parabolic Antenna	135	$12.12	$8.11	Depolyable antenna
Omni. Micro. Ant. x12.57	2	$0.32	$0.21	Fixed Antenna
Omni. Micro. Ant. x25.13	4	$0.55	$0.37	Fixed Antenna
Helix EVA Antenna	3	$0.44	$0.29	Fixed Antenna
VTR (Digital)	23	$3.95	$3.99	tape recorder
Tape Recorder	33	$3.21	$4.79	tape recorder
K Band Transceiver	4	$0.80	$1.83	receiver/transmitter
S Band Transceiver	7	$1.12	$3.68	receiver/transmitter
L Band Transceiver	5	$0.84	$2.03	receiver/transmitter
Stanard Modules				
Inter Comp. Interface Seq. Mod.	1	$1.54	$0.24	Comm. & Data
Shared Memory Module	1	$1.54	$0.24	Comm. & Data
Memory Module	1	$1.54	$0.24	Comm. & Data
Comp. Processor Module	1	$1.54	$0.24	Comm. & Data
I/O Processor Module	1	$1.54	$0.24	Comm. & Data
Power Module	1	$1.54	$0.24	Comm. & Data
I/O Sequencer Module	1	$1.54	$0.24	Comm. & Data
Remote Data Unit	5	$3.83	$0.77	Comm. & Data
Envirmental Housing (computer unit)	7	$1.74	$0.32	complex
Envirmental Housing (RDU)	2	$0.80	$0.12	complex
Fiber Optic Bus	20	$11.94	$0.39	Comm & Data/Wiring
Flight Control EMA	4	$0.09	$0.09	drive mechanism
Human Factors				
EVA				
2 p Airlock	550	$26.40	$9.91	complex

	4 Shuttle EMU	61	$6.73	$1.76	complex
RMS		1,240	$43.81	$18.83	complex
Atmosphere					
	E Ox Tanks	120	$3.83	$0.93	simple
	Nit Tanks	249	$5.33	$1.37	simple
	Filtering System	120	$10.23	$2.98	complex
	Activated Charcoal	51	$5.99	$1.51	complex
	Air System	20	$3.35	$0.73	complex
	Thermal System	100	$4.19	$1.67	Thermal
Water supply					
	Water tanks	20	$1.70	$0.36	simple
Food					
	Storage	5	$0.90	$0.17	simple
	Preparation Unit	5	$1.41	$0.24	complex
	Refrigerator	5	$1.41	$0.24	complex
Sanitation					
	Trash Storage	75	$3.09	$0.72	simple
	Toilet	20	$3.35	$0.73	complex
	Waste holding tanks	10	$1.24	$0.25	simple
Safety Equipment					
	Medical Equipment	4	$1.23	$0.20	complex
	Fire Dectection/Suppression	2	$2.07	$0.35	Comm. & Data
	Emergency Breathing	1	$0.52	$0.07	complex
Crew Cabin					
	Lighting	2	$0.80	$0.12	complex
	Sleeping Berths	20	$1.70	$0.36	simple
	Individual Lockers	5	$0.90	$0.17	simple
	TOTAL		$904		
Software (on-board)			$262		
Software (Ground)			$131		
Ground Support					
Launch Ops.			$130	$100.00	
Recovery Ops.			$4	$1.50	
Facilities			$30	$0.40	
Equipment			$89	$4.60	
Managament				$1.50	
Syst Level (Eng. Support)				$14.50	
	GRAND TOTAL		$1,550		
	cost/misson		$4		